CELLULAR AND MOLECULAR MECHANISMS OF SALINITY ACCLIMATION IN AN AMPHIDROMOUS TELEOST FISH

Jacqueline A. Lee

A thesis submitted in partial fulfilment

of the requirements for the Degree of

Master of Science in Cellular and Molecular Biology

University of Canterbury

2012

ABSTRACT

Inanga (*Galaxias maculatus*) is an amphidromous fish species that is able to successfully inhabit a variety of salinities. Using an integrated approach this thesis has characterised for the first time the physiological characteristics that facilitate acclimation in inanga. Structural studies using scanning electron microscopy (SEM) and laser scanning confocal microscopy (LSCM) revealed freshwater-acclimated inanga have a high density of apical pits and freshwater-type mitochondria-rich cells (MRCs) that can facilitate ion absorption from the hypo-osmotic environment. In seawater, inanga remodel their gills by increased proliferation of seawater-type MRCs to facilitate ion secretion in the hyper-osmotic environment.

Concentration-dependent sodium (Na^+) kinetic analysis revealed that at a whole body level, inanga regulate Na^+ using a saturable, high affinity, low capacity uptake system which makes them extremely adept at extracting Na^+ from very dilute freshwater environments. In fact inanga displayed an uptake affinity (K_m) of 52 ± 29 µM, which is one of the lowest ever recorded in freshwater fish.

The sodium/potassium ATPase transporter (NKA) is central to Na^+ regulation within the gill. In high salinties inanga displayed increased NKA activity (6.42 ± 0.51 µmol ADP mg protein^{-1} h^{-1}) in an effort to excrete the excess Na^+, diffusively gained from the hyper-osmotic environment. This increase in NKA was most likely a reflection of the proliferation of NKA-containing MRCs. The NKA activities seen in freshwater- and 50% seawater-acclimated inanga were similar (2.54 ± 0.19 and 2.07 ± 0.22 µmol ADP mg protein^{-1} h^{-1} respectively) to each other suggesting the inanga gill is capable of supporting ion regulation in brackish waters without a significant increase in NKA activities, and the energetically-expensive changes in gill structure and function that accompany such a change.

Molecular investigation of NKA isoform expression using quantitative PCR (qPCR) showed that inanga displayed salinity-induced changes in the expression of the three α NKA isoform variants investigated. Isoform α1a exhibited a pattern consistent with an important role in freshwater, confirming results from other fish species. While it is generally accepted that α1b isoform is the predominant NKA isoform in seawater, inanga did not display this pattern with a freshwater dominance seen. None of the salinity-induced changes could quantitatively

explain the increased NKA activity in seawater suggesting that different isoforms may convey different activities, that there is also regulation of NKA at a post-transcriptional level, and/or other isoforms or subunits may have a significant role.

The importance of the osmoregulatory hormone cortisol and prolactin is widely accepted and inanga were treated with cortisol, prolactin and a combination of the two in an effort to further elucidate their role. NKA activity and NKA isoform expression were assessed but no specific patterns were deduced, except for a decrease in both NKA activity and isoform expression in 100% seawater-acclimated inanga treated with cortisol and prolactin. The reasons for this decrease were not evident, although the impact of stress induced by the injection protocol was likely to be a confounding factor.

The development of a new confocal-based technique in this study was able to describe, for the first time, intracellular sodium levels ($[Na^+]_i$) as a function of salinity in an intact euryhaline fish gill cell. Using the fluorescent Na^+ indicator dye CoroNa Green this study demonstrated the ability of inanga gill cells to maintain $[Na^+]_i$ in the face of environmental change. Freshwater-acclimated inanga displayed basal $[Na^+]_i$ of 5.2 ± 1.8 mM, with 12 ± 2.3 mM and 16.2 ± 3.0 mM recorded in 50% seawater- and 100% seawater-acclimated cells, respectively. Low $[Na^+]_i$ is advantageous in hypo-osmotic environments as it provides a gradient between the cell and the blood which is essential for generating electrochemical gradients cell volume regulation and other cellular homeostatic mechanisms. A slightly elevated $[Na^+]_i$ seen at the higher sanities would help minimise the diffusive gradient for passive influx from the environment which would be of benefit in hyper-osmotic environments. Upon salinity challenge 50% seawater cells were equally adept at maintaining a constant $[Na^+]_i$ at any salinity, suggesting these cells are have the necessary constituents to regulate Na^+ in both lower and higher salinities. This novel LSCM approach is advantageous relative to existing transport models as it will allow the observation of cellular ion transport in real time, within a native filament structure displaying functional interaction of different cell types.

The extreme ion uptake characteristics of the inanga and their amenability to *in situ* confocal-based studies demonstrated in this study, confirm inanga as a valuable model species for future research.

TABLE OF CONTENTS

LIST OF FIGURES

Chapter 1

Chapter 2

Chapter 3

Chapter 4

Chapter 5

Chapter 6

Appendix A

LIST OF TABLES

Chapter 3

Chapter 4

Chapter 5

Chapter 6

Appendix A

ABBREVIATIONS

18S	18S rRNA
A	amiloride
ACs	accessory cells
ADP	adenosine diphosphate
AM	acetoxymethyl
ANOVA	analysis of variance
ATP	adenosine triphosphate
ATPase	ATP-utilising enzymes
bp	base pair
BSA	bovine serum albumin
CA	carbonic anhydrase
cDNA	complementary DNA
CFTR	cystic fibrosis transmembrane conductance regulator
cort	cortisol
cort + pro	cortisol and prolactin
C_t	threshold cycle
DNA	deoxyribose nucleic acid
DNases	deoxyribose nucleic acid enzymes
dsDNA	double stranded DNA
EF1a	elongation factor 1a
ENaC	epithelial Na^+ channel
ER	endoplasmic reticulum
ER	endoplasmic reticulum
F	fluorescence
F_{max}	fluorescence maximum
F_{min}	fluorescence minimum
FW	freshwater
GAPDH	glyceraldehyde-3-phosphate dehydrogenase
GH	growth hormone
GR	glucocorticoid receptor
GRE	glucocorticoid response element
HA	H^+-ATPase pump
IGF	insulin-like growth factor I
J_{in}	Sodium influx
J_{max}	maximal rate of sosium transport
K_d	dissociation constant
K_m	affinity constant

LDH	lactate dehydrogenase
LSCM	laser scanning confocal microscopy
MRCs	mitochondria-rich cells
mRNA	messenger RNA
NAC	N-acetyl cysteine
NAD+	oxidised nicotinamide adenine dinucleotide
NADH	reduced nicotinamide adenine dinucleotide
NHE	Na^+-H^+ exchanger
NKA	sodium/potassium ATPase
NKCC	Na^+-K^+-$2Cl^-$ cotransporter
NMR	nuclear magnetic resonance
O	ouabain
PBS	phosphate buffered saline
PCR	polymerase cahin reaction
PEP	phosphoenolpyruvate
PK	pyruvate kinase
PMT	photomultiplier tube
PNA	peanut agglutinin
pro	prolactin
PVCs	pavement cells
qPCR	quantitative polymerase chain reaction
RNA	ribonucleic acid
RNases	ribonuclease enzymes
rRNA	ribosomal RNA
RT	reverse transcription
SEM	scanning electron microscopy
SW	seawater
TEM	transmission electron microscopy
T_m	melting temperature
α1a	NKA alpha 1a isoform
α1b	NKA alpha 1b isoform
α1c	NKA alpha 1c isoform
βA	beta actin

CHAPTER 1 GENERAL INTRODUCTION

Fish are arguably the most successful vertebrate group. They have adapted to almost every possible niche in marine and freshwater habitats, and some are even capable of life on land (Farrell, 2011). Aquatic environments present a number of significant challenges, including extremes of salinity, temperature and pH, each of which must be overcome to ensure survival. Irrespective of their external environments, fish have evolved highly efficient ionic and osmotic regulatory mechanisms permitting cellular homeostasis, which is necessary for the effective operation of all biochemical and physiological processes (Hwang and Lee, 2007). Teleosts, the most advanced group of fishes, inhabit aquatic environments ranging from very dilute freshwater to salinities significantly more concentrated than seawater. However, despite the wide ranges in external salinity in the environments they inhabit, all teleosts maintain their plasma osmotic concentrations at a constant level of about one third to one half that of seawater (~280-560 mOsmol kg^{-1}; Nordlie, 2009).

Freshwater teleosts are hyper-osmotic to their surroundings so they face osmotic gain of water and diffusional loss of ions such as sodium (Na^+) and chloride (Cl^-) across their permeable gill epithelium (Figure 1.1). To compensate for these osmotic and ionic changes, freshwater fish excrete large volumes of dilute urine and actively take up Na^+ and chloride ions across the gill epithelium (Evans et al., 1999). Therefore in freshwater the gills behave as ion-absorbing epithelia.

Marine teleosts deal with the opposite challenges. These fish are hypo-osmotic to seawater, so they face osmotic loss of water and diffusional gain of Na^+ and chloride ions across the gill (Figure 1.2). To compensate, seawater teleosts ingest seawater to replace lost water and actively excrete Na^+ and chloride ions via the gill epithelium (McCormick, 2001). Although the kidneys and intestine play an important role, the gill is considered the main site for ionic and osmotic regulation in fish.

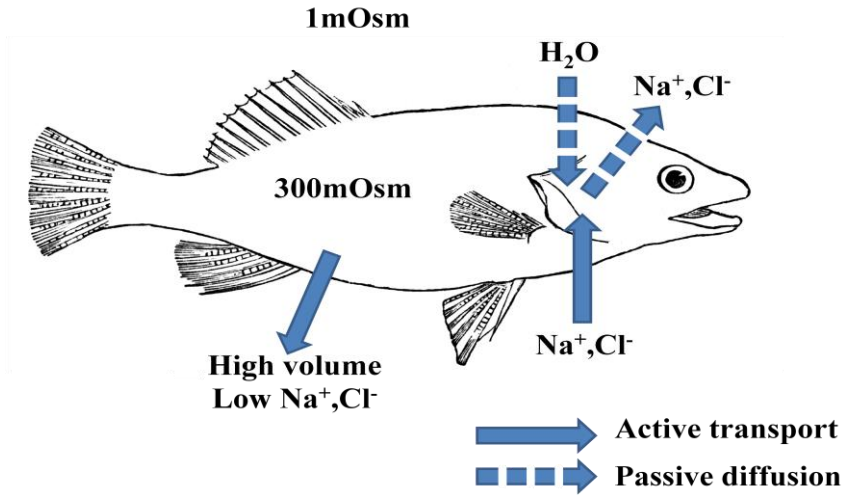

Figure 1.1 Teleost osmoregulation in freshwater. Passive ion movements are denoted by dashed arrows, active by solid arrows. Figure adapted from Evans (2008).

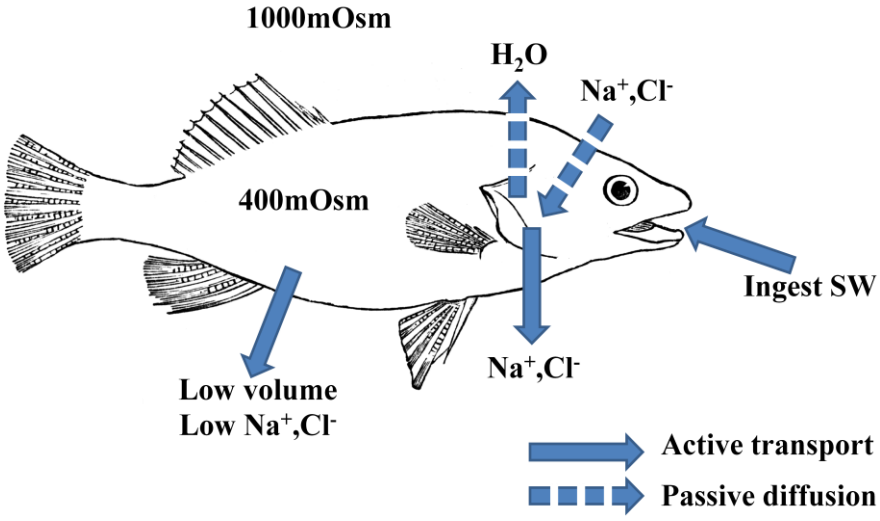

Figure 1.2 Teleost osmoregulation in seawater. Passive ion movements are denoted by dashed arrows, active by solid arrows. Figure adapted from Evans (2008).

The majority of teleosts are stenohaline and live in either freshwater or seawater, and are not exposed to fluctuating salinities. However, a small number (~5%) are euryhaline, meaning that they are able to live in freshwater as well as in varying strengths of seawater (Evans, 1984). These fish may experience waters of distinct salinity either as a function of a life cycle migration, or by inhabiting environments that regularly vary in salinity (e.g. tidally-influenced near-coastal waters). As a consequence these fish must be able to sense osmotic and ionic changes in environmental salinity and activate the appropriate compensatory responses (Fiol and Kültz, 2007). For example, during movement from freshwater to seawater, a euryhaline fish must undertake a major transformation and change their gills from the ion-absorbing epithelium present in freshwater to an ion-secreting epithelium needed in seawater (McCormick, 2001). This dramatic change is thought to be achieved by extensive remodelling of the gill epithelium and includes the turnover of gill epithelial cells, altered differentiation of the gill epithelial cells, and the modulation of ion transporter activity (Kültz, 2001).

Fish which regularly migrate between different salinities at predictable seasons and life stages are known as diadromous (McDowall, 1988). Diadromy encompasses three migratory strategies: anadromy, catadromy and amphidromy (Myers, 1949). Anadromous fish generally live in seawater and enter freshwater rivers as large mature adults to spawn, where as catadromous fish hatch at sea and move to freshwater as small juveniles. Amphidromy involves reproduction in fresh water followed by an immediate migration of the newly hatched larvae to sea. The larvae feed and grow for a period of a few weeks to a few months and then the small juveniles return to fresh water where they mature and grow into adults (Myers, 1949). Amphidromy is rare with less than 80 of the known 20 000 + species of fish exhibiting this strategy (McDowall, 2007).

1.1 Gill Structure

The fish gill is a multifunctional epithelium. It extracts oxygen from the water; excretes carbon dioxide and other, toxic, metabolic wastes (e.g. ammonia); has a central role in acid-base balance; and is also the key regulator of ionic and osmotic balance. The gills are located at the side of the head under the operculum, a thin bony flap that covers the branchial chamber. Water enters the pharynx from the mouth, then passes over the gill and follows the inner wall of the operculum until it exits via the opercular cavity. The flow of water over the gill is counter-current to the blood perfusing the gill and this facilitates gas exchange and ionic and osmotic movements between the gill and its environment. In teleosts the gill consists of four gill arches on each side of the fish. Each gill arch is made up of rows of filaments and each filament is lined with rows of lamellae between which the water flows (Figure 1.3). The water flow strikes the leading edge of the filament, flows across the lamellae and over the trailing filament edge. This flow is countercurrent to the blood perfusing the lamella, with deoxygenated blood entering the gill via the afferent blood vessels (on the trailing edge) and oxygenated blood leaving via the efferent blood vessels (on the leading edge).

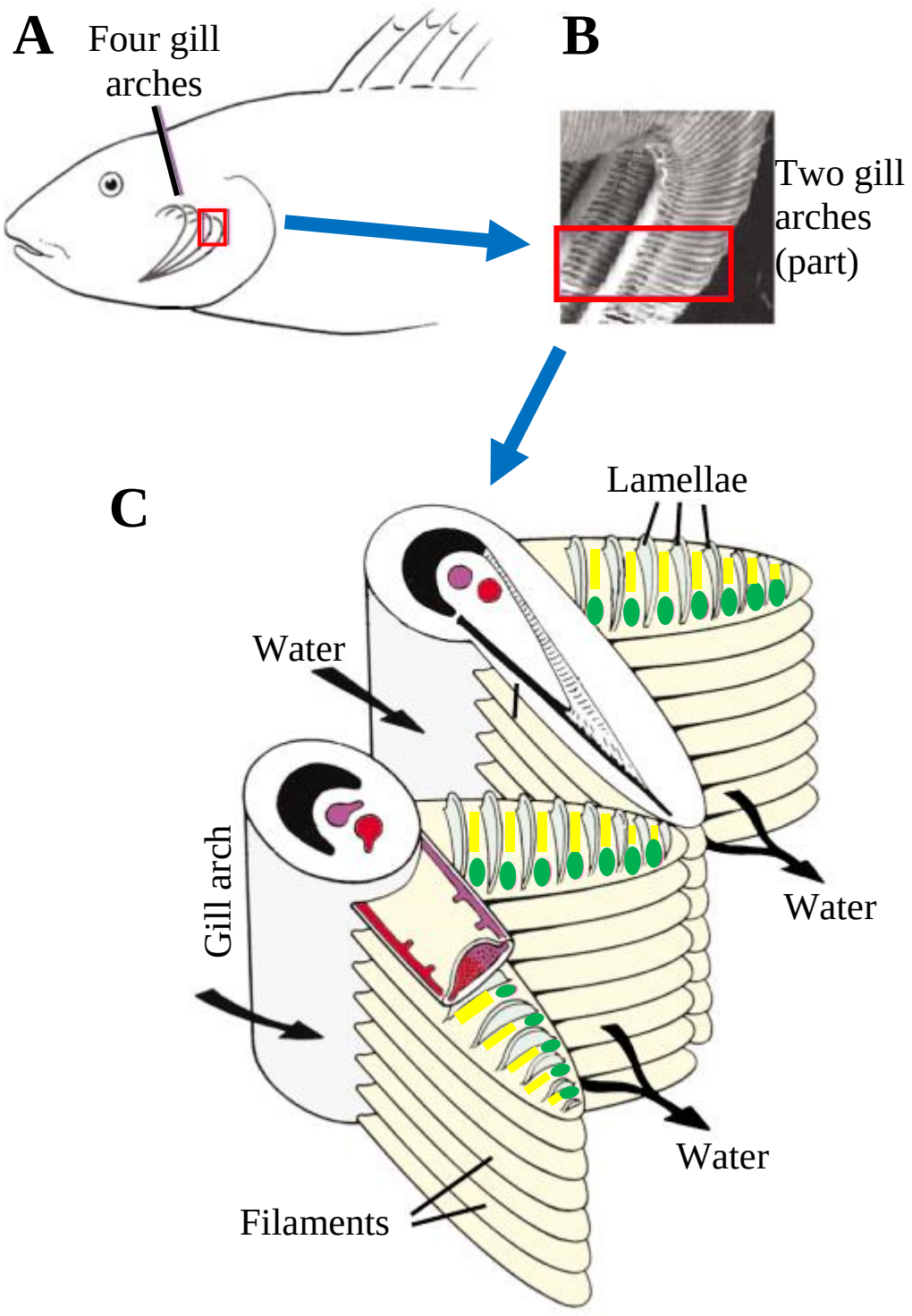

Figure 1.3 Structure of the teleost gill. Each gill is composed of four gill arches (A, B). Each arch is made up of rows of filaments lined with lamellae (C). Green ovals denote the afferent/trailing edge of the filament. Afferent and efferent blood vessels are shown in purple and red respectively. The interlamellar spaces between the lamella are indicated in yellow. Figure adapted from Hirose et al. (2003).

Older literature refers to the filament and the lamellar epithelia as the primary and secondary epithelia, respectively (Laurent and Dunel, 1980). The filaments and lamellae are lined with a single layer of epithelial cells. Opposing sides of each lamella are held apart by pillar cells to form the lamellar blood space (Figure 1.4). This space accommodates a complex series of counter-current blood vessels that perfuse the lamellae, and which facilitate exchange with the environment. This highly organised structural arrangement of filaments and lamellae, results in a very large surface area of gill epithelium, but a very small diffusive distance between the blood that perfuses the lamellae, and the environment (Evans et al., 2005). This arrangement is ideal for the gills role in homeostasis.

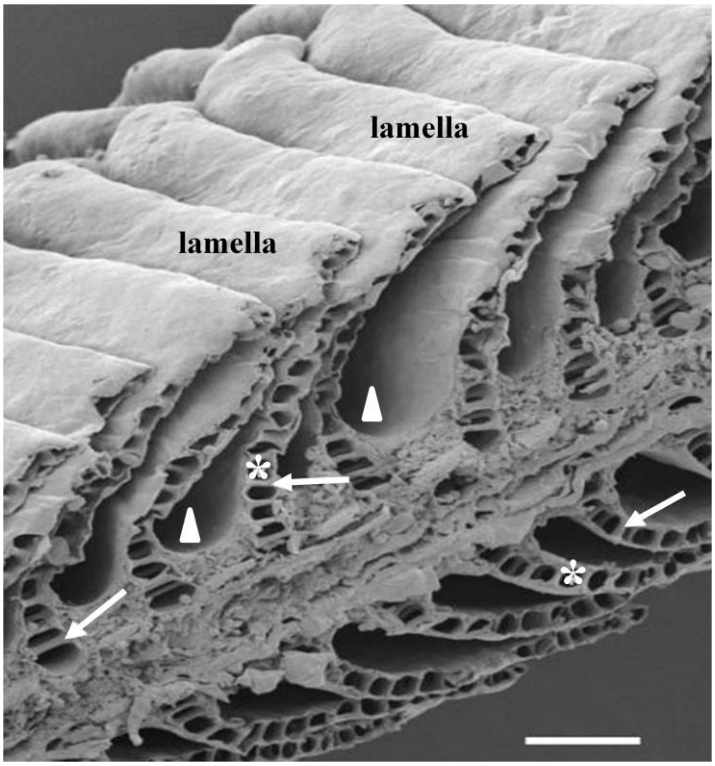

Figure 1.4 Scanning electron micrograph of a longitudinal section through a gill filament (Atlantic stingray, *Dasyatis sabina*). Asterisks indicate lamellar blood spaces formed by pillar cells (arrows) and triangles indicate the interlamellar regions. Bar = 50 µm. Figure adapted from Evans et al. (2005).

The gill epithelium is composed of three main cell types important for ionic and osmotic regulation; pavement cells (PVCs), mitochondria-rich (MRCs) cells and accessory cells (ACs) (Perry, 1997). PVCs are large, generally squamous-shaped cells that have moderate amounts of mitochondria, and well-developed Golgi and rough endoplasmic reticulum. Their apical surface is covered with many microvilli that are thought to be the site of transepithelial gas exchange and may also play a role in acid-base regulation (Evans et al., 1999). The number of mitochondria is often used as a mechanism to differentiate PVCs and MRCs, with the latter having larger numbers of these important organelles (see below). However some studies show that a subset of PVCs, under certain conditions, may also show an abundance of mitochondria (Goss et al., 1994). PVC's form extensive multistranded connections with neighbouring cells resulting in tight intercellular junctions which are impermeable to ions (Karnaky Jr, 1998). PVCs are also generally morphologically unresponsive to environmental change but have been shown be involved in the covering and uncovering of MRCs in response to abrupt salinity change (Daborn et al., 2001; Laurent et al., 2006). Although PVCs comprise approximately 90% of the total cell population within the gills, they are largely considered to play a minor role in ion regulation (Evans et al., 1999).

MRCs (also known as chloride cells or ionocytes) make up ~10% of the gill cell population but are considered to be the primary site of active ion regulation and are subsequently the main focus of ion regulatory studies. MRCs are characterised by an abundance of mitochondria and an extensive tubular system emanating from the basolateral membrane (Perry, 1997). These tubules provide a large surface area for the localisation of transport proteins such as the Na^+ pump (sodium/potassium ATPase; NKA). MRCs are usually found in the interlamellar spaces and on the trailing edge of the filament (Figure 3), but have also been found on the lamellar epithelium in some freshwater fish species (Pisam et al., 1988; Uchida et al., 1996).

Many morphological subtypes of MRCs have been described in variety of fish. Atlantic salmon (*Salmo salar*), striped bass (*Morone saxatilis*), tilapia (*Oreochromis mossambicus*), and killifish (*Fundulus heteroclitus*) all demonstrate distinct freshwater- and seawater-type MRCs (Pisam et al., 1988; King and Hossler, 1991; Kültz et al., 1995; Katoh et al., 2001). Goss et al. (2001) described the presence of two distinct subpopulations of MRCs in rainbow trout (*Oncorhynchus mykiss*) based on their ability to bind to peanut agglutinin (PNA). PNA^+

and PNA^- showed differential expression of the proton pump (H^+-ATPase), with the PNA^- subtype showing higher expression levels. Hiroi et al. (2008) described four MR cell types in tilapia (*Oreochromis mossambicus*) based on ion transporter-specific immunofluorescence staining.

The third main cell type, ACs, resemble MRCs in many respects. They have numerous mitochondria but are smaller, with a less-developed tubular system, and display a lower expression of NKA compared to MRCs. Their specific function is unknown but they appear to form multicellular complexes with MRCs, indicating an accessory role in ion transport (Wilson and Laurent, 2002).

1.2 Ion transport

Much controversy surrounds the exact roles PVCs, MRCs and ACs play in ion regulation. Ionic and osmotic homeostasis is thought to occur mainly through MRCs and based on this several models for gill ion regulation have been proposed. Central to all models is NKA. NKA is a ubiquitous, membrane-bound transport protein that not only actively transports Na^+ ions out of the cell and potassium (K^+) ions into the cells, but also provides the driving force for many other transporters within the fish gill (Hwang and Lee, 2007). NKA is composed of two subunits (α and β) that pair to form an αβ heterodimer. The α-subunit is the main catalytic unit where Na^+, K^+ and ATP all bind. The β-subunit is thought to assist in the folding and placement of the α-subunit in the cell membrane (Blanco and Mercer, 1998). A third subunit, γ, is a member of the FXYD protein family and appears to have a regulatory role, affecting the conformation and kinetic properties of the β subunit (Garty et al., 2002).

Different isoforms for each NKA subunit have been identified in a few species of teleost, including the European eel (*Anguilla anguilla*, Cutler et al., 1995), killifish (*Fundulus heteroclitus*, Semple et al., 2002) and rainbow trout (*Oncorhynchus mykiss*, Richards et al., 2003). The appearance of different NKA isoforms is thought to be a result of genome duplication. For example, a whole genome duplication in the teleost lineage is known to have occurred between 25 and 100 million years ago (Allendorf and Thorgaard, 1984). Such duplication events are thought to have provided the raw genetic material that helped promote

the radiation of the teleosts (Venkatesh, 2003). Following gene duplication one of the resulting gene copies may be silenced and eliminated or it can take on novel functions independent of the other copies. It is suggested that the different NKA isoforms confer different kinetic or biochemical properties that allow the fish to adapt to different physiological demands (Hwang and Lee, 2007).

The current model by which seawater teleosts excrete ions via the gill is well established. Excretion of sodium chloride (NaCl) occurs in the MRCs of the gills and is mediated by NKA (Figure 1.5). NKA is located on the basolateral membrane of the cell and maintains cytoplasmic Na^+ concentration lower than that of the blood and environment. In so doing it creates an electrochemical gradient that drives other ion movements into and out of the cell. A basolateral Na^+-K^+-$2Cl^-$ cotransporter (NKCC) mediates the entry of Na^+ and Cl^- into the cell, down the electrochemical gradient generated by NKA. Chloride ion then builds up inside the cell until it generates a favourable gradient for diffusion and exits the MRC through a chloride channel that is homologous to the human cystic fibrosis transmembrane conductance regulator (CFTR). NKA actively transports Na^+ out of the MRC and into the paracellular space. Once in the paracellular space, the Na^+ concentration builds up until it reaches a level whereby it diffuses passively into the environment through paracellular pathway between the tight-junction separating the MRC and the AC. This movement is also facilitated by the favourable transepithelial potential created by the movement of Cl^- out of the cell (Evans et al., 1999).

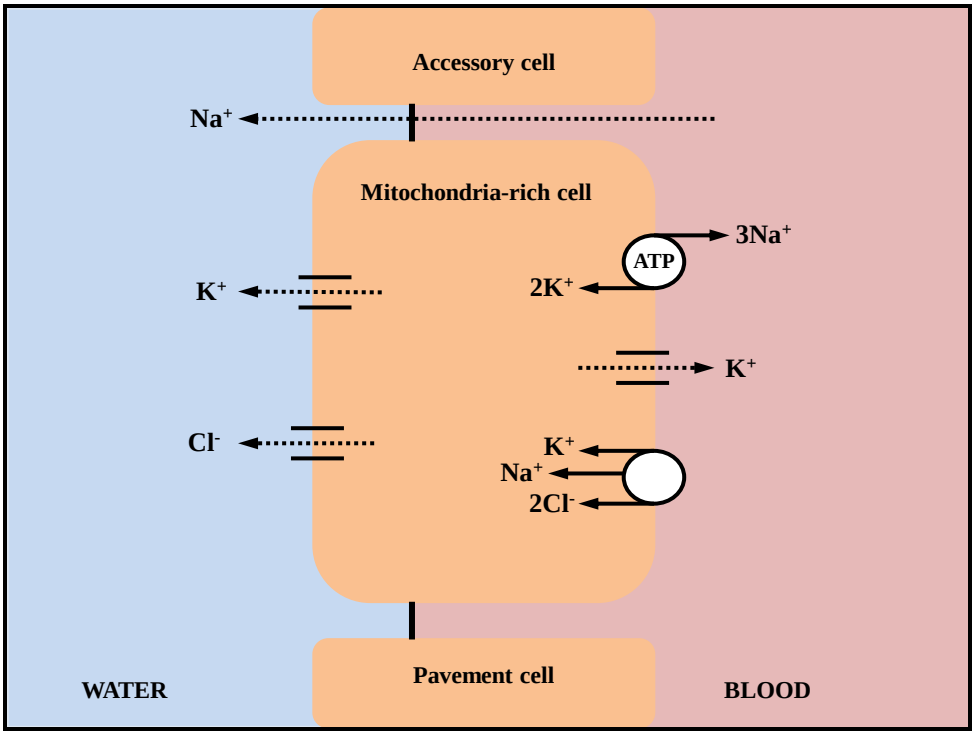

Figure 1.5 Sodium excretion in the MRCs of seawater teleosts. Passive ion movements are denoted by dashed arrows, active by solid arrows. Figure adapted from Evans et al. (1999).

In contrast, the mechanism by which freshwater teleosts absorb Na^+ from their environment is controversial and is hotly debated among fish physiologists (Evans, 2008). Currently there are two proposed models for the absorption of Na^+ into gill cells: (1) the exchange of Na^+ and H^+ via an apical Na^+-H^+ exchanger (NHE) and (2) an apical H^+-ATPase pump (HA) electrochemically-linked with Na^+ absorption via an epithelial Na^+ channel (ENaC).

In the first model the NHE located on the apical membrane, mediates the exchange of a Na^+ ion for a hydrogen ion (Figure 1.6). This model relies on the creation of a favourable electrochemical gradient for Na^+ influx, likely generated by the actions of the basolateral NKA and by the efflux of hydrogen down a concentration gradient. Function of the NHE is driven solely by the environment and the cellular concentrations of Na^+ and H^+ and is not affected by the membrane potential (Parks et al., 2008). This means that in order for the NHE to function either environmental Na^+ concentration must be higher than the internal Na^+ and/or environmental pH must be higher than intracellular pH. There are a number of theories to explain how this might be achieved. Intracellular Na^+ could be maintained at a low level by

the numerous NKA transporters present in the basolateral membrane (Evans et al., 2005). Wright (1991) calculated that the H^+ gradient alone could drive the NHE as long as intracellular pH was at least 0.3 units below environmental pH. Intracellular pH can be lowered through the actions of the intracellular enzyme, carbonic anhydrase (CA). CA acts by catalysing the hydration of intracellular CO_2 to form bicarbonate (HCO_3^-) and H^+. The bicarbonate is transported into the blood space via a basolateral HCO_3^-/Cl^- transporter and the H^+ is used to drive the NHE. The production of HCO_3^- and H^+ also produces charges that counter those produced by Cl^- and Na^+ flux respectively (Perry and Gilmour, 2006).

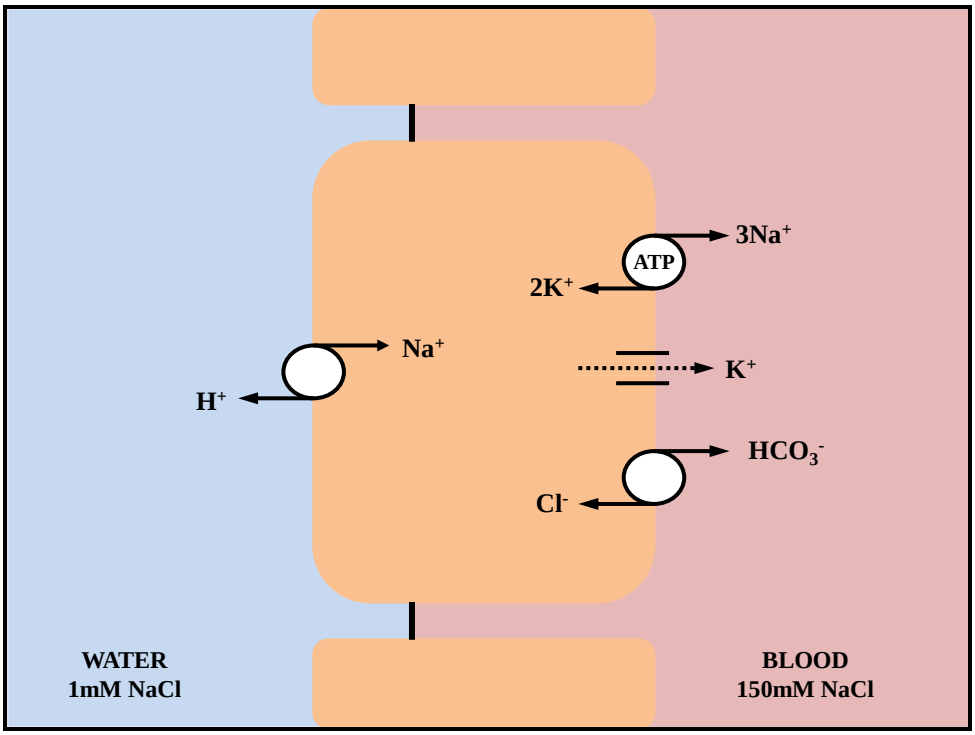

Figure 1.6 The apical Na^+-H^+ exchanger (NHE) model in the MRCs of freshwater teleosts. An apical NHE exchanger absorbs Na^+ into the MRCs of freshwater teleosts. Passive ion movements are denoted by dashed arrows, active by solid arrows. Figure adapted from Evans et al. (1999).

NHE has been implicated in freshwater Na^+ absorption after immunological studies showed the presence of NHE in blue-throated wrasse (*Pseudolabrus tetrious*), rainbow trout (*Oncorhynchus mykiss*) and tilapia (*Oreochromis mossambicus*) (Edwards et al., 1999; Wilson et al., 2000a). Evidence for a role of NHE has also been provided by the use of

transport inhibitors such as amiloride. Amiloride and its analogues are widely used pharmacological agents that inhibit the function of NHE (Kleyman and Cragoe, 1988). For example, exposure of skin ionocytes from zebrafish embryos to amiloride resulted in the blockage of over 90% of Na^+ accumulation (Esaki et al., 2007). Molecular studies, utilising polymerase chain reaction (PCR) also support this model with multiple copies of the NHE gene having been found in a small number of species (Hirata et al., 2003; Scott et al., 2005). Hirata et al. (2003) also identified and localised NHE in the apical membranes of gill MRCs of the Osorezan dace (*Tribolodon hakonensis*) using homologous antibodies and molecular probes.

There are, however, several major drawbacks to the NHE model. The use of inhibitors is controversial as some lack specificity and their exact mechanism of action is not always known. For example, amiloride not only blocks NHE but it has also been shown to block other transporters such as ENaC (Masareel et al., 2003). Immunological studies have sometimes used heterologous antibodies that lack the required specificity to accurately identify their NHE targets (Wilson et al., 2000a). Thermodynamic evidence also casts doubt on the NHE model suggesting that the Na^+ ion concentration of freshwater (1 mM) is too low to drive the NHE as the intracellular Na^+ concentration is thought to be greater than 10 mM (Parks et al., 2008). Environmental pH is also an issue as acidic waters will actually cause the NHE to work in reverse resulting in a loss of intracellular Na^+ and uptake of H^+ (Parks et al., 2008). Unfortunately measuring intracellular Na^+ has proven to be extremely difficult (Amorino and Fox, 1995; Morgan et al., 1994) and must be successfully overcome in order to more accurately assess the validity of this model.

In the alternate model, an apical V-type H^+-ATPase (HA) works in conjunction with the basolateral NKA to provide an electrochemical gradient that allows the movement of Na^+ into the cell via an epithelial Na^+ channel (ENaC) (Figure 1.7). The NKA moves Na^+ into the blood, decreasing the intracellular Na^+ concentration. This creates a gradient for the influx of Na^+ via the ENaC. The HA also assists with Na^+ influx by removing H^+ from the cell thus making the cell more electrochemically negative.

Immunocytochemical evidence using heterologous antibodies suggests ENaC is present on the apical surface of gill filaments in rainbow trout and tilapia (Lin et al., 1994; Wilson et al., 2000a). Antibodies have also been used to localise H^+-ATPase in the gills of rainbow trout

(*Oncorhynchus mykiss*, Lin et al., 1994; Wilson et al., 2000a), tilapia (*Fundulus heteroclitus*, Wilson et al., 2000a) and the mudskipper (*Periophthalmodon schlosseri*, Wilson et al., 2000b). Inhibitors of the H^+-ATPase such as bafilomycin have also been shown to decrease Na^+ influx in tilapia (*Oreochromis mossambicus*) and carp (*Cyprinus carpio*, Fenwick et al., 1999). To date partial gene sequences for fish H^+-ATPase have been published (Perry et al., 2000; Lin et al., 2006) but no gene sequences resembling the mammalian ENaC have been found in any of the fish genomes that have thus far been sequenced (Kumai and Perry, 2011).

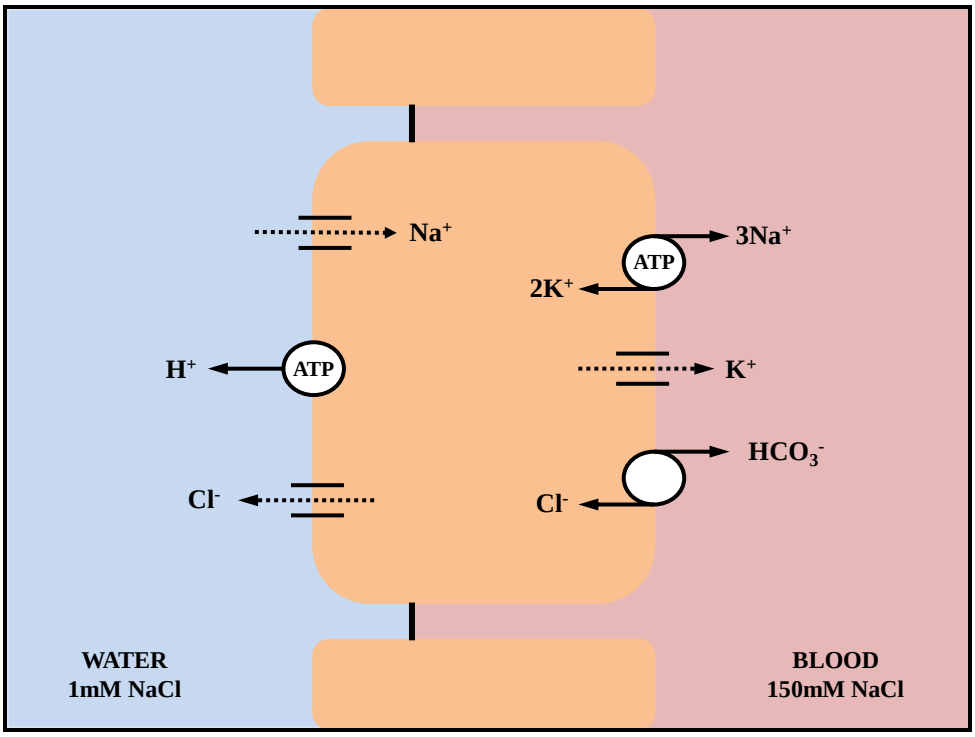

Figure 1.7 The apical H^+-ATPase/ ENaC model in the MRCs of freshwater teleosts. An apical H^+-ATPase pump (HA) creates an electrochemical gradient that drives Na^+ absorption via an epithelial Na^+ channel (ENaC). Passive ion movements are denoted by dashed arrows, active by solid arrows. Figure adapted from Evans et al. (1999).

Given the diversity among teleosts, and the different acclimation responses and survival strategies that have evolved, it is not surprising that all teleosts do not fit one model (McCormick, 2001). It is possible that different species of freshwater teleost fish utilise different mechanisms for Na^+ uptake and the two models reflect species-specific differences. However, only a few species of teleosts have been studied, and with examination of further species rationalisation of the current data may be possible. It is also hoped that the

development of molecular and cellular tools such as gene cloning and expression measurement, and homologous immunohistochemistry techniques may allow further clarification. The development of an accurate mechanism for measuring intracellular ion levels in the cells of fish gills *in situ* would also be of immense benefit in helping to resolve ion transport mechanisms.

1.3 Hormones

Ionic and osmotic homeostasis requires an effective communication system that allows an integrated response in the face of change. The endocrine system works in a signalling capacity to turn environmental, developmental and physiological cues into physiological change. Hormones act as signalling molecules to modulate transport of ions across the gill epithelium through a variety of complex pathways.

1.3.1 Prolactin

Prolactin belongs to a family of structurally- and functionally-related polypeptides that includes growth hormone, placental lactogen, proliferin and somatolactin (Prunet and Auperin, 1995). Prolactin is produced by prolactin cells in the *pars distalis* of the pituitary gland. It initiates its actions by binding to a specific cell surface prolactin receptor (Eyckmans et al., 2010). The prolactin molecule needs to bind with two receptors to produce an active form. The active form is unstable so there is a rapid dissociation to the inactive form (Bole-Feysot et al., 1998).

Prolactin is a pleiotropic hormone, with wide-ranging effects on metabolism, behaviour, reproduction, immunoregulation, and ionic and osmotic regulation (Hirano, 1986; Manzon, 2002). The importance of prolactin in osmoregulation was first shown in freshwater-adapted killifish (*Fundulus heteroclitus*) whose pituitary glands had been removed. Pickford and Phillips (1959) demonstrated that exogenous prolactin was necessary for survival of these hypophysectomised killifish in hypo-osmotic environments. Subsequent research led to prolactin being labelled as “the” freshwater-adapting hormone (Utida et al., 1972). The main

function of prolactin appears to be the maintenance of ion and water permeability in the epithelia of osmoregulatory organs such as the gill, intestine, kidney and bladder in freshwater-acclimated fish (Hazon and Balment, 1998). Treatment with exogenous prolactin increases the ion uptake capacity by altering the morphology of MRCs to an ion absorbing phenotype and by inhibiting the development of seawater MRCs (Herndon et al., 1991; Pisam et al., 1993).

1.3.2 Cortisol

The production of cortisol is under the control of the hypothalamus-pituitary-interrenal axis (Mommsen et al., 1999). Cortisol is produced within the mitochondria of the steroidogenic cells that make up the interrenal gland. It is synthesised from cholesterol via the microsomal enzymatic pathway.

The signalling pathway for cortisol involves the binding and activation of glucocorticoid receptors (GR) within target tissues (Figure 1.8). Glucocorticoid receptors are a nuclear receptor family of ligand-bound transcription factors that bind with cortisol to form a cortisol-GR complex (Prunet et al., 2006). This complex moves into the nucleus and forms a homodimer with another cortisol-GR complex. The cortisol-GR homodimers then bind to a specific DNA region called the glucocorticoid response element (GRE). This leads to the activation or repression of glucocorticoid responsive genes (Prunet et al., 2006). The primary sites of cortisol action are the gills and the intestinal epithelia, with specific receptors having been identified in these tissues (Chakrabotri et al., 1987).

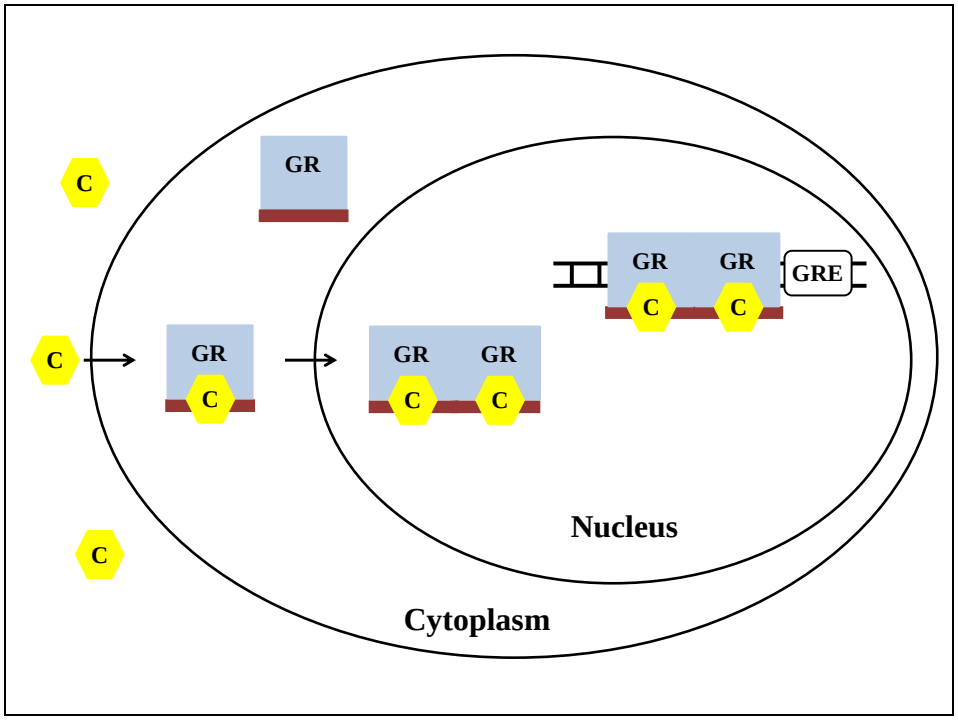

Figure 1.8 Action of cortisol in a target cell. Cortisol (yellow C) enters the cell and binds to a glucocorticoid receptor (GR). The cortisol-GR complex forms a homodimer with another cortisol-GR complex and moves inside the nucleus. Once inside it binds to a glucocorticoid response element (GRE) and leads to the activation or repression of specific genes. Picture adapted from Aluru and Vijayan (2009).

The major functions of cortisol include energy metabolism, ion regulation and the stress response (Hazon and Balment, 1998). In terms of ionic and osmotic regulation, cortisol was traditionally regarded as "the" seawater-adapting hormone due to its effect of enhancing salinity tolerance in seawater-adapted teleosts (McCormick, 2001). This enhanced tolerance is thought to occur via an increase in gill MRC size and density and an increase in NKA activity (Madsen et al., 1995; McCormick, 2001). However, cortisol may play an important role in freshwater as well. For example, freshwater-adapted fish treated with cortisol show an increase in ion uptake and gill MRC surface area (Laurent and Perry, 1990; Mancera et al., 2002). Euryhaline fish transferred from freshwater to seawater, and *vice versa*, show an increase in circulating cortisol, which indicates the importance of this hormone in both freshwater and seawater (Hazon and Balment, 1998).

It has also been suggested that cortisol works in cooperation with prolactin in freshwater to promote ion uptake. In this scenario cortisol maintains ion transporters and prolactin

promotes the development of freshwater MRCs (McCormick, 2001). However, there is, as yet, very little direct evidence for this hypothesis (Sakamoto and McCormick, 2006).

1.3.3 Other hormones

Prolactin and cortisol are not the only hormones known to impact salt and water balance in fish. Growth hormone (GH) and insulin-like growth factor I (IGF-1) have also been shown to have an osmoregulatory role in the teleost gill. GH is a member of the same family as prolactin and has been shown to play a role in osmotic regulation (McCormick, 1995). GH has been shown to increase gill NKA activity and mRNA levels (Madsen et al., 1995; McCormick, 1995) and stimulates the proliferation of MRCs (Sakamoto and McCormick, 2006). IGF-I is a hormone secreted by the liver as a result of stimulation by GH. IGF-1 has a similar effect to GH and has promotes salinity tolerance via an increase in gill NKA activity and by enhancing development of MRCs (McCormick, 1996).

In addition to the independent osmoregulatory roles of GH and IGF-1 they also interact with prolactin and cortisol. Madsen and Bern (1992) showed that prolactin can antagonise the hyper-osmoregulatory actions of GH and IGF-1 by decreasing NKA activity in two salmonids, *Salmo trutta* and *Oncorhynchus kisutch*. GH and cortisol, in contrast, have a synergistic effect when administered together. For example, killifish (*Fundulus heteroclitus*) exhibit higher salinity tolerance with GH and cortisol when compared to either hormone alone (McCormick, 1996). One suggested mechanism of interaction between these two hormones is through the regulation of cortisol receptors, as GH treatment is associated with increased receptor expression in MRCs (Shrimpton and McCormick, 1998).

1.4 Methods for studying branchial ionic and osmotic regulation

The complexity of the intact gill and its regulation has led to the development of techniques and surrogate preparations that have attempted to simplify the gill in order to elucidate the principles of ion regulation. In the 1930s Ancel Keys developed a heart-gill preparation that allowed gill function to be isolated from the rest of the fish (Marshall and Bellamy, 2010). Although a significant advance, this technique did not find favour among other researchers due to the relative inaccessibility of the chemicals and radioisotopes Keys used. In 1961 Bellamy developed a protocol using excised gill arches from eels that were bathed in either freshwater or seawater and the gain or loss of ions could be measured (Bellamy, 1961). This technique allowed several experimental replications to be performed per animal. Shuttleworth (1972) further developed the isolated arch method to include cannulation and perfusion of the arch. The major drawback with this technique was fluctuations in perfusion pressure over time and with exposure to certain hormones. The complexity of the gill also meant that identification of the surface area over which ion fluxes were occurring was impossible to determine. In an effort to remove the issue of complexity, a reductionist approach was taken and flat epithelial preparations were developed. Early attempts used the gill-like epithelia of frog skin and toad bladder epithelia in a membrane chamber which is now known as an Ussing chamber (Marshall and Bellamy, 2010).

In an Ussing system a piece of epithelial tissue is slotted between two voltage sensors and chambers on either side are filled with solutions of known ionic composition. The voltage sensors monitor changes in currents that indicate net ion transport across the epithelium. Movement of radioisotopes across the membrane can also be used to monitor ion transport. The use of the Ussing chamber with skin and bladder epithelium was instrumental in the understanding of active ion transport processes in general, but it was not known how well these principles applied to the fish gill (Marshall and Bellamy, 2010). Another type of epithelia commonly used to study ion transport is the opercular epithelium from the killifish (*Fundulus heteroclitus*). This epithelium lines the operculum and it contains MRCs that are essentially indistinguishable from those in the gill epithelium (Karnaky Jr, 1998). The use of this preparation has been instrumental in establishing many ionoregulatory principles and transporters, such as the basolateral locus of the NKA (Karnaky, Jr. et al., 1976) and the identification of the CFTR channel (Marshall et al., 1995).

The development of primary gill cell culturing techniques in the 1990s (Avella et al., 1994; Pärt and Wood, 1996), led to a resurgence in the use of gill cells for research. Initially cell suspensions were routinely used. However these lack cellular polarity (an important requirement for transporter organisation) and have limited viability, leading to alternative preparations. Wood and Pärt (1997) developed a method in which primary gill cell cultures were grown on permeable supports ('filter inserts'). When gill cells were grown on these inserts, the resulting epithelia had polarity (i.e. apical and basolateral morphologies). This preparation was also advantageous in that it allowed the bathing medium on the apical side of the monolayer culture to be replaced with freshwater in an effort to replicate *in vivo* conditions. However, while a significance advance in that these preparations replicated the passive electrical and flux properties of the intact gill, they proved unable to provide information about active ion transport (Wood and Pärt, 1997). The major drawback of these methods was that the culture consists mainly of PVCs and very few MRCs. This led to the development of double-seeded cultures where a second application of gill cells is applied to a primary culture. This results in a culture containing MRCs, and which more closely resembles a native gill epithelium (Kelly et al., 2000; Kelly and Wood, 2002a, 2002b). These epithelia are amenable to alteration of ion environments on both the apical and basolateral sides and show many physiological and morphological characteristics similar to those of the gill epithelium *in vivo* (Kelly et al., 2000; Kelly and Wood, 2002a, 2002b). However, attempts to stimulate active Na^+ uptake in these preparations have failed to replicate *in vivo* transport rates (Kelly et al., 2000; Wood et al., 2002). Another important aspect lacking in cultured preparations is three-dimensional structure. The gill structure is complex and facilitates cooperation between the cell types that make up the epithelia. These interactions are not present in laminar culture preparations and these may therefore present a false picture of *in vivo* ion regulation. Despite these shortcomings, cell cultures are routinely used in research as they are advantageous in terms of their low cost and labour demands, and from an animal use perspective.

Confocal microscopy may be a technique with significant utility for examining ion transport in the intact fish gill. Confocal microscopy makes use of filters to eliminate out-of-focus light from the focal plane to produce an image with greater resolution and contrast than conventional microscopy. This is advantageous as it allows for clear visualisation of the individual cells that make up the tissue. *Ex vivo* models such as lung tissue from mice and

cornea from rats have been used in conjunction with confocal microscopy to demonstrate the functional interaction of different cell types (Grupcheva et al., 2003; De Proost et al., 2008). Many *in vivo* models have also been developed. These include eye tissue (Petroll et al., 1993), mammalian brain tissue (Svoboda et al., 1997; Trachtenberg et al., 2002), melanoma skin tumours (Chernyavskiy et al., 2009) and kidney tubules (Andrews et al., 1991). A confocal microscopy approach to studying gill ion transport would be highly advantageous in that it would permit real-time visualisation of cellular ion levels in intact gill cells that replicate the *in vivo* condition.

1.5 Fish for studying ion and osmotic regulation

August Krogh, who was one of the earliest proponents of comparative physiology, based much of his work on animals that exhibit extreme physiological characteristics. He argued that these 'extreme' animals were those best studied to ascertain the principles of a given physiological process (Krebs, 1975). This maxim became known as Krogh's Principle. Because fish successfully inhabit a wide range of environments, they are therefore ideally suited as "Krogh" models for research.

As vertebrates, fish share most developmental pathways, physiological mechanisms and organ systems with humans, and so may provide valuable information when human studies are not possible (Cossins and Crawford, 2005). For example, fish models have provided insights into the function of the CFTR chloride channel and its role in cystic fibrosis. Fish genomes are also considered more diverse and 'plastic' than other vertebrates due to frequent genome changes such as gene and chromosome duplications that have occurred (Venkatesh, 2003). This rich source of naturally-occurring genetic variation within and between species, provides an opportunity to investigate biological processes that are adaptively important (Cossins and Crawford, 2005). The low cost of maintenance and rearing of fish in comparison to mammalian, avian, reptilian or amphibian models, as well as their amenability to field and laboratory experiments, also makes them an attractive research model (Bolis et al., 2001).

1.5.1 Salmon

The Salmonidae are a family of ray-finned fish that include salmon and trout. They are native to the Pacific coast of North America and Russia, and have been introduced into waterways around the world. Salmonidae are one of the most extensively studied species having been used as research models into the study of carcinogenesis, toxicology, comparative immunology, disease ecology, physiology and nutrition (Thorgaard et al., 2002). *Oncorhynchus*, *Salmo* and *Salvelinus* genera are commonly used in research and can be sourced both from wild and commercially-farmed populations. There are no native salmonids in New Zealand, with all species currently residing in New Zealand having been introduced (McDowall, 2001). Introduced species include Chinook salmon (*Oncorhynchus tshawytscha*), Sockeye salmon (*Oncorhynchus nerka*), rainbow trout (*Oncorhynchus mykiss*), Atlantic salmon (*Salmo salar*), brown trout (*Salmo trutta*), brook char (*Salvelinus fontinalis*), and mackinaw (*Salvelinus namaycush*).

The Chinook salmon (also known as King salmon) was successfully introduced into the Waitaki River of New Zealand's South island in the early 1900s (McDowall, 2001). They are now found in rivers throughout Canterbury, Otago, Marlborough and the West Coast of the South Island Adults two to five years old return to the river to spawn in April/May (McDowall, 2001). Eggs are laid and fertilised in depressions in gravel streambeds where they develop over the next two months. The eggs hatch into alevins (fry with yolk sacs attached) and then develop into fry (Figure 1.9). The fry gradually make their way downstream over a period of a few months before entering the ocean during summer. While at sea they develop into adults and after a few years will return to rivers to spawn (McDowall, 2001). The ecology, behaviour and physiology of salmonids have been studied extensively (Thorgaard et al., 2002), which makes them an ideal model for comparative studies that also utilise more sparsely studied species.

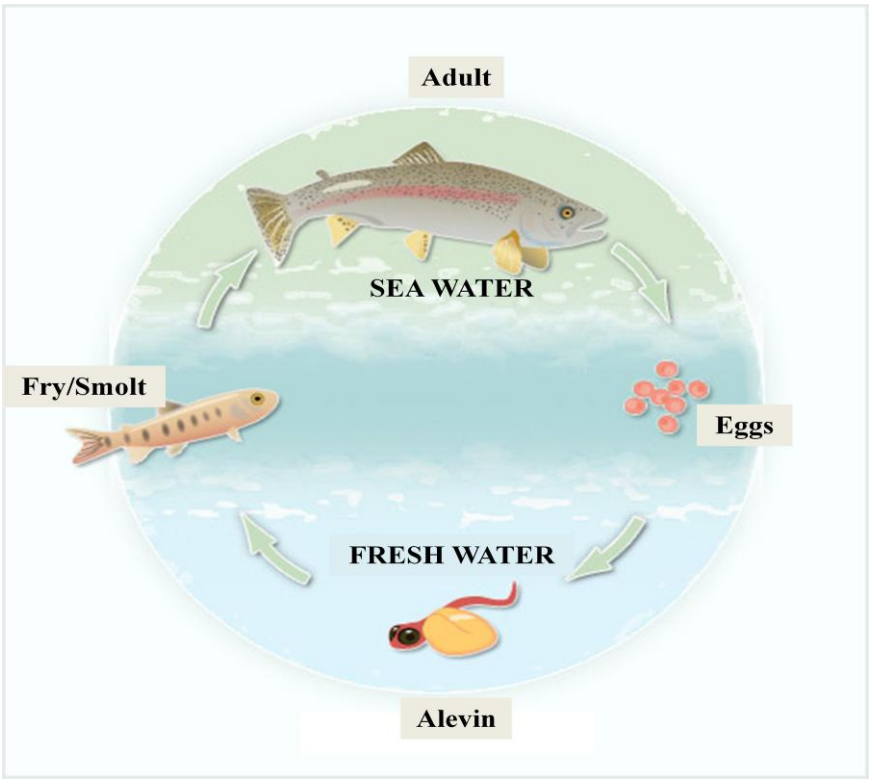

Figure 1.9 Life cycle of the King salmon (*Oncorhynchus tshawytscha)*. Picture modified from Walrond (2009).

1.5.2 Galaxiids

The Galaxiidae are a large family of fish that are found in a wide range of habitats, from subtropical to sub-Antarctic regions, in the Southern hemisphere (Waters et al., 2000; McDowall, 2006a). The widespread distribution of the galaxiids is thought to have been facilitated by the break-up and subsequence drift of Gondwanaland (Burridge et al., 2012), a process that started approximately 180 million years ago (Raven and Axelrod, 1972). This break-up and drift lead to the development of the landmasses now known as Antarctica, Australia, Africa, South America and New Zealand. The Galaxiidae family comprises approximately 50 different species that are characterised by their lack of both adipose fin and scales (Waters et al., 2000). Many species are found throughout New Zealand with fossil evidence suggesting their presence in New Zealand's South Island as early as 20 million years ago (McDowall and Pole, 1997).

Perhaps the most iconic of all galaxiid species, *Galaxias maculatus* (known as inanga in New Zealand) are an amphidromous species found in both freshwater and coastal waters in New Zealand, as well as in Australia, South America and South Africa (McDowall, 2001). Adult inanga lay their eggs on vegetation that lines the banks of near-coastal freshwater streams during high spring tides. When the larvae hatch ~2-4 weeks later, they migrate to sea where they spend the winter developing into juveniles (McDowall et al., 1994; Baker and Hicks, 2003). Once developed, the juveniles, known as whitebait, return to freshwater and develop into breeding adults (Figure 1.10).

Inanga are exposed to different salinities throughout their life cycles, and also face the challenge of daily tidal cycles when they are in, or near, estuarine environments. Inanga are euryhaline and have been shown to be very tolerant to a wide range of salinities (from 0.2 to 60 parts per thousand; ‰) (Chessman and Williams, 1975). The whitebait of *G. maculatus* and other closely-related species are an important component of New Zealand's freshwater fish fauna partly because of their contribution to the whitebait fishery (McDowall, 2001). The decline in whitebait numbers over the years has resulted in the implementation of restricted fishing by New Zealand's Department of Conservation. This decline has been attributed to the overharvesting of the juvenile whitebait stage, habitat destruction including that of spawning areas and loss of waterways, pollution of waterways, and the impact of introduced species (McDowall, 2001).

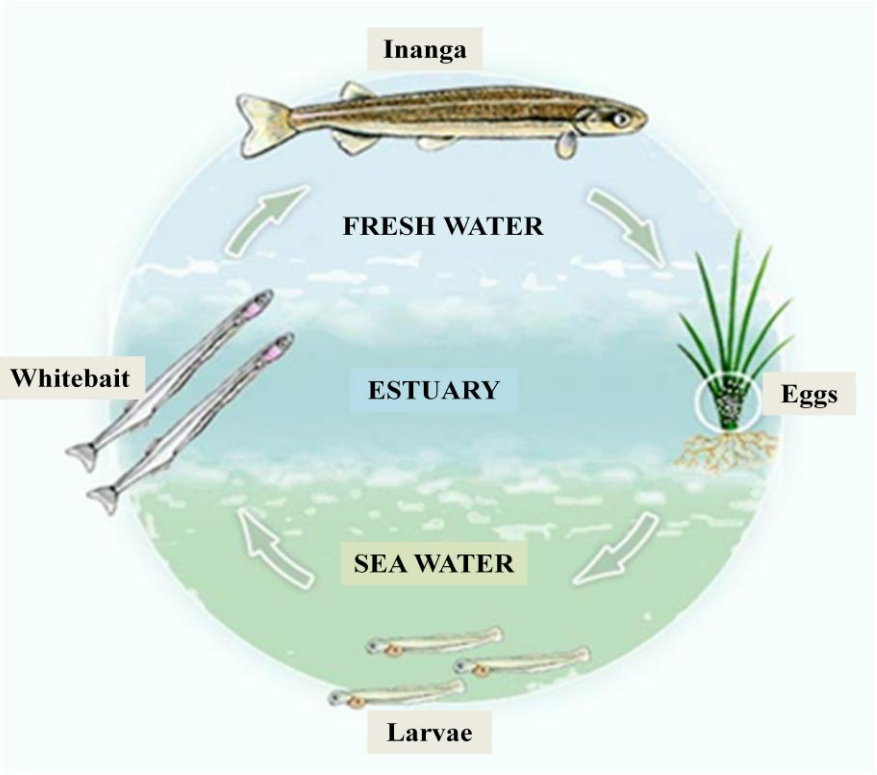

Figure 1.10 The life cycle of inanga (*Galaxias maculatus*). Picture adapted from Walrond (2011).

Species with wide geographic distributions are often exposed to a diversity of environments that impose different selective pressures on life history traits (Waters et al., 2000). The ability of inanga to live in such a wide range of habitats makes them an attractive Krogh research model, especially for investigations into their physiological, cellular and molecular responses to differing salinities.

1.6 Thesis Aims

Euryhaline fish have the remarkable ability to change their gills from an ion-absorbing epithelium in freshwater to the ion-secreting epithelium required for life in seawater (McCormick, 2001). The current knowledge of the exact mechanisms that allow euryhaline fish to successfully acclimate is surprisingly limited (Fiol and Kültz, 2007). The primary aim of this thesis is to examine the physiological, cellular and molecular responses of inanga to changes in salinity. As an amphidromous fish that can inhabit a very diverse range of environments, the inanga is an ideal research model for this study.

The complex structural arrangement of the fish gill allows it to be multifunctional. As there are currently no published reports about inanga gill structure, an important aspect of this research is to characterise the microscopic structure of the inanga gill using scanning electron microscopy (SEM) and laser scanning confocal microscopy (LSCM). For comparison inanga gill will be compared to the widely-studied salmon gill.

NKA is central to ion transport as it not only facilitates the movement of the important ions Na^+ and K^+, but also provides the driving force for other transporters (Hwang and Lee, 2007). Assessment of NKA activity and the possibility of isoform switching in response to salinity changes may offer valuable insights into its roles and regulation. Although NKA isoform switching has been shown in fish previously (e.g. Richards et al., 2003) it is not known how widespread this phenomenon is, and its functional implications are not well understood. In addition, the response of NKA to two important osmoregulatory hormones, cortisol and prolactin will be investigated in an effort to help resolve the role of cortisol and prolactin in ion regulation, and to determine whether these roles are similar in inanga as they are in the better-studied Northern hemisphere fish species.

Many of the specific mechanisms of ion transport are still debated due to differences in species, experimental design, and limitations in methodologies. In an effort to help resolve outstanding controversies in fish ion transport, a new confocal microscopy-based method will be developed to monitor Na^+ ion transport within cells using whole live gill filaments. This approach is advantageous relative to existing transport models as it will allow the observation of cellular ion transport in real time, within a native filament structure.

CHAPTER 2 GENERAL METHODS

All research for this thesis was carried out at the School of Biological Sciences, University of Canterbury, Christchurch, New Zealand. This chapter details various general methods referred to in the thesis. Specific experimental protocols are found within the method section of each chapter.

2.1 Fish Husbandry

Adult freshwater inanga (*Galaxias maculatus*; ~0.5–2 g) were collected by seine net from small coastal streams in Canterbury, New Zealand. Juvenile freshwater King salmon (*Oncorhynchus tshawytscha*; ~4-5 g) were provided by New Zealand King Salmon, Southbridge, Canterbury, New Zealand and Fish & Game New Zealand's Montrose hatchery in Rakaia, South Canterbury, New Zealand. All fish were transported to the School of Biological Sciences aquarium, University of Canterbury, where they were maintained in flow-through freshwater tanks with constant aeration. The water temperature was maintained at ~15°C and a 12 hour light: 12 hour dark photoperiod was observed. The water had a Na^+ concentration in the range of 315 – 330 µM and a pH ranging from 6.8 – 7.2. The fish were held under these conditions for a minimum of 2 weeks prior to the commencement of any procedure. The animals were fed *ad libitum* daily with either commercial pellet food (salmon) or commercial flake food (inanga). All procedures carried out in this thesis were approved by the University of Canterbury Animal Ethics Committee (AEC application numbers 2010-02R and 2011-03R)

2.2 Gradual Salinity Acclimation

Freshwater fish were acclimated to 50% seawater or 100% seawater to permit investigation of morphological, molecular and physiological changes in the gill relating to environmental salinity. Fish were acclimated to the required salinity using a gradual acclimation protocol. Inanga were housed in 60 litre plastic tanks under static water conditions with constant aeration, at a biomass of ~0.67 grams per litre. Salmon were housed similarly, except in 100

litre tanks, at a biomass of ~1 gram per litre. Acclimation to 50% seawater was carried out over a 2 week period with salinity being increased at a rate of 7% per day up until the 50% seawater level was reached. The fish were then held at 50% seawater for at least 1 week prior to use. Acclimation to 100% seawater was carried out over a 4 week period. Fish were first acclimated to 50% seawater, as described above. After the one week hold at 50% seawater, however, fish were then acclimated to 100% seawater by increasing salinity at a rate of 7% per day until 100% seawater was attained. Again the fish were held at this salinity for at least 1 week prior to use.

2.3 Hormone treatments

Acclimated inanga (freshwater, 50% seawater or 100% seawater) were placed into 6 L plastic tanks at a biomass of ~1 gram per litre and left to settle in the holding tanks for 48 hours before commencement of hormonal treatment. Each fish was individually weighed before receiving an intraperitoneal injection of one of the following treatments:

1. **Cortisol 50 µg/g**

   Hydrocortisone 21-hemisuccinate sodium salt (Sigma) was resuspended 1:1 in sunflower oil to a concentration of 50 µg/µL. The cortisol:oil suspension was warmed to 18°C and 10 µL per gram of wet body weight was injected intraperitoneally using a Hamilton syringe, to give a final dose of 50 µg of cortisol per gram of wet body weight.

2. **Prolactin 5 µg/g**

   Ovine prolactin 20-50 IU/mg (Sigma) was resuspended 1:1 in sunflower oil to a concentration of 5 µg/µL. The prolactin:oil suspension was warmed to 18°C and 10 µL per gram of wet body weight was injected intraperitoneally using a Hamilton syringe, to give a final dose of 10 µg of prolactin per gram of wet body weight.

3. **Cortisol 50 µg/g + Prolactin 5 µg/g**

   Hydrocortisone was resuspended 1:1 in sunflower oil to a concentration of 100 µg/µL. Ovine prolactin 20-50 IU/mg was resuspended 1:1 in sunflower oil to a concentration of 10 µg/µL. The two hormone solutions suspensions were then combined at a ratio of 1:1 to produce a final working solution of 50 µg/µL cortisol + 5 µg/µL prolactin. The cortisol/prolactin solution was warmed to 18°C and 10 µL per gram of wet body weight of was injected intraperitoneally using a Hamilton syringe, to give a final dose of 50 µg of cortisol and 5 µg of prolactin per gram of wet body weight.

4. **Sham**

   To account for any changes associated with the injection procedure alone, the sham fish were injected intraperitoneally with warmed (18°C) sunflower oil at a volume of 10 µL per gram of wet body weight.

5. **Control**

   These inanga were held under identical conditions to the groups above. However, no injection was given and the fish were not handled, except for introducing them and removing them from the holding containers.

After injection the inanga were returned to holding tanks and left undisturbed for 24 hours. The dosing procedure was repeated 24 and 48 hours after the initial injection, with each fish receiving a total of three injections. On the fourth day the fish was euthanised and the tissues isolated via dissection as described above.

All hormone doses were chosen to be within the range commonly used in osmoregulatory hormone studies in fish. Previous studies have used cortisol concentrations ranging from 1 to 50 µg/g and prolactin concentrations ranging from 4 to 5 µg/g (Seidelin and Madsen, 1999; Mancera et al., 2002; Kajimura et al., 2003; Sangiao-Alvarellos et al., 2006; McCormick et al., 2008; Breves et al., 2011). A recent study by McCormick et al. (2008) found that a cortisol dose of 50 µg/g per gram of body weight produced statistically significant changes in NKA activity and isoform mRNA expression in Atlantic salmon whereas a lower

concentration of 10 µg/g did not induce any significant changes. For this reason the higher cortisol dose was chosen as the dose for this study. A dose of 5 µg/g prolactin was chosen in accordance with previous literature. Ovine prolactin and the synthetic cortisol (hydrocortisone 21-hemisuccinate sodium salt) are the most commonly used forms of prolactin and cortisol in fish studies due to the inaccessibility of teleost-derived prolactin and cortisol. Ovine prolactin has been shown to be an almost universal ligand of prolactin receptors in vertebrates (Prunet and Auperin, 1995).

The dosing protocol (three doses spaced 24 h apart) was determined by a survey of the literature, which shows that multiple doses are often required to engender effects (Mancera et al., 2002; McCormick et al., 2008). A pilot study was conducted to determine the tolerance of inanga to multiple injections. This found that inanga health was compromised by protocols that involved more than three injections (data not shown).

2.4 Dissection of Gill Tissue

2.4.1 NKA Activity

Fish were euthanised by severing the spinal cord, and the gills from each side of the head were removed and placed into labelled 2.5 mL tubes. The tubes were immediately immersed in liquid nitrogen to rapidly preserve the samples, and were then stored at -80°C until use.

2.4.2 NKA Isoform Assessment

Gill dissections for molecular work were conducted under RNase-free conditions. Ribonuclease enzymes (RNases) degrade mRNA, the template for molecular reactions. Dissection equipment and consumables were all autoclaved and treated with RNase Zap® (Invitrogen) before use. Following spinal cord transection, gills from each side of the head were removed and placed into labelled 2.5 mL tubes. The tubes were immediately immersed in liquid nitrogen and stored at -80°C until use.

2.4.3 Confocal Microscopy

For whole filament analysis, the gill arches were excised and placed into a sample of the experimental water with salinity identical to that which the fish were acclimated to. The mucus surrounding the gills was left intact to act as a protective barrier and ensure prolonged survival of the filament post-dissection. Before use, each arch was carefully blotted with tissue paper to remove the mucus and then loaded with the appropriate dye (see section 3.2.3). While gill cells were shown to be viable up to 245 minutes post-dissection (see section 6.3.1), every attempt was made to use the tissue as soon after dissection as possible to minimise cell deterioration.

2.4.4 Scanning Electron Microscopy (SEM)

For SEM analysis gills from inanga and salmon were excised similarly to those described above (section 2.4.1). The arches were separated and carefully blotted with tissue paper to remove the adhering mucus. The gill arches were then place in 1% (w/v) N-acetyl cysteine (NAC) in phosphate buffered saline (PBS: 137 mM NaCl, 8.1 mM Na_2HPO_4, 1.47 mM KH_2PO_4 and 2.68 mM KCl; pH 7.7) for 10 minutes to remove excess mucus. NAC is a widely used mucolytic drug that reduces the viscosity of mucus by rupturing the disulfide bridges of the high molecular weight glycoproteins present in the mucus (Rochat et al., 2004). The arches were then removed from the NAC solution and blotted to remove mucus. The NAC wash was repeated another two times before the gills were placed in PBS and processed for SEM immediately.

2.5 Confocal Microscopy

2.5.1 Technique overview

Confocal microscopy is a technique that produces high resolution and high contrast images (Dailey et al., 2006). This therefore permits visualisation of individual cells within a tissue without having to fix the cells. In confocal microscopy, light is emitted by a laser unit (excitation source) and passes through a pinhole aperture, before it is reflected off a dichroic mirror and scanned across the specimen (Figure 2.1). Fluorescence from the specimen's focal point passes back through the dichroic mirror, towards the detector pinhole aperture where light from the focal point is able to pass through to the photomultiplier tube (PMT) detector. The PMT detects the light and then, using an image processor, converts it into an image of the specimen. Fluorescence from other focal planes is also emitted from the specimen but this out-of-focus light cannot pass through the detector pinhole aperture. Therefore the resulting image is primarily composed of in-focus light and produces an image with superior resolution and contrast compared to other microscopic techniques (Smith, 2011).

In LSCM, an image is generated by scanning the excitation beam across the specimen (Pawley, 2006). The light is moved across the specimen in the *x* and *y* dimensions, either by movement of the stage or movement of the beam of light with mirrors. LSCM can also collect information from the *z* plane to acquire optical sections, which can then be collated and processed with *x* and *y* plane images to form a three-dimensional image (Pawley, 2006).

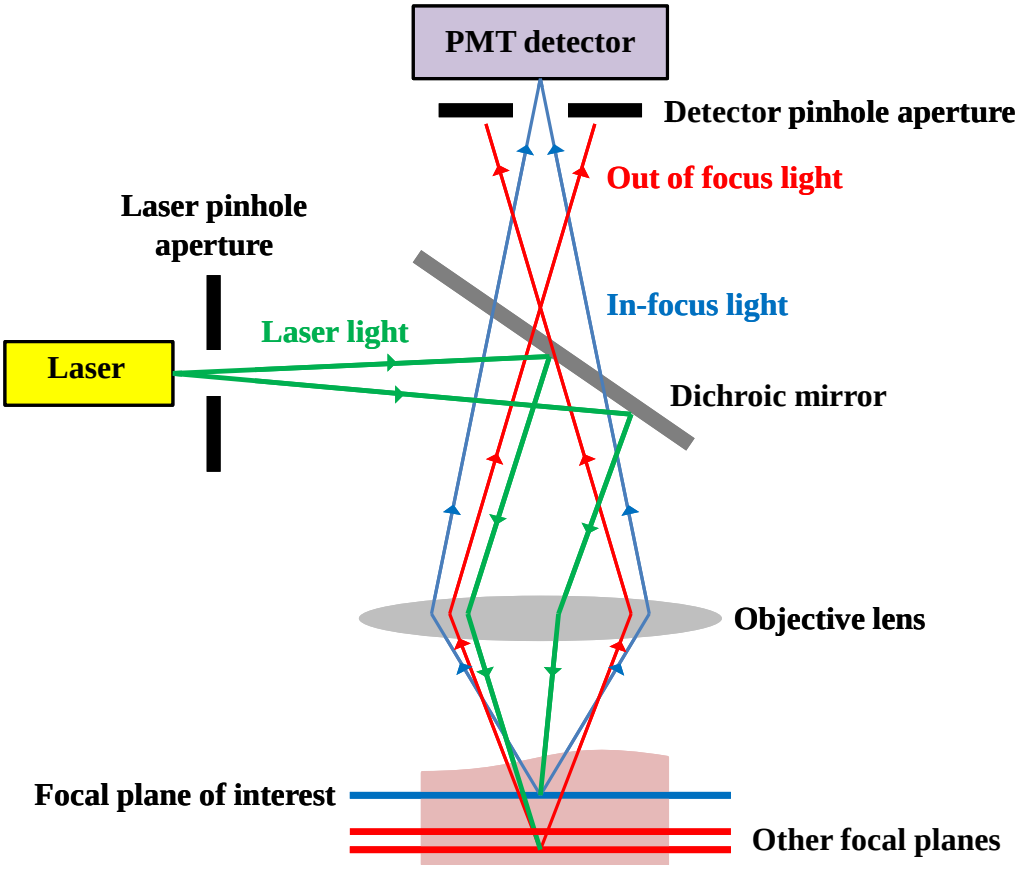

Figure 2.1 The basic operation of the confocal microscope. Figure adapted from Paddock et al. (2012).

For a specimen to be visualised using LSCM, it must first be stained with a fluorescent dye. The choice of fluorescent dyes is dependent on the lasers and detectors the microscope is fitted with, the type of specimen, and the cellular structures that are to be visualised (Albrecht and Oliver, 2011; Smith, 2011). Fluorescent dyes are available in forms such as simple salts, dextran conjugates, or as acetoxymethyl (AM) forms. AM dyes are membrane permeable and freely diffuse across cell membranes when placed into the extracellular environment adjacent to the cell. Once inside the cell, enzymes called esterases cleave off the acetate moieties to convert the dye into an active form. AM dyes are commonly used when working with live cells as they are less toxic than other dye forms (Takahashi et al., 1999; Paredes et al., 2008). As certain dyes are excited by specific lasers, the choice of a dye will also depend on the lasers available.

2.5.2 Confocal Microscope and Consumables

Confocal imaging was conducted on an inverted confocal microscope (Leica model SP5, Wetzlar, Germany) located in the School of Biological Sciences, University of Canterbury, Christchurch, New Zealand. Dyes were sourced from Invitrogen New Zealand and Sigma-Aldrich New Zealand.

2.5.3 Visualisation

For specific information such as dye name, loading concentration, loading time and confocal settings please refer to the methods and material section in the relevant chapter. In general, however, dyes were freshly diluted to the appropriate concentration just before use owing to the deterioration of reconstituted dyes with time (Reynolds, 2001). Inanga and salmon gill tissue were loaded with the dye of choice before being rinsed in distilled water. The specimen was then placed on a FluoroDish cell culture dish (World Precision Instruments) and covered with a 32 mm x 0.015 mm glass coverslip (to help immobilise the tissue and prevent desiccation), and positioned in the confocal microscope.

Using a HCX PL APO 20.0 x 0.70 glycerol immersion lens, the specimen was first visualised and aligned using bright-field microscopy. Bright-field microscopy uses transmitted light to illuminate the tissue and allows visualisation without excessive exposure to the laser light. Lengthy exposure of tissues and dyes to laser light can cause damage and photobleaching (Reynolds, 2001). Once the tissue was in the centre of the field of view, and in focus, the tissue was examined at a higher magnification using a HCX PL APO 63.0 x 1.30 glycerol immersion lens and the appropriate laser. Once the cell or cellular structure of interest was identified, a fluorescent image and a transmitted light image were collected. Images were collected in a 512 pixels x 512 pixels format with 8-bit resolution and averaged twice (via software-selected repeated line scan mode) to improve the signal-to-noise ratio. For time series images one frame was collected every 30 seconds for 5 minutes to produce a total of 31 frames. Because the cells were not adhered to the FluoroDish, cell movement sometimes occurred. In an effort to keep the cells in the same focal plane, the focus was manually adjusted throughout the time series to account for any movement. Focal planes were

determined in the transmitted light image using the nuclear membrane as the reference point. The use of a visual reference point allowed for correction of any cell movement by adjusting the focal plane, thus ensuring consistency.

2.5.4 Image processing and analysis

CoroNa Green, a fluorescent Na^+ indicator dye was used in this study. It exhibits large changes in fluorescence upon binding with Na^+ and can therefore be used to monitor changes in intracellular Na^+ (Johnson and Spence, 2010). To measure and quantify Na^+ changes the fluorescence of individual cells was observed and recorded, with images analysed using Leica Microsystems LAS AF Lite software. As MRCs are thought to be the primary site of active ion regulation (Evans, 1998), these cells were selected for analysis. Identification of MRCs was based on size, location within the lamellar epithelium, and staining patterns (see section 3.3.2). A region of interest (ROI) was selected around, and incorporating, the cell of interest using the software tools (Figure 2.2). As the entire cell may not fluoresce, the transmitted light image was used as a guide to ensure the ROI was correctly placed around the entire cell in the fluorescent image. The Leica software assesses the ROI and evaluates each pixel in the image, giving it an intensity of fluorescence score, based on an arbitrary scale of 1 to 255. A value of 1 denotes the weakest intensity, while 255 is the strongest intensity. The software calculates a variety of statistics including the minimum, maximum and average fluorescence intensity within the cell of interest. The average fluorescence intensity of each cell was used in subsequent calculations to determine the changes in Na^+ concentration (see section 6.2.6).

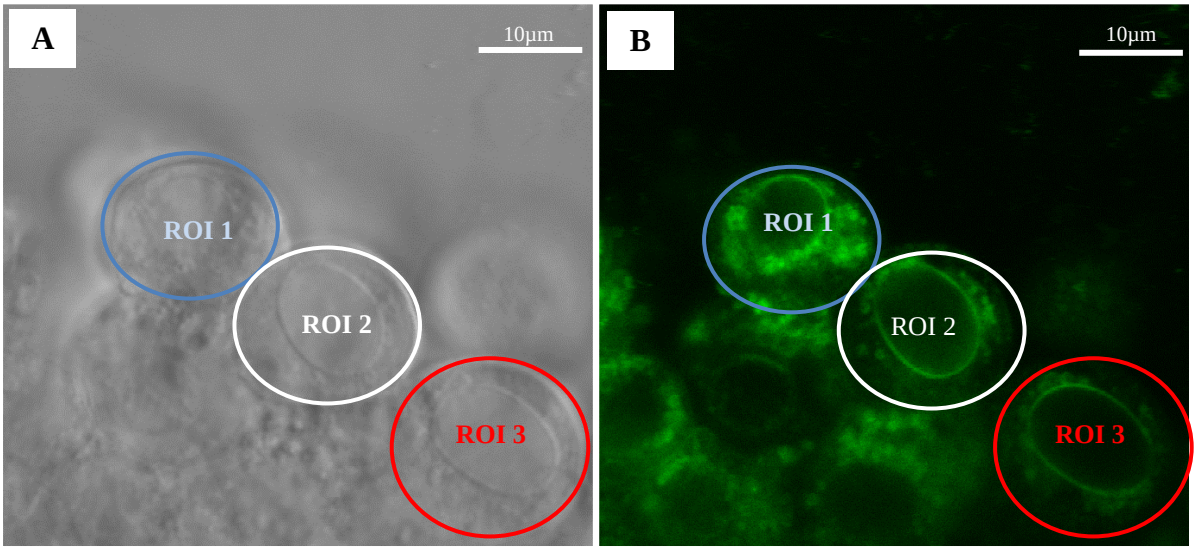

Figure 2.2 Example of region of interest (ROI) selection. Using Leica Microsystems LAS AF- LAS AF Lite software, ROIs were drawn. The ROI is first positioned on the transmitted light image (A) to ensure the entire cell is included. The software automatically aligns the corresponding ROI on the fluorescent light image (B).

2.5.5 Correction for autofluorescence

All unstained tissues show some level of autofluorescence due to natural peptides present within the tissue (Albrecht and Oliver, 2011). If the autofluorescence is small compared to the fluorescent contribution from the dye, then it can be disregarded. Otherwise levels of autofluorescence must be accounted for. At the start of all experiments the autofluorescence levels of unloaded cells were measured under similar experimental conditions and microscope settings as for the dye-loaded cells. This background fluorescence was then subtracted from all data measurements to correct for the autofluorescence.

2.6 SEM

2.6.1 Technique overview

Scanning electron microscopy (SEM) is a technique that uses electrons instead of light to produce high-resolution images of the surface structure of a solid specimen (Goldstein et al., 2003). In a vacuum column, an electron beam is produced by an electron gun and is directed down towards the specimen by a condenser (Figure 2.3). The beam then passes through a series of magnetic lenses and into a scan coil that moves the beam of electrons back and forth across the specimen. The primary electrons hit the sample and interact with atoms on the samples surface causing the emission of secondary and back-scatter (reflected) electrons. Detectors collect the signal from these electrons as the beam is scanned across the samples surface. The signal is then amplified by a PMT and sent to an image processor. The processor synchronises the position of the beam and the intensity of the signal to produce an image of the scanned surface of the sample.

There are four steps to producing a good quality SEM image: fixation, drying, coating and imaging (Goldstein et al., 2003). These are discussed below.

2.6.2 Fixation

Following their removal, arches were placed immediately in 5% glutaraldehyde/PBS for 24 hours to fix. Fixation stabilises and preserves the structure of the tissue so it remains as close to the living state as possible. It was therefore important that the gill arches were fixed immediately after dissection to ensure they did not degrade.

2.6.3 Critical Point Drying

Critical point drying is a procedure in which all of the liquid is removed from the tissue in a precise and controlled way to ensure the tissue structure is preserved (Goldstein et al., 2003). This is achieved by forcing the liquid to its critical point, that is, the temperature and pressure where the liquid will change from a liquid phase to a gas phase without boiling or evaporating. Boiling and evaporation are detrimental to the cell as changes to the surface tension of the liquid during these processes can break apart delicate structures within the cells, thus distorting morphology. At a liquid's critical point there is no surface tension so it

can leave the tissue without any morphological change (Martill and Harper, 1990). Because water has a very high critical point (375°C at 3212 pounds per square inch (psi)), it is replaced with a transient fluid, carbon dioxide, which has a more practical critical point (35°C at 1200 psi) (Chandler and Roberson, 2009).

After fixation gill arches were removed from the 5% glutaraldehyde/PBS solution, blotted with tissue paper, and then placed into increasing concentrations of ethanol (25%, 50%, 75%, 90% and 100%; 1 hour per concentration) to dehydrate the tissue. Gill arches were then placed in a fresh solution of 100% ethanol for 24 hours before being desiccated in the critical point drier.

2.6.4 Coating

Once dry, gill arches were mounted onto a metal stub using carbon adhesives. The arches were mounted in a variety of different orientations so they could be examined from multiple points of view. Gills were then coated in a very thin layer of gold for one minute at 1.2kV and 20mA, to give a coat thickness of approximately 100 Angstroms. This sputter-coating electrically grounds the specimen to prevent an accumulation of electrostatic charge that would degrade the image (Bozzola and Russell, 1999).

2.6.5 SEM Imaging

Inanga and salmon gill filaments were visualised using a Leica S440 scanning electron microscope. Images were exported as TIFF files and imported into PhotoShop CS5 (Adobe) where only minimal processing, such as adjustment of colours or contrast, was performed.

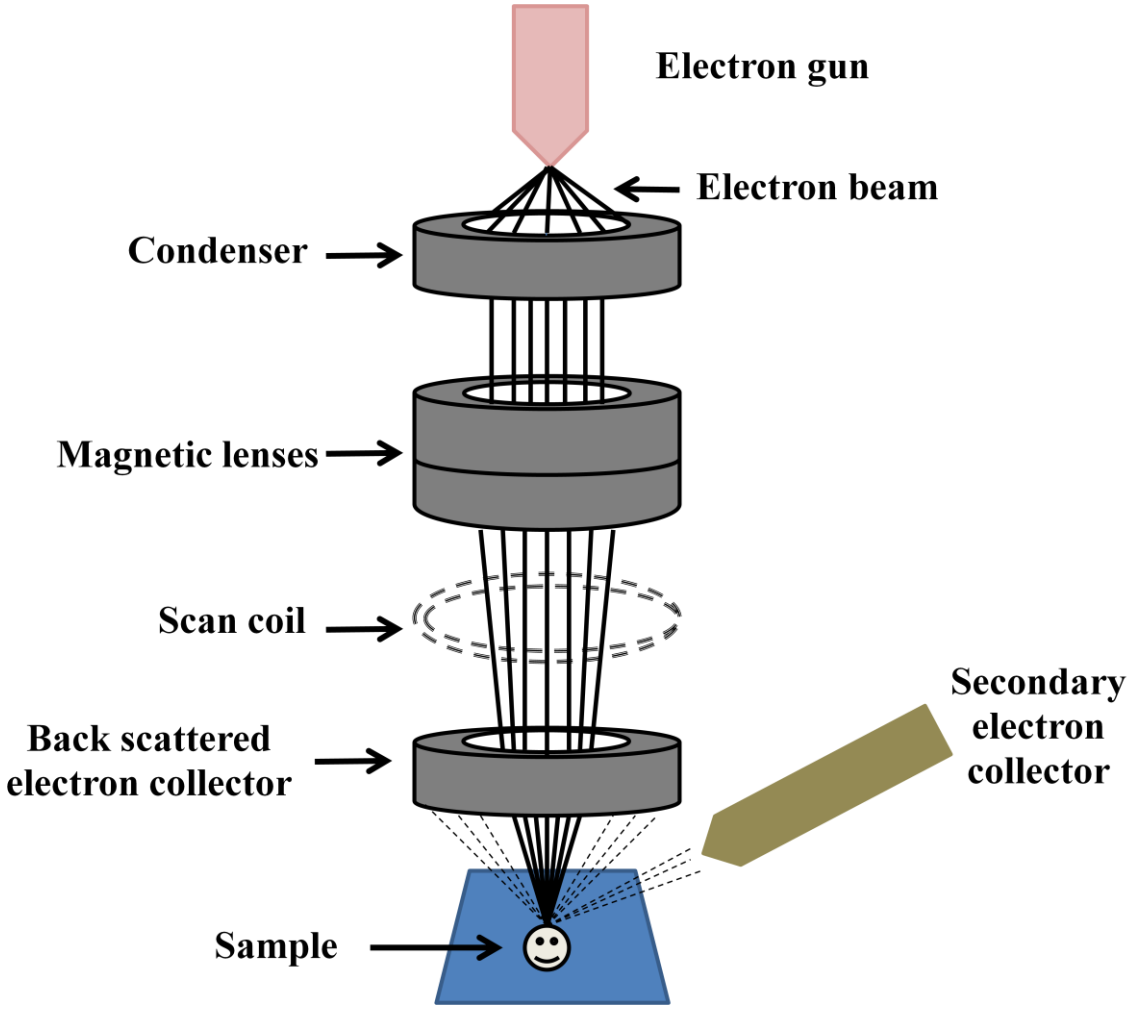

Figure 2.3 The basic operation of a scanning electron microscope (SEM). Figure adapted from Goldstein et al. (2003).

2.7 Flame photometry

Actual sodium concentrations of solutions were measured using a flame photometry (Sherwood Instruments). A standard curve was first established using standards of known concentrations before each sample was analysed in triplicate.

CHAPTER 3 GILL STRUCTURE AND MORPHOLOGY

3.1 Introduction

3.1.1 General structure

The complex structural arrangement of the fish gill facilitates its multiple functions (Evans et al., 2005). Each teleost gill is made up of four branchial arches that are lined with multiple filaments and are further partitioned into many lamellae. The filaments and lamellae create a very large surface area with a relatively small diffusion distance between the blood and the environment allowing maximum exchange between the animal and the environment, and *vice versa* (Evans et al., 1999).

The gill epithelium lining the filaments and lamellae are made up of three main cell types; PVCs, MRCs and ACs. These were detailed in Chapter 1, but are briefly reintroduced here. Around 90% of the gill epithelium is composed of PVCs, which are thought to be the main loci of gas exchange (Evans et al., 1999). MRCs are typically smaller than PVCs and comprise only ~10% of the gill cell population. MRC's are considered to be the primary site of active ion regulation in the gills (Evans et al., 1999). Structurally they are well suited to an ionoregulatory function with abundant mitochondria and basolateral infoldings that enhance surface area and provide microenvironments for generation of local electrochemical gradients. ACs, as their name implies, are thought to perform an accessory role in ion transport (Wilson and Laurent, 2002).

While the overall gross structure and cellular components of the gill are conserved among teleosts, there is considerable interspecies variation with respect to apical membrane surface morphology (Perry, 1997). MRC numbers, their arrangement and size can also vary greatly between different fish species. The reason for this variation is not clear (Perry, 1997).

3.1.2 Salinity-related changes

Euryhaline fish such as salmon and inanga regularly experience waters of distinct salinity. This may be as part of a life cycle migration, or due to inhabiting near-coastal waters that are

subjected to tidal-based variations in ionic composition. In order to maintain ionic and osmotic homeostasis during salinity changes, a euryhaline fish must be able to reorganise both the structure and function of their gills, from the ion-absorbing epithelium present in freshwater to one that secretes ions in seawater.

A number of morphological changes in the gill have been reported in response to salinity change. On transfer of freshwater-acclimated fish to seawater, a proliferation of MRCs is often seen (Laurent and Dunel, 1980; Laurent et al., 1985; Perry and Walsh, 1989; Uchida et al., 1996). This may result in a thickening of the lamellar epithelium (Wilson and Laurent, 2002). The increase in MRCs is often accompanied by an increase in NKA activity, suggesting an increase in ion regulatory capacity in seawater (McCormick et al., 2003). However in some species, such as killifish (*Fundulus heteroclitus*), no change in NKA activity is observed between freshwater and seawater-acclimated fish, suggesting that NKA activity stimulation is not a universal trait of euryhaline fish (Katoh et al., 2001). However, while there is no change in NKA activity morphological changes are evident in killifish gill, with the transformation of seawater-type MRCs to freshwater type MRCs upon freshwater exposure (Katoh and Kaneko, 2003).

3.1.3 Microscopy Techniques

SEM and transmission electron microscopy (TEM) have long been used to investigate the structure of the gill (Evans et al., 2005). SEM provides a detailed image of the surface structure of the gill arch whereas TEM allows the internal structure to be examined. SEM and TEM are advantageous over conventional light microscopy as they have a higher magnification and resolution that can provide a more detailed image (Goldstein et al., 2003). However, both techniques require fixation of the tissue prior to use and subsequently cannot image live cells. While chemical fixation methods have been shown to be more successful than temperature fixation (heat or freezing; Chandler and Roberson, 2009), chemical fixation does have its drawbacks. Membrane distortion and fusion, and loss of soluble cellular components have been reported as possible complications induced by chemical fixation methods (Chandler and Roberson, 2009).

Confocal microscopy offers many advantages over SEM and TEM. Confocal microscopy can be used in conjunction with fluorescent dyes, probes and antibodies to localise and visualise cellular and subcellular structures. Optical sectioning allows various layers within the tissues to be examined, without destroying the tissue. While fixed specimens can be also be visualised by confocal microscopy, the significant advantage of this technique is that it can be used to examine live cells and their cellular processes in real time (Dailey et al., 2006). Early work by Cornell-Bell et al. (1990) demonstrating the presence of calcium waves in astroglia and O'Rourke and Fraser (1990) showing neuronal axons in developing tadpoles, highlighted the vast potential of confocal microscopy. Since these pioneering studies, confocal microscopy has become an increasing popular method of studying a wide range of biological processes in a diverse array of tissue types (Dailey et al., 2006).

3.2 Chapter Aims

The basic structure of the gill was outlined nearly 60 years ago (Evans et al., 2005) and since then the gills of a number of species, including salmon have been widely characterised (Pisam et al., 1988; Evans et al., 1999; Evans et al., 2005). In contrast, the inanga, which exhibits similar physiological characteristics to salmon, and which has the potential to be a valuable model species, has not been studied. There are currently no published reports on the inanga gill structure. Therefore the aim of this chapter is to characterise the microscopic structure of the inanga gill using scanning electron microscopy (SEM) and laser scanning confocal microscopy (LSCM), and to compare to it the widely-studied salmon gill.

3.3 Methods

3.3.1 Fish

Inanga (~0.5 – 2g) and salmon (~4 – 5g) were acclimated to freshwater, 50% seawater and 100% seawater as previously described (section 2.2).

3.3.2 SEM

Gill tissue from inanga and salmon were prepared as previously described (section 2.4.4) and visualised following the protocol in section 2.6.5).

3.3.3 LSCM

Gill tissue from inanga and salmon was prepared as previously described (section 2.4.3). The gills were visualised following the protocol outlined in section 2.5.3 with a few modifications (see below).

Different tissues can respond differently to dyes (Johnson and Spence, 2010) so it is important that each dye is tested thoroughly in the tissue of choice. Incubation times and dye concentrations were experimentally determined in freshwater inanga and salmon to ensure optimal visualisation of cellular structures. Information on the fluorescent dyes used is found in Table 3. 1. Fresh gill tissue was exposed to each dye separately and cellular structures were identified and images recorded. When the labelling of more than one cellular structure at a time was required in an image, dyes were evaluated for any possible negative interactions such as decreased fluorescence or abnormal staining patterns.

When more than one dye was used in an image, sequential multiple channel fluorescence scanning was used to avoid and/or reduce crosstalk of fluorescence signals. Crosstalk can occur when the excitation and/or emission of more than one dye overlaps, making it difficult to isolate the activity of each individual dye (VandeVen et al., 2010). With sequential scanning only one laser line is active at a time. This ensures only one dye is excited, allowing its fluorescence to be collected before the laser is switched and excitation of the second dye occurs. The Leica software then collects the information from each scan and compiles this data.

Table 3.1 Properties of dyes used for LSCM

Fluorescent Dye	**Cell structure**	**Laser**	**Emission band width (nm)**	**Working Concentration (µM)**	**Incubation Time (minutes)**	**Source**
9-anthroyl ouabain	NKA	405	410-510	2	60	Invitrogen
CoroNa Green	Intracellular Na^+	488	500-580	5	10	Invitrogen
3,3'-dihexyloxacarbocyanine iodide ($DiOC_6$)	Endoplasmic reticulum (ER), mitochondria & vesicles	488	500-550	10	10	Sigma-Aldrich
LysoTracker Red DND-99	Acidic organelles (e.g. lysosomes)	561	580-620	0.5	10	Invitrogen
MitoTracker Orange	Mitochondria	561	571-671	0.5	10	Invitrogen
Propidium iodide	Nucleus	561	599-700	10	10	Sigma-Aldrich

3.4 Results

3.4.1 SEM

SEM examination of inanga gills showed that they have a similar gill structure to salmon and other teleosts (Figure 3.1 and 3.2). Salmon and inanga have four arches on each side of the head and each arch is lined with filaments. Filament size was proportional to fish size, with salmon having longer filaments than the smaller inanga (data not shown). The lamellae are evenly spaced across the filaments creating a large surface area across which water can flow (Figure 3.2 A). Recessed cells formed apical crypts or pores that can be seen on the surface of the lamellae (Figure 3.2 A and B). On average inanga lamella had twice as many apical pores (8 apical pores per 100 μm^2) as salmon (4 per 100 μm^2).

The lamellae of the seawater-acclimated inanga and salmon had a different appearance from those of freshwater-acclimated fish (Figures 3.3 and 3.4). The cells were raised and pronounced and the lamellar thickness was more than double that of a freshwater-acclimated equivalent (4 µm versus 10 µm in inanga). The recessed cells were not evident in the seawater-acclimated inanga or salmon. On closer inspection microplicae on the apical surface of some cells could also be seen in seawater-acclimated salmon and inanga (Figures 3.3B and 3.4B). Cells with microplicae were not specifically localised to a particular region of the lamella in both species, although such cells appeared to be more abundant in salmon.

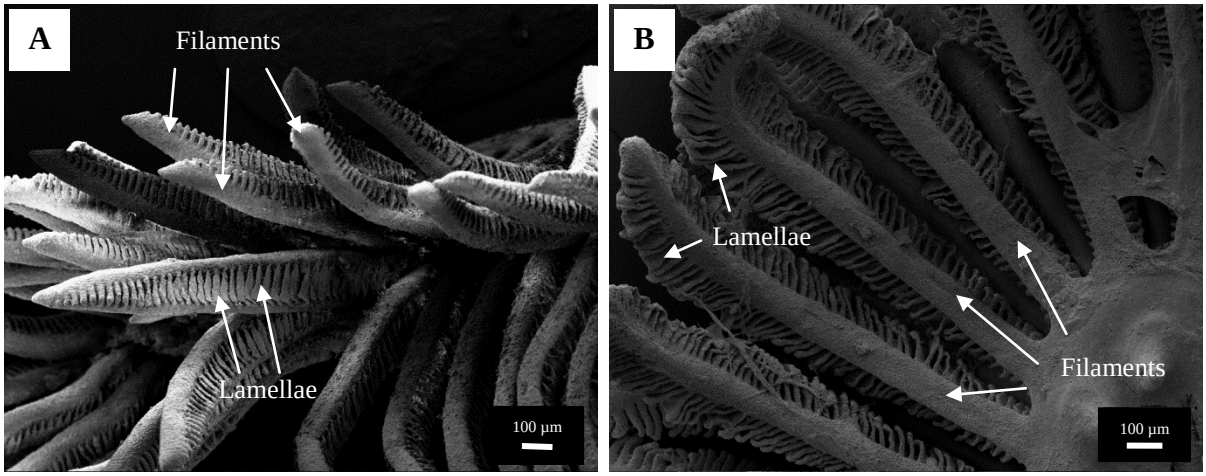

Figure 3.1 SEM images of freshwater-acclimated salmon (A) and inanga (B) gill filaments. The gill filaments are lined with regularly spaced lamella as indicated by the arrows. Scale bars = 100 µm.

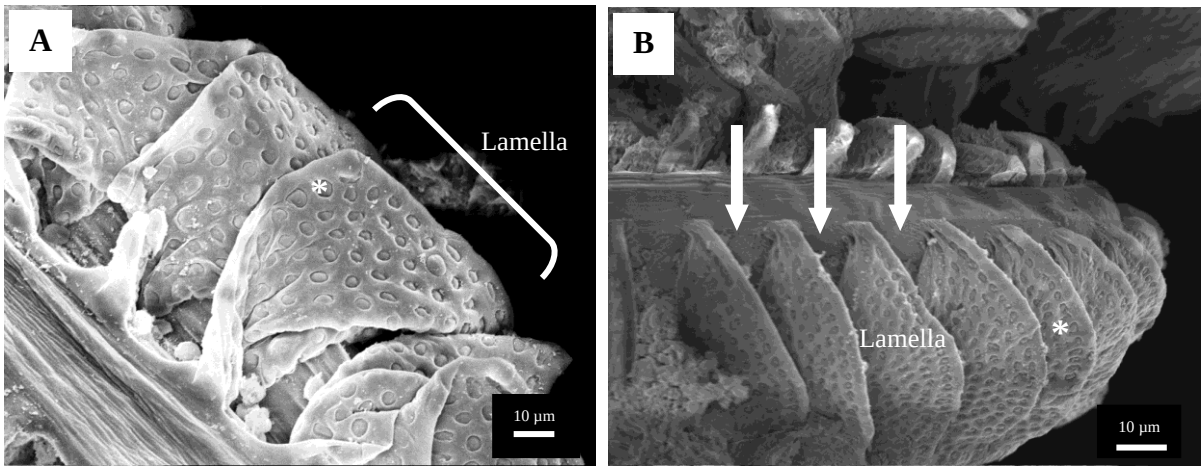

Figure 3.2 SEM images of freshwater-acclimated salmon (A) and inanga (B) lamellae. The lamellae are covered in an epithelium made up of PVCs, MRCs and ACs. Apical crypts or pores (*) are formed by recessed cells. Arrows represent the spaces where water perfuses between the lamella. Scale bars = 10 µm.

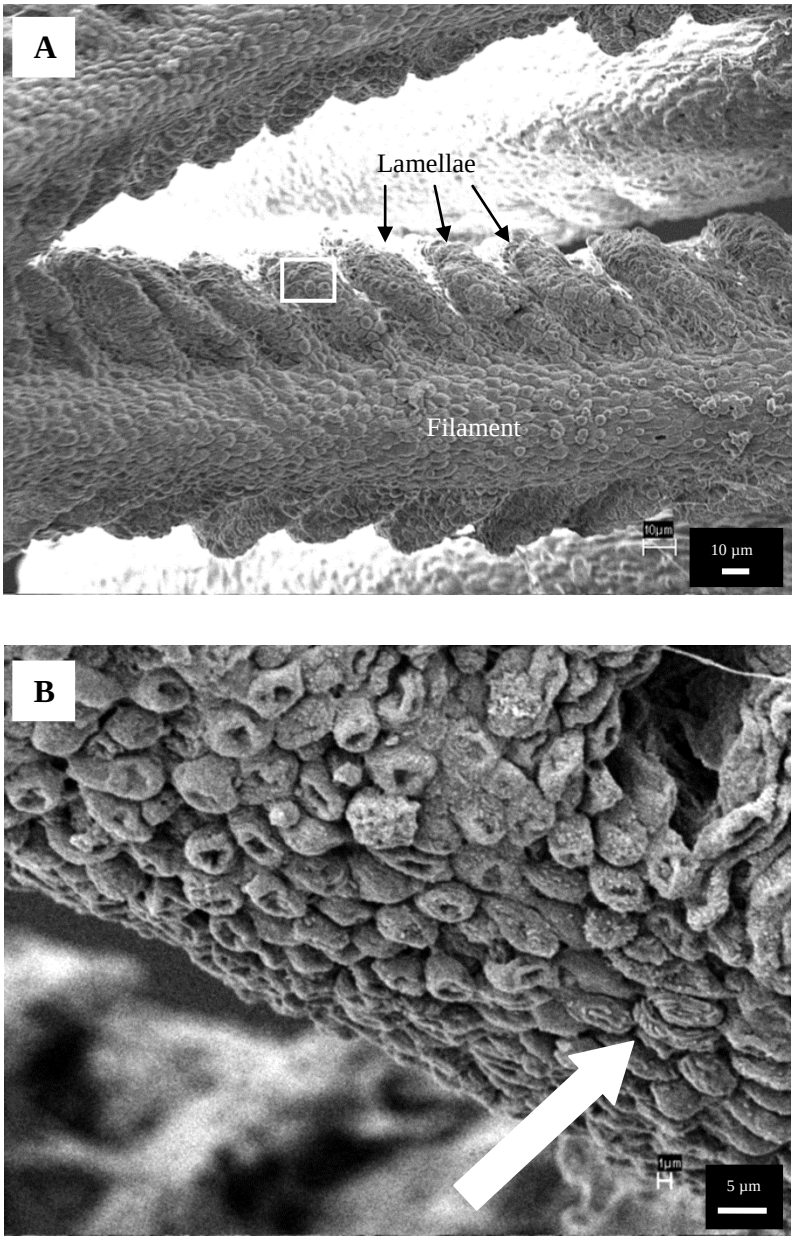

Figure 3.3 SEM images of a seawater-acclimated inanga gill. The cells lining the filament and lamella are more raised and pronounced than the freshwater equivalent (A). Upon higher magnification of the selected region (white box in A), microplicae (arrow) on the apical surface of some cells lining the lamella can be seen (B).

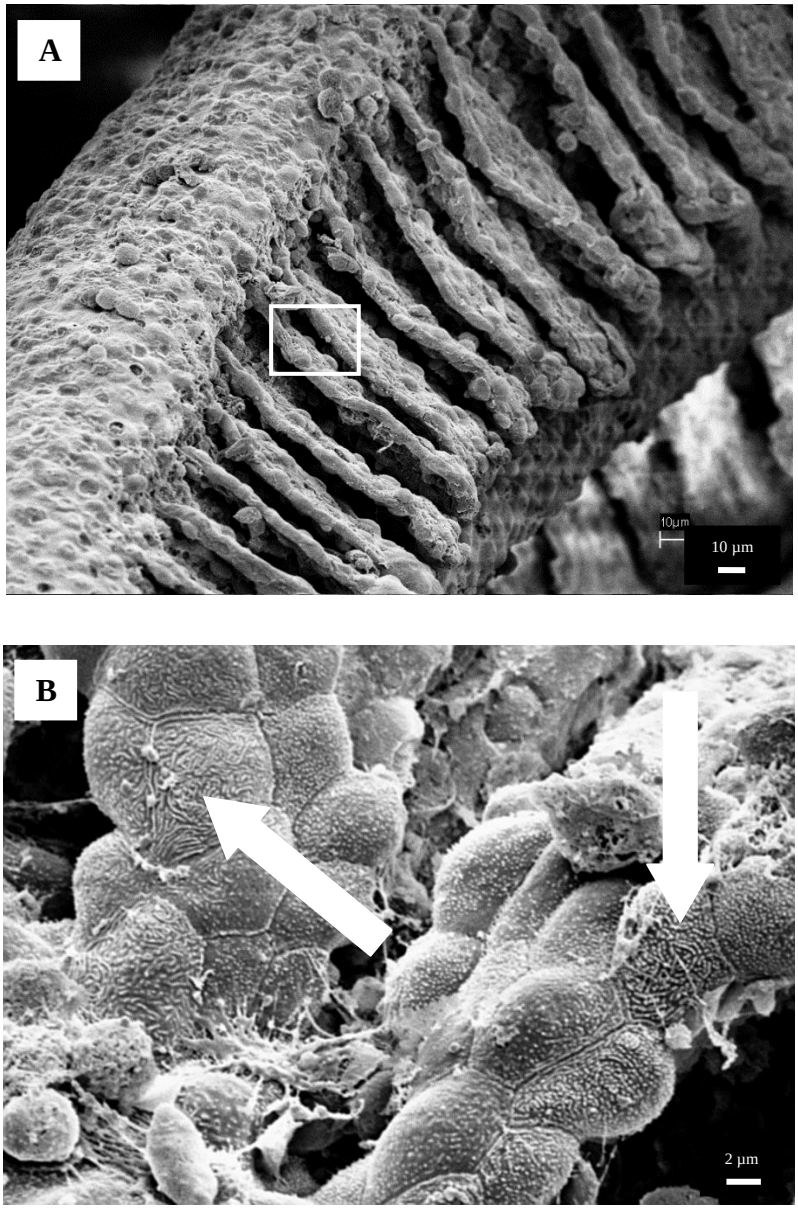

Figure 3.4 SEM images of a seawater-acclimated salmon gill. The filamental and lamella are more raised and pronounced in appearance compared to the freshwater acclimated salmon (A). Higher magnification of the selected region (white box A) shows the presence of microplicae (arrows) on the apical surface of the cells lining the lamella can be seen (B).

3.4.2 LSCM

CoroNa Green and MitoTracker Red rely on the presence of intracellular esterases present in living cells to convert the dye into its active form. As these dyes can therefore only be visualised in live cells they are commonly used as an indicator of cell viability (Steward et al., 1999). The presence of a fluorescence signal when using these dyes indicated the cells were still alive post-dissection. A formal cell viability test can be found in section 6.2.4.

LSCM confirmed the gill structure observed in the SEM images (Figure 3.5). Close examination of the lamellae revealed cellular features such as mitochondria, lysosomes, endoplasmic reticulum, nucleus and cytosol. Mitochondria were commonly found in the lamellae with seawater-acclimated inanga showing more mitochondrial staining than freshwater-acclimated inanga (Figure 3.6). The ER, mitochondria and vesicles stain 3,3'-dihexyloxacarbocyanine iodide (**$DiOC_6$**), revealed a difference in the arrangement of these organelles between freshwater- and seawater-acclimated inanga (Figure 3.7). The fluorescence produced by $DiOC_6$ was decreased in the seawater-acclimated inanga and showed movement of the organelles towards the nucleus of the cells. LysoTracker Red revealed the presence of many acidic organelles within the cytoplasm of the gill cells (Figure 3.8A and B) but no difference was seen between freshwater- and seawater-acclimated inanga.

Exposure of the gill cells to CoroNa Green, a Na^+ indicator, showed a general fluorescence throughout the cell with small regions of high fluorescence (Figure 3.9 A). Sequential staining with MitoTracker Red revealed that these high fluorescence CoroNa Green regions did not co-localise with the MitoTracker Red fluorescence, indicating these were not mitochondria (Figure 3.9 B). The high fluorescence regions were not present when the cells were loaded with a lower concentration of CoroNa Green dye (5 µM; data not shown). Staining with CoroNa Green also highlighted the structural arrangement of cell types on the lamellae (Figure 3.10 A). Cells formed a circular structure with a central cell recessed below the others. The dye 9-anthroyl ouabain, which binds to NKA, revealed these central recessed cells had a higher NKA content than the surrounding cells, and were most likely MRCs (Figure 3.10 B).

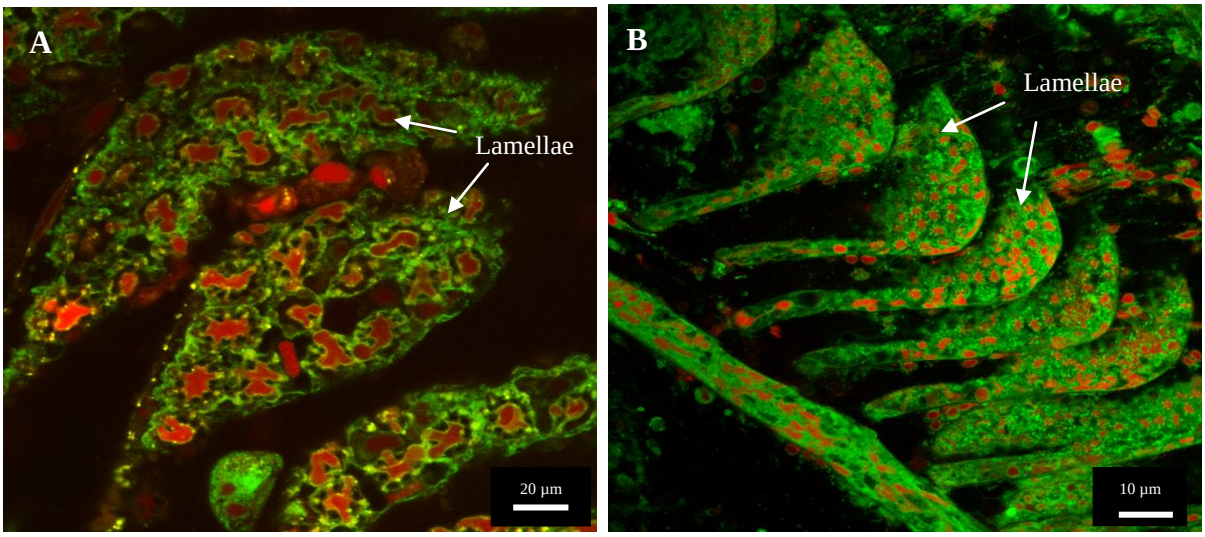

Figure 3.5 LSCM images of freshwater-acclimated salmon (A) and inanga (B) lamellae. The gill tissue was incubated with 10 µM $DiOC_6$ (green) that stained ER, mitochondria and vesicles and 10 µM propidium iodide (red) that stained nucleus of gill cells.

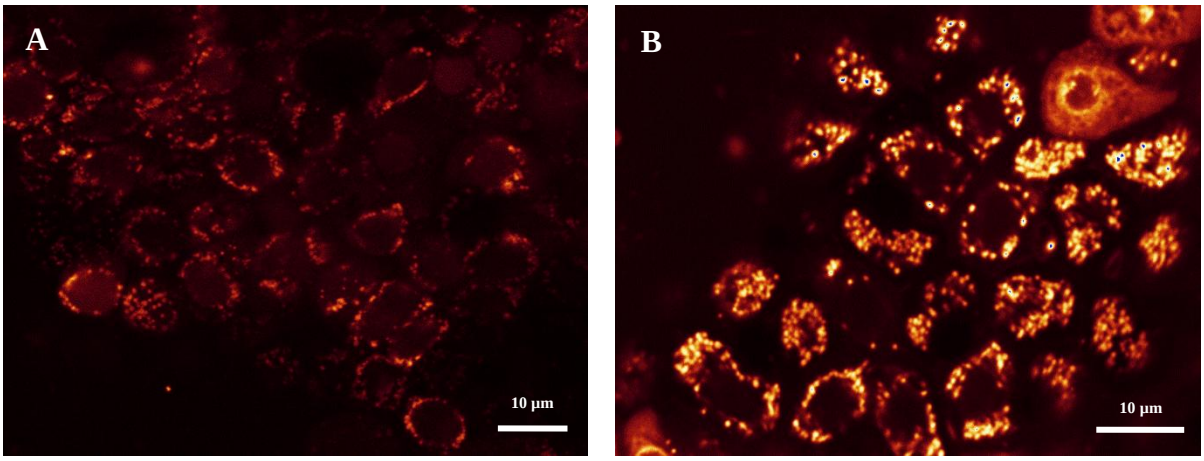

Figure 3.6 LSCM images of mitochondria in the lamellar epithelium of freshwater-acclimated inanga (A) and seawater-acclimated inanga (B). 0.5 µM MitoTracker Orange revealed the presence of numerous mitochondria in the cells that make up the lamellae.

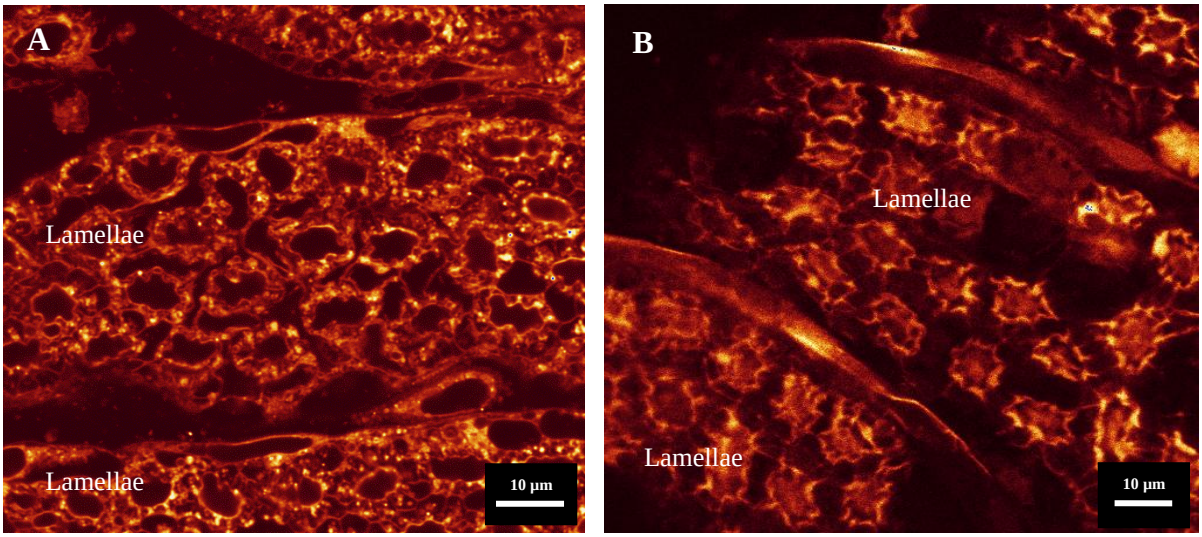

Figure 3.7 LSCM images of freshwater-acclimated (A) and seawater-acclimated (B) inanga gill lamellae. Incubation with 10 µM $DiOC_6$ (ER, mitochondria and vesicle stain) shows organisation of cytoplasmic organelles.

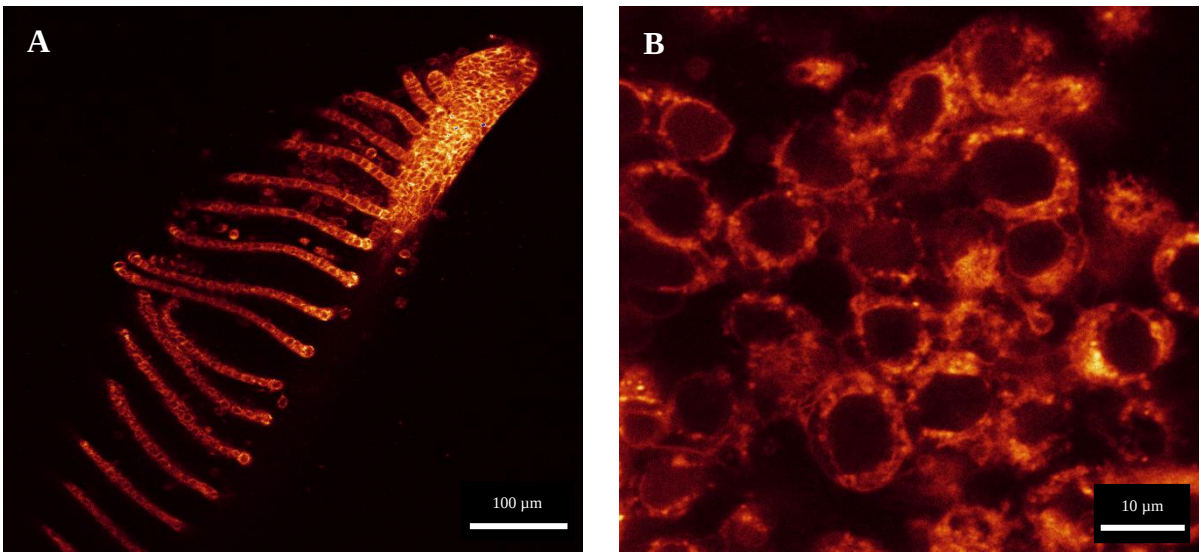

Figure 3.8 LSCM images of acidic organelles in the filament (A) and the cytoplasm of the lamellar cells (B) of freshwater-acclimated inanga. 0.5 µM LysoTracker shows the presence of acidic organelles in the cytoplasm of lamellae cells.

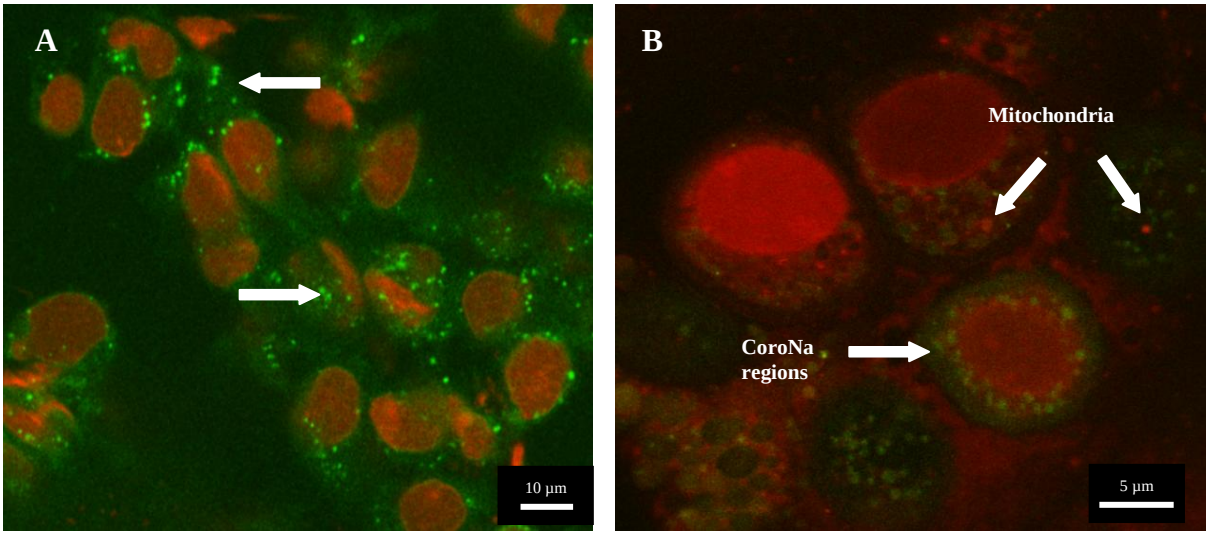

Figure 3.9 LSCM images of freshwater-acclimated inanga gill cells. 10 µM CoroNa Green (sodium-specific dye) stained the cytoplasm (A) and produced high fluorescence regions (arrows), nuclei stained red with propidium iodide. Sequential scanning with MitoTracker Red (B) showed these high fluorescence regions (green dots) were not mitochondria (red dots).

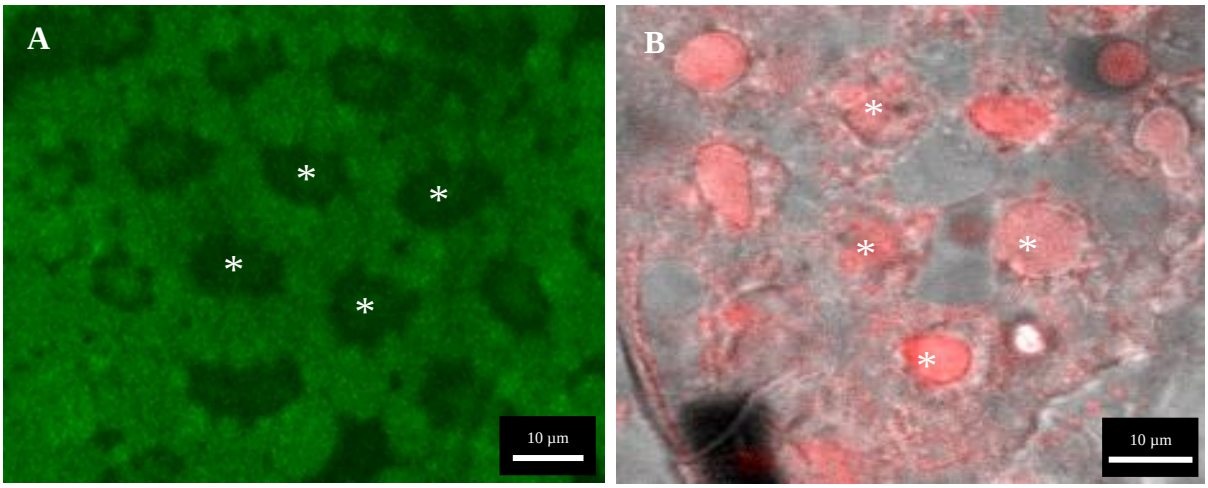

Figure 3.10 LSCM images showing the structural arrangement of PVCs and MRCs in seawater-acclimated inanga lamellae. (A) 5 µM CoroNa Green (green) showed the presence of a circular arrangement of cells with a central recessed cell (asterisks). (B) 2 µM 9-Anthroyl ouabain (red) showed these central cells have high NKA content (asterisks and red dye) when overlaid on the transmitted light image.

3.5 Discussion

The general structure of the teleost fish gill is conserved (Evans et al., 2005) and this study using SEM and LSCM demonstrated that salmon and inanga have a typical teleost gill structure. Both species have four gill arches on each side of the body and both display a reduced interbranchial septum compared to other classes of fish (Wilson and Laurent, 2002). There were, however, distinct differences in gill morphology between freshwater- and seawater-acclimated fish. SEM images showed that some cells in seawater-acclimated inanga and salmon had a raised and pronounced appearance compared to those from the freshwater-acclimated gill. In many freshwater species MRCs are only present on the afferent edge and interlamellar region of the gill filament (Evans, 2005). MitoTracker staining indicated the presence of MRCs on the lamellar surface of the gill which has also been noted in some species (Uchida et al., 1996). These freshwater- type MRCs generally contain moderate numbers of mitochondria (Katoh et al., 2001). In seawater fish the lamellae were thicker and the recessed apical pits evident in freshwater were not evident. An increase in mitochondrial numbers was also noted in seawater-acclimated fish. This increase may indicate a proliferation of seawater-type MRCs which generally have more mitochondria than their freshwater counterparts. These salinity-induced changes are similar to those that have been observed in other fish species. A proliferation of MRCs is often seen when freshwater-acclimated fish are transferred to seawater (Laurent and Dunel, 1980; Laurent et al., 1985; Perry and Walsh, 1989). This proliferation often results in a thickening of the lamellae epithelium (Wilson and Laurent, 2002). MRCs are the primary site of active ion regulation in the gills (Laurent and Perry, 1990; Laurent et al., 1985), therefore an increase in MRC and NKA in seawater is beneficial for osmoregulation. The increased diffusion of ions into the gill when the fish is in hyper-osmotic water can therefore be compensated for by the increased functional surface area and by an increase in excretion of these ions by the NKA present in MRCs.

Lamellar thickening can have a negative impact on the blood to water diffusion distance. From the perspective of ionoregulation this may be advantageous in that it would have a small effect in decreasing diffusive ion influx in hyper-osmotic environments. However, it may also inhibit gas exchange, leading to a decreased hypoxia tolerance (Wilson and Laurent, 2002). Recent studies by Urbina et al. (2012) showed that in inanga skin plays an important

role in oxygen uptake during hypoxic conditions. Therefore an increase in lamellar thickness due to MRC proliferation could be advantageous to inanga osmoregulation without compromising gas exchange.

$DiOC_6$, which stains ER, mitochondria and vesicles, revealed a difference in the arrangement of these organelles between freshwater- and seawater-acclimated inanga. A decrease of fluorescence accompanied by a centralisation of fluorescence towards the nucleus was evident in seawater-acclimated inanga. Changes in ER distribution have been observed in response to chemical stresses and toxicants (Pawert et al., 1998). The changes observed in this study may thus represent a protective response in the face of ionic and osmotic stress. PVCs have been shown to cover MRCs when exposed to seawater in an effort to reduce ion permeability (Daborn et al., 2001).

Microplicae (or microridges) are small projections that are often present on the apical surface of PVCs (Wilson and Laurent, 2002) and were present in seawater-acclimated inanga and salmon. PVCs are important for gas exchange and the microplicae are thought to increase the functional surface area and help mucus adhere to the surface of the gill (Evans et al., 2005). The increased surface area created by the microplicae, and the subsequent increased gas exchange, may help counteract the gas exchange issues associated with increased diffusion distance created by the lamellar thickening. An increase in the mucus layer covering the gills is beneficial in hyper-osmotic waters as the mucus acts as a barrier reducing diffusive gain of ions (Shephard, 1992). A decreased number of microplicae were seen in inanga compared to salmon. This may be a reflection of the ability of inanga to take up oxygen via the skin, meaning that they may not need to rely as much on the gill PVCs. Consequently the enhanced surface area of these cells is more important for a salmonid that does not utilise the skin as a respiratory surface.

The SEM images of the freshwater-acclimated salmon and inanga have a similar appearance, both exhibiting recessed apical crypts/pits lining the lamellae. The use of CoroNa Green dye was able to highlight the same arrangement of cells in seawater-acclimated gills, a morphology that was not able to be determined from SEM images of seawater-acclimated fish. The use of 9-anthroyl ouabain, which binds to NKA, revealed these centrally-recessed cells had a high NKA content and were most likely MRCs. In fact 9-anthroyl ouabain has long been used to identify MRCs (McCormick, 1990). This arrangement is similar to that

observed in the euryhaline tilapia (*Oreochromis mossambicus*; Perry et al., 1992; Van Der Heijden et al., 1997). In freshwater-acclimated tilapia, the apical membrane is substantially recessed below the adjacent pavement cells to form an apical crypt. This typically "marine" arrangement of MRCs in some freshwater species is thought to be a reflection of the evolution of freshwater species from a marine ancestry (Evans et al., 2005). It has been hypothesised that the immediate ancestor of the galaxiid lineage was diadromous (i.e. moves between freshwater and seawater), but whether their original ancestor was an inhabitant of marine or fresh waters is unknown (McDowall, 2002).

One notable difference between the salmon and inanga was the density of recessed apical crypts/pits. Inanga exhibited a higher density of recessed apical crypts/pits on their lamellae surface than the salmon. This may reflect an increase in MRC density and therefore ion absorbing capacity of inanga in freshwater. Adult inanga have an exceptional ability to extract Na^+ from very dilute freshwater environments (see Chapter 3) which may be facilitated by the increase MRC density.

Lysosomes are acidic cellular organelles that help break down waste and unwanted cellular debris (Alberts et al., 2002). Lysosomes have also been shown to play a role in urea excretion in uroetelic fish which excrete the majority of their nitrogenous waste as urea (Laurent et al., 2001). Inanga excrete ~27% of their nitrogenous waste as urea (M.A. Urbina, unpublished observation). Therefore positive LysoTracker staining may indicate the presence of large numbers of acidic lysosomal organelles participating in excretion of urea. Lysosomes are also involved in the autophagy of cellular waste such as that produced by proliferation and remodelling induce by stressful conditions such as salinity changes (Yabu et al., 2011). This action may also reflect the large numbers of lysosomes observed.

PVCs and MRCs are traditionally differentiated on the basis of morphological features and stains such as those for mitochondrial and NKA. However recent research suggests a plethora of different subtypes of MRCs and PVCs may be present in the gill, each with their own morphological traits and staining patterns (Hwang et al., 2011). This extra layer of complexity adds to the challenge of discriminating cell types. In this chapter the classic parameters of cell size, and mitochondrial and NKA staining patterns were used to differentiate cell types, but it is important to note that there is likely a continuum of cell types between PVCs and MRCs and this may greatly confound interpretation.

3.6 Conclusion

Inanga have a conserved teleost gill structure with morphological features that are similar to other euryhaline teleosts. Freshwater-acclimated inanga displayed a high apical crypt and freshwater-type MRC density that likely allows for a greater ion absorption in hypo-osmotic freshwater environments, and which would therefore be a critical factor ensuring survival in very dilute waters. Upon acclimation to seawater, inanga remodelled their gills to facilitate active ion excretion in light of diffusive ion influx in the hyper-osmotic environment. The gill epithelium of seawater fish was thickened due to an increase in seawater-type MRCs which are essential for ion excretion.

CHAPTER 4 BIOCHEMISTRY AND PHYSIOLOGY

4.1 Introduction

Freshwater teleosts are hyper-osmotic regulators that maintain their body ion concentration at levels higher than those of their environment. As a consequence they lose ions to the environment down a concentration gradient and must therefore replace them via active transport in order to maintain homeostasis (Evans et al., 1999). Seawater teleosts face the opposite challenge and passively gain ions from the environment. To compensate they actively transport ions from the body in order to remain hypo-osmotic to their environment (Evans et al., 1999). The movement of these ions, and in particular Na^+, has long been studied in an effort to elucidate osmoregulatory mechanisms (Krogh, 1939).

The rate of Na^+ ion transport generally increases with environmental salinity up to a maximal rate (Wilmer et al., 2004). This saturation only occurs if the rate-limiting step is mediated by a transport protein rather than by a channel or via simple diffusion (Cornish-Brown, 1979). The maximal rate of transport (J_{max}) is determined in part by the number of transport proteins present. An important aspect of saturation kinetics is the affinity constant (K_m) which reflects the affinity a transporter has for the substrate it moves. The lower the K_m, the higher affinity, and thus the lower the range of concentrations over which the transporter can effectively operate (Cornish-Brown, 1979). A low K_m (high affinity) is beneficial in freshwater as it means the fish is better able to extract Na^+ from its environment in an effort to counteract diffusive loss. Theoretically K_m increases with salinity as there is less for need for Na^+ influx due to the passive gain of ions from the hyper-osmotic environment (Evans, 1984). Examining ion influx kinetics at a whole organism, tissue or a cell level, will reflect the overall kinetic properties of the transporters that achieve uptake.

In fish the main tissue that facilitates Na^+ influx is the gill, and within the gill it is NKA that drives ion transport (Hwang and Lee, 2007). Using the energy of ATP to translocate three Na^+ ions from inside the cell to the blood in exchange for two K^+ ions, this transporter generates an electrochemical gradient favouring Na^+ movement into the cell. Although the mechanism of apical Na^+ entry from the environment into the cell is controversial (see Chapter 1) in freshwater fish, the electrochemical gradient created by NKA in concert with accessory transporters, is sufficient to drive absorption from dilute water (Evans et al., 1999).

In seawater NKA has a similar role. In seawater, however, NKA acts in association with accessory transporters driven by the NKA-generated electrochemical gradient, to excrete Na^+ (see Chapter 1). In general, levels of NKA are thought to increase in euryhaline fish in seawater relative to levels in freshwater (Tipsmark et al., 2002; Richards et al., 2003; Hawkings et al; 2004; Bystriansky et al 2006). Other changes in the gill that occur in response to seawater acclimation include those related to gill morphology that are thought to facilitate ion excretion over ion absorption (see Chapter 3).

These changes that occur in the gill are mediated by hormones, in particular prolactin (considered to be the freshwater hormone) and cortisol (the seawater hormone) (McCormick, 2001). These hormones and their roles in ion regulation were discussed in detail in Chapter 1.

The challenge of maintaining ion homeostasis is much greater in those fish that inhabit a variety of salinities, such as the euryhaline inanga. Inanga are migratory and also inhabit near-coastal waters and are thus subjected to variations in salinity in relation to life-cycle stage and the tides. As a consequence inanga are known to be highly tolerant to a wide range of salinities (Chessman and Williams, 1975). This tolerance must rely on effective mechanism for maintaining Na^+ ion homeostasis in light of the diametrically-opposed challenges of diffusive ion influx (in seawater) and ion loss (in freshwater). These characteristics make them an idea model organism for studying ion transport systems and in particular Na^+ metabolism and transport. However, nothing is known regarding the mechanism of ion transport in inanga and whether there are special physiological and biochemical mechanism that they employ in order to deal with the salinity extremes of the environments they inhabit.

4.2 Chapter Aim

The aim of this chapter is to examine Na^+ metabolism and transport in inanga acclimated to different salinities. The concentration-dependent kinetics of Na^+ transport can be determined by monitoring Na^+ influx in response to a graded series of water Na^+ levels. The resulting kinetic parameters of J_{max} and K_m can be compared across different salinities, to determine how the properties of Na^+ influx change as a function of environmental salinity. Enzymatic assessment of NKA activity in response to different salinities, and in response to cortisol and prolactin, will also be performed in an effort to determine the role of this transporter in facilitating inanga survival in such a wide range of salinities.

4.3 Methods

4.3.1 Unidirectional sodium flux

In a given tissue there is a large number of transporters responsible for achieving Na^+ uptake, and each will have slightly different properties with respect to the substrate. As environmental Na^+ levels increase those transporters with highest affinity are able to bind the substrate and facilitate uptake. As levels increase further, more and more transporter binding sites are occupied, until the environmental Na^+ level increases to the point where all transporters are saturated. This point therefore represents the maximal rate of transport (J_{max}), and this will reflect the number of NKA transporters present. The Na^+ concentration at which there is half maximal transport is known as the affinity constant, K_m, and this reflects the affinity the transporter population has for Na^+ ions. J_{max} and K_m can be determined experimentally by analysing the transport kinetics of radiolabelled sodium isotope (^{22}Na). Use of a sodium isotope allows 'new' sodium to be differentiated from the 'old' sodium already in the fish. Because of the large pool of 'old' sodium present, it takes some time for equilibrium between the 'old' and 'new' Na^+ to be reached. Therefore if the assay is short enough the accumulation of the radiolabel will reflect only unidirectional uptake (i.e. none of the 'new' sodium will be excreted as it has not yet fully equilibrated with the total sodium pool within the fish).

Fish are exposed to a known amount of ^{22}Na in a controlled environment and Na^+ influx (J_{in}) is then calculated from Equation 4.1:

Equation 4.1

$$J_{in} = \frac{\gamma \text{ cpm}}{SA.m.t}$$

where γ cpm is the whole body gamma counts per minute of the fish, *SA* is the specific activity of the exposure water (i.e. the ratio of radiolabelled Na^+ to total Na^+), *m* is the mass of the fish and *t* is the time of exposure. Na^+ influx is then expressed as nmol g^{-1} h^{-1}.

If when Na^+ concentration is plotted against J_{in}, the data results in a rectangular hyperbola the transporter is said to conform to Michaelis-Menten kinetics (Figure 4.1).

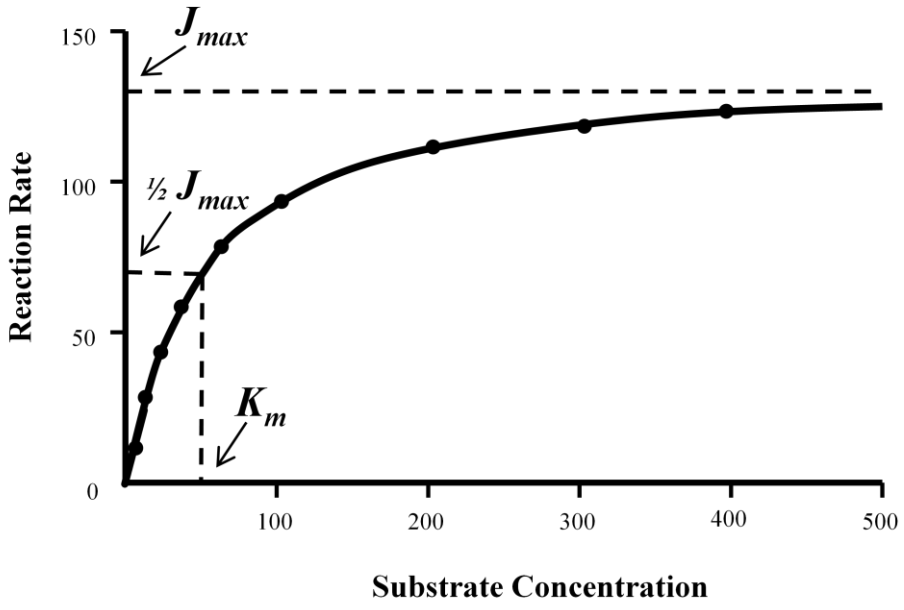

Figure 4.1 The relationship between substrate concentration and reaction rate (e.g. sodium uptake). The hyperbolic curve illustrates that in the presence of excess substrate the transporter becomes saturated and reaches a maximal rate (J_{max}). The reaction conforms to Michaelis-Menten kinetics and the affinity constant (*Km*) can be derived.

The shape of this curve shows that in the presence of excess substrate, the transporter becomes saturated and the transport rate reaches a maximal rate (J_{max}). This pattern is characteristic of Michaelis-Menten kinetics, and thus permits the calculation of J_{max} and K_m according to the Michaelis-Menten Equation 4.2:

.

Equation 4.2

$$J_{in} = \frac{J_{max} \,.\, [Na^+]}{K_m + [Na^+]}$$

4.3.1.1 Sodium Influx Method

Adult inanga were acclimated to one of three salinities - freshwater, 50% seawater and 100% seawater as described in section 2.2. Following acclimation, 30 fish from each salinity (freshwater, 50% seawater and 100% seawater) were randomly selected for the Na^+ flux experiment. Flux chambers consisting of a 4 L plastic bag containing 2 L of one of five nominal Na^+ concentrations (0, 50, 100, 1000, 2000 µM) were set-up. Triplicate initial water samples from each chamber were taken to determine the exact water Na^+ concentration via flame photometer (Sherwood Instruments) (section 2.7). Each chamber was then spiked with radiolabelled ^{22}Na (as NaCl; ~5 μC_i L^{-1}; Perkin-Elmer). Six freshwater-acclimated inanga were then placed into each of the five flux chambers. The fish were then left undisturbed for one hour. At this point exposed fish were removed from the flux chambers and euthanised *in situ* via the introduction of an overdose of 3-aminobenzoic acid ethylester (MS222; 1 g L^{-1}) into the chamber. The fish were then rinsed in 1 M NaCl to displace any ^{22}Na adhering to the skin or gill (i.e. adsorbed rather than absorbed label) before a final rinse in two changes of milli-Q water (to remove any traces of radiolabelled water from the fish). Each fish was then weighed and whole body gamma counts per minute (γ cpm) were determined using a gamma counter (Wallac Wizard 1470; Perkin-Elmer). This procedure was repeated with inanga acclimated to 50% freshwater and 100% seawater.

4.3.1.2 Influx Data Analysis

Sodium influx was determined for each fish using Equation 4.1. The mean and SE for each group were calculated and then plotted against Na^+ concentration to determine if the data conformed to Michaelis-Menten kinetics. The kinetic parameters of Na^+ influx, J_{max} and K_m were determined according to the Michaelis-Menten Equation 4.2 using nonlinear regression (SigmaPlot, Version 11.0).

4.3.2 NKA Activity

NKA activity can be assessed with a coupled-enzymatic assay that measures the ouabain-sensitive ATPase activity. In this assay adenosine diphosphate (ADP) is formed when ATP-utilising enzymes (ATPases) hydrolyse adenosine triphosphate (ATP) and this reaction is enzymatically coupled to the oxidation of reduced nicotinamide adenine dinucleotide (NADH) (Figure 4.2) (Barnett, 1970).

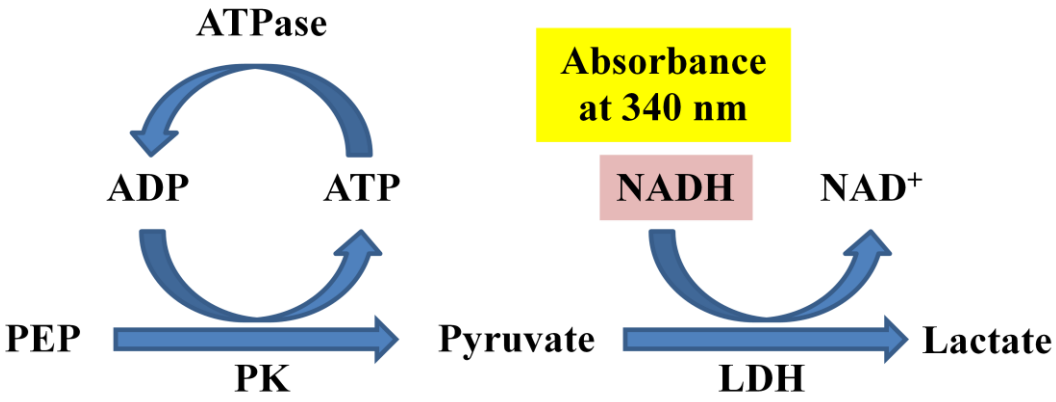

Figure 4.2 Sequence of the ATPase-coupled enzymatic reaction to determine NKA activity. See text for details. Abbreviations; adenosine diphosphate (ADP), adenosine triphosphate (ATP), ATP-utilising enzymes (ATPases), lactate dehydrogenase (LDH), oxidised nicotinamide adenine dinucleotide (NAD^+), reduced nicotinamide adenine dinucleotide (NADH), phosphoenolpyruvate (PEP) and pyruvate kinase (PK).

Following each cycle of ATP hydrolysis, pyruvate kinase (PK) converts phosphoenolpyruvate (PEP) to pyruvate and subsequently ADP is converted back to ATP. Pyruvate is then converted to lactate by lactate dehydrogenase (LDH) resulting in the oxidation of NADH to NAD^+. NADH absorbs light at 340 nm whereas NAD^+ does not, therefore the conversion of NADH to NAD^+ can be monitored spectrophotometrically by a decrease in absorbance at 340 nm. The oxidation of NADH is directly proportional to the hydrolysis of ATP by ATPases (Barnett, 1970). There are many types of ATPases present in cells so to determine the activity of NKA, the NKA-specific inhibitor ouabain is added to the reaction. Activity in the presence of ouabain is subtracted from the total activity (no ouabain) to give the ouabain-sensitive

component, which reflects the ATP hydrolysis related specifically to NKA (McCormick, 2003).

NKA activity is then normalised to the protein concentration present in each sample by Bradford assay. The Bradford assay is a dye-binding assay in which binding of protein to the Coomassie dye produces a shift in absorbance from 465 nm to 595 nm. Protein standards are constructed using bovine serum albumin (BSA) and run with all samples. The protein concentration of each sample can then be determined from the standard curve using the following equation 4.3:

Equation 4.3 μg/μl sample = ((mean absorbance - intercept) / slope) x dilution factor

4.3.2.1 Method

Thirty adult inanga were acclimated to each of the three salinities (freshwater, 50% seawater and 100% seawater) and treated with hormone injections as described in section 2.3. Following acclimation and hormone treatment, gill tissue was isolated as described in section 2.4.1.

NKA activity was measured using a modified microplate assay (McCormick, 1993). Stock salt solution containing 189 mM NaCl, 10.5 mM $MgCl_2$, 42 mM KCl, 50 mM imidazole (pH 7.5) was made on the day of the assay. The salt solution was divided in half and 3 mM ouabain was added to one half and stored in a light-proof container to protect the light-sensitive ouabain. The other half was kept as salt solution without ouabain.

An enzyme solution containing 8 U/mL LDH, 10 U/mL PK, 2.8 mM PEP, 3.5 mM ATP, 0.22 mM reduced NADH, 50 mM imidazole (pH 7.5) was made on the day of the assay and tested before use. To determine the activity of the enzyme solution and ensure its optimal performance, the enzyme solution was tested with an ADP standard curve. To make the ADP standard, a stock solution of 4 mM ADP in 57 mM sodium acetate buffer (pH 6.8) was made and then diluted in 50 mM imidazole buffer (pH 7.5) to the following concentrations: 0, 5, 10, 20 nM ADP . Ten μL of each standard was added to 4 wells in a NUNC™ 96-well plate

(Thermo Fisher Scientific) and 50 µL of salt solution without ouabain was added to all wells. The enzyme solution was then warmed to 25°C and 150 µL was added to every well. The plate was sealed and read at 340 nm with a FLUOstar OPTIMA microplate reader at 25°C. The data was exported to Microsoft Office Excel and a standard curve produced. An optimal enzyme solution is one that produces a standard curve slope of -0.014 to -0.010 OD units per nM of ADP per well (McCormick, 1993). If the curve did not meet these criteria the solution was remade and retested until it did.

The gill tissue was homogenised in 100 µL of homogenising buffer (150 mM sucrose, 10 mM EDTA, 50 mM imidazole, 0.5% w/v sodium deoxycholate, pH 7.3) using a plastic pestle. The tubes were then immediately centrifuged for 5,000g for 30 seconds to separate the homogenate from the supernatant. Supernatant (~10 µL) was added to four wells in a chilled 96-well plate. Fifty µL of salt solution without ouabain was added to two wells and 50 µL of salt solution with ouabain was added to the other two wells. The enzyme solution was warmed to 25°C and 150 µL was added to every well. This set-up was repeated for each gill sample. The plate was sealed and read at 340nm over a 10 minute period to measure the reduction of absorbance of NADH. The difference in slope of the samples with ouabain and without ouabain were calculated to obtain the NKA-specific activity.

Protein standards for the Bradford (1976) assay were generated by diluting 2 mg/mL bovine serum albumin (BSA) with milli-Q water to give the following concentrations: 0, 0.25, 0.5, 0.75, 1.0, 1.25, 1.5, 1.75 and 2.0 µg/µL BSA. Ten µL of each standard was added to three wells in a 96-well plate, along with 200 µL of Bradford reagent. The plate was sealed and incubated at room temperature for 30-45 minutes before being read at 595nm. NKA activity was expressed as µmol ADP mg protein^{-1} h^{-1} with the NKA specific activity being normalised to amount of ADP and protein present.

4.3.2.2 Data Analysis

All data were subjected to tests of normality (Kolmogorov-Smirnov test) and homogeneity of variance (Levene's test) using SigmaPlot Version 11.0. Data that passed these assessments were analysed parametrically via one-way analysis of variance (ANOVA) and pairwise multiple comparison procedures (Holm-Sidak method) using SigmaPlot. Data are presented

as the mean and standard error of the mean (S.E.M.) for each treatment group. For statistical testing of the kinetic parameters (J_{max} or K_m) the following approach was taken (Glover et al., 2005). Parameters from curve-fitting were subjected to paired t-tests (a total of three tests per parameter to test each combination), using the standard error values derived from the curve fitting as the variance measure. To alleviate the issues associated with multiple comparisons, a conservative approach whereby each Na^+ concentration, rather than each individual plotted point, was counted as an observation, thereby reducing the degrees of freedom used to determine significance.

4.4 Results

4.4.1 Unidirectional sodium influx

The concentration-dependent kinetics of Na^+ influx in inanga acclimated to freshwater, 50% seawater and 100% seawater were examined (Figure 4.3, 4.4 and 4.5). As the Na^+ concentration increased, the influx increased. In all three salinities, the relationship between Na^+ concentration and Na^+ influx best-fitted a hyperbolic curve, conforming to Michaelis-Menten kinetics. Values for J_{max} and K_m were then derived from the data. The maximal rate of Na^+ transport capacity (J_{max}) in 100% seawater-acclimated inanga (615 ± 83 nmol g^{-1} h^{-1}) was statistically significantly different than that seen in freshwater and in 50% seawater-acclimated inanga (288 ± 33 nmol g^{-1} h^{-1} and 243 ± 43 nmol g^{-1} h^{-1} , respectively) (Figure 4.6).

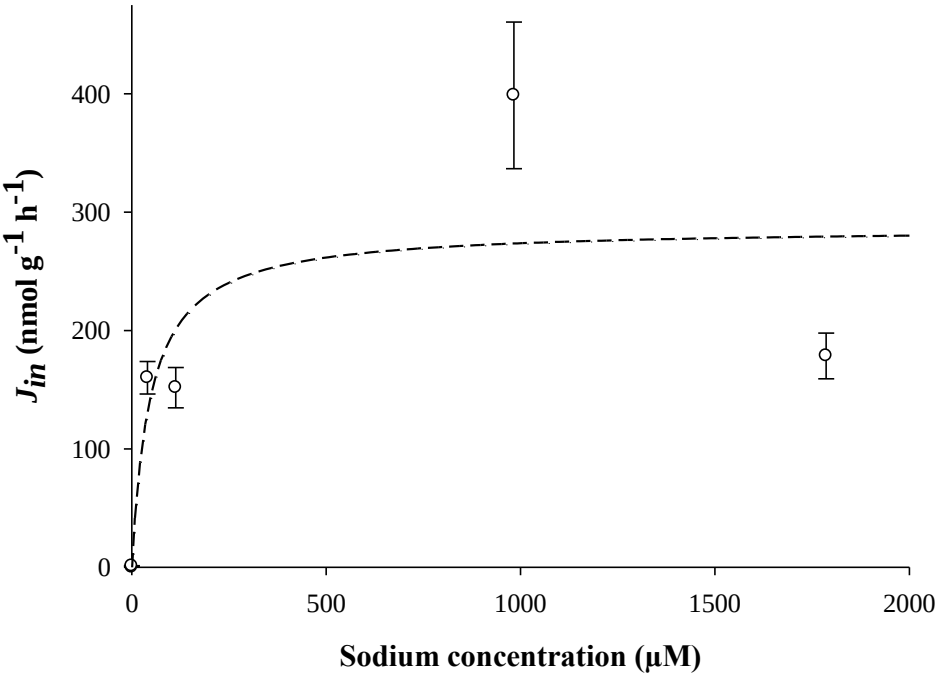

Figure 4.3 Concentration-dependence of sodium influx (J_{in}; nmol g^{-1} h^{-1}) in inanga acclimated to freshwater. Plotted points represent the mean ± SE of 6 individuals. Fitted lines were derived from raw values and determined by non-linear regression using Sigmaplot.

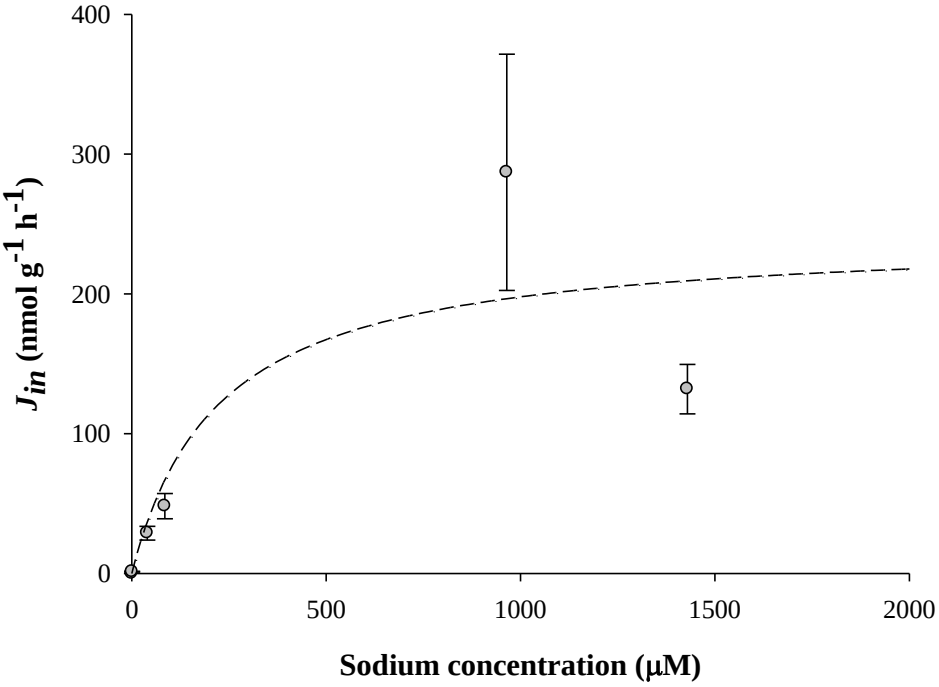

Figure 4.4 Concentration-dependence of sodium influx (J_{in}; nmol g^{-1} h^{-1}) in inanga acclimated to 50% seawater. Plotted points represent the mean ± SE of 6 individuals. Kinetic parameters (J_{max}, maximal sodium influx rate; K_m, affinity constant) and fitted lines were derived from raw values and determined by non-linear regression using Sigmaplot.

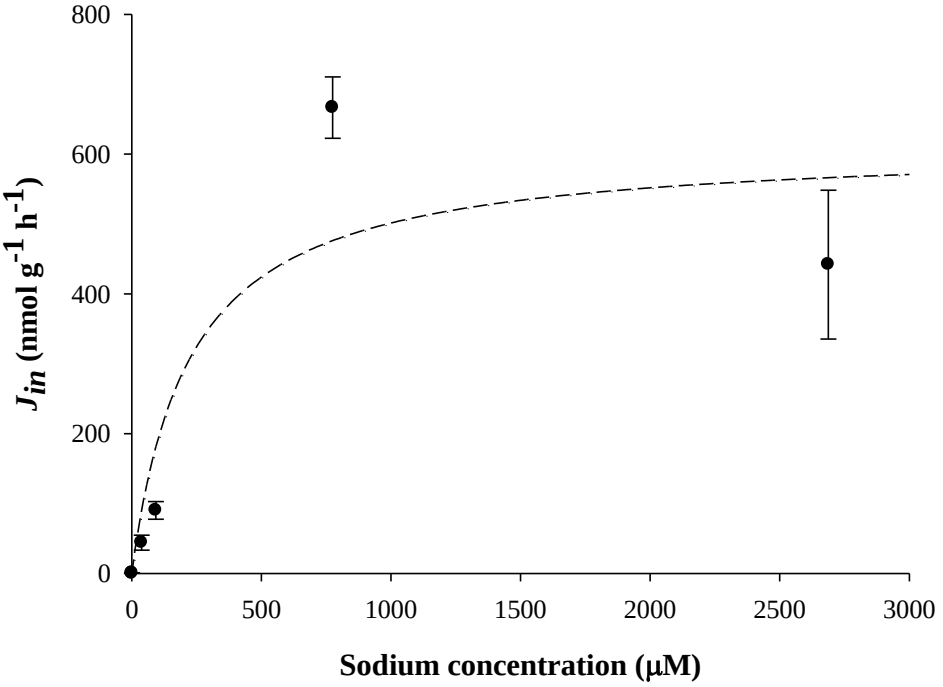

Figure 4.5 Concentration-dependence of sodium influx (J_{in}; nmol g^{-1} h^{-1}) in inanga acclimated to 100% seawater. Plotted points represent the mean ± SE of 6 individuals. Kinetic parameters (J_{max}, maximal sodium influx rate; K_m, affinity constant) and fitted lines were derived from raw values and determined by non-linear regression using Sigmaplot.

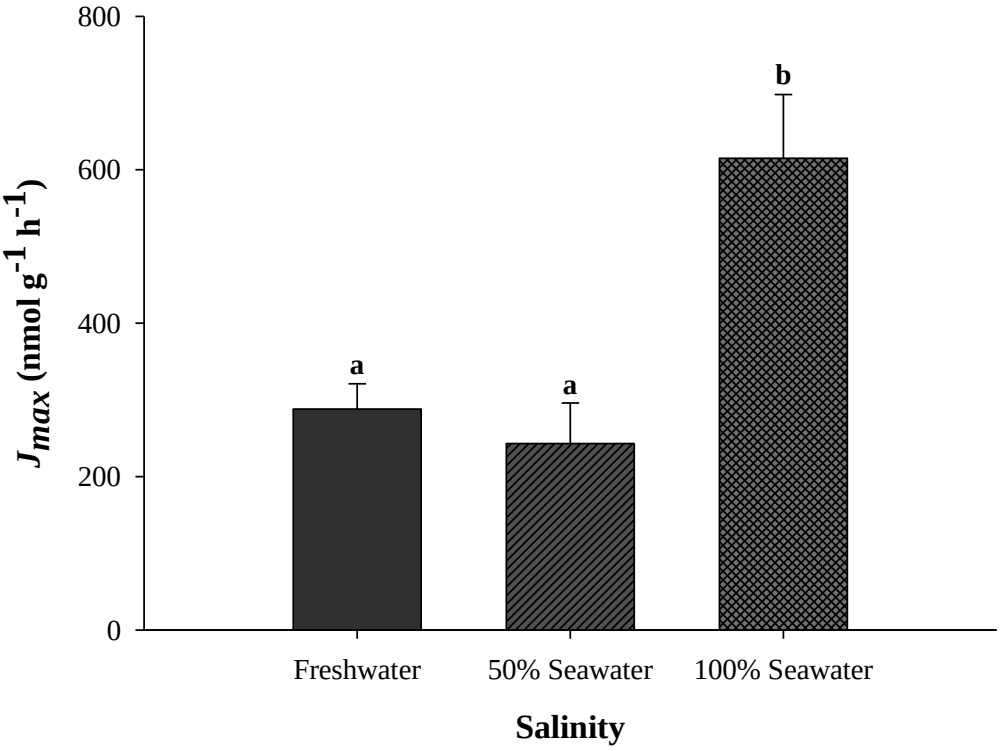

Figure 4.6 The effect of salinity acclimation on the sodium transport capacity (J_{max}, nmol g^{-1} h^{-1}) of inanga. Mean values sharing letters are not statistically significantly different ($p < 0.05$).

Although statistically-significant differences in Na^+ transport capacity were observed, the 50% and 100% seawater-acclimated groups had similar Na^+ influx affinity constants (230 ± 123 µM and 243 ± 43 µM, respectively) (Figure 4.7). Although the K_m value for the freshwater-acclimated group (52 ± 30 µM) was less than a quarter that of the 50% and 100% seawater-acclimated groups, the associated large error value negated any statistically-significant difference (Figure 4.7).

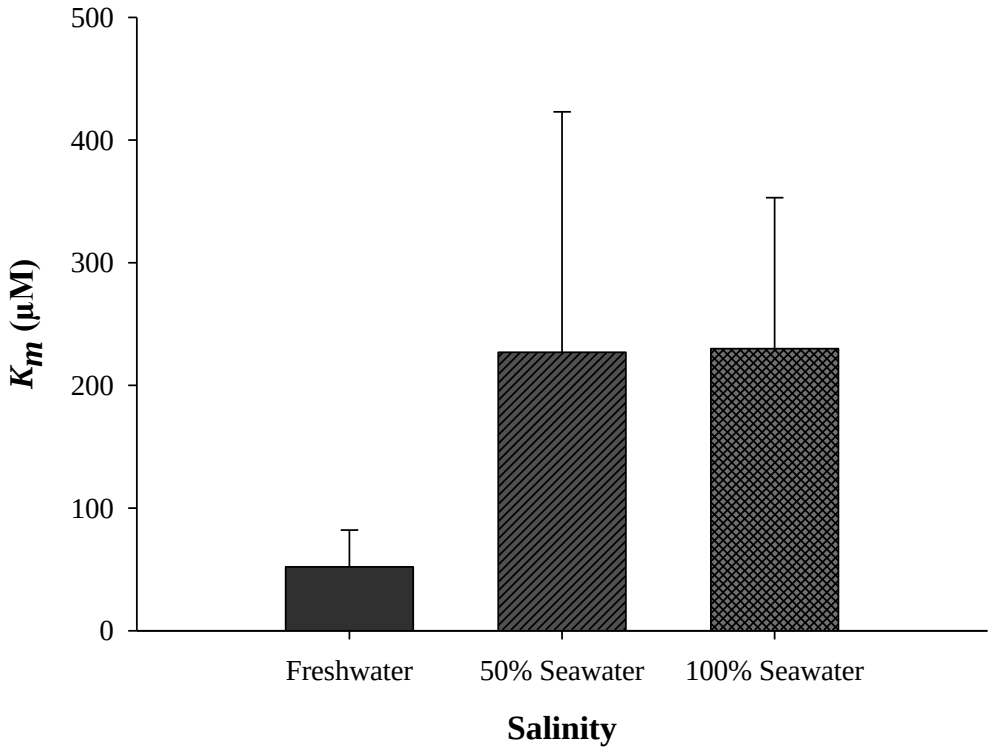

Figure 4.7 The effect of salinity acclimation on the sodium transport affinity constant (K_m, µM) in inanga. No significant difference was found between treatments (one-way ANOVA).

4.4.2 NKA Activity

NKA activity in the gills of 100% seawater-acclimated inanga was significantly higher than the activity seen in freshwater and 50% seawater-acclimated fish (Figure 4.8). Freshwater and 50% seawater-acclimated inanga showed less than half as much NKA activity (2.54 ± 0.19 and 2.07 ± 0.22 µmol ADP mg protein^{-1} h^{-1} respectively) as that seen in 100% seawater-acclimated inanga (6.42 ± 0.51 µmol ADP mg protein^{-1} h^{-1})

Figure 4.8 The effect of acclimation to three salinities on NKA activity of inanga gill (µmol ADP mg protein^{-1} h^{-1}). Plotted values represent mean ± SE of 6 individuals. Mean values sharing letters are not statistically significantly different ($p < 0.05$), as determined by one-way ANOVA, followed by a Holm-Sidak post-hoc analysis (SigmaPlot).

Cortisol, prolactin and cortisol + prolactin hormone treatments decreased NKA activity in freshwater-acclimated inanga (Figure 4.9). The control group (2.54 ± 0.19 µmol ADP mg protein^{-1} h^{-1}) was statistically significantly different from the three hormonal treatments (cortisol 0.77 ± 0.05, prolactin 1.23 ± 0.25, cortisol + prolactin 1.26 ± 0.25 µmol ADP mg protein^{-1} h^{-1}) but not from the sham group (1.68 ± 0.36 µmol ADP mg protein^{-1} h^{-1}). Treatment with cortisol caused a significant decrease in NKA activity compared to the sham. In contrast, there was no significant effect of hormones on gill NKA activity relative to the control or the sham in 50% seawater-acclimated inanga (p = 0.18) (Figure 4.9).

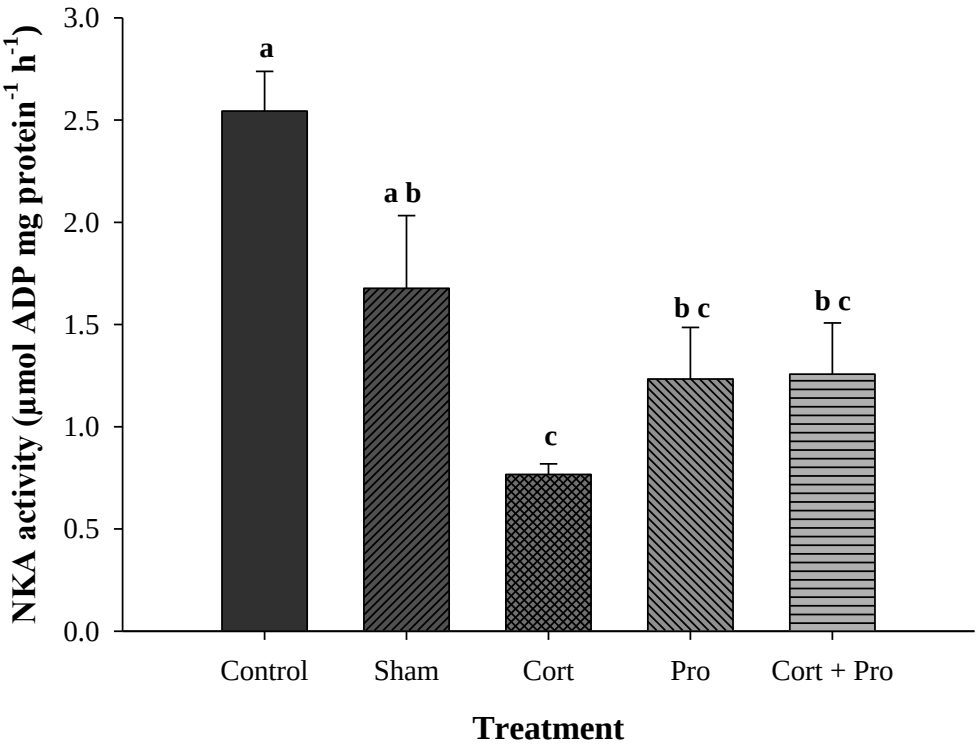

Figure 4.9 The effect of cortisol 50 µg/g (Cort), prolactin 5 µg/g (Pro), cortisol 50 µg/g and prolactin 5 µg/g (Cort + Pro) hormone treatment (intraperitoneal injection) on NKA activity of freshwater-acclimated inanga gill (µmol ADP mg protein^{-1} h^{-1}). Sham represents an injection control (vehicle only) and the control is a no-injection/handing control. Plotted values represent mean ± SE of 6 individuals. Mean values sharing letters are not statistically significantly different ($p < 0.05$), as determined by one-way ANOVA and Holm-Sidak post hoc analysis (SigmaPlot).

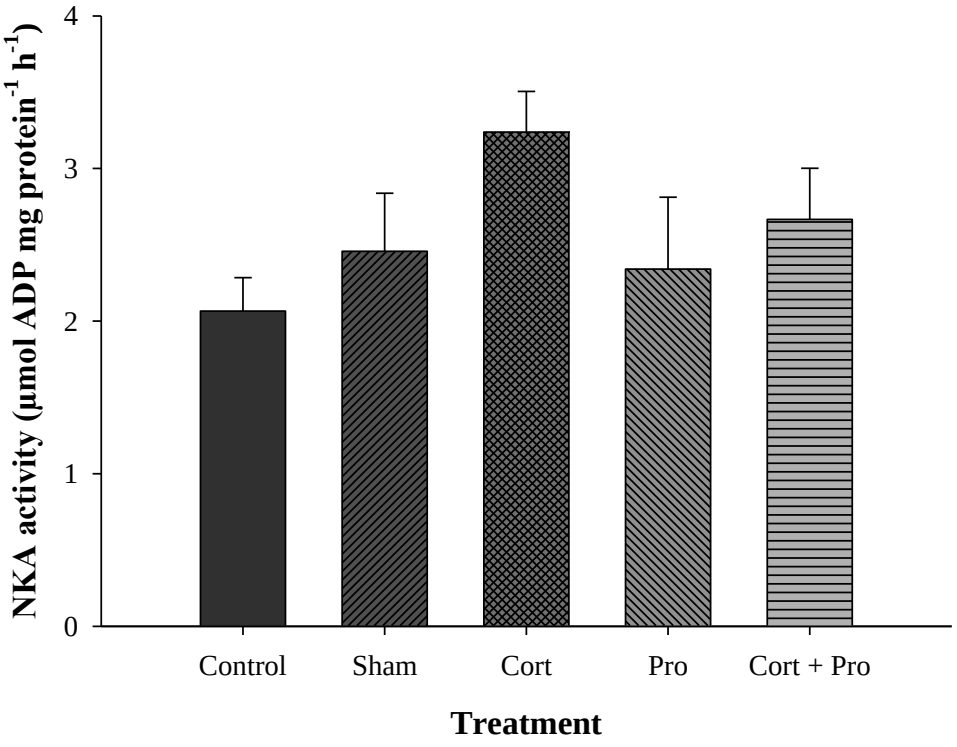

Figure 4.10 The effect of cortisol 50 µg/g (Cort), prolactin 5 µg/g (Pro), cortisol 50 µg/g and prolactin 5 µg/g (Cort + Pro) hormone treatment (intraperitoneal injection) on NKA activity of 50% seawater-acclimated inanga gill (µmol ADP mg protein^{-1} h^{-1}). Sham represents an injection control (vehicle only) and the control is a no-injection/handing control. Plotted values represent mean ± SE of 6 individuals. No significant difference was found between treatments (one-way ANOVA).

There was no significant effect of cortisol or prolactin on gill NKA activity, relative to the control or the sham in 100% seawater-acclimated inanga (Figure 4.11). However hormone treatment with both cortisol + prolactin significantly decreased NKA activity.

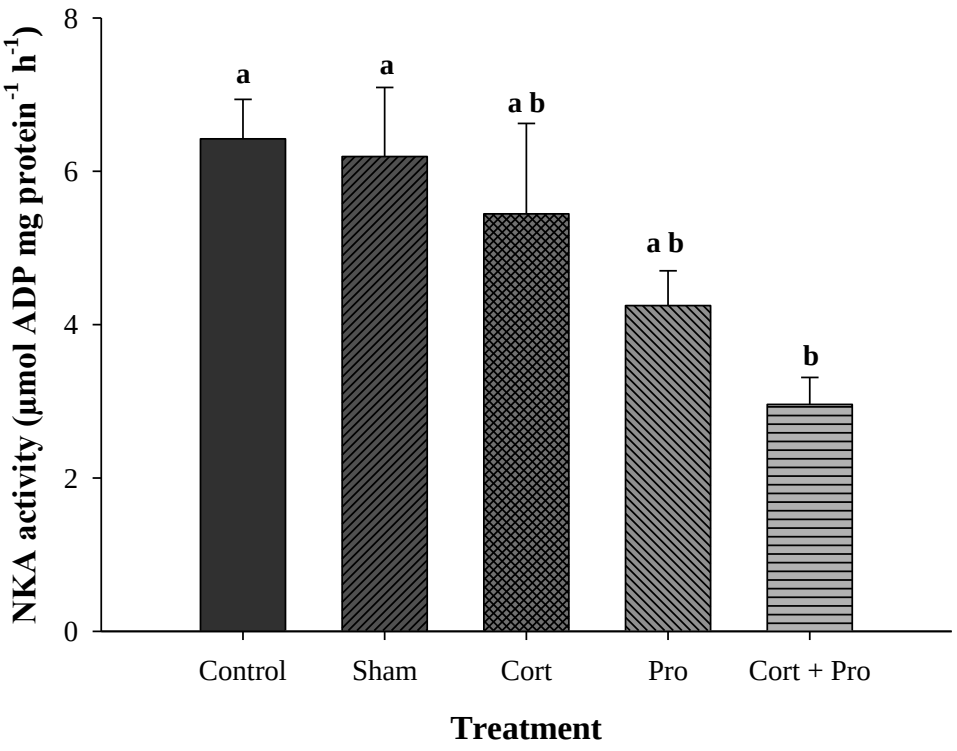

Figure 4.11 The effect of cortisol 50 µg/g (Cort), prolactin 5 µg/g (Pro), cortisol 50 µg/g and prolactin 5 µg/g (Cort + Pro) hormone treatment (intraperitoneal injection) on NKA activity of 100% seawater-acclimated inanga gill (µmol ADP mg protein^{-1} h^{-1}). Sham represents an injection control (vehicle only) and the control is a no-injection/handing control. Plotted values represent mean ± SE of 6 individuals. Mean values sharing letters are not statistically significantly different ($p < 0.05$), as determined by Holm-Sidak ANOVA.

4.5 Discussion

There is limited information regarding the physiology of inanga (*Galaxias maculatus*) but a previous study by Chessman and Williams (1975), demonstrated the high tolerance of this fish to the varied salinities it encounters during its life. The present work corroborates the findings of Chessman and Williams and affirms inanga as an idea model organism for studying ion transport systems.

4.5.1 Sodium Influx

In freshwater fish Na^+ influx is achieved by a high affinity, low capacity system. This is in contrast to seawater fish, which display a low affinity, high capacity system (Evans, 1984). Fish with high affinity systems (low K_m) are better able to extract Na^+ from the environment. Adult freshwater inanga display a saturable, high affinity, low capacity uptake system for Na^+ influx, in line with the findings for most other freshwater teleosts. That Na^+ influx conformed to Michaelis-Menten kinetics for all salinities studied, suggests that Na^+ influx in inanga is achieved by a specific transport process rather than by passive diffusion. There has been limited work examining Na^+ kinetics in fish as a function of salinity but the low J_{max} value seen in the freshwater-acclimated inanga in line with previous findings in other freshwater teleosts (see Table 4.1). However the affinity constant for freshwater-acclimated inanga derived from these experiments is the lowest ever recorded (see Table 4.1). This indicates that inanga have an exceptional ability to extract Na^+ from very dilute freshwater environments in order to counteract diffusive loss. In accordance with Krogh's Principle (Krebs, 1975) this extreme ability suggests that inanga will be an ideal organism for examining mechanisms of ion uptake, with relevance to both the function of fish and the fish gill, and also for ion transport in general (e.g. Marshall et al., 1995).

Table 4.1 Kinetics of sodium uptake in teleost fish

Species	Medium	K_m (µM)	J_{max} (nmol g^{-1} h^{-1})	Reference
Inanga (*Galaxias maculatus*)	Freshwater	52	288	This study
Killifish (*Fundulus heteroclitus*)	Freshwater	2000	-	Potts and Evans, 1966
Killifish (*Fundulus heteroclitus*)	Freshwater ('soft')	74	1160	Boisen et al., 2003
Killifish (*Fundulus heteroclitus*)	Freshwater ('hard')	160	525	Boisen et al., 2003
European flounder (*Platichthys flesus*)	Freshwater	800	350	Maetz, 1971
Rainbow trout (*Salmo gairdneri*)	Freshwater	500	400	Kerstetter et al., 1970
Rainbow trout (*Oncorhynchus mykiss*)	Freshwater ('soft')	161	605	Matsuo et al., 2004
Rainbow trout (*Oncorhynchus mykiss*)	Freshwater ('hard')	204	1453	Matsuo et al., 2004
Goldfish (*Carassius auratus*)	Freshwater	300	650	Maetz, 1973
Sailfin molly (*Poecilia latipinna*)	Freshwater	8000	12000	Evans, 1973
Pinfish (*Lagodon rhomboides*)	Freshwater	5000	7000	Carrier and Evans, 1976
Inanga (*Galaxias maculatus*)	50% seawater	227	243	This study
Inanga (*Galaxias maculatus*)	Seawater	230	615	This study
Sailfin molly (*Poecilia latipinna*)	Seawater	17000	33000	Evans, 1973
Pinfish (*Lagodon rhomboides*)	Seawater	22000	32000	Carrier and Evans, 1976

Sodium influx in 50% and 100% seawater-acclimated inanga was also assessed. Inanga acclimated to 100% seawater showed a significantly higher maximal rate of transport (J_{max}) than the other acclimation groups, indicating a higher capacity for transport. This is suggestive of a large population of transporters available to carry out Na^+ uptake. It is probable that this reflects the higher levels of NKA that were present in 100% seawater fish. As NKA drives ion transport the higher levels of this transporter in the seawater gill suggest an overall higher level of transport activity. The relative differences in Na^+ influx properties of fish reflect the different ionic challenges these fish face. A freshwater fish is constantly losing ions to the environment and therefore must absorb Na^+ ions back into their body in order to maintain homeostasis. Conversely fish in seawater are faced with diffusive ion influx and therefore do not require high affinity Na^+ influx pathways. In fact, the presence of Na^+ influx in seawater fish initially seems to be counterproductive. It is, however, important to note that pathways of ion transport in the gill are strongly linked to other gill-based processes such as acid-base metabolism and nitrogen excretion. For example, proton excretion in fish may occur via the NHE, which exchanges an intracellular proton with an environmental Na^+ (Claiborne et al., 1999). Although Na^+ influx is not required in seawater, proton excretion still is. Consequently Na^+ influx must still occur in marine fish in order to drive acid-base balance. A similar mechanism occurs for ammonia excretion (Wilkie, 1997). The significant differences in Na^+ transport capacity between the 100% seawater-acclimated fish and other groups may therefore reflect a higher demand for acid-base balance and/or ammonia excretion in this group. There is sound physiological evidence for this. For example, in seawater fish drink, and secrete base into the gut in order to precipitate ions and create a favourable gradient for water influx (e.g. Gilmour et al., 2012). However the increased demand for base also creates an elevated acid status (through the actions of carbonic anhydrase in the gill), and this therefore increases gill acid excretion (Claiborne et al., 1994), which, if linked to Na^+ uptake would increase Na^+ influx and therefore explain the observed pattern in the current study.

The inanga used in these experiments were all sourced from freshwater environments and then acclimated to other salinities. Their efficient performance in freshwater may be a reflection of this and it would be interesting to repeat the same experiment on seawater juveniles (whitebait). Similarly, adult inanga spend most of their time in freshwater. Although they show excellent tolerance for acclimation to other salinities it may be that the

characteristics of their Na^+ influx differ from juvenile forms that are 'hard-wired' for life in a marine environment.

4.5.2 NKA Activity

4.5.2.1 Impact of salinity

Inanga spend most of their life cycle in freshwater and brackish water. On a daily basis they encounter both freshwater and brackish salinities as a consequence of tidal cycles. In this study freshwater and 50% seawater-acclimated inanga showed similar NKA activities. This suggests that in natural environments the assortment of transporters that achieve Na^+ uptake may be able to adequately deal with elevated salinities, and that no increase in NKA levels are required. Consequently acclimation to 50% seawater would not require a significant change in gill structure and function. This would be a valuable attribute as it would mean that inanga would not need to deal with the large energy demands associated with acclimation/gill remodelling (Febry and Lutz, 1987) in order to enter brackish waters. Conversely there was a significant change in NKA activity in 100% seawater, suggesting a significant change in the functional properties of the gill. The increased NKA activity seen in freshwater is most likely a reflection of the increase proliferation of MRCs (Chapter 3). The pattern of increased NKA activity in euryhaline fish acclimated to seawater is consistent with most previous studies (Tipsmark et al., 2002; Richards et al., 2003; Hawkings et al; 2004; Bystriansky et al 2006).

4.5.2.2 Impact of hormones

4.5.2.2.1 Cortisol

Hormones play an integral role in adaptation to different salinities. Cortisol is typically known as the ‘seawater-adapting' hormone but it has been shown to play a role in freshwater adaption (McCormick, 2001). NKA is involved in both salt excretion and ion uptake in the gill of teleost fish (Evans et al., 2005), and in both freshwater and seawater fish exogenous cortisol has been shown to increase NKA activity to aid adaptation (McCormick, 1995, 2001; Mancera et al., 2002). However in the data presented in this chapter, the NKA activity of

freshwater, 50% seawater and 100% seawater-acclimated inanga gills did not increase when treated with cortisol. Decreased NKA activity has been observed in conjunction with increased endogenous cortisol in plasma in some studies (e.g. Wu et al., 2008), so the decrease of NKA activity observed in this chapter is not without precedent. High plasma cortisol concentrations result in a higher plasma glucose that fuels the "fight or flight' response. This results in the diversion of energy away from all but essential homeostatic functions (Schreck, 1981). If *de novo* expression of NKA is not considered essential in a stressful situation, then a decrease in NKA activity may be observed.

Exogenous treatments with hormone such as cortisol and prolactin have long been used as a technique to decipher ionic and osmotic regulation. For accurate interpretation of results, a suitable control for the injection procedure itself must be run in parallel with the hormone treatments. In this study a sham control as well as a no-treatment control was used. The sham control consisted of an injection of vehicle (oil) only and therefore accounted for any effects of the injection and handling. Acute stress can be simulated with a single injection of cortisol which can result in the release of endogenous cortisol (Mommsen et al., 1999). Cortisol is the major corticosteroid produced in fish and dramatic rises in plasma cortisol concentrations are seen in response to stress (Mommsen et al., 1999).In freshwater-acclimated inanga, NKA activity showed a general decrease in response to the sham control relative to the true control. This was similar to the response of the cortisol treatment. This suggests the injection protocol was stressful for the fish and the cortisol supplement along with endogenous cortisol may have resulted in the significant decrease in NKA activity.

McCormick (2001) hypothesised that cortisol is important in freshwater as it induces ion uptake via an increase in NKA activity. This has been supported by studies using Atlantic salmon (*Salmo salar*) (McCormick et al., 2008; Tipsmark and Madsen, 2009). In contrast freshwater inanga treated with 50 µg/g cortisol showed a significant decrease in NKA activity. This suggests that if cortisol does play a role in the stimulation of ion uptake in freshwater inanga, it is by a route other than by increasing NKA activity. Conversely, the discrepancies between this study and others may be a reflection of the species of fish used and/or the treatment regime. McCormick et al. (2008) administered one injection of 50 µg/g of cortisol per day over six days whereas Tipsmark and Madsen (2009) administered one injection of 4 µg/g of cortisol per day over two days. Both studies used Atlantic salmon and

saw increased NKA activity. While inanga and Atlantic salmon are both diadromous, inanga spend most of their lives in freshwater while adult Atlantic salmon are predominantly in seawater. Therefore their life histories may account for the different responses to cortisol. Another possible source of difference is the levels of circulating cortisol that are available to the receptors. The actual circulating concentration of cortisol may not reflect the dose administered due to species differences, stress, maturity, salinity and nutritional status (Mommsen et al., 1999). Plasma cortisol levels were not measured in this experiment due to the small size of the inanga used and their inability to yield sufficient quantities of plasma for analysis. Therefore the actual circulating concentration of cortisol within the fish is unknown.

4.5.2.2.2 Prolactin

As 'the' freshwater-adapting hormone, prolactin has been show to regulate several aspects of ion regulation such as lowering the water permeability of the gill and increasing ion uptake by stimulating the development of freshwater-type MRCs (Mancera and McCormick, 2007). The limited work that has been conducted with prolactin has revealed a variety of responses in NKA activity (Madsen and Bern; 1992; Kelly et al., 1999; Mancera et al., 2002; Sangiao-Alvarellos et al., 2006). It has been suggested that this variety in results may reflect in part, from the difference in the relative importance of NKA in ion uptake among freshwater teleosts (Mancera and McCormick 2007). Therefore the decrease in NKA seen in prolactin-treated freshwater-acclimated inanga may be a reflection of the reduce role NKA plays in ion absorption from hypo-osmotic environments.

4.5.2.2.3 Prolactin and cortisol

It has been suggested that cortisol and prolactin work together to promote acclimation to low salinities (McCormick, 2001). While prolactin supports the development and maintenance of freshwater MRCs, cortisol promotes freshwater acclimation by maintaining ion transporters and MRCs (McCormick, 2001). This was not supported in the current study as the cortisol-prolactin treatment had no effect on freshwater NKA activity, relative to the sham group. However, in 100% seawater-acclimated inanga, a significant decrease in NKA activity was

observed upon cortisol and prolactin treatment. Little work has been conducted using cortisol in combination with prolactin on seawater-acclimated fish. Seawater-acclimated salmon showed no change in NKA activity upon treatment of cortisol and prolactin (Tipsmark and Madsen, 2009). Clearly further investigations are needed to show if these differences are species-specific or another reason is evident.

4.5.2.2.4 Methodological considerations

Hormone treatments were run one salinity at a time and all effort was made to lessen any variance between salinity experiments. All fish were approximately the same size (1-1.5g) and the acclimation procedure progressed at the same rate. However due to the disruption caused by the Christchurch earthquakes in 2011, the seawater-acclimated inanga hormonal experiment was carried out approximately 8 weeks after the experiments in freshwater- and 50% seawater-acclimated fish. Inanga display seasonal variations on behaviour (i.e. spawning and migration) (McDowall et al., 1984) so the temporal separation of the experiments may have been a confounding factor. The expression of hormone receptors has been shown to vary according to reproductive cycles and migration (Shiraishi et al., 1999; Kiilerich et al., 2007b). If at the time of treatment the expression of a hormone's particular receptor is low, then administration of that hormone may have little effect.

Due to the inaccessibility of teleost-derived hormones, synthetic and/or heterogeneous hormones are routinely used in fish studies (McCormick, 1995). While ovine prolactin has been shown to be an almost universal ligand from prolactin receptors in vertebrates, it does show less affinity for teleost receptors than the fish-derived hormones (Prunet and Auperin, 1995). It has been shown that a hormone from one species may have a very different activity profile and potency when given to other, even closely-related, species (Hazon and Balment, 1998). Consequently the effects seen may not necessarily be reflective of the native hormones, and could explain why differences between this study and previous findings exist.

The NKA assay measures the activity of the NKA transporter population but does not provide any insight into the individual transporters that comprise that population. As described in Chapter 1 the NKA is made up of three subunits, each of which has different isoforms (Blanco and Mercer, 1998). A certain salinity or hormone may result in a change in subunit

isoform, without having an overall significant effect on NKA activity. Hence hormonal effects could cause subtle changes in the NKA transporter that may not be reflected in an increase or decrease in activity (Kiilerich et al., 2011). This concept is investigated further in Chapter 5 – Molecular Expression of NKA Isoforms.

4.6 Conclusions

Adult freshwater inanga display a saturable, high affinity, low capacity uptake system for Na^+ influx indicating they are highly adept at extracting Na^+ from their freshwater environment to counteract diffusive loss. Freshwater- and 50% seawater-acclimated inanga displayed similar levels of NKA activity but when acclimated to 100% seawater, inanga increased NKA activity, presumably in an effort to excrete the excess Na^+, gained by diffusion from the hyper-osmotic environment. This increase in NKA activity was most likely a reflection of the increased proliferation of MRCs seen in Chapter 3. Freshwater-acclimated inanga significantly decreased their NKA activity in response to cortisol which contrasts with other studies. In 100% seawater acclimated inanga, a significant decrease in NKA was observed upon cortisol and prolactin treatment. The incongruity of these responses may be a reflection of the differences between species and experimental design and therefore warrant further investigation. These results may also be potentially compromised by the underlying effect of stress induced by the handling and hormonal treatments themselves.

CHAPTER 5 MOLECULAR EXPRESSION OF NKA ISOFORMS

5.1 Introduction

NKA is the key entity involved in cellular ion transport in all cells, including the gills of fish, a tissue exquisitely designed to regulate ion exchange. Owing to the variety of different environmental factors that are known to impact ion transport in the gills, it is important that NKA is responsive to environmental change. For example, as shown in Chapter 4, the levels of NKA activity can change in response to salinity. However in recent years it has become apparent that changes in NKA can also be more subtle. Molecular characterisation of NKA in fish led to the discovery of the presence of different isoforms of the NKA subunits (see Chapter 1) in species such as the European eel (*Anguilla anguilla*, Cutler et al., 1995), killifish (*Fundulus heteroclitus*, Semple et al., 2002) and rainbow trout (*Oncorhynchus mykiss*, Richards et al., 2003). As well as identifying five different α isoforms, Richards and colleagues also demonstrated "isoform switching", a differential expression pattern upon salinity transfer. Upon transfer to seawater, a decrease in α1a expression and an increase in α1b expression were observed in the gill tissue.

The discovery of this phenomenon has important consequences for our understanding of NKA. Traditionally NKA changes have been assessed by monitoring total NKA activity and although this approach has been useful, it represents the summed activity of the many different isoforms and may mask the contribution of the individual isoforms present (Glover, 2007). The current thought is that each isoform provides different functionalities to the NKA which may be invoked under different conditions (Hwang et al., 2011). Advancements in molecular technologies such as quantitative PCR (qPCR) have allowed identification of individual isoforms and has allowed monitoring of how these may change in response to salinity in osmoregulatory tissues.

Endocrine factors such as cortisol and prolactin are responsible for coordinating the physical changes necessary during changes in salinity (Sakamoto and McCormick, 2006). As NKA is central to salinity acclimation, its response to cortisol and prolactin has previously been investigated. The incongruity of the results has lead to the examination of the NKA isoforms

which contribute of the overall enzymatic activity of NKA. Investigations into the relationship between isoform expression and hormones, is still in its infancy and only a few studies have been performed. Cortisol has been shown to increase the expression of α1a and α1b in freshwater Atlantic salmon (Kiilerich et al 2007a; McCormick et al., 2008) and expression of α1a isoform has shown to be dependent on prolactin in freshwater tilapia (Kiilerich et al., 2011).

5.1.1 Technical overview

In the Central Dogma reactions of molecular biology, genetic information is passed from DNA to RNA via transcription and then the RNA is translated into a protein (Alberts et al., 2002). The relationship between messenger RNA (mRNA) and proteins leads to the underlying assumption that differences in mRNA levels result in different protein levels and therefore different biologically relevant phenotypes (Gry et al., 2009). Real time reverse transcription qPCR is now the most common method for quantifying gene expression and variations in mRNA levels (Orlando et al., 1998; Van Guilder et al., 2008).

There are 4 steps that make up the real time RT-qPCR reaction:

1. Isolation of mRNA from the tissue of choice
2. The reverse transcriptase-dependent conversion of mRNA into single stranded complementary DNA (cDNA)
3. The amplification of cDNA using PCR
4. The detection and quantification of PCR products in real time

In the first step, tissue samples are collected and mRNA is isolated. There is a variety of different methods used for isolation and these include organic extraction and solid phase isolation. The specific method used depends on the tissue type and the amount of RNA to be isolated (Pfaffl, 2004). The mRNA is then converted into single stranded cDNA using a reverse transcriptase enzyme. mRNA must be converted into cDNA as the DNA polymerase used in PCR can only use DNA as its template (Valasek and Repa, 2005). The reverse

transcriptase transcribes single stranded RNA into double stranded cDNA using random primers to initiate first strand synthesis. The small numbers of target cDNA is then amplified using PCR.

In PCR the double stranded cDNA is first heated to ~95°C to denature the two strands. The temperature is then dropped to ~54°C, allowing sequence-specific primers to anneal to the complementary sequence on the cDNA. Finally the temperature is raised to ~72°C to allow the extension of the primers by the DNA polymerase enzyme and therefore to produce a complementary strand of DNA. The three PCR cycles are repeated a total of 40 times to produce an exponential number of cDNA copies.

In the final step of real time qPCR, the progress of the PCR is monitored as it happens (i.e. in real time) by the use of a PCR-product detection dye. The most common detection method is intercalating dyes, such as SYBR Green, which binds to the double-stranded DNA (dsDNA) formed during the PCR. Upon binding to dsDNA, the SYBR Green emits fluorescence that is 1,000 fold greater than when it is free in solution (Wittwer et al., 1997). The fluorescence is measured at the end of every cycle and because fluorescence intensity is proportional to double-stranded DNA concentration, the amount of product produced in each cycle can be quantified. The greater the quantity of target DNA in the tissue, the more rapidly an increase in fluorescent signal is seen.

The fluorescent signals are collected and graphed by software to produce amplification curves (Figure 5.1). The threshold line represents the point at which the fluorescent signal begins to increase above the background fluorescence. As the reaction progresses and more double-stranded DNA is produced, more fluorescence is emitted. The cycle number at which the fluorescence signal for each reaction line (represented by different starting cDNA levels in Fig 5.1; see below) crosses the threshold is known as the threshold cycle (C_t). The C_t value is inversely related to the amount of starting cDNA template. For example in Figure 5.1 sample A has a lower C_t value than B, C or D indicating a higher initial amount of cDNA present.

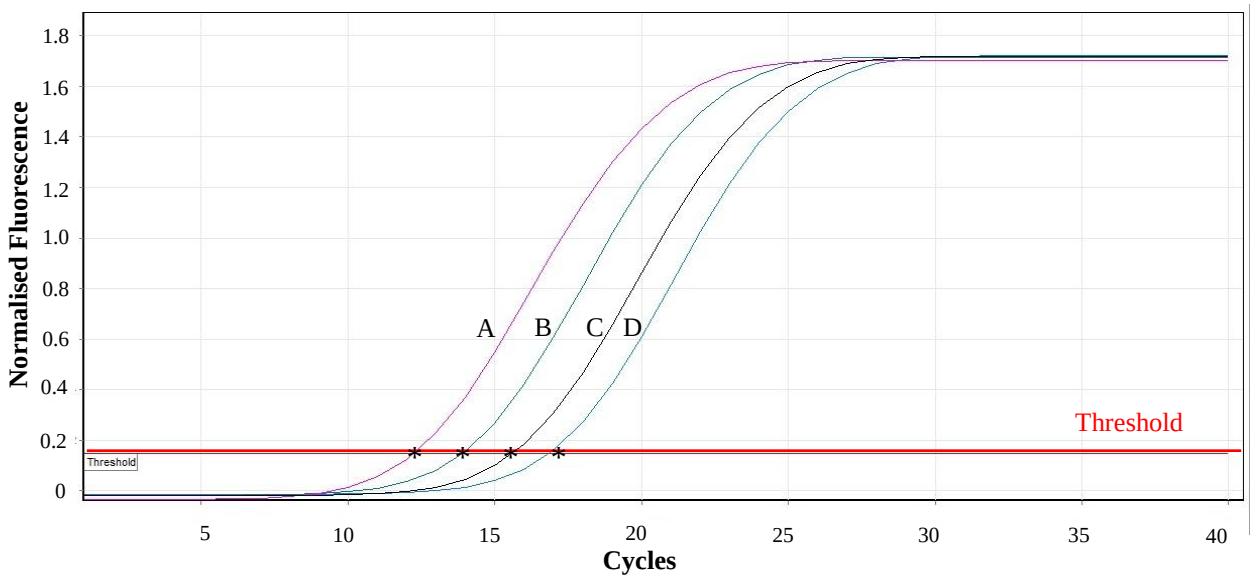

Figure 5.1 Amplification curves of qPCR reaction. Asterisks (*) indicated the threshold cycle (C_t) for each of the four samples A, B, C and D..

When the qPCR reaction is operating at 100% efficiency, the amount of product will double during each cycle. To determine the efficiency of a reaction, a dilution series of representative cDNA is used to make a standard curve (e.g. the multiple reaction curves seen in Fig. 5.1). The log of the concentration is plotted against the C_t value for the corresponding concentration and the slope of the line formed is calculated. The efficiency can then be calculated with the following Equation 5.1:

Equation 5.1 $\text{Efficiency} = 10^{(-1/\text{slope})} - 1$

Ideally the efficiency of the reaction should be 1 i.e. 100% efficiency but efficiency ranging from 0.9 – 1.1 (90% - 110%) is acceptable (Bustin, 2004).

There are two different methods for analysing the data arising from qPCR assessment: absolute quantification and relative quantification. Absolute quantification determines the initial input copy number of the gene of interest. This method requires the samples to be compared against a sample with a known copy number. The most common mechanism of relative quantification is the Comparative ($2^{-\Delta\Delta Ct}$) method (Livak and Schmittgen, 2001). In

this technique the expression of a gene of interest in an experimental sample is compared to a control sample and variations in the amounts of total RNA in the starting tissue are normalised by the use of a reference gene. The fold difference is calculated using the following Equation 5.2:

Equation 5.2 $2^{-\Delta\Delta Ct}$

where $\Delta\Delta C_t = \Delta C_t$ sample $- \Delta C_t$ control

ΔCt sample $= C_t$ gene of interest $- C_t$ reference gene

ΔC_t control $= C_t$ gene of interest $- C_t$ reference gene

Ideally a reference gene is a one that is relatively stable in expression over a variety of experimental conditions, and commonly more than one reference gene is used to account for any possible variability (Vandesompele et al., 2002; Olsvik et al., 2005). Some commonly used reference genes are β-actin (βA), 18S rRNA and glyceraldehyde-3-phosphate dehydrogenase (GAPDH). For the Comparative method to be valid, the amplification efficiencies of the gene of interest and reference genes must be approximately equal (Livak and Schmittgen, 2001).

5.2 Chapter Aims

The aim of this chapter is to examine the gene expression patterns of the NKA isoforms α1a, α1b and α1c in the gills of inanga acclimated to freshwater, 50% seawater and 100% seawater. and determine if inanga show salinity-dependent expression patterns.

Endocrine factors such as cortisol and prolactin have been shown to play a role in NKA isoform expression but their exact effect in unclear. Therefore the impact of the exogenous cortisol and prolactin on the expression of the NKA isoforms will also be assessed using a intraperitoneal hormone injection protocol.

5.3 Methods

5.3.1 Tissue isolation

To examine the effect of salinity on isoform expression inanga were acclimated to freshwater, 50% seawater and 100% seawater, and gill tissue was isolated and prepared as described in section 2.4.2. To assess the impact of the hormones prolactin and cortisol inanga were first acclimated to freshwater, 50% seawater and 100% seawater before being treated with hormones as described in section 2.3.

5.3.2 RNA extraction

Total RNA was extracted from the gill tissue using TRIzol Reagent (Invitrogen) following the manufacturer's instructions. Seven hundred mL of TRIzol Reagent was added to each tube containing four gill arches and the tissue was homogenised using an Omni Bead Ruptor 24 and 2 mm ball bearings. The tubes were incubated at room temperature for 5 minutes before 200 mL of chloroform was added to each tube. The tubes were then capped and shaken vigorously for 15 seconds and incubated at room temperature for a further 3 minutes. Tubes were then centrifuged at 4°C at 12,000 g for 15 minutes. The top colourless aqueous phase was removed from each tube with a pipette and placed into a fresh, labelled 1.5 mL tube. Isopropyl alcohol (500 µL) was added, inverted to mix and incubated for 10 minutes before being centrifuged at 12,000 g for 10 minutes at 4°C to form an RNA pellet. The supernatant was removed from each tube using a pipette, taking care not to disturb the pellet. The pellet was then washed with 500 µl of 75% ethanol and vortexed briefly. Tubes were then centrifuged at 7,500 g for 5 minutes at 4°C and the supernatant removed with a pipette and discarded. The tubes were then inverted to ensure all of the 75% ethanol was removed. The total RNA pellet was then dissolved in 25 µL of molecular grade RNase free water and incubated in a heat block for 10 minutes at 55-60°C.

5.3.3 DNase Treatment

Any contaminating DNA present in the extracted RNA can be used as a template in the reverse transcription reaction (Bustin, 2004). This can lead to interference and inaccurate quantification of RT-PCR products. DNases are enzymes that degrade DNA and can be used to remove contaminating DNA from a sample. Each extracted RNA sample was treated with DNA-*free* (Invitrogen) following the manufacturer's instructions. Ten µL of total RNA was diluted into 30 µL of molecular-pure water and 4 µL of 10X DNase I Buffer and 1 µL of rDNase I were then added. The sample was mixed gently and incubated in a heat block at 37°C for 30 minutes. The rDNase was inactivated by the addition of 5 µL of Inactivation Reagent, mixed well and incubated for 2 minutes while occasionally mixing. The sample was then centrifuged at 10,000 g for 1.5 minutes to pellet the rDNase. The supernatant, containing the RNA, was then carefully transferred into a fresh tube.

5.3.4 RNA Analysis

5.3.4.1 RNA Integrity

Analysis of total RNA integrity was determined by agarose gel electrophoresis. Intact RNA should appear as sharp bands on the stained gel. A band at ~5 kb represented 28S and a band at ~1.9kb represents 18S. The presence of smears rather than bands indicates the RNA sample is degraded. The 28S band should also appear twice as bright as the 18S band and any change in this ratio also suggests degradation has occurred (Jankowski and Polak, 1996). RNA samples were mixed with bromophenol loading dye and were separated on a 2% agarose gel containing 0.01% SYBR-Safe dye (Invitrogen) at 100 volts for approximately 60 minutes. A Hyperladder I molecular weight ladder was included to allow the size of the bands to be determined. RNA bands were imaged using a Syngene G:Box Gel Documentation system (Synoptics Group).

5.3.4.2 Concentration and Purity

The concentration and purity of the extracted and DNA-free total RNA in each sample was determined using a ND1000 NanoDrop spectrophotometer (ThermoScientific). RNase-free molecular grade water was used to clean the spectrophotometer pedestal before use and to zero the instrument before assessment of the samples. The NanoDrop spectrophotometer determines RNA concentration (ng/µL) by analysis of the absorbance at 260 nm. Sample purity can be determined by assessing the ratio of the absorbance at 260 nm/280 nm ($A_{260/280}$), and 260 nm/230 nm ($A_{260/230}$). Good quality RNA will have an $A_{260/280}$ ratio of 1.8 – 2 and an $A_{260/230}$ of around 2 (Wilfinger et al., 1997). Anything less than these values may indicate the presence of proteins, salts, solvents or other contaminants that absorb at or near 230 and 280 nm. Each sample was analysed in duplicate and concentration and purity were recorded. Samples that did not meet the above criteria were discarded or re-extracted.

5.3.5 Reverse Transcription (RT)

The isolated RNA was converted into cDNA using a High-Capacity cDNA Reverse Transcription Kit (Invitrogen), following the manufacturer's instructions. This kit uses random primers to initiate cDNA synthesis and convert all RNA present into cDNA. Each RT reaction was set up as shown in Table 5.1. No-RT controls for all samples were also prepared at the same time. These controls show if there are any contaminants present in the RNA that can be amplified instead of the target, and consist of all the mastermix components except for the Multiscribe RT enzyme. Water was added instead of the enzyme to make up the reaction volume.

The RNA was diluted with molecular grade water to give a concentration of 100 ng/µL. Ten µL of diluted RNA and 10 µL of master mix was added to a labelled 0.5 mL PCR tube and gently mixed by flicking. The PCR tube was briefly centrifuged and then loaded onto the thermal cycler (Total Lab Solutions LTD) and run using the thermal cycling protocol in Table 5.2.

The quantity of cDNA produced by the RT reaction was not directly determined, so cDNA quantity was assumed to be equal to the quantity of RNA used as a template (i.e. 1000 ng per

20 µL reaction). The cDNA was stored at -80^{o}C until use. All experimental samples were reverse transcribed at the same time to eliminate inter-experimental variation.

Table 5.1 Mastermix of RT reaction components

Component	**RT reaction Volume (µL)**	**No RT reaction Volume (µL)**
10x RT Buffer	2	2
25x dNTP	0.8	0.8
10x Random Primers	2	2
Multiscribe RT	1	-
RNase Inhibitor	1	1
Nuclease-free H_2O	3.2	4.2
Total per reaction	**10**	**10**

Table 5.2 Thermal Cycling Conditions

	Step 1	**Step 2**	**Step 3**	**Step 4**
Temperature (°C)	25	37	85	4
Time (min)	10	120	5	∞

5.3.6 Sequences

Sequences for the inanga α1a (JQ885968), α1b (JQ885969), α1c (JQ885968) isoforms and 18S (HQ615533) were accessed from GenBank. Limited molecular work has been conducted on inanga and no other sequences for potential reference genes were available. Beta actin (βA) and elongation factor 1a (EF1a) are two genes that have been shown to be good candidate reference genes for qPCR evaluation in salmon (Olsvik et al., 2005). These authors ranked EF1a in the top two most suitable genes with βA fourth and 18S was ranked last of the six genes evaluated in the gill tissue. As there was no sequence available for inanga βA and EF1a, primers for these genes were based on conserved regions of sequences from closely related Salmonidae fish and (McDowall, 1990; Johnson and Patterson, 1996; McDowall, 1997). βA and EF1a sequences for three species *Oncorhynchus mykiss*, *Oncorhynchus tschawytscha* and *Salmo salar* were obtained from GenBank (Table 5.3). sequences were aligned using the alignment software MEGA Version 5.0 (Tamura et al., 2011). A conserved region was identified and primers designed for this region.

Table 5.3 GenBank accession numbers of sequences for reference genes

Species	**β-Actin**	**EF1a**
Oncorhynchus mykiss	AF157514.1b AJ438158.1b	AF498320.1 NM001124339.1
Oncorhynchus tshwaytscha	FJ546418.1 FJ890357.1	FJ890356.1
Salmo salar	BG933897.1	AF321836.1

5.3.7 Primer Design and Optimisation

Selection of appropriate primers is a fundamental step in a qPCR reaction. Primers must be specific to the intended target. If primers have poor specificity they may inadvertently prime and amplify off-target sequences. Primers were designed using IDT online tool PrimerQuest^{SM} (www.idtdna.com) using the guidelines outlined in Appendix A. in addition primer optimisation allows specificity, sensitivity and reproducibility of the assay (Nolan et al., 2006). This is an important step, especially when working with highly conserved sequences as in this study. Primer optimisation protocols are outlined in Appendix A.

5.3.8 Primer ordering and reconstitution

All primers were ordered from IDT technologies and were received in a desiccated and desalted form. Primers were centrifuged and then resuspended to a stock concentration of 1 mM using molecular pure water according to the manufacturer's instructions.

5.3.9 qPCR of experimental samples

Experimental samples were run as 20 µL reactions in duplicate, using the parameter in Table 5.4 as determined by the various optimisation steps in Appendix A). EF1a and βA primers were deemed not specific enough so only 18S was used as a reference gene (for details see Appendix A). Standard curves were placed in every qPCR run to continually assess reaction efficiency. The cDNA for the standard curves was made up of pooled experiment samples to ensure the entire dynamic range of the specimens was covered. One primer set was analysed at a time and all experimental samples including the experimental controls were run simultaneously. Realtime qPCR was performed on a Rotor-Gene Q Realtime PCR instrument (Qiagen), in strip tubes and a 72 reaction rotor, using the thermal cycling program in Table 5.5.

Table 5.4 qPCR reaction components for experimental samples

Reaction components	**Volume (µL) per reaction**	**Final concentration**
Water	8.2	-
Forward primer - α1a = 7.5 µM - α1b, α1c, 18s = 10 µM	0.4	α1a = 150 nM α1b, α1c, 18s = 200 nM
Reverse primer - α1a = 7.5 µM - α1b, α1c, 18s = 10 µM	0.4	α1a = 150 nM α1b, α1c, 18s = 200 nM
KAPA SYBR® qPCR FAST Master Mix (2X)	10	1X
Template DNA (100 ng/µL)	1	5 ng/µL

Table 5.5 qPCR thermal cycling conditions for experimental samples

Step	**Temperature °C**	**Duration**	**Cycles**
Enzyme activation	95	10 minutes	hold
Denature	95	30 seconds	40
Annealing	60	30 seconds	
Extension	72	30 seconds	
Melt curve analysis	60 - 95	1 second per step	

5.3.9.1 Controls

To ensure validity and integrity of the qPCR, a number of controls were run alongside the standard curve and experimental samples. A no-amplification control containing all reaction components except the KAPA SYBR® Fast qPCR master mix (2X) was run in every qPCR experiment. Fluorescence produced in this sample would be indicative of a fluorescent contaminant present in the reaction. A no-template control consisted of all reaction components except the template cDNA of interest. Any amplification detected in this sample would be indicative of primer dimerisation or a contaminating template. Finally a no-reverse transcription control (no-RT) from the reverse transcription experiment (section 5.2.5) was also run. Any amplification seen in this control would indicate DNA contamination in the starting RNA that was not removed by the DNA-*free* treatment.

5.3.10 Data analysis

Standard curves were generated using Rotor-Gene Q Series Software (Qiagen). Samples that did not fall within the curve were repeated after undergoing a dilution. Samples that did not amplify correctly were discarded. Melt curve analysis was performed to identify any primer dimerisation or misamplification events and these samples were repeated. Samples which showed a discrepancy between the duplicate samples were identified and repeated. Data was exported to an Excel spreadsheet and further analysed using the Delta Delta Ct method (Livak and Schmittgen, 2001) (Equation 5.2) where the relative quantity of the NKA α1a, α1b and α1c mRNA was normalised to the reference gene 18S and expressed as a fold-change relative to the control in each experiment.

All data were subjected to tests of normality (Kolmogorov-Smirnov test) and homogeneity of variance (Levene's test) using SigmaPlot Version 11.0. Data that passed these assessments were analysed parametrically via one-way analysis of variance (ANOVA) and pairwise multiple comparison procedures (Holm-Sidak method or Dunn's post hoc analysis) using SigmaPlot. Data are presented as the mean fold-change relative to the control and standard error of the mean (SE) for each treatment group.

5.4 Results

5.4.1 RNA analysis

Gel analysis for assessment of RNA integrity showed two distinct bands denoting 28S and 18S (Figure 5.2). Some degradation of the RNA was also evident by the slight smearing either side of the bands.

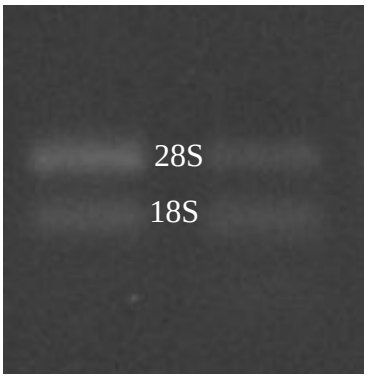

Figure 5.2 Electrophoresis gel of extracted RNA. Two bands are present in each sample showing 18S and 28S RNA.

NanoDrop spectrophotometer analysis showed the average $A_{260/280}$ ratio of the RNA samples was 1.83 and the average $A_{260/230}$ ratio was 1.9, indicating good quality RNA. Although the isolated RNA concentrations varied amongst samples, all were diluted to the same concentration for the RT reaction (100 ng/µL). The RNA concentration dropped by 25% after DNA-*free* treatment, so concentration readings were taken after this treatment.

5.4.2 DNase Treatment

Treatment with DNA-*free* resulted in the appearance of only a single band at ~100 bp and therefore a single product on the gel (Figure 5.4). Untreated cDNA resulted in two products indicating genomic DNA contamination of the initial RNA sample.

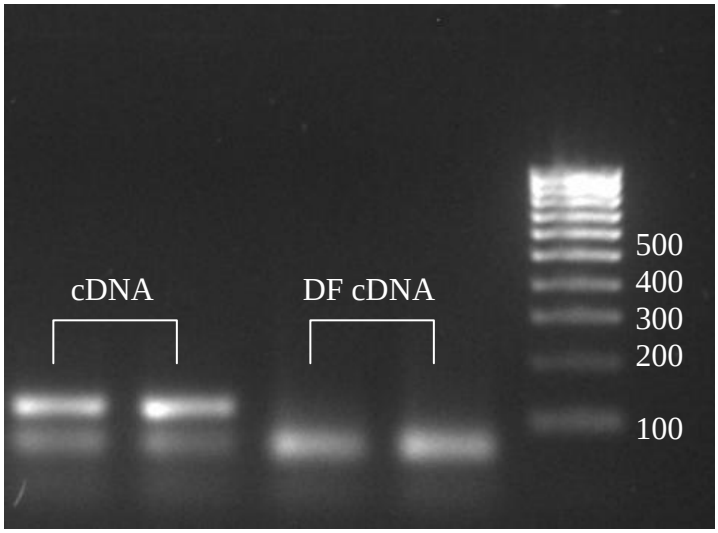

Figure 5.3 Electrophoresis gel image of DNA-*free* treatment (DF cDNA) and untreated cDNA (DNA) samples. A DNA-*free* treated and untreated RNA samples were reversed transcribed to produce cDNA and then run on a gel for comparison. The Hyperladder IV indicates the band size in basepairs.

5.4.3 Primer Selection

The primers for NKA α1a were designed by Mauricio Urbina (University of Canterbury) and Prof. Patricia Schulte (University of British Columbia) for ongoing work that is currently unpublished. Primers for NKA α1b, NKA α1c, 18S, EF1a and βA were designed as part of this thesis and, along with the α1a primers, are shown in Table 5.6.

Table 5.6 Sequences and parameters of primers used for qPCR

Gene	Primers	Primer length (bp)	Product length (bp)	GC content %	T_m °C
α la	**F 5'** CAT CGT AAC AGG AGT GGA AGA GG **3'** **R 5'** AAG GGC GAC ATC TCT GGA ATC **3'**	F 23 R 21	99	F 52.2 R 52.4	F 56.6 R 56.6
α 1b	**F 5'** AGC AAT GGA CGT ACG AGC AGA GAA **3'** **R 5'** AGA TGA TCA GGT CGG CCC ATT GAA **3'**	F 24 R 24	99	F 50 R 50	F 59.9 R 60.1
α 1c	**F 5'** ACT GGT GAA TCT GAG CCA CAG TCT **3'** **R 5'** CAC ACA GTT GGT GGA GAA GAA AGC **3'**	F 24 R 24	96	F 50 R 50	F 59.6 R 58
18S	**F 5'** AGT TGG TGG AGC GAT TTG TCT GGT **3'** **R 5'** ACG CCA CTT GTC CCT CTA AGA AGT **3'**	F 24 R 24	116	F 50 R 50	F 60.5 R 59.6
EF1a	**F 5'** AAG TTC CTG AAG TCT GGA GAC GCT **3'** **R 5'** GCC TTG ATG ACA CCA ACA GCA ACA **3'**	F 24 R 24	146	F 50 R 50	F 59.5 R 60
β A	**F 5'** ATG AAG TGT GAC GTG GAC ATC CGT **3'** **R 5'** AGG TGA TCT CCT TCT GCA TCC TGT CA**3'**	F 24 R 26	109	F 50 R 50	F 60.1 R 60.9

5.4.4 qPCR of experimental samples

5.4.4.1 Standard curves

Standard curve analysis showed that the α1a, α1b, α1c and 18S primers had amplification efficiencies close to a value of one (Figure 5.4A, B, C and D). This means that the amount of PCR product generated from these primers was doubling with every cycle. This also means that the Delta Delta Ct method of analysing the data can confidently be used (Livak and Schmittgen, 2001). Subsequent runs with experimental samples all showed similar efficiencies (data not shown). The reaction efficiencies for α1a (1.00), α1b (1.02) and α1c (0.97) were all similar to that of the reference gene 18S (0.99) and therefore the Comparative method of relative quantification (relating expression of genes of interest to a housekeeping gene) was valid.

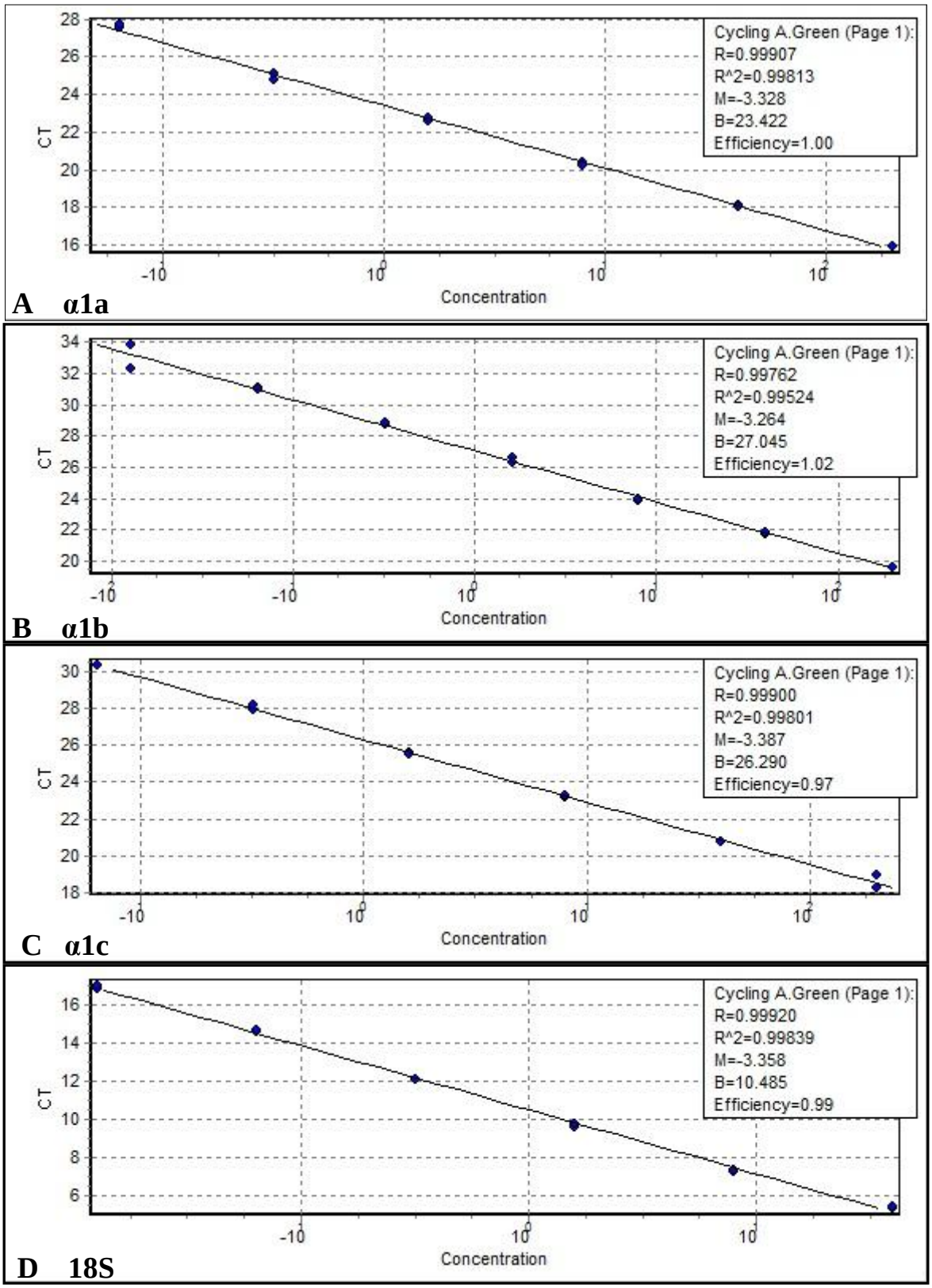

Figure 5.4 Standard curves for α1a, α1b, α1 and 18S. Curves were generated using Rotor-Gene Q series software.

5.4.4.2 Melt curve analysis

Melt curve analysis showed only one product was produced by each of the primers as indicated by the single peak at 84°C (Figure 5.5). A shoulder to the left of the product peak was also noted. In order to determine whether the shoulder might represent the presence of other products, a gel was run (Pål Olsvik, personal communication). This also confirmed the present of a single product (Figure 5.6).

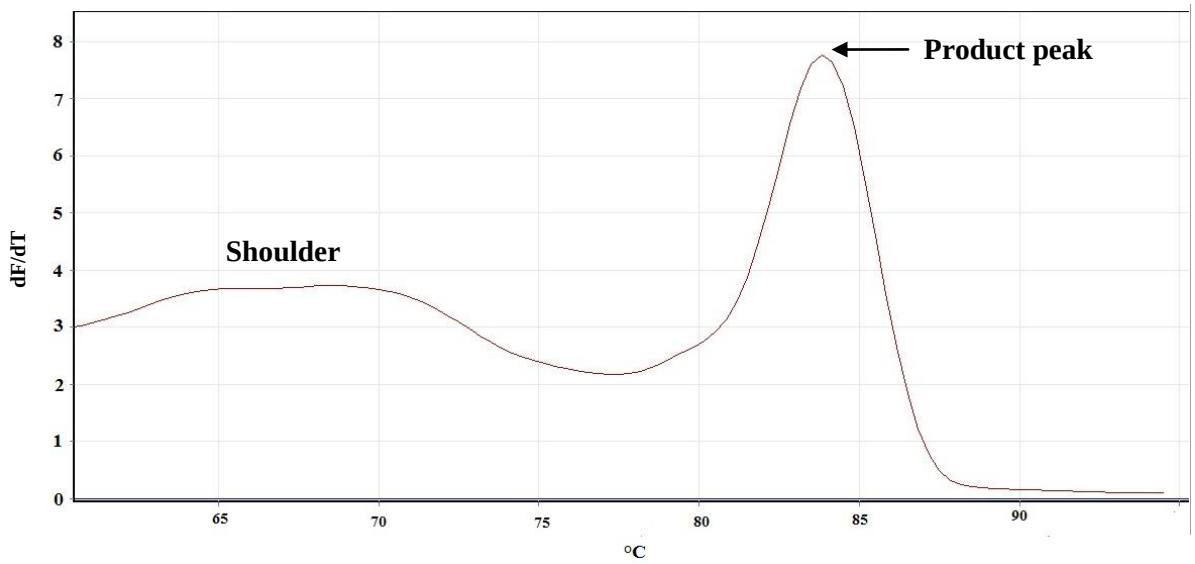

Figure 5.5 Melt curve analysis of 18S primers. Curves were generated using Rotor-Gene Q series software.

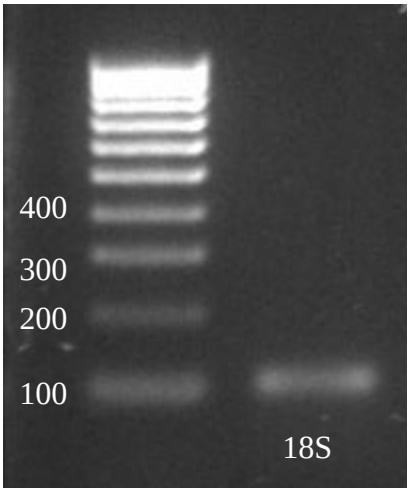

Figure 5.6 Electrophoresis gel of qPCR product using 18S primers. The presence of a single band indicates a single product is produced. The Hyperladder IV indicates the band size in basepairs.

5.4.5 Effect of salinity

Salinity-induced changes were observed in the α1a isoform of acclimated inanga. The α1a isoform showed a significant down-regulation of expression in the gill tissue of 100% seawater-acclimated inanga compared with the freshwater control and 50% seawater-acclimated inanga (Figure 5.7). Inanga acclimated to 50% seawater showed a 3.67 ± 0.94 fold increase in expression of α1a mRNA compared to the freshwater control, although this was not statistically-significant.

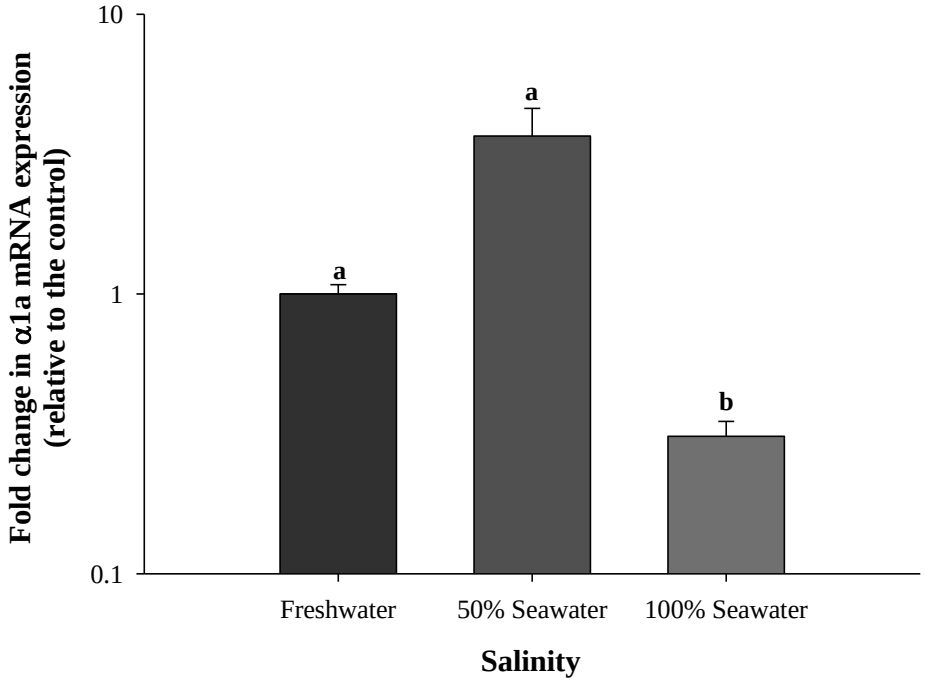

Figure 5.7 mRNA expression of the α1a NKA isoform in response to salinity. Plotted values represent the fold change in α1a mRNA expression is relative to the freshwater control ± SE of 6 individuals. Mean values sharing letters are not statistically significantly different ($p < 0.05$), as determined by Kruskal-Wallis ANOVA and Dunn's post hoc analysis (SigmaPlot).

There was a significant down-regulation of α1b mRNA expression in the 100% seawater-acclimated inanga compared to the freshwater control (Figure 5.8). Expression in the 50% seawater-acclimated gill tissue was not statistically significantly different from the freshwater control or the 100% seawater-acclimated inanga.

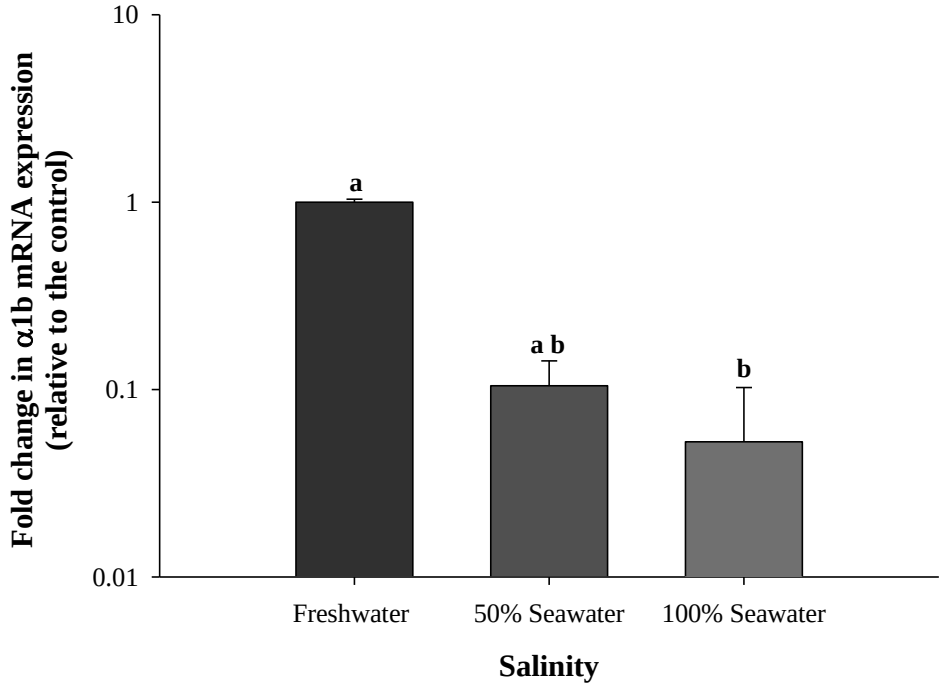

Figure 5.8 mRNA expression of the α1b NKA isoform in response to salinity. Plotted values represent the fold change in α1b mRNA expression is relative to the freshwater control ± SE of 6 individuals. Mean values sharing letters are not statistically significantly different ($p < 0.05$), as determined by Kruskal-Wallis ANOVA and Dunn's post hoc analysis (SigmaPlot).

There was a significant down-regulation of α1c mRNA expression in the 50% seawater-acclimated inanga compared to the freshwater control (Figure 5.9). Expression in the 100% seawater-acclimated gill tissue was not statistically significantly different from the freshwater control or the 50% seawater-acclimated inanga.

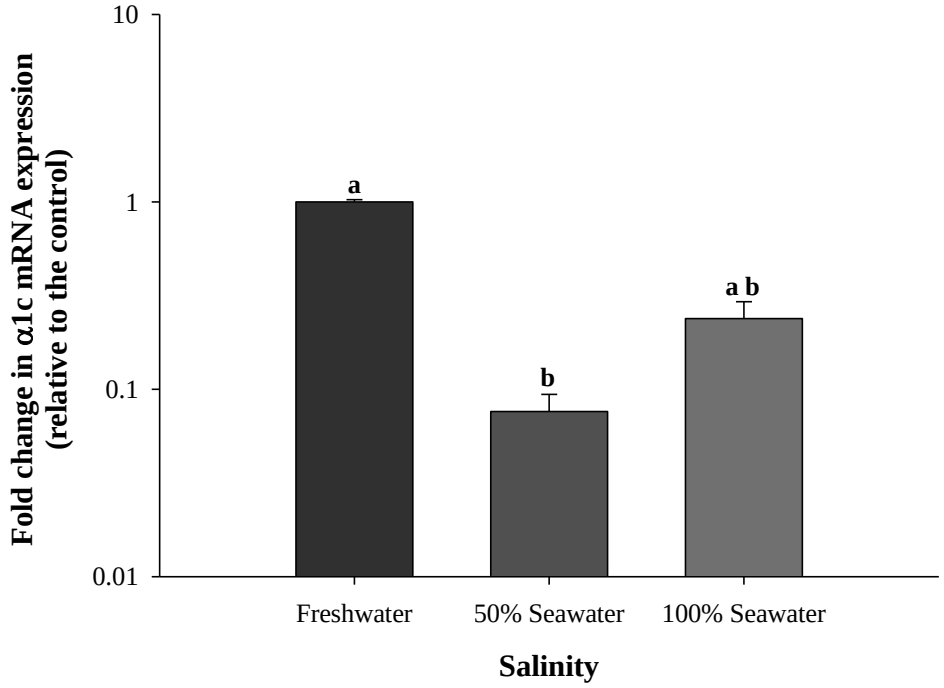

Figure 5.9 mRNA expression of the α1c NKA isoform in response to salinity. Plotted values represent the fold change in α1c mRNA expression is relative to the freshwater control ± SE of 6 individuals. Mean values sharing letters are not statistically significantly different ($p < 0.05$), as determined by Kruskal-Wallis ANOVA and Dunn's post hoc analysis (SigmaPlot).

5.4.5.1 Effect of hormones

A significant up-regulation of α1a mRNA expression was seen in freshwater-acclimated inanga treated with 5 µg/g prolactin compared to the untreated freshwater-acclimated control and freshwater-acclimated inanga treated with both cortisol (50 µg/g) and prolactin (5 µg/g) (Figure 5.10). None of the treatments was, however, statistically significantly different from the sham injection control.

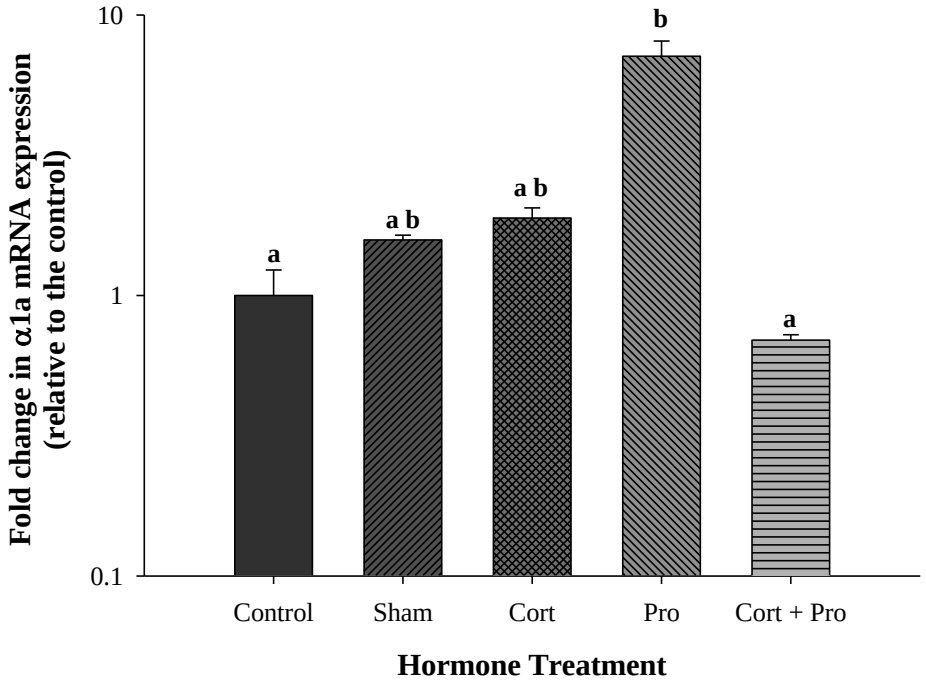

Figure 5.10 The effect of cortisol 50 µg/g (Cort), prolactin 5 µg/g (Pro), cortisol 50 µg/g and prolactin 5 µg/g (Cort + Pro) hormone treatment (intraperitoneal injection) on α1a mRNA expression in freshwater-acclimated inanga gill. Sham represents an injection control (vehicle only) and the control is a no-injection/handing control. Plotted values represent the mean fold change (± SE) in α1a mRNA expression relative to the freshwater control for 4-5 individuals. Mean values sharing letters are not statistically significantly different ($p < 0.05$), as determined by Kruskal-Wallis ANOVA and Dunn's post hoc analysis (SigmaPlot).

There was no significant difference in any treatments relative to the 50% seawater-acclimated control fish (Figure 5.11). However 50% seawater-acclimated inanga treated with cortisol (50 µg/g) showed significant up-regulation of α1a mRNA expression compared to both the sham and prolactin (5 µg/g) treated fish. Inanga treatment with both cortisol and prolactin did not change the mRNA expression compared to the controls.

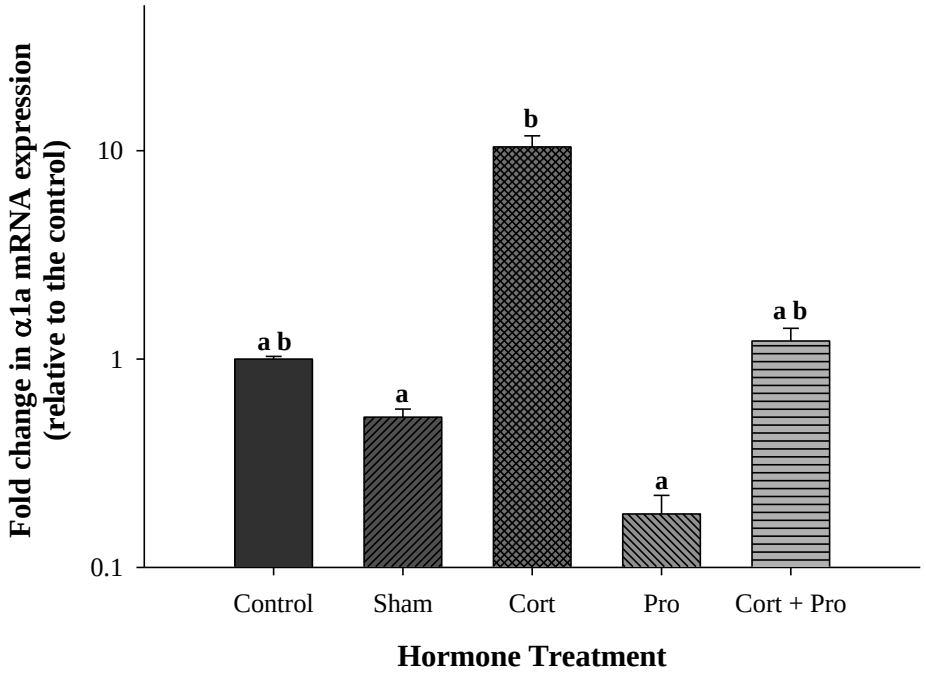

Figure 5.11 The effect of cortisol 50 µg/g (Cort), prolactin 5 µg/g (Pro), cortisol 50 µg/g and prolactin 5 µg/g (Cort + Pro) hormone treatment (intraperitoneal injection) on α1a mRNA expression of 50% seawater-acclimated inanga gill. Sham represents an injection control (vehicle only) and the control is a no-injection/handing control. Plotted values represent the fold change in α1a mRNA expression is relative to the 50% seawater control ± SE of 4-6 individuals. Mean values sharing letters are not statistically significantly different ($p < 0.05$), as determined by Kruskal-Wallis ANOVA and Dunn's post hoc analysis (SigmaPlot).

.

A significant down-regulation of α1a mRNA expression was seen in 100% seawater-acclimated inanga treated with prolactin (5 µg/g) and both cortisol (50 µg/g) and prolactin (5 µg/g) compared to the untreated 100% seawater-acclimated control (Figure 5.12). A significant down regulation of α1c mRNA expression was seen in the prolactin (5 µg/g) treated fish compared to the sham injection control. This was the only significant effect relative to the sham group.

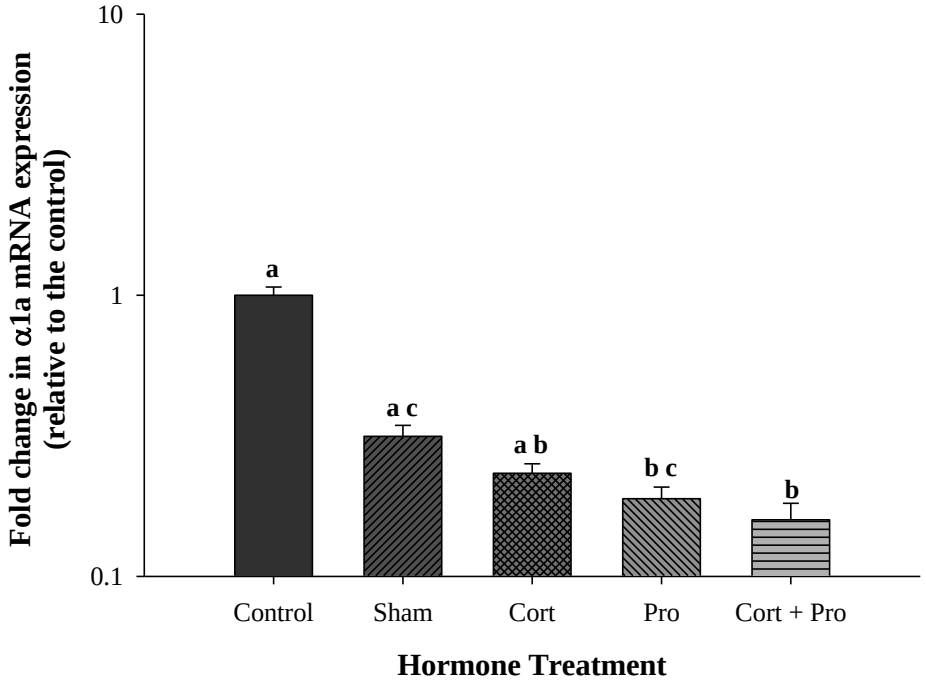

Figure 5.12 The effect of cortisol 50 µg/g (Cort), prolactin 5 µg/g (Pro), cortisol 50 µg/g and prolactin 5 µg/g (Cort + Pro) hormone treatment (intraperitoneal injection) on α1a mRNA expression of 100% seawater-acclimated inanga gill. Sham represents an injection control (vehicle only) and the control is a no-injection/handing control. Plotted values represent the fold change in α1a mRNA expression is relative to the 100% seawater control ± SE of 4-6 individuals. Mean values sharing letters are not statistically significantly different ($p < 0.05$), as determined by Kruskal-Wallis ANOVA and Dunn's post hoc analysis (SigmaPlot).

A significant up regulation of α1b mRNA expression was seen in freshwater-acclimated inanga treated with 5 µg/g prolactin compared to the untreated freshwater-acclimated control and the sham (Figure 5.13). This up regulation represents a 10-fold increase in the expression of the α1b isoform compared to the sham. All other treatments showed similar expression levels to the freshwater control.

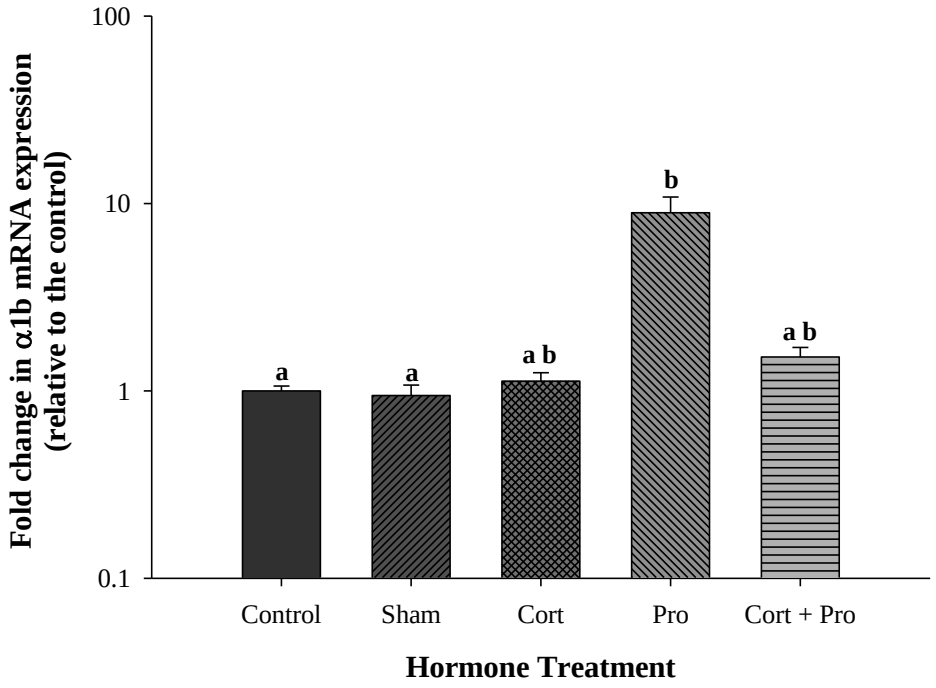

Figure 5.13 The effect of cortisol 50 µg/g (Cort), prolactin 5 µg/g (Pro), cortisol 50 µg/g and prolactin 5 µg/g (Cort + Pro) hormone treatment (intraperitoneal injection) on α1b mRNA expression of freshwater-acclimated inanga gill. Sham represents an injection control (vehicle only) and the control is a no-injection/handing control. Plotted values represent the fold change in α1b mRNA expression is relative to the freshwater control ± SE of 4-5 individuals. Mean values sharing letters are not statistically significantly different ($p < 0.05$), as determined by Kruskal-Wallis ANOVA and Dunn's post hoc analysis (SigmaPlot).

Gill tissue from 50% seawater-acclimated inanga showed no change in α1b mRNA expression with any of the hormone treatments (Figure 5.15). Expression of α1b was not affected by the injection protocol as indicated by the similarity between the sham and the control.

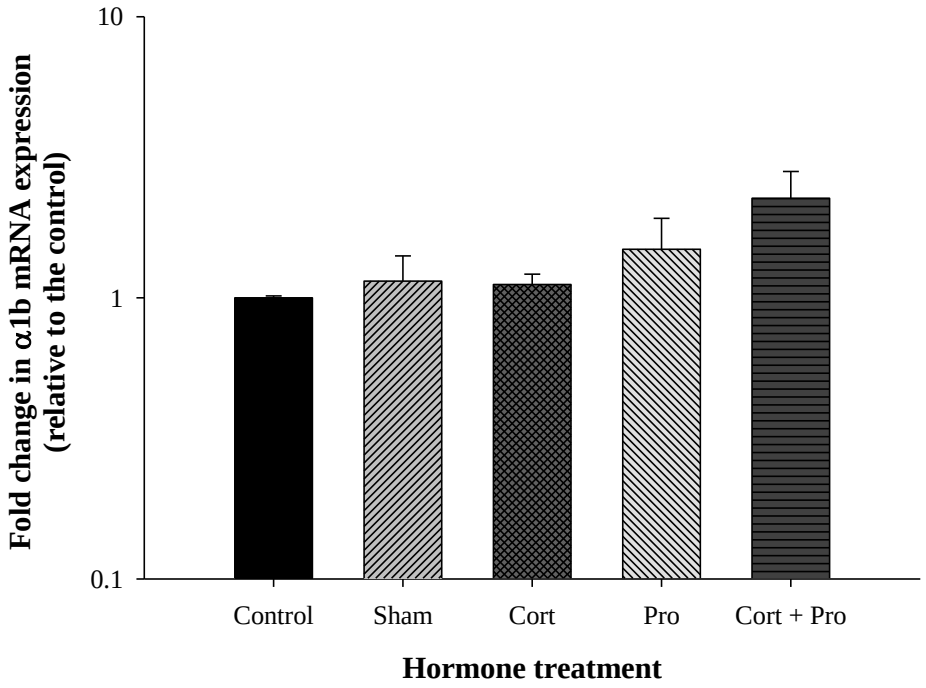

Figure 5.14 The effect of cortisol 50 µg/g (Cort), prolactin 5 µg/g (Pro), cortisol 50 µg/g and prolactin 5 µg/g (Cort + Pro) hormone treatment (intraperitoneal injection) on α1b mRNA expression of 50% seawater-acclimated inanga gill. Sham represents an injection control (vehicle only) and the control is a no-injection/handing control. Plotted values represent the fold change in α1a mRNA expression is relative to the 50% seawater control ± SE of 4-5 individuals. No significant difference was found between treatments (one-way ANOVA).

A significant down-regulation of α1b mRNA expression was seen in the prolactin-treated (5 µg/g) 100% seawater-acclimated fish compared to the sham injection control (Figure 5.15). The combination of cortisol (50 µg/g) and prolactin (5 µg/g) also produced a marked 10-fold decrease in α1b mRNA expression compared to the sham. The cortisol-treated 100% seawater inanga showed similar expression levels to the untreated control and the sham injection control.

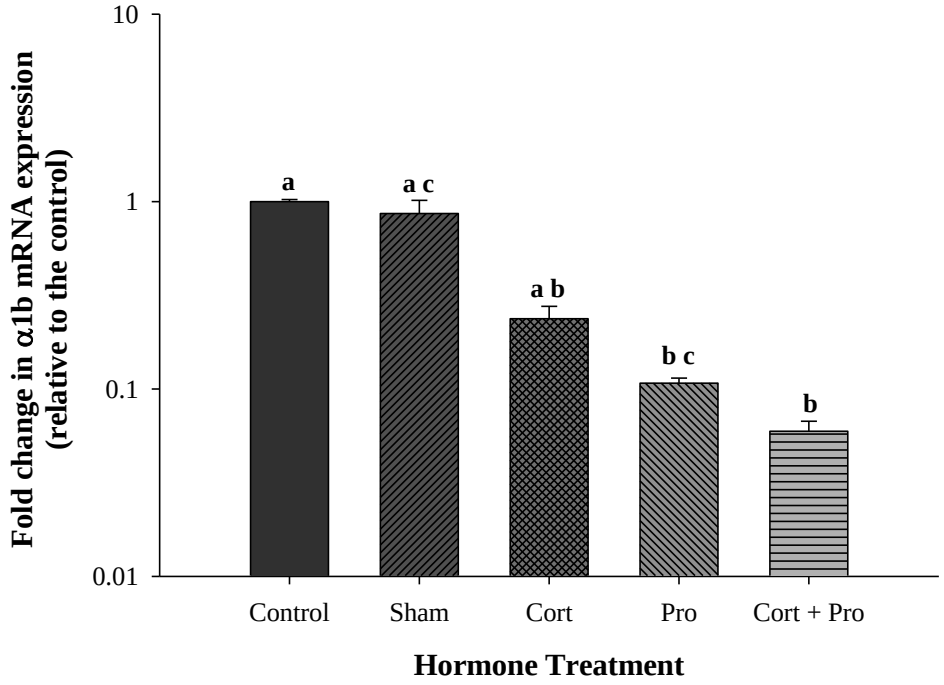

Figure 5.15 The effect of cortisol 50 µg/g (Cort), prolactin 5 µg/g (Pro), cortisol 50 µg/g and prolactin 5 µg/g (Cort + Pro) hormone treatment (intraperitoneal injection) on α1b mRNA expression of 100% seawater-acclimated inanga gill. Sham represents an injection control (vehicle only) and the control is a no-injection/handing control. Plotted values represent the fold change in α1b mRNA expression is relative to the 100% seawater control ± SE of 5 individuals. Mean values sharing letters are not statistically significantly different ($p < 0.05$), as determined by Kruskal-Wallis ANOVA and Tukey's post hoc analysis (SigmaPlot).

Treatment of freshwater-acclimated inanga with cortisol, prolactin or cortisol + prolactin did not result in any changes in α1c mRNA expression compared to the sham injection control (Figure 5.16). An up-regulation of α1c mRNA expression was seen in prolactin (5 µg/g) and cortisol (50 µg/g) + prolactin (5 µg/g) fish compared to the untreated freshwater-acclimated control.

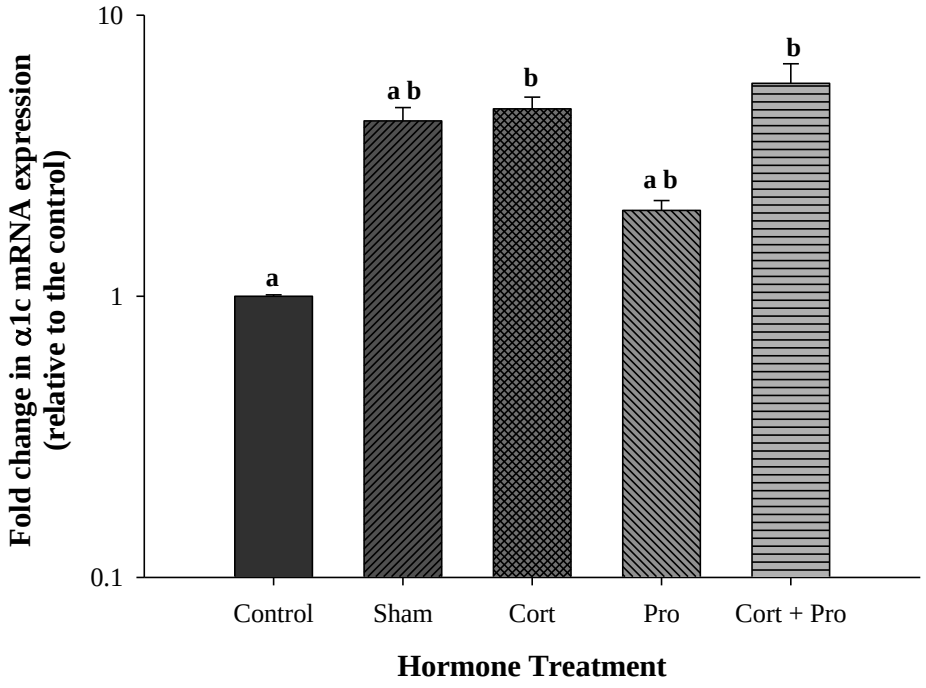

Figure 5.16 The effect of cortisol 50 µg/g (Cort), prolactin 5 µg/g (Pro), cortisol 50 µg/g and prolactin 5 µg/g (Cort $^{+}$ Pro) hormone treatment (intraperitoneal injection) on α1c mRNA expression of freshwater-acclimated inanga gill. Sham represents an injection control (vehicle only) and the control is a no-injection/handing control. Plotted values represent the fold change in α1c mRNA expression is relative to the freshwater control ± SE of 5 individuals. Mean values sharing letters are not statistically significantly different ($p < 0.05$), as determined by Kruskal-Wallis ANOVA and Dunn's post hoc analysis (SigmaPlot).

Expression of α1c isoform in the gill tissue of 50% seawater-acclimated inanga was not significantly affected by treated with cortisol (50 µg/g), prolactin (5 µg/g) or cortisol (50 µg/g) + prolactin (5 µg/g) compared to the sham injection control (Figure 5.17). A significant difference was observed between the prolactin-treated (5 µg/g) tissue and the cortisol-treated (50 µg/g) tissue with prolactin resulting in an almost 13-fold decrease in expression.

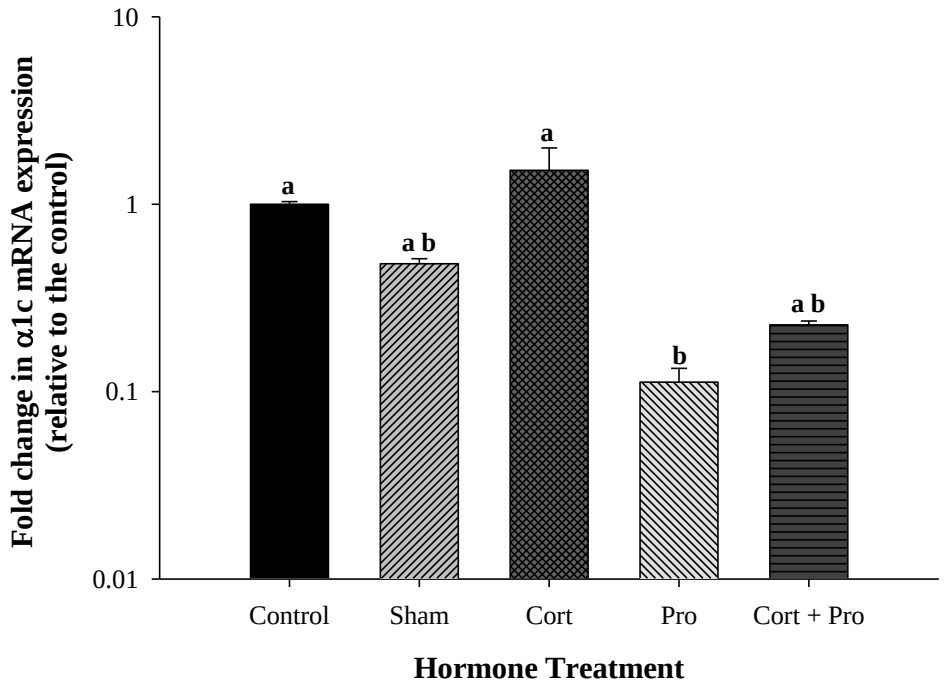

Figure 5.17 The effect of cortisol 10 µg/g (Cort), prolactin 5 µg/g (Pro), cortisol 50 µg/g and prolactin 5 µg/g (Cort + Pro) hormone treatment (intraperitoneal injection) on α1c mRNA expression of 50% seawater-acclimated inanga gill. Sham represents an injection control (vehicle only) and the control is a no-injection/handing control. Plotted values represent the fold change in α1c mRNA expression is relative to the 100% seawater control ± SE of 4-5 individuals. Mean values sharing letters are not statistically significantly different ($p < 0.05$), as determined by Kruskal-Wallis ANOVA and Dunn's post hoc analysis (SigmaPlot).

.

A significant down-regulation of α1c mRNA expression was seen in the gill tissue of 100% seawater-acclimated inanga treated with both prolactin (5 µg/g) and cortisol (50 µg/g), compared to the sham injection control (Figure 5.18). Expression levels in the cortisol + prolactin treated group significantly lower than that of the sham injection control. Individually cortisol and prolactin had no affect on expression levels compared to the sham injection control. Gill tissue from 100% seawater-acclimated inanga showed no change in α1c mRNA expression with any of the hormone treatments compared to the 100% seawater control.

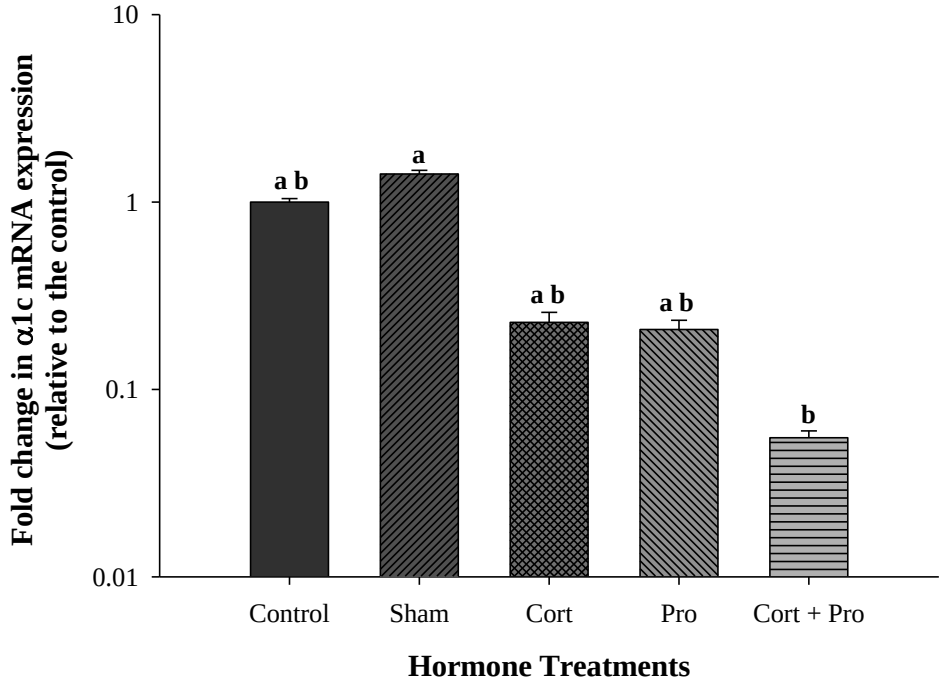

Figure 5.18 The effect of cortisol 50 µg/g (Cort), prolactin 5 µg/g (Pro), cortisol 50 µg/g and prolactin 5 µg/g (Cort + Pro) hormone treatment (intraperitoneal injection) on α1c mRNA expression of 100% seawater-acclimated inanga gill. Sham represents an injection control (vehicle only) and the control is a no-injection/handing control. Plotted values represent the fold change in α1c mRNA expression is relative to the 100% seawater control ± SE of 4-5 individuals. Mean values sharing letters are not statistically significantly different ($p < 0.05$), as determined by Kruskal-Wallis ANOVA and Dunn's post hoc analysis (SigmaPlot).

5.5 Discussion

5.5.1 Effect of salinity

Salinity-specific isoform expression has been shown in a number of euryhaline salmonids (Richards et al., 2003; Bystriansky et al., 2006; McCormick et al., 2009), and this study reveals for the first time the presence of salinity-specific isoform expression in galaxiids. This is a significant finding as it shows isoform switching is not confined to salmonids but is present in other families as well. This is not suprsing considering how closely related salmonids and galaxiids are (McDowall, 1990; Johnson and Patterson, 1996; McDowall, 1997). Isoform switching in salmonids has been attributed to a whole genome duplication in this lineage thought to have occurred between 25 and 100 million years ago (Allendorf and Thorgaard, 1984). These gene duplication events promote the development of physiological plasticity, and may have played a major role in the adaptation of teleost fish to a variety of environmental niches. In the case of salmonids and galaxiids the presence of multiple isoforms of NKA is likely to have conferred the ability to survive in different salinities, and may therfore have been responsible for the development of eurhalinity and diadromy in these groups.

Inanga displayed salinity-induced changes in the expression of all three α isoform variants. Expression of the α1a and α1b isoform in freshwater inanga was greater than that seen in seawater-acclimated inanga suggesting these isoforms play a more significant role in freshwater then seawater. This pattern of expression is slightly different from that observed in salmonids. Previous studies have shown that α1a mRNA expression of freshwater-acclimated fish gills quickly decreased following seawater exposure while α1b levels increased (Richards et al., 2003; Scott et al., 2004; Bystriansky et al., 2006; Bystriansky et al., 2007; McCormick et al., 2009). These observations have led to the conclusion that α1a isoform may be responsible for active ion absorption in freshwater salmonids and that the α1b isoform is responsible for active ion excretion in seawater. So while this study supports the role of α1a in freshwater, it highlights a difference between the species with respect to α1b expression.

An important difference between this study and previous research is the acclimation protocol. Most of the previous studies have examined changes in isoform expression in response to immediate changes in salinity (Richards et al., 2003; Bystriansky et al., 2006; McCormick et al., 2009). Expression would therefore reflect the changes required to acclimate in the short term. After a few weeks expression will reach a steady state with the isoform required for long-term survival at a particular salinity predominating. In this study acclimation was a gradual and long-term process so the results are indicative of the 'steady state' rather than the rapid response. It would be interesting to monitor changes in isoform expression in inanga in response to rapid acclimation to identify if α1b is necessary for rapid acclimation as it is in salmonids.

NKA α1c isoform expression has only been described in a few studies to date (Richards et al., 2003; Nilsen et al., 2007; Madsen et al., 2009). These salmonid-based studies all showed the α1c isoform exhibited no change in response to salinity and it was suggested that it may have a house-keeping function rather than an active osmoregulatory function. Inanga did display salinity-dependent expression with both α1a and α1b decrease as salinity increases, suggesting it does have an active role in ion regulation in this species. The α1c isoform showed a U-shaped expression pattern with the lowest expression levels seen in 50% seawater.

NKA activity was shown to increase in a salinity-dependent manner upon seawater exposure (Chapter 4) however none of the three α isoforms in this study showed a significant increase in expression in seawater compared to the other salinities. There are a number of possible explanations for this dichotomy. It is possible that an isoform not quantified in the present study may have a role in ion regulation in the gills of seawater inanga. Richards et al. (2003) showed that although α3 isoform was also present in the gill, it was not differentially-regulated in response to seawater and may have a housekeeping role. It is possible that α3 may play more of an active role in species other than salmonids and further characterisation of other isoform expression patterns in inanga may help to resolve this. A role of the other two subunits β and γ in modifying NKA activity also cannot be eliminated. An increase in NKA activity may also be due to an increase in overall numbers of NKA without a change in expression patterns. This may result from a decrease in protein degradation which is not apparent when

measuring mRNA expression. Further studies using isoform-specific antibodies and Western Blot technique would be needed to resolve this issue.

The α subunit is the main catalytic subunit of NKA and therefore the differential expression of the α sunbunit isoforms enables cells to precisely corodinate NKA activity to their physioloigcal requirements (Blanco and Mercer, 1998). It has long been known that different isoforms of NKA confer different activities and have different affinities for Na^+ and K^+ (Lingrel, 1992; Blanco and Mercer, 1998). This may explain why expression levels of a paticular isoform may not change (or can even decline) even though activity remains elevated.

5.5.2 Effects of hormones

While cortisol has been shown to increase the expression of α1a and α1b in freshwater Atlantic salmon (Kiilerich et al 2007a; Killerich et al., 2010; McCormick et al., 2008), it had no significant effect any of the isoform when administered in freshwater-acclimated inanga. It did however cause a significant increase in α1a expression in 50% seawater-acclimated inanga but this change was not reflected in the overall NKA activity (Chapter 4). This suggests that while cortisol can upregulate α1a, another mechanism such as protein degradation or decreased expression of another unknown isoform may be working to decrease NKA activity.

In freshwater-acclimated inanga prolactin caused an significant increase in α1b expression relative to the sham control which is in contrast a study done on Mozambique tilapia which showed no effect of prolactin on α1b expression either freshwater or seawater-acclimated fish (Killerich et al., 2011). Once again this increase was not reflected in the NKA activity (Chapter 4).

Perhaps the most striking effect and consistent effect of hormone treatment was that seen in seawater-acclimated inanga. All three isoforms showed a significant decrease in expression when treated with both cortisol and prolactin. This is the same pattern as that observed for NKA activity of seawater-acclimated inanga treated with cortisol and

prolactin (Chapter 4). In contrast seawater–acclimated Atlantic salmon showed no change in α1a and α1b expression or NKA activity upon treatment with cortisol and prolactin (Tipsmark et al., 2009). One possible reason for this discrepancy maybe the hormone dose and injection protocol Tipsmark and colleagues used (two injections 24 hours apart; dose of 4 µg/g cortisol and 0.2 µg/g prolactin).

5.5.3 Experimental Design

Variations in qPCR can have a significant impact on data and the many variables need to be controlled for successful gene expression analysis (Vandesompele et al., 2002). Because of the many steps needed to measure gene expression via qPCR, there are many opportunities where error may inadvertently be introduced. Theoretically this might explain some why the results diverge from the traditional patterns of expression such as the high expression of α1b in freshwater. However this is unlikely due to the careful trouble shooting of all the critical steps involved in the qPCR experiments as described in the methods section and Appendix A.

The inanga used in this study were caught in freshwater streams (0.1ppt, personal observation). Juvenile inanga (whitebait) reside in seawater and it would be interesting to compare the two life stages to see if the response to salinity and hormones was a general response in inanga or a life stage-dependent response. Salmon undergo a process known as smoltification where they prepare themselves for migration to seawater (Hoar, 1988; Prunet and Auperin, 1995). Smoltification is associated with increased plasma cortisol levels, increased gill NKA activities, chloride cell proliferation and enhanced SW tolerance (McCormick, 2001). Differential expression of NKA subunits has been observed salmon undergoing smoltification and post-smolting (Björnsson et al., 2011). Variations in hormone receptors such as the desensitisation of glucocorticoid receptor to cortisol in fish undergoing smoltification have been reported (Shrimpton et al., 1994). If inanga show these same life stage variations that salmon do, then this may confound results.

Another important variable is the fact that whole tissue samples such as the gill are composed of many cell types and the gene expression result will give an average expression value of the different cell types present. McCormick et al. only found the α1a and α1b isoforms present in MRCs and with salinity dependent localisation with regards to filamentous and lamellar epithelium (McCormick et al., 2009). If a specialised osmoregulatory isoform is localised to a specific region on the filament its significance may be masked by an abundant non- osmoregulating isoform which is present over the entire gill surface. Therefore the relative expression changes seen may not be truly representative of the functional importance of the particular isoform.

5.6 Conclusions

Inanga displayed salinity-induced changes in the expression of all three α isoform variants. While isoform α1a showed a similar pattern than what was seen in other fish species, α1b expression suggested it also played more of a role in freshwater then seawater. Treatment with the hormones cortisol and prolactin also induced isoform expression changes with injection of cortisol and prolactin resulting in a significant decrease in expression of all three isoforms in seawater-acclimated inanga.

CHAPTER 6 MEASURING INTRACELLUAR SODIUM IN INANGA GILL CELLS

6.1 Introduction

Sodium plays an important role in fundamental biological processes such as membrane transport, membrane potential and the regulation of other intracellular ions (Campbell and Reece, 2005). Any changes in Na^+ concentration can lead to the disruption of cellular homeostasis and function. For this reason intracellular concentrations of Na^+ ions are tightly regulated (Taylor and Windhager, 1979). The mechanisms behind Na^+ regulation within the gills of fish are widely debated (see Chapter 1). Many approaches have been taken to study and quantify intracellular Na^+ concentrations within the gill in an effort to elicit mechanistic detail. These studies have resulted in a variety of measured intracellular Na^+ concentrations ranging from 6.2 to 90 µM. Whether this range is a true reflection of the actual Na^+ levels within a cell or whether it is also reflects method-induced error is unknown. Accurate quantification of Na^+ within gill cells would allow for the monitoring of intracellular Na^+ changes and would greatly contribute to the understanding of homeostatic control of ion balance in fish.

6.1.1 Methods of Quantifying Sodium

Several techniques are available to measure Na^+ concentrations. These include X-ray microanalysis, nuclear magnetic resonance (NMR), ion-specific microelectrodes and laser scanning confocal microscopy (LSCM). The variety of techniques used to date all have distinct advantages and disadvantages.

6.1.1.1 X-ray Microanalysis

X-ray microanalysis is a technique based on the principle that when atoms of an element are struck with a beam of electrons, they emit X-rays which are characteristic of that

element (Van Grieken and Markowicz, 2001). This method can be used to identify and quantify each element present in a specimen. Papers using this technique to measure Na^+ have reported concentrations in the range of 50–90 mM in trout gills (Wood and Le Moigne, 1991; Eddy and Chang, 1993; Morgan et al., 1994). However the preparation of the tissues for X-ray microanalysis may introduce errors into the measurement, with the greatest problem being the cryofixation of the tissue. For X-ray microanalysis whole gill tissues are frozen with liquid nitrogen before being cut into thin sections with an ultramicrotome. Incomplete freezing or any partial thawing can cause the formation of ice crystals that can damage the cells and subsequently result in the relocation of ions (Morgan et al., 1994). Furthermore, because the tissues are fixed, this technique does not allow real-time monitoring of Na^+ concentrations.

6.1.1.2 Sodium-23 nuclear magnetic resonance (^{23}Na NMR)

Sodium-23 nuclear magnetic resonance (^{23}Na NMR) is a technique that measures the response of an isotope to a magnetic field. Each isotope produces specific spectra depending on its atomic properties. Intracellular and extracellular Na^+ concentrations can be differentiated using shift reagents applied to the external medium, but which are excluded from the intracellular environment owing to the impermeability of the cell membrane. These reagents cause a chemical shift in the spectra obtained from the extracellular Na^+ so it can be isolated from the intracellular Na^+ spectra. ^{23}Na NMR studies have been successfully conducted on the elasmobranch *Narcine brasiliensis* electric organ and have demonstrated an intracellular Na^+ concentration of 20 ± 10 mM (Blum et al., 1990). However, this technique has never been applied to examine intracellular Na^+ levels in the fish gill. ^{23}Na NMR is non-destructive but does require large amounts of tissue, expensive instrumentation and exposure of the tissue to shift reagents which are hazardous to the user (Amorino and Fox, 1995).

6.1.1.3 Ion-specific Microelectrodes

Ion-specific microelectrodes allow for the direct measurement of intracellular Na^+ using a small electrode that is inserted into isolated cells. The electrodes are calibrated to

known concentrations of Na^+ before insertion. The disadvantage of this technique is that it is invasive and the cell can potentially become damaged during electrode insertion (Voipio et al., 1994). Ion-specific microelectrodes are better suited for large cells (>50 µm in diameter) which would require the use of large fish. Adult inanga range in size from 0.2 – 2 g with an MRC size approximately 5-10 µM (Chapter 3), rendering them too small for this technique. Microelectrodes have been used in fish studies for assessing ion fluxes (Shephard, 1992; Clarke and Potts, 1998) but have not been directly used to measure ion concentration.

6.1.1.4 Laser Scanning Confocal Microscopy (LSCM)

The use of fluorescence dyes and laser scanning confocal microscopy is rapidly becoming the method of choice for monitoring intracellular ion levels due to the relative simplicity of its use over other techniques (Dailey et al., 2006). The key to confocal microscopy is its ability to examine individual ions in real time without causing tissue artefacts. More detailed information on LSCM is found in Chapter 2.

To date the majority of research conducted on fish gills using LSCM has used isolated gill cell cultures or fixed gill tissue. A study by Li et al. (1997) using the Na^+ indicator Sodium Green showed intracellular Na^+ concentrations between 6.4 to 16.5 mM in the cultured opercular cells of the tilapia *Oreochromis mossambicus*. Opercular epithelial cells line the opercular bone in fish and are often used as a surrogate for gill tissue. Opercular epithelium is laminar and therefore more accessible to physiological and morphological studies than gill epithelium (Mazon et al., 2007). This epithelium also contains MRCs (albeit in low numbers) and so may offer an insight into MRC transport properties (Marshall, 1995). The opercular epithelium has been gradually superseded by cultured gill cell preparations (see also section 1.4). Initially these cultures contained only homogenous population of cells (mitochondria-rich or pavement cells). This was later overcome by double-seeded techniques that incorporated multiple gill cell types (Kelly et al., 2000; Wood et al., 2002). However these preparations are still not ideal as they have undergone chemical and physical manipulation to isolate the cells. These manipulations may introduce artefacts which may perturb characteristics of ion balance

and they also cannot give any information about the natural organisation and cooperation between cells that may occur when they are part of a tissue. Fixed tissue allows for the study of cells within a tissue structure but only represents a snapshot of what has already happened.

Within the last few years a new Na^+ indicator dye CoroNa Green (CoroNa) (Invitrogen) has become available. CoroNa is excited at 492 nm by an argon laser and displays emission maxima of 516 nm. The manufacturer states that CoroNa is brighter and exhibits larger changes in fluorescence after binding of Na^+ when compared to the commonly used Na^+ indicator Sodium Green (Johnson and Spence, 2010). The cell permeant acetoxymethyl (AM) form of CoroNa is able to freely diffuse across cell membrane and once inside the cell esterases cleave off the acetate moieties to convert the dye into a Na^+-responsive form (Figure 6.1).

As well as being able to resolve spatial and temporal variations of Na^+, CoroNa can also be used to measure intracellular sodium concentrations ($[Na^+]_i$). This is achieved by performing a response calibration in which the fluorescence intensity of the CoroNa in solutions with precise known free Na^+ concentrations is measured. The values are then incorporated into the following Equation 6.1:

Equation 6.1: $$[Na^+]_i = K_d\,(F - F_{min})/(F_{max} - F)$$

where K_d is the dissociation constant of the CoroNa-Na^+ complex, F is the fluorescence intensity of the sample of interest, F_{min} and F_{max} are the fluorescence intensities corresponding to the minimum and maximum calibration solutions, respectively.

As CoroNa is relatively new to the market only a few studies on its use have been published. A study on *Arabidopsis thaliana* showed that CoroNa was useful for comparing Na^+ uptake between the salt-sensitive mutant and wild-type forms of this model plant species (Park et al., 2009). A comparative study between CoroNa and

Sodium Green concluded that CoroNa was useful for monitoring $[Na^+]_i$ changes in the neurons of mice, and may prove to be an important tool in the investigation of Na^+-mediated cellular processes (Meier et al., 2006).

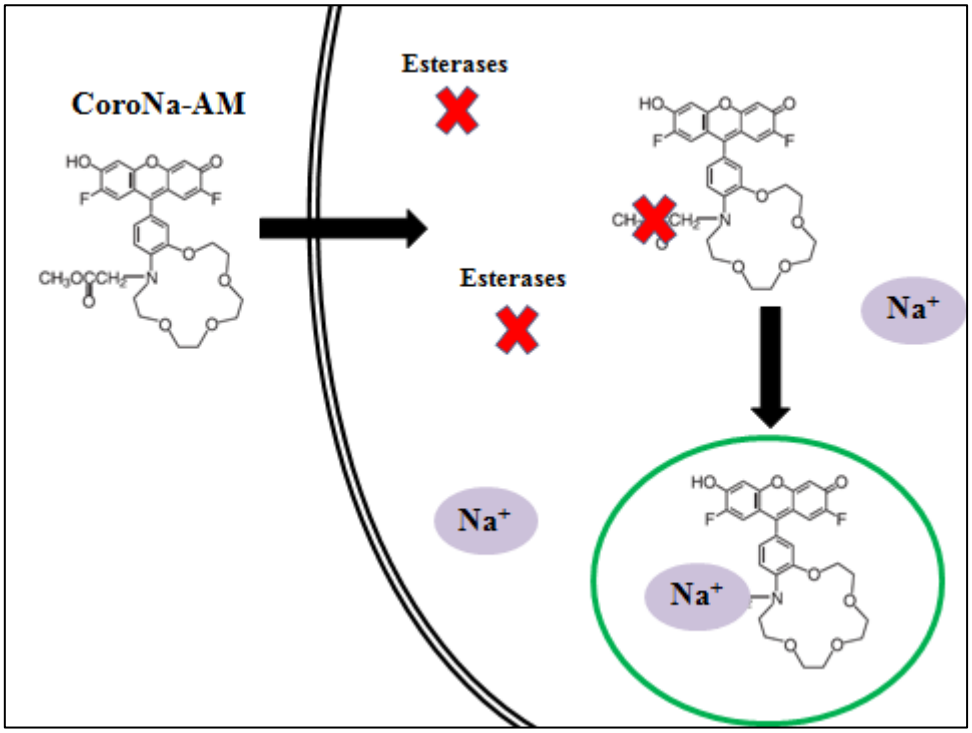

Figure 6.1 Action of CoroNa Green AM sodium dye. CoroNa Green AM sodium dye freely diffuses through the cell membrane into the cell where it is converted by esterases into a sodium-responsive form.

6.2 Chapter Aim

To my knowledge no attempt has been made to measure the intracellular Na^+ concentrations in live, intact gill tissue. Therefore the aim of this chapter is to develop a LSCM-based method for measuring intracellular Na^+ within live gill tissue, using the Na^+ indicator CoroNa. Once a protocol has been established, measurement of Na^+ in the gill cells of fish acclimated to freshwater, 50% seawater and 100% seawater under a variety of *in vitro* conditions will be attempted in an effort to extend the current knowledge on Na^+ metabolism of the fish gill.

6.3 Methods

6.3.1 Microscope

All experiments were conducted on an inverted confocal microscope (Leica model SP5, Wetzlar, Germany) using a HCX PL APO lambda blue 20.0 x 0.70 IMM UV glycerol immersion lens and a HCX PL APO 63.0x1.30 UV glycerol immersion lens. All specimens were first visualised and aligned using bright-field microscopy to protect the tissue and dye from excessive exposure to the laser light by avoiding photobleaching. General methods for LSCM and image processing were conducted as described in Chapter 2 (section 2.5), with any modifications noted.

6.3.2 Gill tissue

Fish were dissected as described in Chapter 2 (section 2.4.3) with a few minor modifications. Upon removal of the gill basket, it was placed directly into a 1.5 mL tube containing 1 mL of water to which the inanga was acclimated. The mucus surrounding the gills was left intact to help maintain the gill microenvironment and ensure prolonged survival of the filament post-dissection. Immediately before use each arch was carefully blotted with tissue paper to remove the protective mucus and thus facilitate dye loading. All measurements were taken from MRCs lining the lamella.

6.3.3 Storage and Reconstitution of dye

CoroNa Green AM Sodium indicator dye was purchased from Invitrogen in a desiccated form and stored at -20°C. The dye was reconstituted when needed with anhydrous dimethylsulphoxide to give a stock solution with a concentration of 1 mM and stored in aliquots at -20°C. Working solutions were made by diluting the stock solution in ultrapure water (>18 MΩ, Milli-Q, Millipore). Fresh aliquots were used for each experiment.

6.3.4 Viability of tissue

Tissue can only last so long outside of its natural environment before the cells begin to break down and die. To check if the gill tissue was still viable post-dissection, a viability test was performed using CoroNa. To allow binding with Na^+, CoroNa must first have its acetate moieties cleaved by esterases. Esterases are enzymes that are only functional in living cells therefore CoroNa can also be used as a means of assessing if a cell is still alive. Esterase activity is commonly used as a viability test in other cell systems (Steward et al., 1999; Franklin et al., 2001).

Freshwater-acclimated fish were euthanised by severing the spinal cord, with the time of death being noted, and the gill basket was removed. One gill arch was removed from the dissected gill basket, blotted and incubated with 10 µM CoroNa for 15 minutes. The arch was rinsed in freshwater before being visualised and images collected using the protocol in Chapter 2. A series of images was collected for each arch with one frame being captured ever 30 seconds for a total of 5 minutes. The procedure was repeated every 15 minutes with the remaining tissue for a total of 4 ½ hours. This experiment was repeated with a 50% seawater-acclimated and 100% seawater-acclimated inanga. Fluorescence intensity of an average of 6 gill cells at each time point from each fish was plotted against the difference in time-from-death to visualisation on the microscope.

6.3.5 Confirmation of dye properties

CoroNa Green has not been used to visualise gill Na^+ in any fish species. Therefore confirmation of the properties of the dye in this cellular system is an important step in the validation of this method. Unless stated all preliminary experiments were carried out using freshwater-acclimated inanga.

6.3.5.1 Wavelength scans

Product information states that CoroNa Green has an absorbance maximum of 492 nm and an emission maximum of 516 nm. To test the emission maxima, wavelength scans were performed using a 405, 488 and 561 nm laser. A wavelength scan records a series of individual images within a user-defined wavelength range, with each image detecting a specific emission wavelength. This is then used to measure the emission spectrum of a dye and determine which laser is best suited to the dye.

After dissection gill arches were placed in 10 µM of CoroNa Green for 10 minutes and then rinsed in freshwater to remove any excess dye. The gills were then placed into a solution containing 1 M NaCl, 3 µM gramicidin, 10 µM monensin and 100 µM ouabain. Gramicidin and monensin are ionophores, making the cell permeable to Na^+ which allows for rapid equilibration of intracellular and extracellular Na^+ (Harootunian et al., 1989). Ouabain is an inhibitor of the basolateral NKA transporter (McCormick, 1993). NKA removes intracellular Na^+ and therefore creates a gradient between intracellular and extracellular Na^+, an undesirable outcome in this experiment, hence its inhibition via ouabain. The tissue was then placed onto a 50 mm FluoroDish cell culture dish (World Precision Instruments) and covered with a 32 mm x 0.015 mm glass coverslip to help immobilise the tissue and prevent desiccation. Using each laser, a series of scans over a range of wavelengths at 5 nm intervals was performed and images collected. For the 405 laser, emission wavelengths between 415 and 700 nm were collected, for the 488 laser wavelengths between 495 and 700 nm were collected and for the 561 laser wavelengths between 570 and 700 nm were collected. Different filaments from the same arch were used for each laser experiment. The images were collected and

processed as described in Chapter 2. Fluorescence from an average of three cells was recorded per interval for each scan. The mean fluorescence was then normalised to the highest fluorescence value recorded and graphed against wavelength (SigmaPlot 11). From the graph the best laser for excitation and the size of the emission detection window for the CoroNa dye was then determined.

6.3.5.2 Response to sodium

CoroNa Green dye reportedly allows spatial and temporal resolution of Na^+. To confirm a response to Na^+, the gill cells were exposed to a Na^+-free environment and then a Na^+-saturated environment (1 M NaCl).

A gill arch was incubated in 10 µM CoroNa Green for 10 minutes. The gill arch was then rinsed in freshwater to remove any excess dye and placed onto a 50 mm FluoroDish with a small volume of Na^+-free PBS (124 mM choline chloride ($C_5H_{14}ClNO$), 11.9 mM choline bicarbonate ($HOCH_2CH_2N(CH_3)_3HCO_3$), 1.5 mM $CaCl_2$, 6 mM HEPES, 2 mM $C_6H_{12}O_6$, 3.3 mM KH_2PO_4 and 4 mM KCl; pH 7.7), and covered with a glass coverslip. The sample was incubated for 10 minutes before being visualised and images collected. The Na^+-free PBS bathing medium was removed using tissue paper and replaced with 1M NaCl. The sample was again incubated for 10 minutes. Fluorescence intensity of the sample in a Na^+-free environment was compared to the sample in a Na^+-saturated environment.

6.3.5.3 Dye concentration and loading time

Invitrogen suggests a working concentration of 0.5 - 10 µM for CoroNa. The fluorescence generated by the CoroNa-Na^+ complex is a reflection of a steady state that exists between the dye, the unbound Na^+ and the cells buffering mechanisms for Na^+ (Reynolds, 2001). To reduce the impact of cellular function on fluorescence, the lowest concentration of dye that still exhibits fluorescence with little noise should be selected. Noise (random variations in the colours of the pixels that make an image) may be

introduced into an image at high magnification and can give a false localisation of fluorescence.

To determine the best concentration of CoroNa, gill tissue was exposed to 0.5, 1, 5, 10 and 20 µM of CoroNa for 10 minutes, rinsed in freshwater before being visualised and imaged. The mean fluorescence intensity of a minimum of four cells at each concentration was calculated and plotted against dye concentration. Non-linear regression was performed using SigmaPlot 11.

The incubation time for loading of the dye into the tissue is another important parameter. A short loading time will result in only a small number of dye molecules entering the cells, whereas a long loading time will promote loading of dye into organelles (Reynolds, 2001). Once sequestered into an organelle, the dye is no longer available to the free Na^+ within the cytoplasm. Therefore a time which gives adequate fluorescence with little noise and no organelle loading is preferential. To test this gill tissue was loaded with 10 µM of CoroNa and incubated for 1, 5, 10, 15, 20, 30 and 45 minutes. Tissue was then rinsed in freshwater before being visualised and images collected. Cells were examined for staining of organelles within the cytoplasm.

6.3.5.4 Determination of the Dissociation Constant (K_d)

The dissociation constant (K_d) describes the relationship between a dye and an ion. It is the ion concentration at which half the dye's binding sites are occupied by the ion. K_d essentially measures the affinity the dye has for the specific ion of interest and is a fundamental factor when attempting to measure ion concentration with confocal microscopy.

Dissociation constant values can vary depending on the presence of other ions, temperature, pH, ionic strength, viscosity, protein binding, and other factors within a cell (Takahashi et al., 1999). Consequently it is important that the K_d is measured in the specific cell type to be used (i.e. *in situ*), as it may not have the same value as *in vitro* measurements or measurements done within other cell types. Typically ion

concentrations can be determined within a 10-fold range above and below the value of the apparent dissociation constant (Szmacinski and Lakowicz, 1997; Takahashi et al., 1999). Product information claims CoroNa has a K_d of 80 mM and therefore should be able to determine ion concentrations between 8 and 800 mM.

To determine the K_d, an *in situ* response calibration was performed. The calibration consists of recording fluorescence signals corresponding to a series of precisely manipulated Na^+ concentrations. Fifteen calibration solutions were made ranging in Na^+ concentration between 0 and 500 mM, with actual Na^+ concentrations being confirmed via flame photometry (section 2.7). Solutions of known Na^+ concentration were made to calibrate the levels of Na^+-specific fluorescence observed in confocal images. These solutions were based on a HEPES-Cortland saline buffer commonly used in fish physiology (Pärt and Wood, 1996). Sodium concentration was controlled by varying the amount of NaCl and $NaHCO_3^-$ added to the saline. Choline chloride ($C_5H_{14}ClNO$) and choline bicarbonate ($HOCH_2CH_2N(CH_3)_3HCO_3$) were also added to as a Na^+ substitute to ensure other ion concentrations and osmolarity (~300 mOsmol/kg) of all solutions was similar (Onken et al., 2003). The pH of all solutions was adjusted to 7.7 using HCl. Sodium transport modifiers (3 µM gramicidin, 10 µM monensin and 100 µM ouabain) were added to the solutions to equilibrate the internal ion concentration with the external ion concentration.

Sections of gill arches with intact filaments were incubated in 10 µM CoroNa Green for 10 minutes. They were then rinsed in freshwater to remove any excess dye and placed onto a 50 mm FluoroDish cell culture dish with a small volume of each calibration solution. Fluorescence intensity of a minimum of 6 cells exposed to each calibration solution was measured after a ten-minute incubation. The procedure was repeated with each calibration solution, using fresh gill tissue. The calibration experiment was repeated a total of three times, with the order of exposures varied to ensure this had no impact on the results. The experiment was also repeated in 50% and 100% seawater-acclimated fish.

6.3.5.4.1 Data analysis

Fluorescence intensity data was obtained as described in Chapter 2 (section 2.5.3) and corrected for background fluorescence (Chapter 2, section 2.5.5). The fluorescence intensity of a minimum of 6 cells at each calibration solution concentration were first averaged and then normalised to the minimum Na^+ concentration (F_{min}) and to the fluorescence intensity of the sample exposed to the maximum Na^+ concentration (F_{max}) using Equation 6.2.

Equation 6.2: $$\text{Normalised fluorescence} = (F - F_{min}) / (F_{max} - F)$$

The log of the actual Na^+ concentration of the calibration solution (log [Na^+]), as determined by flame photometry (section 2.7), was then plotted against the log of the normalised fluorescence intensity of each calibration sample (Grynkiewicz et al., 1985; Kowalczyk et al., 1997; Petr and Wurster, 1997; Johnson and Spence, 2010). Linear regression was performed using SigmaPlot to determine the x-intercept, which is the log of the K_d of CoroNa expressed in nM.

6.3.6 Measuring internal sodium concentration $[Na^+]_i$

6.3.6.1 Intracellular sodium concentrations in freshwater-, 50% seawater- and 100% seawater-acclimated inanga

Once the CoroNa had been proven suitable for use and a robust method developed for its application to the fish gill, an attempt to measure gill internal Na^+ concentration was performed. The basal $[Na^+]_i$ was first determined by visualising the cells bathed in the medium to which they were acclimated (i.e. freshwater-acclimated inanga gills cells in freshwater). Freshwater-, 50% seawater- and 100% seawater –acclimated inanga gill cells were then exposed *in situ* to various salinities within the range of those the inanga encounter during their lifetime (i.e. freshwater, 50% seawater and 100% seawater), and the resulting change in Na^+ concentration was observed.

A protocol (detailed in the paragraph below) for measuring intracellular Na^+ was determined using the results from the confirmation of spectral properties experiments and the experience gained in their development. All procedures including confocal settings, dye concentrations, loading, handling and image processing were kept constant throughout all of the following experiments to allow comparisons.

Fish were euthanised by severing the spinal cord and the entire gill basket was removed and placed directly into a 1.5 mL tube containing 1 mL of water identical in composition to that which the inanga was acclimated to. A single gill arch was removed from the gill basket, carefully blotted with tissue paper to remove the surrounding mucus and placed into a fresh tube containing 10 µM CoroNa. After 10 minutes the gill was removed from the dye and rinsed in a fresh change of acclimation water. The gill arch was placed onto a 50 mm FluoroDish cell culture dish with a small volume of the acclimation water and covered. The dish was placed onto the microscope and the gill arch was aligned so that a single lamella was in the field of view. Cells were visualised using the settings in Table 6.1.

Table 6.1 Confocal setting for measuring internal sodium concentration in inanga gill filaments

Parameters	**Settings**
Laser	488 argon laser, 20% power
Objective	HCX PL APO 63.0x1.30 glycerol immersion lens
Emission band width	500 – 580 nm
Format	512 x 512
Gain	708.1
Pinhole	1.00
Zoom	3.7
Line average	2
Frame average	1

After basal measurements had been recorded, the bathing medium in the FluoroDish was removed by wicking it away with tissue paper and was replaced with water of a distinct salinity (i.e. for freshwater-acclimated fish, 50% or 100% seawater was used). The coverslip was replaced and the filament was incubated for 10 minutes before visualising. The procedure was repeated with the final salinity (i.e. for freshwater gill, the remaining seawater concentration 50 or 100% seawater). The freshwater, 50% seawater and 100% seawater used for these experiments was sampled directly from the water the inanga were acclimated to. The Na^+ concentration of these waters was measured using flame photometry (section 2.7) and was determined to be 1 mM for freshwater, 189 mM for 50% seawater and 421 mM for 100% seawater. A full calibration using all 15 calibration solutions could not be performed after every experiment as there was insufficient gill tissue. Therefore at the end of each experiment

a modified response calibration was performed using four calibration solutions (0, 50, 15, 300 mM Na^+). These four data points were compared to the corresponding concentrations in previous full calibration curves to determine if the same calibration curve, and therefore K_d, could be applied to the experiment. Images were processed as described in Chapter 2. Intracellular Na^+ concentrations were calculated using Equation 6.2. The experiment was repeated with a total of three freshwater, three 50% and three 100% seawater-acclimated inanga.

6.3.6.2 Intracellular sodium concentration in the presence of amiloride and ouabain

Amiloride and ouabain are membrane transport inhibitors. Amiloride is known to inhibit both the NHE and ENaC (Kleyman and Cragoe, 1988) and ouabain is an inhibitor of NKA. Both of these drugs have been widely used to elucidate the mechanisms of ion regulation in fish (see Chapter 1). To test what effect, if any, amiloride and ouabain may have on the intracellular Na^+ concentrations of inanga MRCs, gill arches were exposed to solutions containing each inhibitor and a variety of salinities.

Gill arches were dissected, stained and visualised as previously described. Basal measurements, consisting of the gill in the acclimation salinity alone, were first taken as a control. Subsequently the media surrounding the arches was removed and replaced with one of six solutions:

1. Freshwater (1 mM Na^+) $^+$ 50 µM amiloride
2. 50% seawater (189 mM Na^+) $^+$ 50 µM amiloride
3. 100% seawater (421 mM Na^+) $^+$ 50 µM amiloride
4. Freshwater (1 mM Na^+) $^+$ 1 mM ouabain
5. 50% seawater (189 mM Na^+) $^+$ 1 mM ouabain

6. 100% seawater (421 mM Na^+) $^+$ 1 mM ouabain

Inhibitor concentrations were determined based on a previous study by Li et al., (1997) which used LSCM to measure intracellular Na^+ changes in tilapia (*Oreochromis mossambicus*) opercular gill cell cultures. The gill cells were incubated in the given experimental medium for 10 minutes before being visualised. A fresh gill arch was used for each exposure to avoid any carry-over effect. Sodium concentrations were determined using flame photometry (section 2.7). At the end of each experiment a calibration was performed (0, 50, 15, 300 mM Na^+). The experiment was performed with freshwater-, 50% seawater- and 100% seawater-acclimated inanga.

6.3.7 Statistical analysis

Fluorescence intensity data was obtained as described in Chapter 2 (section 2.5.3) and corrected for background fluorescence (Chapter 2, section 2.5.5). Data are presented as mean fluorescence intensity (arbitrary units) and standard error if the mean (SE) for each group.

Data for intracellular sodium concentration was then converted into concentration using Equation 6.1. Data was then subjected to tests of normality (Kolmogorov-Smirnov test) and homogeneity of variance (Levene's test) using SigmaPlot Version 11.0. Data that passed these assessments were analysed parametrically via one-way analysis of variance (ANOVA) and pairwise multiple comparison procedures (Holm-Sidak method or Dunn's post hoc analysis) using SigmaPlot. Data are presented as the mean intracellular sodium concentration and standard error of the mean (SE) for each treatment group.

6.4 Results

6.4.1 Viability of tissue

AM-forms of dyes rely on the presence of intracellular esterases present in live cells to convert the dye into its active form. Gill cells from freshwater, 50% seawater- and 100% seawater-acclimated inanga loaded with 10 µM CoroNa, exhibited fluorescence and therefore viability post-dissection (Figure 6.2). Gill cells were examined over a 270 minute period and freshwater-acclimated inanga still exhibited fluorescence 245 minutes post-dissection. Gill cells from 50% seawater- and 100% seawater-acclimated inanga still showed fluorescence 194 and 152 minutes post-dissection, respectively. This data shows the gill cells are viable for some time after dissection and all subsequent experiments were performed within 3 hours of the inanga being euthanised.

Each point in figure 6.2 represents a single frame, with runs of points representing a 5 minute time series. The downward trend of each series indicates a loss in fluorescence over this time period, most likely caused by photobleaching. Repeated exposure to the laser light can cause photobleaching of the dye and a loss of signal (Reynolds, 2001). Therefore all subsequent experiments were conducted under conditions that reduced laser exposure by limiting frame collection in a series to less than 2 minutes. If any cell degradation or loss of signal was observed, the experiment was immediately terminated

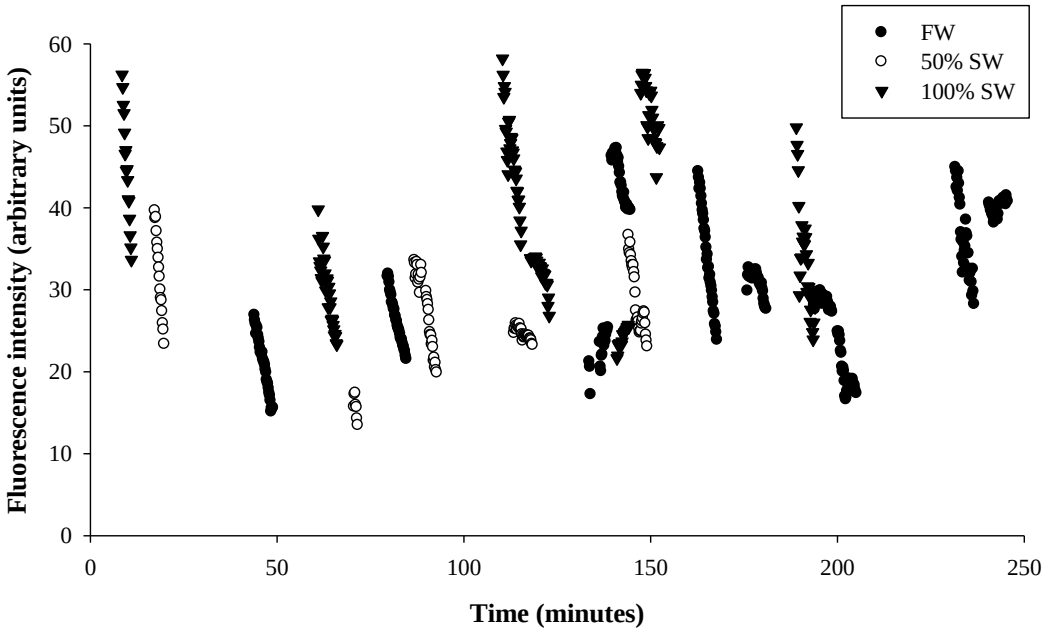

Figure 6.2: Viability of gill cells in freshwater-, 50% seawater- and 100% seawater-acclimated inanga post-dissection. Each point represents a single frame in which the mean fluorescence of a minimum of 6 cells was recorded. Time 0 is the time of death of the inanga. Fluorescence intensity is expressed in arbitrary units.

.

6.4.2 Confirmation of spectral properties

6.4.2.1 Wavelength scans

Normalised wavelength scans recorded at three different excitation wavelengths (405, 488 and 561 nm) produced emission spectra showing three peaks (Figure 6.3). The 405 nm laser produced a very small shoulder at 490 nm and a larger peak at 540 nm; whereas the 488 nm laser produced a large peak at 527 nm. The 561nm laser did not produce any peaks. The 488 nm laser produced the highest and cleanest (single) peak which supports Invitrogen's claims that this CoroNa is best excited by this laser. All subsequent experiments were performed with the 488 nm laser and emission wavelengths between 500 and 580 nm were collected.

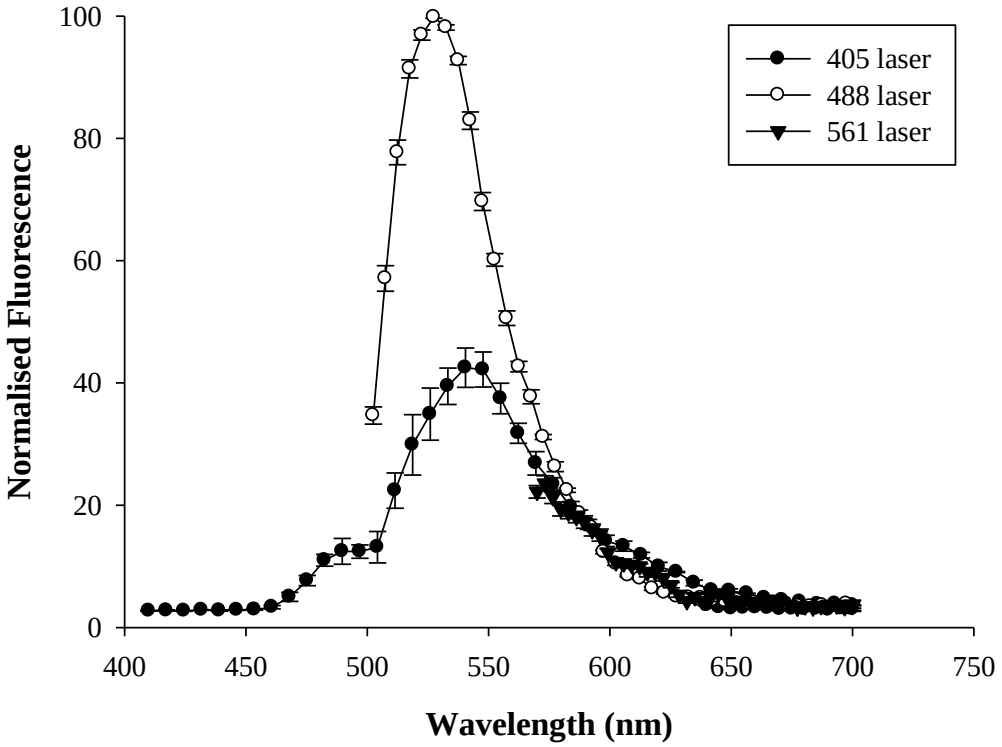

Figure 6.3 Normalised wavelength scans recorded with three different lasers (405, 488 and 561nm). The fluorescence intensity of a minimum of three cells per interval was averaged, normalised and plotted against wavelength (±SE) to produce the emission spectra.

6.4.2.2 Response to Sodium

Freshwater-acclimated inanga gill cells loaded with 10 µM CoroNa and exposed to a Na^+-free environment showed a small amount of fluorescence in the cytoplasm of the cells (Figure 6.4A). Upon exposure to 1 M NaCl, the cells exhibited a dramatic increase in fluorescence intensity as shown by the change in colour from orange to blue (Figure 6.4B). Blue indicates that saturation of the dye with Na^+ has occurred. CoroNa is therefore confirmed as a Na^+-responsive dye.

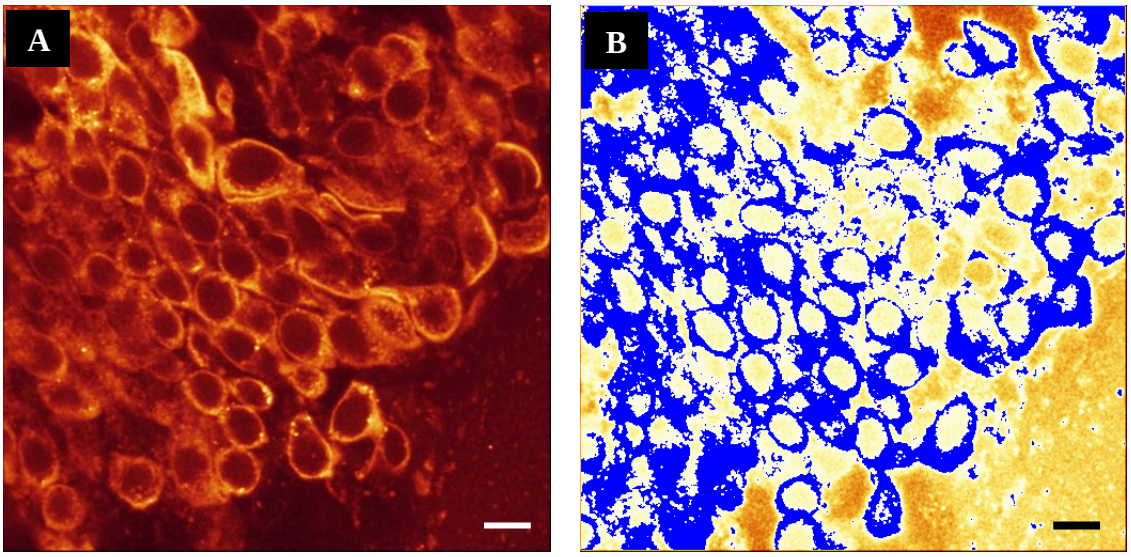

Figure 6.4 Freshwater-acclimated inanga gill cells exposed to a sodium-free environment (A) and 1 M NaCl (B). A change in fluorescence intensity is represented as a change in colour with the lowest fluorescence intensity (0 arbitrary units) coloured black and the highest fluorescence (255 arbitrary units) coloured blue. Scale bar = 10 µm.

6.4.2.3 Dye concentration and loading time

Gill cell fluorescence increased as dye concentrations increased. Five µM CoroNa produced the highest fluorescence intensity of 59.3 ± 4.3 arbitrary units (Figure 6.5). Higher dye levels (10 and 20 µM) produced similar fluorescence intensities (58.7 ± 0.9 and 55.4 ± 0.7 arbitrary units, respectively). A concentration of 10 µM CoroNa was

selected as the loading dye concentration for future experiments as it showed similarly high fluorescence intensity to 5 µM CoroNa but with less variation (smaller SE).

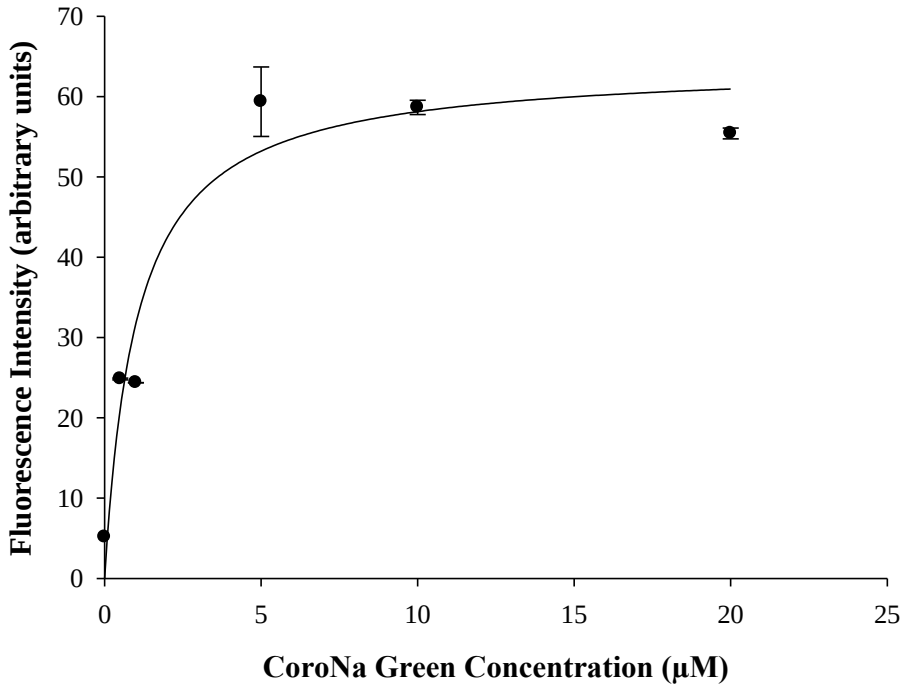

Figure 6.5 Freshwater-acclimated inanga gill cells loaded with increasing concentrations of CoroNa (0, 0.5, 1, 5, 10 and 20 µM) for 10 minutes. Each point represents the mean fluorescence intensity of a minimum of four cells (± SE).

Increased loading time corresponded to an increase dye loading into organelles (Figure 6.6). Ten minutes was selected as the optimum loading time as it was long enough to allow dye to load but short enough to avoid dye loading into the organelles.

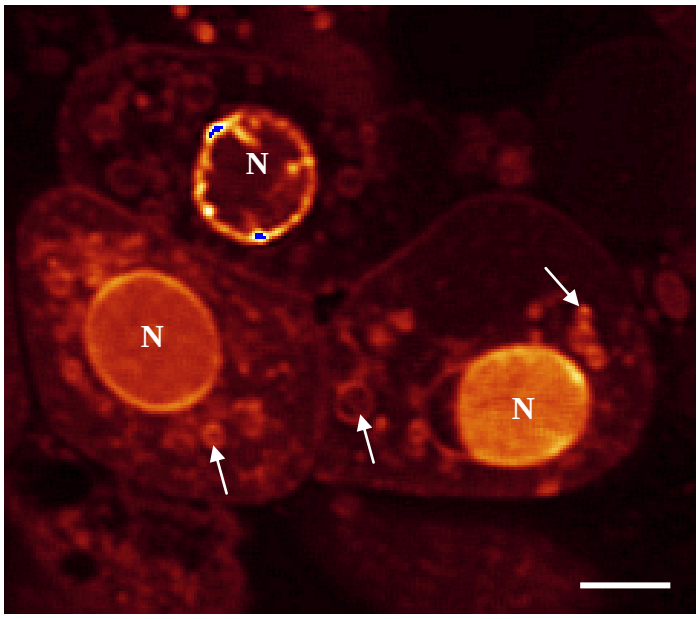

Figure 6.6 Loading of intracellular organelle in freshwater-acclimated inanga gill cells with 10 µM CoroNa incubated for 45 minutes. Prolonged incubation resulted in dye loading into nuclei (N) and intracellular organelles (arrows). Scale bar = 5 µm.

6.4.2.4 Determination of the Dissociation Constant (K_d)

As Na^+ concentration of the calibration solutions increased the fluorescence intensity exhibited by the cells increased (Figure 6.7A, B, C and D). This sigmoidal relationship showed that the CoroNa intensity was dependent on Na^+ concentration (Figure 6.8). A double log plot of the Na^+ concentration (mM) versus the normalised fluorescent intensity ((*F* - *Fmin*) / (*Fmax* - *F*)) yielded a K_d of 87.8 mM (Figure 6.9). Inanga acclimated to 50%- and 100% seawater showed similar dissociation constants, 86.0 mM and 96.3 mM respectively (data not shown). A one-sample t-test showed there was no statistical difference between the any of the three acclimation groups. For all subsequent Na^+ calculations the corresponding K_d for each acclimation group was used.

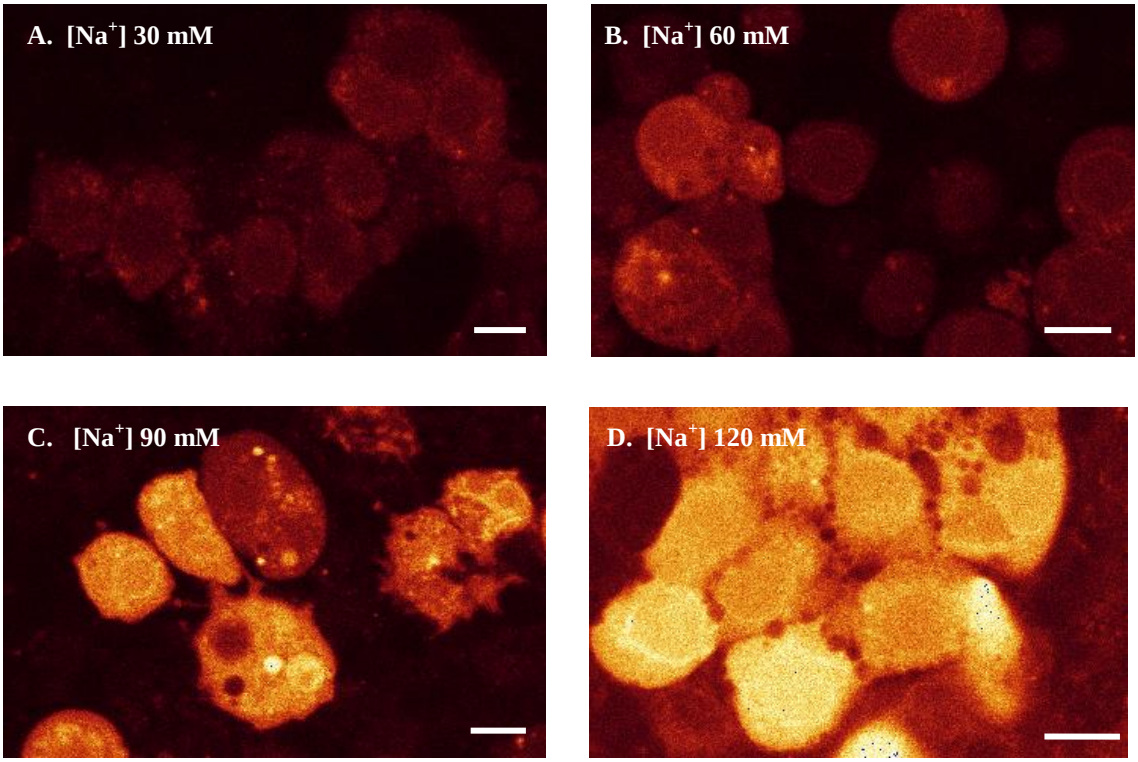

Figure 6.7 Freshwater-acclimated inanga gill cells loaded with 10 µM CoroNa and exposed to a variety of calibration solutions with variable nominal concentrations of Na^+ and containing ionophores. Scale bar = 5 µm

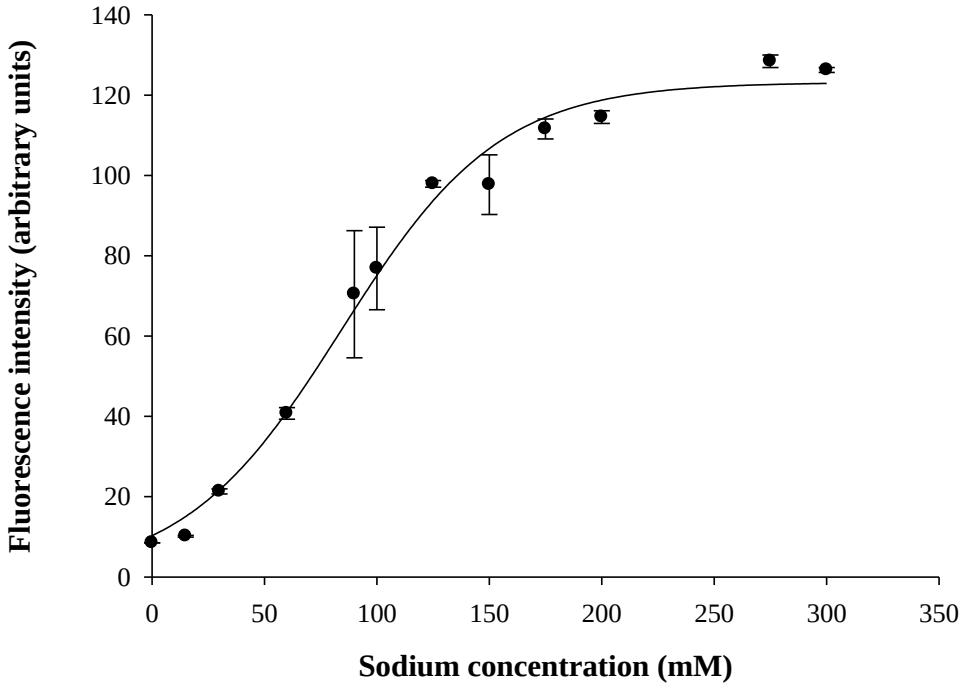

Figure 6.8 Fluorescence intensity of freshwater-acclimated inanga gill cells exposed to increasing concentrations of sodium expressed in arbitrary units. Each point represents the mean ± SE of a minimum of six cells. This experiment is representative of all calibrations performed.

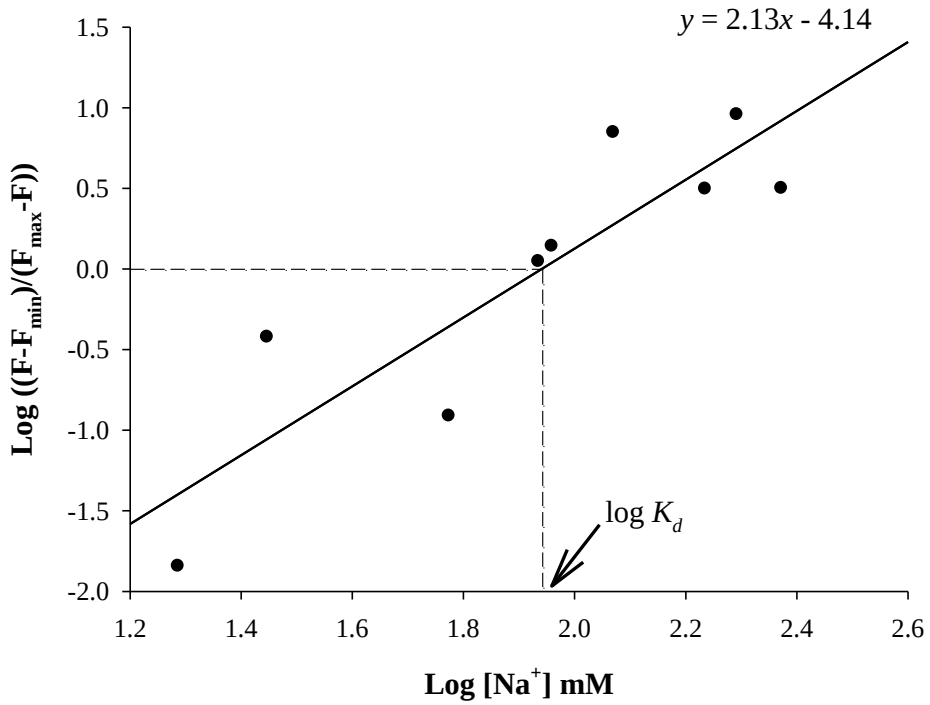

Figure 6.9 Determining the *in situ* dissociation constant (K_d) in freshwater-acclimated inanga gill cell. Linear regression was performed using SigmaPlot to determine the x-intercept, which is the log of the K_d of CoroNa expressed in nM.

The calibration curve was replicated in its entirety at several separate occasions throughout the course of LSCM experiments and proved to be reproducible providing the calibration solutions were made fresh prior to each experiment. Calibrations were also attempted using solutions that did not contain any ionophores. This resulted in minimal fluorescence at all concentrations (results not shown).

6.4.3 Intracellular sodium concentrations $[Na^+]_i$ in freshwater, 50% and 100% seawater-acclimated inanga

The average basal $[Na^+]_i$ for freshwater inanga gill cells bathed in freshwater was 5.2 ± 1.8 mM with values ranging from 2.0 – 13.3 mM (Figure 6.10).Following gradual acclimation to 100% seawater over a 4 week period the average basal $[Na^+]_i$ significantly increased to 16.2 ± 3.0 mM. Inanga acclimated to 50% seawater showed no significant increase in $[Na^+]_i$.

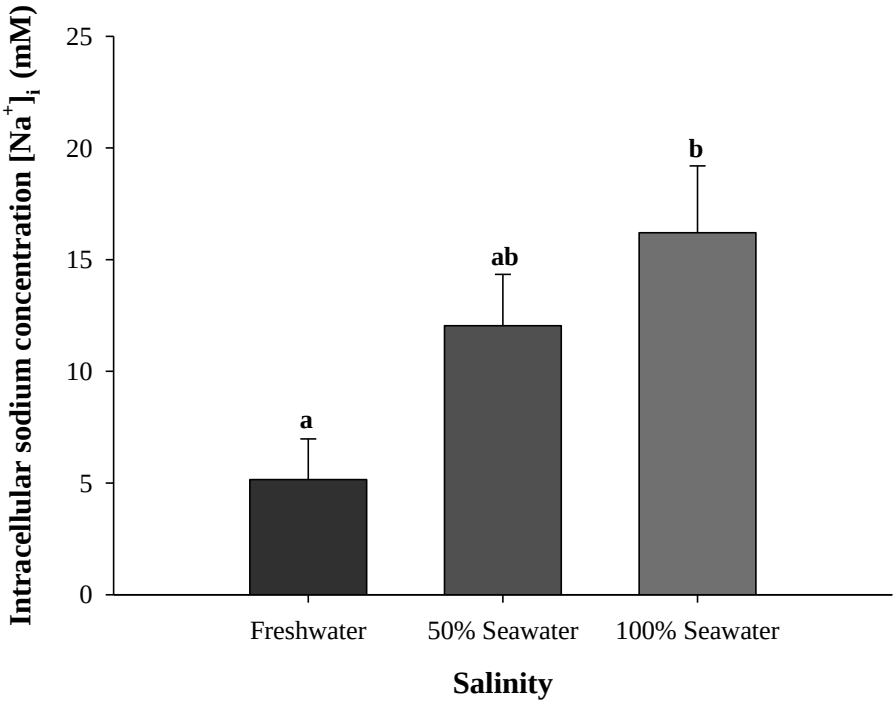

Figure 6.10 Basal intracellular sodium concentration $[Na^+]_i$ of cells in the gills of inanga acclimated to freshwater, 50% seawater and 100% seawater. Cells were bathed in the medium they were acclimated to. Bars represent mean values ± SE of three experiments and a minimum of 10 cells per experiment. Bars that share letters are not statistically significantly different ($p < 0.05$), as determined by one-way ANOVA followed by a Holm-Sidak post-hoc analysis (SigmaPlot).

6.4.3.1 Changes in intracellular sodium concentration $[Na^+]_i$ in response to different salinities

Freshwater-, 50% seawater- and 100% seawater-acclimated inanga gill cells were exposed to various salinities within the range of those the inanga encounter during their lifetime. When the bathing medium was changed to 100% seawater, a significant increase in $[Na^+]_i$ was seen within the gill cells of freshwater–acclimated inanga (Figure 6.11). The 10 minute exposure resulted in a $[Na^+]_i$ increase from 5.2 ± 1.8 mM to 18.15 ± 1.4 mM. There was no significant change in $[Na^+]_i$ when the freshwater cells were exposed 50% seawater. When gill cells from a 50% seawater-acclimated inanga were exposed to freshwater and 100% seawater for 10 minutes, no significant change in $[Na^+]_i$ was observed (p = 0.186) (Figure 6.12).

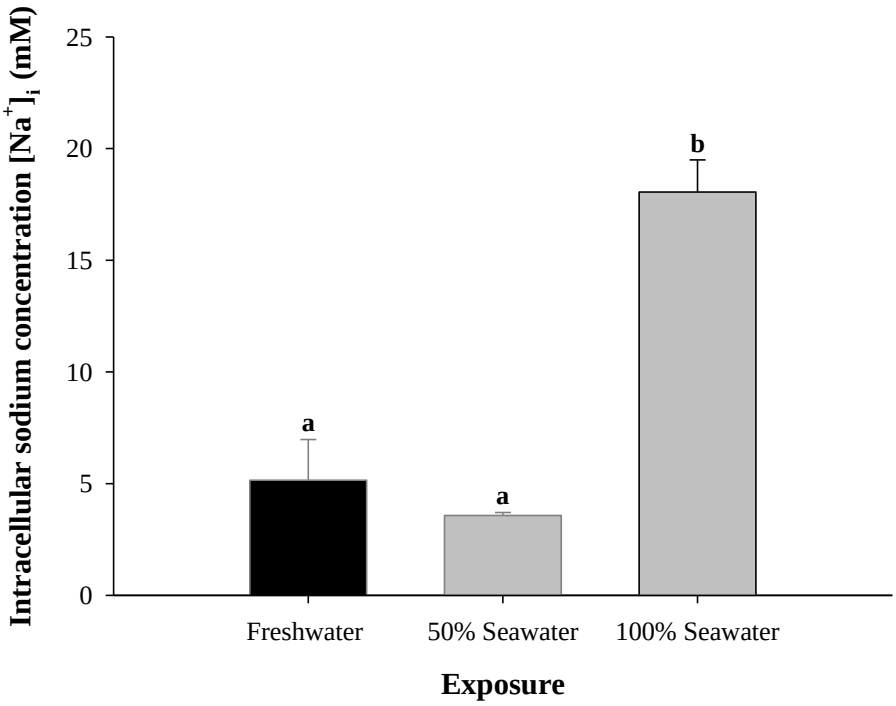

Figure 6.11 Intracellular sodium concentration $[Na^+]_i$ in gill cells of freshwater-acclimated inanga exposed to freshwater, 50% seawater and 100% seawater for 10 minutes. Bars represent mean values ± SE of a minimum of 10 cells. Bars that share letters are not statistically significantly different ($p < 0.05$), as determined by one-way ANOVA followed by a Dunn's post-hoc analysis (SigmaPlot).

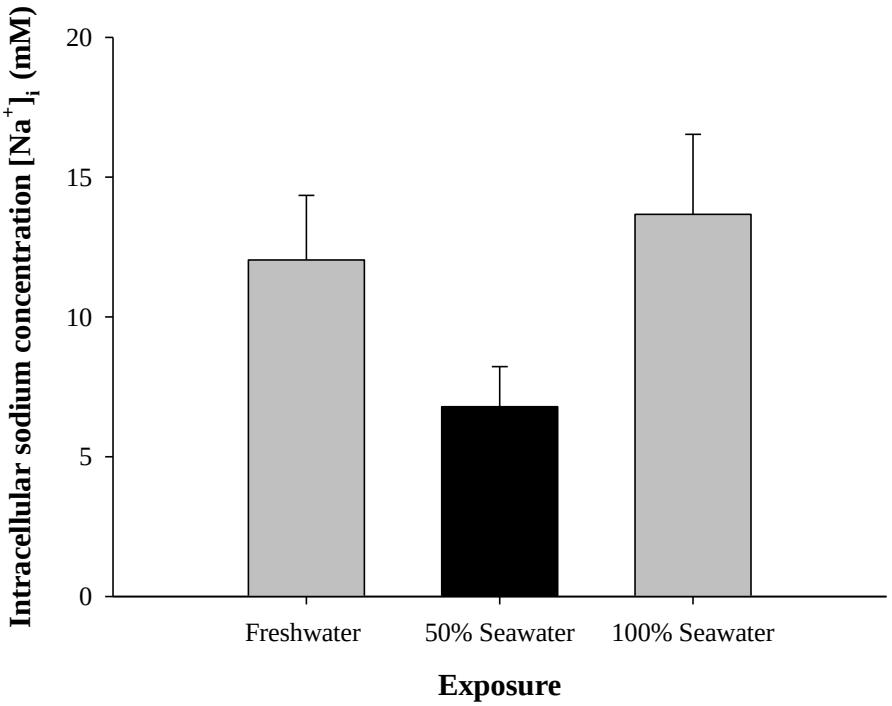

Figure 6.12: Intracellular sodium concentration $[Na^+]_i$ in gill cells of 50% seawater-acclimated inanga exposed to freshwater, 50% seawater and 100% seawater for 10 minutes. Bars represent mean values ± SE a minimum of 10 cells. No significant difference was found between exposures (one-way ANOVA; SigmaPlot).

Gill cells from 100% seawater-acclimated inanga showed a significant decrease in $[Na^+]_i$ when exposed to freshwater (Figure 6.13). The 10 minute exposure resulted in a $[Na^+]_i$ decrease from 16.2 ± 3.0 mM to 5.0 ± 1.8 mM. There was no significant change in $[Na^+]_i$ when the 100% seawater cells were exposed to 50% seawater.

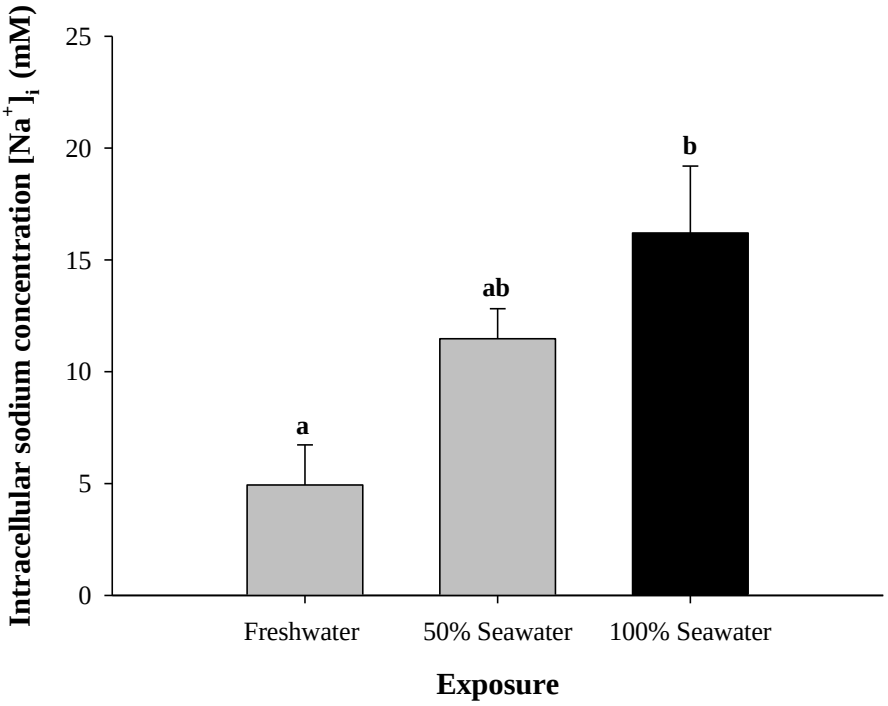

Figure 6.13 Intracellular sodium concentration $[Na^+]_i$ in gill cells of 100% seawater-acclimated inanga exposed to freshwater , 50% and 100% seawater for 10 minutes. Bars represent mean values ± SE of two experiments and a minimum of 10 cells per experiment. Bars that share letters are not statistically significantly different ($p < 0.05$), as determined by one-way ANOVA followed by a Holm-Sidak post-hoc analysis (SigmaPlot).

6.4.3.2 Internal sodium concentration $[Na^+]_i$ in the presence of amiloride and ouabain

To determine the effects of inhibitors on intracellular Na^+, the salinity response experiment was repeated as above but in the presence of ouabain and amiloride. The results from the salinity response experiment (no inhibitors) have been overlaid on the following graphs to aid comparison.

The $[Na^+]_i$ of freshwater inanga gill cells significantly increased when exposed to 100% seawater in the presence of amiloride (Figure 6.14). Comparison of the freshwater control (FW) to the freshwater and amiloride (FW + A) treatment showed the addition of amiloride alone was not enough to change $[Na^+]_i$ of freshwater-acclimated inanga gill cells. In the absence of amiloride (see Figure 6.11 and the blue diamond) an increase in intracellular Na^+ was also observed, but the presence of amiloride has significantly decreased the response.

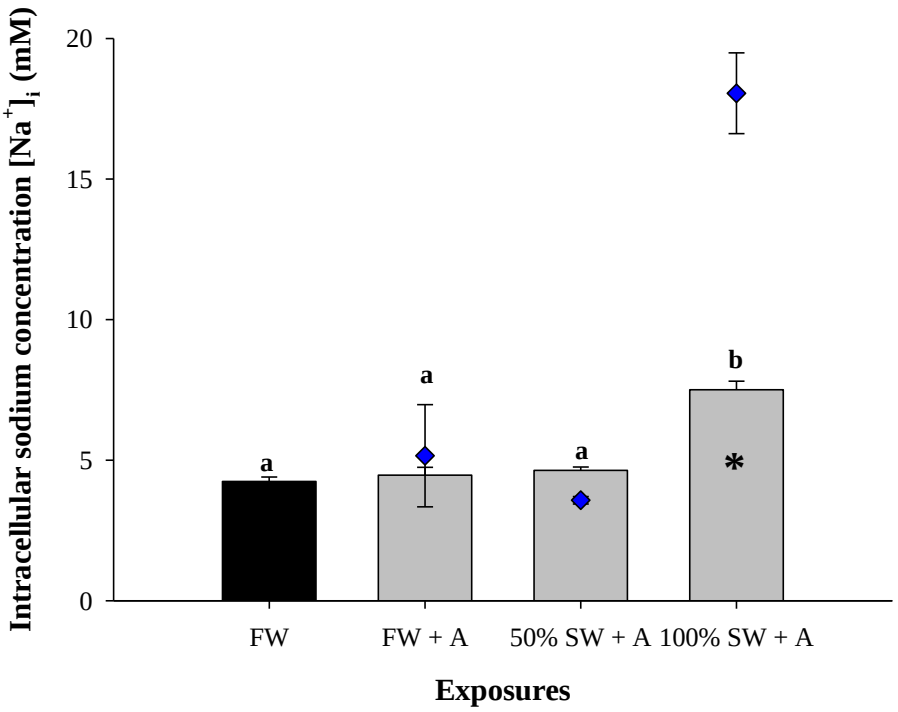

Figure 6.14: Intracellular sodium concentration $[Na^+]_i$ in gill cells of freshwater-acclimated inanga exposed to freshwater (FW), freshwater and 50 µM amiloride (FW + A), 50% seawater and 50 µM amiloride (50% SW + A) and 100% seawater and 50 µM amiloride (100%SW + A) for 10 minutes. Bars represent mean values ± SE of a minimum of 10 cells. Bars that share letters are not statistically significantly different ($p < 0.05$), as determined by a Kruskal-Wallis ANOVA followed by a Dunn's post-hoc test (SigmaPlot). Blue diamonds represent the no-inhibitor salinity exposure in Figure 6.11. Asterisks indicate statistical significance ($p < 0.05$) between the bars and diamonds as determined by Kruskal-Wallis ANOVA followed by a Dunn's post-hoc test (SigmaPlot).

Exposure to 100% seawater and amiloride significantly increased the $[Na^+]_i$ of gill cells acclimated to 50% seawater compared to the control and the 50% seawater $^+$ amiloride treatment (Figure 6.15). This increase was not seen in the absence of amiloride with no significant difference seen between the exposures (Figure 69). There was a statistically significant effect of increased $[Na^+]_i$ in 50% seawater cells exposed to freshwater in the presence of amiloride relative to the same manipulation in the absence of amiloride (blue diamonds and Figure 6.12).

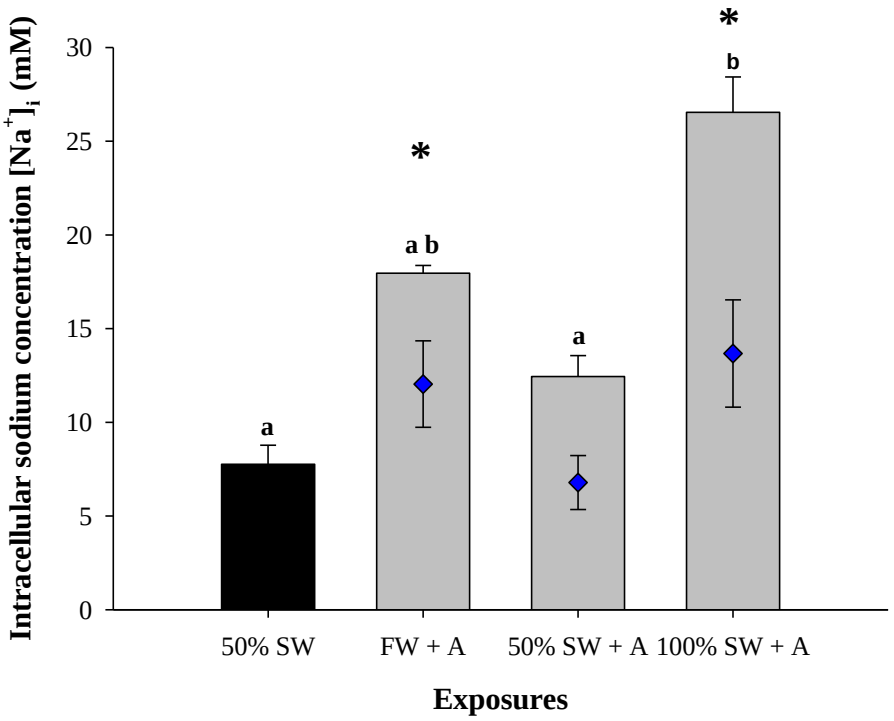

Figure 6.15 Intracellular sodium concentration $[Na^+]_i$ in gill cells of 50% seawater-acclimated inanga exposed to 50% seawater (50% SW), freshwater and 50 µM amiloride (FW $^+$ A), 50% seawater and 50 µM amiloride (50% SW $^+$ A), and 100% seawater and 50 µM amiloride (100%SW $^+$ A) for 10 minutes. Bars represent mean values ± SE of two experiments and a minimum of 10 cells per experiment. Bars that share letters are not statistically significantly different (p < 0.05), as determined by one-way ANOVA followed by a Holm-Sidak post-hoc analysis (SigmaPlot). Blue diamonds represent the no-inhibitor salinity exposure in Figure 6.12. Asterisks indicate statistically significant differences (p < 0.05) between the bars and diamonds as determine by Kruskal-Wallis ANOVA followed by a Dunn's of Holm-Sidak post-hoc test (SigmaPlot).

When 100% seawater-acclimated gills were exposed to 50% seawater and amiloride (50% SW $^{+}$ A) there was a significant 10-fold increase in $[Na^+]_i$ when compared to all other exposures (Figure 6.16). This increase was significantly greater to the response with 50% seawater alone (i.e. no amiloride) (blue diamonds and Figure 6.13). A significant decrease in $[Na^+]_i$ was seen when the gill cells were exposed to freshwater and amiloride but was statistically similar to the pattern observed with freshwater alone (blue diamonds and Figure 6.13).

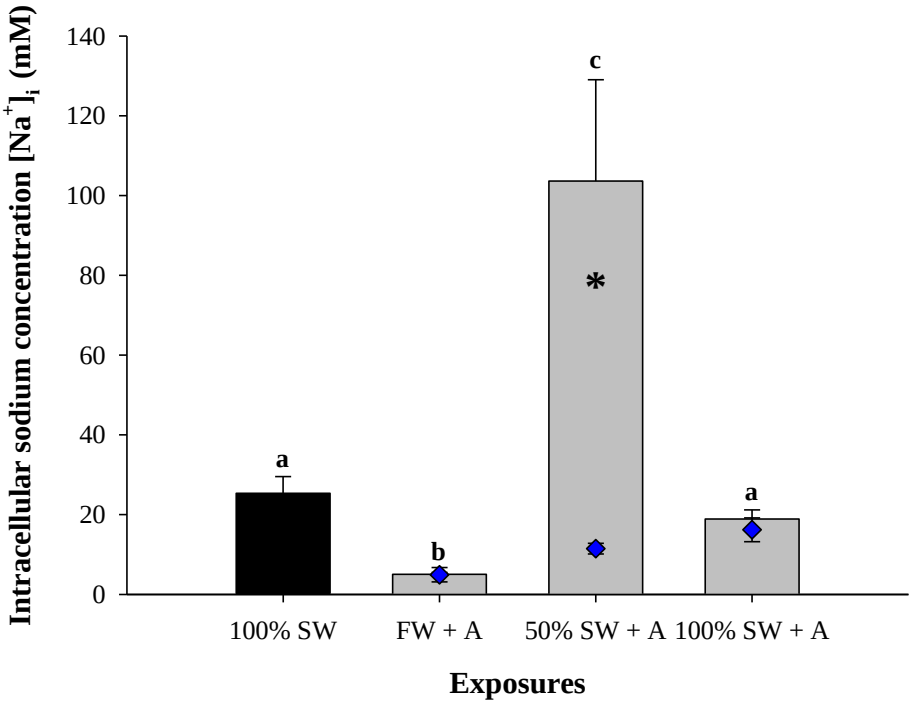

Figure 6.16 Internal sodium concentration $[Na^+]_i$ in gill cells of 100% seawater-acclimated inanga exposed to 100% seawater (100% SW), freshwater and 50 µM amiloride (FW + A), 50% seawater and 50 µM amiloride (50% SW + A) and 100% seawater and 50 µM amiloride (100%SW + A) for 10minutes. Bars represent mean values ± SE of two experiments and a minimum of 10 cells per experiment. Bars that share letters are not statically significantly different ($p < 0.05$), as determined by one-way Kruskal-Wallis one-way ANOVA followed by a Dunn's post-hoc test (SigmaPlot). Blue diamonds represent the no-inhibitor salinity exposure in Figure 6.13.

Exposure to 100% seawater and ouabain (100% SW $^{+}$ O) significantly increased the $[Na^{+}]_i$ in the gill cells of freshwater-acclimated inanga from 4.2 ± 0.2 mM to 8.3 ± 1.8 mM (Figure 6.17). This was similar to the pattern observed in the absence of ouabain, but the magnitude of this response was significantly lower in the presence of ouabain (blue diamond, Figure 6.11). Ouabain (FW + O) also significantly increased $[Na^{+}]_i$ when compared with the freshwater control (FW). No statistically significant difference was observed between the freshwater control group (FW) and the 50% seawater and ouabain group (50% SW $^{+}$ O), consistent with the pattern observed for freshwater-acclimated gill cells in the absence of ouabain.

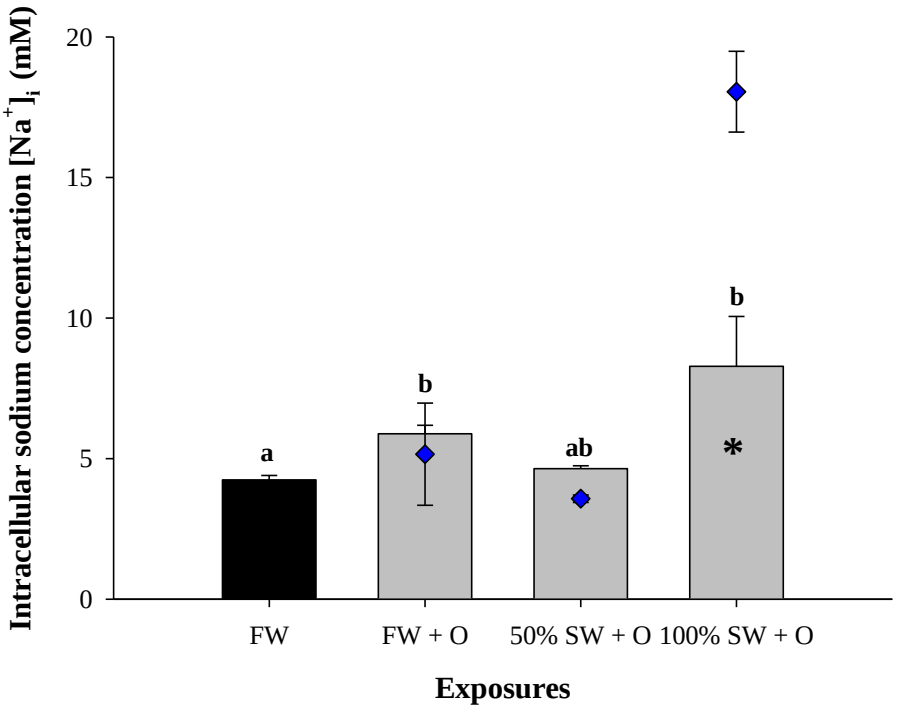

Figure 6.17 Intracellular sodium concentration $[Na^{+}]_i$ in gill cells of freshwater-acclimated inanga exposed to freshwater (FW), freshwater and 1 mM ouabain (FW + O), 50% seawater and 1 mM ouabain (50% SW + O) and 100% seawater and 1 mM ouabain (100%SW + O) for 10 minutes. Bars represent mean values ± SE of two experiments and a minimum of 10 cells per experiment. Bars that share letters are not statistically significantly different ($p < 0.05$), as determined by Kruskal-Wallis ANOVA followed by a Dunn's post-hoc test (SigmaPlot). Blue diamonds represent the no-inhibitor salinity exposure in Figure 6.11. Asterisks indicate statistical significance ($p < 0.05$) between the bars and diamonds as determine by Kruskal-Wallis ANOVA followed by a Dunn's or Holms-Sidak post-hoc test (SigmaPlot).

The $[Na^+]_i$ of 50% seawater-acclimated significantly increased upon exposure to 50% seawater and ouabain (50% SW $^+$ O) (Figure 6.18). This increase was greater than what was observed with 50% seawater alone (blue diamonds and Figure 6.13). It is also important to note here that the 50% seawater cells differed markedly in their $[Na^+]_i$ between the inhibitor-free treatment and the control of the experiments that incorporated the inhibitor, even though these treatments were essentially identical. Exposure of 50% seawater-acclimated gill cells to freshwater and 100% seawater in the presence of ouabain had no significant effect on $[Na^+]_i$ when compared to the control (50% SW) or when compared to the ouabain-free experiments (blue diamonds and Figure 6.13).

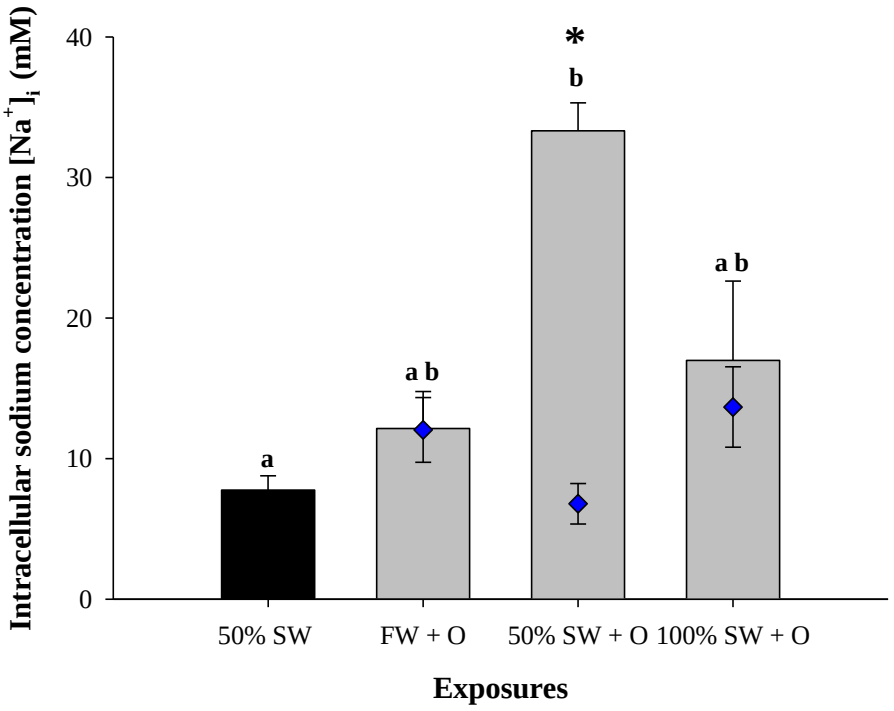

Figure 6.18 Intracellular sodium concentration $[Na^+]_i$ in gill cells of 50% seawater-acclimated inanga exposed to 50% seawater (50% SW), freshwater and 1 mM ouabain (FW + O), 50% seawater and 1 mM ouabain (50% SW + O), and 100% seawater and 1 mM ouabain (100%SW + O) for 10 minutes. Bars represent mean values ± SE of two experiments and a minimum of 10 cells per experiment. Bars that share letters are not statistically significantly different ($p < 0.05$), as determined by Kruskal-Wallis ANOVA followed by Dunn's post-hoc analysis (SigmaPlot). Blue diamonds represent the no-inhibitor salinity exposure in Figure 6.12. Asterisks indicate statistical significance ($p < 0.05$) between the bars and diamonds as determine by Kruskal-Wallis ANOVA followed by a Dunn's or Holm-Sidak post-hoc test (SigmaPlot).

Exposure to ouabain had no significant impact on $[Na^+]_i$ in the cells of 100% seawater-acclimated inanga (Figure 6.19). There was, however, a trend for decreasing $[Na^+]_i$ with decreasing salinity. There was also no significant change seen between the exposures 'with' ouabain to the 'without' ouabain exposures (blue diamonds and Figure 6.13)

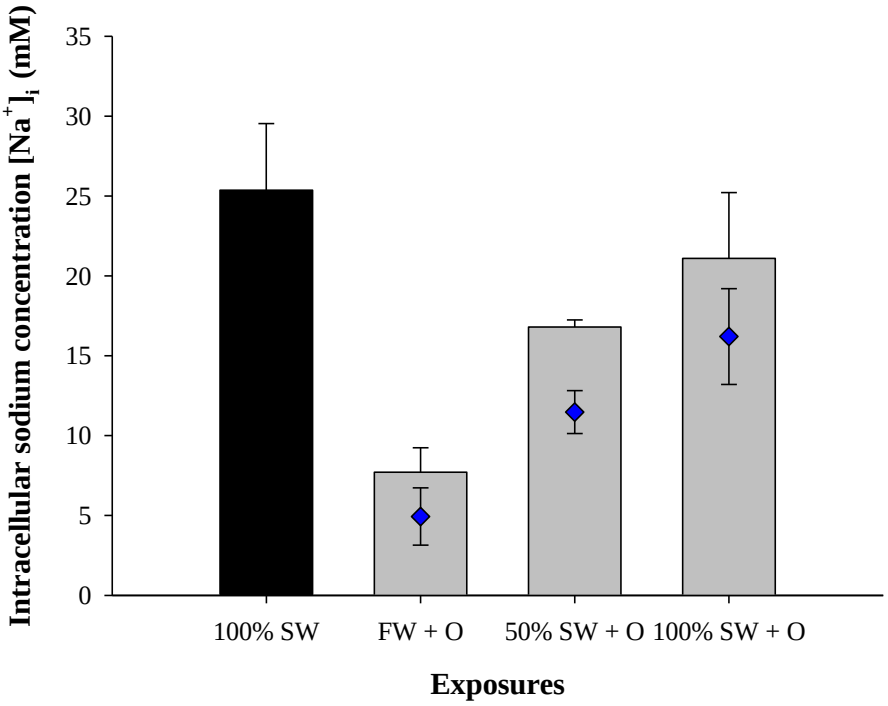

Figure 6.19 Intracellular sodium concentration $[Na^+]_i$ in gill cells of 100% seawater-acclimated inanga exposed to 100% seawater (100% SW), freshwater and 1 mM ouabain (FW $^+$ O), 50% seawater and 1 mM ouabain (50% SW $^+$ O) and 100% seawater and 1 mM ouabain (100%SW $^+$ O) for 10 minutes. Bars represent mean values ± SE of two experiments and a minimum of 4 cells per experiment. No significant difference was found between exposures (Kruskal-Wallis one-way ANOVA; SigmaPlot). Blue diamonds represent the no-inhibitor salinity exposure in Figure 6.13

6.5 Discussion

In freshwater, teleosts passively lose Na^+ to their environment and must actively replace the lost Na^+ ions via the gill epithelium. In seawater, the teleost gill actively excretes the Na^+ which is passively gained from the hyper-osmotic seawater (Evans, 1999). However, cells are generally considered to function within a very narrow range of ion concentrations. In part this is because ions perturbing osmolytes, meaning that they can significantly disrupt cellular processes such as enzyme function (Hochachka and Somero, 2002). For this reason levels of intracellular Na^+ within the fish gill are likely to be regulated. However the range of Na^+ ion concentrations that the gill cells of fish can operate within is unknown (Parks et al., 2008). Intracellular Na^+ is likely to reflect the net changes in Na^+ uptake and Na^+ loss within a cell. This will be primarily controlled by the actions of NKA which translocates Na^+ ions from inside the cell into the blood or paracellular spaces. Other transporters will also play a role, with NHE and/or ENaC facilitating apical exchange of Na^+ between the cell and the environment. Environmental salinity and the blood Na^+ concentration will also be important factors. Teleosts maintain their blood plasma Na^+ concentration around 130 mM in freshwater and 180 mM in seawater (Evans et al., 2005). Recent measurements of inanga plasma Na^+ show that inanga fall close to these values (120 – 130 mM in freshwater and 135 mM in seawater; M.A. Urbina, unpublished data). By maintaining a low $[Na^+]_i$ there will always be a gradient between the cell and the blood which is essential for generating electrochemical gradients (Evans et al., 2005), cell volume regulation (Lang, 2007) and other cellular homeostatic mechanisms. The data gathered in the current chapter shows that inanga appear capable of rapidly regulating MRC $[Na^+]_i$ within a range of Na^+ levels between ~5 mM in freshwater and 16 mM in seawater (Figure 6.20). This is the first known description of intracellular Na^+ levels as a function of salinity in a euryhaline fish gill cell.

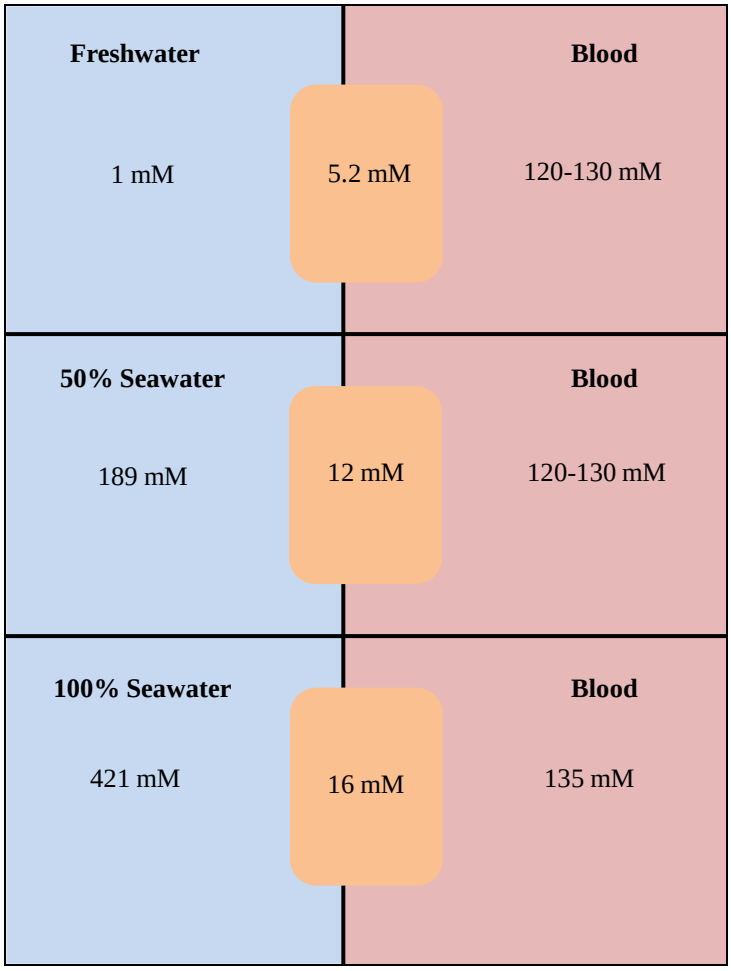

Figure 6.20 Summary of sodium gradients in inanga gill cells acclimated to different salinities

6.5.1 Intracellular sodium concentration $[Na^+]_i$

Studies investigating $[Na^+]_i$ in fish have reported a variety of concentrations ranging from 6.4 to 90 mM in freshwater fish (Wood and Le Moigne, 1991; Eddy and Chang, 1993; Morgan et al., 1994; Li et al., 1997). In this study inanga were shown to exhibit a mean $[Na^+]_i$ levels of 5.2 mM in freshwater. This value is the lowest recorded but within the range of most other measurements. It is notable, however, that the range previously reported varies by an order of magnitude. This is likely to be related to the method of analysis. Higher concentrations were found in studies using X-ray microanalysis where the Na^+ within the entire tissue (total cellular Na^+) cannot be differentiated from the Na^+

within an individual cell (intracellular Na^+) (Morgan et al., 1994). Techniques such as confocal microscopy and ion-specific microelectrodes, which employ live cells, tend to report lower $[Na^+]_i$. The concentrations reported in this work are in line with other observations reported in various vertebrate cells using confocal microscopy (Harootunian et al., 1989; Negulescu et al., 1990; Ahlemeyer et al., 1992; Tornquist and Ekokoski, 1993; Despa et al., 2002; Despa and Bers, 2003).

It is important to note that in freshwater the $[Na^+]_i$ is higher than that of the external Na^+ concentration, and therefore seems to counter the idea that absorption is achieved by reducing $[Na^+]_i$ to levels lower than that of the external environment. However the measurements in the this chapter do not account for local microenvironments in which levels of ions and, importantly, pH can vary significantly leading to favourable gradients for Na^+ uptake (Playle and Wood, 1989). Although the LSCM technique applied here is capable of examining changes in microenvironments, changes at a local scale were not the focus of the present work.

6.5.2 The effect of salinity

This study shows that in inanga, freshwater cells can maintain a Na^+ balance in response to a rapid *in vitro* exposure to 50% seawater, but did not maintain a freshwater $[Na^+]_i$ in response to rapid *in vitro* exposure to 100% seawater. Cells from 100% seawater fish were similar in that they can also maintain a Na^+ balance in 50% seawater but when exposed to freshwater, $[Na^+]_i$ dropped significantly. That cells were able to maintain a relatively constant $[Na^+]_i$ in light of salinity change implies that regulation of this parameter does not require central control. A fish's acclamatory responses to salinity stresses is based on its efficiency to sense osmotic stress and then mount a response via the osmotic stress signalling pathway (Fiol and Kültz, 2007). Osmotic sensors include membrane proteins, molecular chaperones, DNA damage sensors, baroreceptors, changes in cell membrane structure and cytoskeletal organisations that sense cell volume changes (Fiol and Kültz, 2007) are able to sense local changes in the environment and respond rapidly.

These findings also suggest inanga acclimated to freshwater or to 100% seawater possess a distinct freshwater or seawater cell phenotype where they maintain $[Na^+]_i$ at a specific ‘freshwater' or 'seawater' level. In contrast 50% seawater cells are equally adept at maintaining $[Na^+]_i$ at any salinity. This suggests one of two scenarios. These 50% seawater cells may have a stricter range of $[Na^+]_i$ that they must operate within, and therefore more tightly regulate $[Na^+]_i$. Alternatively they have regulatory components that are common to both freshwater and 100% seawater cells and therefore are capable of regulating at all salinities. These two scenarios are not mutually exclusive. The ability of 50% seawater acclimated cells to maintain $[Na^+]_i$ in the face of salinity change is advantageous to inanga as they may encounter daily variations in salinity particularly around the time of spawning. Similarly, both freshwater and 100% seawater fish are most likely to encounter 50% seawater if faced with a different salinity. In all these scenarios (50% seawater fish in either freshwater or 100% seawater, freshwater fish in 50% seawater, and 100% seawater fish in 50% seawater) $[Na^+]_i$ was maintained. This would ensure that cellular processes are kept in an optimal ionic environment and therefore will operate efficiently.

A study by Katoh and Kaneko (2003) showed acute exposure (24 hours) of killifish to freshwater induced seawater MRCs to transform into freshwater-type cells, whereas chronic exposure induced a replacement of seawater MRCs with newly differentiated freshwater MRCs. This supports the idea of distinct phenotypes in inanga as they have undergone a gradual acclimation process and may therefore only possess the distinct MRC phenotype required for that salinity. This is also supported by the findings of Chapter 2, which clearly showed differentiation of MRCs between the two salinities. Unfortunately this study did not examine 50% seawater-acclimated inanga, so it is not possible to determine whether cells at this salinity are more like freshwater or seawater MRCs.

6.5.3 The effect of amiloride and ouabain

Amiloride is a pharmacological agent that is proposed to inhibit the apical NHE in fish (Kleyman and Cragoe, Jr., 1988; McCormick, 1993). The presence of apical NHE in the fish gill remains controversial, and an alternative mechanism of apical Na^+ transport via an ENaC has been proposed (Evans et al., 1999). In freshwater, fish are faced with diffusive Na^+ loss, and the gill is tasked with maintaining homeostasis by absorbing Na^+ from the environment. If NHE is the mechanism by which Na^+ enters the freshwater cell, and it is inhibited by amiloride, a decrease in the $[Na^+]_i$ compared to the freshwater control (no amiloride) would be expected. This did not occur in the present study, suggesting that NHE may not be involved in Na^+ influx in the freshwater inanga gill. When the salinity on the apical side of the freshwater inanga gill cell was increased to 100% seawater and amiloride was present, an increase in $[Na^+]_i$ was observed. This effect was similar to that observed in the absence of amiloride, although the extent of the effect was significantly less in the presence of the inhibitor (Figure 6.14). Upon a rapid increase in environmental Na^+ it might be expected that pathways used for Na^+ absorption are overwhelmed. That amiloride reduces $[Na^+]_i$ to a significant extent could be evidence that an NHE is present (blocking a proportion of the influx). There is, therefore, conflicting evidence as to the presence of NHE in the freshwater inanga gill, suggesting that either there is no NHE on the apical surface of inanga gill cells or the Na^+ absorption is by an amiloride-insensitive pathway (e.g. ENaC).

At higher environmental salinities, the gill excretes Na^+ to rid the fish of excess ions that have accrued via diffusive ion influx. The mechanism of Na^+ efflux in the fish gill is not thought to directly involve NHE, and therefore it was not anticipated that amiloride would have an effect on $[Na^+]_i$. However the addition of amiloride to the bathing medium of 50% seawater-acclimated gill cells exposed to 100% seawater increased the $[Na^+]_i$. The 50% seawater cells were shown to be adept at maintaining a Na^+ balance at any salinity but this mechanism appears to be disrupted by amiloride. In 100% seawater-acclimated cells, amiloride had a large and significant effect on increasing $[Na^+]_i$ upon exposure to 50% seawater, an effect similar to that observed for the 50% sewater cells exposed to 100% seawater.

Overall the effects of amiloride do not present a cohesive picture of a role for NHE in Na^+ ion transport in inanga. There are a number of possible explanations for this. Amiloride is a promiscuous agent and it has been shown to inhibit other transporters and exchangers (Masareel et al., 2003). This is especially true at high concentrations (0.1 – 1 mM) where it is known to inhibit ion exchange, block ENaC and even inhibit NKA (Kleyman and Cragoe, 1988). The amiloride concentration used in this study (50 µM) was in line with other studies (10 - 100 µM) that have shown NHE-specific responses. However these studies were performed on MRCs from tilapia opercular epithelium and MRCs from zebrafish yolk sacs (Li et al., 1997; Esaki et al., 2007) and these epithelia may have a different response to amiloride than the preparation used in this study. The use of more specific inhibitors such as phenamil for ENaC (Kleyman and Cragoe, Jr., 1988; Alvarez de Canessa et al., 2000) and HOE 694 for NHE (Woll et al., 1993; Reid et al., 2003) may offer a greater insight, but this would require careful investigation of their exact inhibitory targets in inanga.

An alternative explanation relates to NHE isoforms. This thesis has already indicated the presence of ion transporter isoforms in inanga (Chapter 5), so there is a strong likelihood that if NHE is involved in apical Na^+ transport that multiple isoforms of this exchanger may exist. Some NHE isoforms have been shown to be resistant to amiloride such as the NHE3 isoform found in fish (Hirata et al., 2003; Choe et al., 2005). The presence of this isoform in inanga could account for the lack of consistent amiloride effect in freshwater. This inconsistency in $[Na^+]_i$ response in inanga gill cells treated with amiloride particularly in the freshwater inanga gill, coupled with the possibility of non-target effects of this drug, suggests that NHE is unlikely to be an important component of apical gill Na^+ transport in inanga.

Ouabain has been well characterised as an inhibitor of NKA. NKA lowers $[Na^+]_i$, creating a gradient for absorption of Na^+ from the environment, and this gradient is also utilised by other transporters, such that NKA is directly or indirectly responsible for all transport processes within the gill. Gill cells isolated from freshwater-acclimated inanga showed increased $[Na^+]_i$ on treatment with ouabain (in both freshwater and 100% seawater conditions). This increase in $[Na^+]_i$ likely reflect inhibition of the NKA by ouabain, which can no longer effectively maintain a lowered $[Na^+]_i$. A similar effect

was observed in 50% seawater-acclimated gill cells exposed to 50% seawater. However, no other treatment showed a significant effect of ouabain, with NKA having no effect at all in 100% seawater-acclimated inanga gills. In high Na^+ environments inhibition of NKA would be expected to cause an increase in $[Na^+]_i$ as the diffusively gained Na^+ is not able to be transported across the basolateral membrane. The lack of a ouabain effect suggests Na^+ has another route out of the cell. NHEs have been shown to be present on the basolateral membrane of MRCs in seawater teleosts and play a role in acid-base regulation where they move Na^+ into the cell in exchange for a proton (Claiborne et al., 1999). NHE's are known to be able to function in reverse (e.g. Demaurex et al., 1995), so it is possible that when $[Na^+]_i$ start to elevate, the basolateral NHE acts to limit the $[Na^+]_i$ increase. In this regard the NHE would act as a safety valve, ensuring that $[Na^+]_i$ do not rise to levels where it impacts cellular processes.

Different isoforms of NKA differ in their affinity for ouabain (Scheiner-Bobis and Schoner, 2001). In Chapter 5 it was shown that there is a salinity-dependent expression of isoforms, so it is possible that the lack of effect of ouabain in 100% seawater-acclimated inanga, for example, might indicate that the predominant NKA isoform expressed in this salinity is relatively insensitive to ouabain. Countering this argument is the observation (Chapter 3) that NKA activity is higher in 100% seawater-acclimated fish. An alternative explanation may relate to the method used. In this study ouabain was added to the bathing medium, whereas NKA is located on the basolateral membrane. It might be that ten minutes was an insufficient time for the drug to traverse the cell and reach its target. This would be especially true for seawater-acclimated fish, which display a thicker lamellae that could potentially impair diffusion.

This study has focussed on MRCs as they are thought to be the predominant cells type involved in ion regulation (Evans et al., 1999). A comparison of the responses of other cells types such as PVCs and ACs to this method may offer further insight into ionic regulation.

6.5.4 Technical issues

The use of fluorescent dyes and confocal microscopy is rapidly becoming the method of choice due to the relative simplicity of its use over other methods (Dailey et al., 2006), but it is not without its challenges. Quantification with confocal dyes relies heavily on the proper set-up and alignment of the confocal microscope. Every effort was made to keep experimental conditions consistent through the experiments but possible alignment issues with the confocal microscope caused by the Christchurch earthquakes 2010/2011 can not be ruled out.

6.6 Conclusion

This novel LSCM approach is advantageous relative to existing transport models as it will allow the observation of cellular ion transport in real time, within a native filament structure displaying functional interaction of different cell types. The development of a new confocal-based technique enabled the description of intracellular Na^+ levels as a function of salinity in a euryhaline fish gill cell for the first time. The low $[Na^+]_i$ recorded in freshwater-acclimated inanga would be advantageous in hypo-osmotic environments while the increase observed at in higher salinities minimise the diffusive gradient for passive influx from the environment which would be of benefit in hyper-osmotic environments.

Cells from 50% seawater-acclimated inanga were shown to be very adept at maintaining $[Na^+]_i$ in the face of salinity changes, a beneficial characteristic for the amphidromous lifestyle. Freshwater and 100% seawater cells were not as success full at regulating $[Na^+]_i$ in the face of significant salinity change (i.e. freshwater cells exposed to 100% seawater and 100% seawater cells exposed to freshwater). This suggests inanga acclimated to freshwater or to 100% seawater possess a distinct freshwater or seawater cell phenotype, where they maintain $[Na^+]_i$ at a specific ‘freshwater' or 'seawater' level.

This inconsistency in $[Na^+]_i$ response in inanga gill cells treated with amiloride, particularly in the freshwater inanga gill, coupled with the possibility of non-target effects of this drug, suggests that NHE is unlikely to be an important component of apical gill Na^+ transport in inanga. This is an important finding in light of the controversy that surrounds osmoregulation in freshwater (Chapter 1)

CHAPTER 7 GENERAL DISCUSSION

7.1 Summary of findings

Euryhaline fish have the remarkable ability to change their gills from an ion-absorbing epithelium in freshwater to the ion-secreting epithelium needed in seawater (McCormick, 2001). The work in this thesis supports this view and illustrates the remarkable ability of inanga to be successful in a variety of salinities (Chessman and Williams, 1975). Not only are inanga capable of survival in a range of salinities, they are able to do so over two distinct temporal regimes. As part of their development juvenile inanga migrate from seawater nurseries to freshwater adult habitat, and once in this environment their occupation of a niche near the saltwater wedge exposes them to daily fluctuations in salinity (McDowell, 2006). The physiology of inanga must be able to deal with these variations, although prior to this thesis almost nothing has been reported about the physiology of inanga is different salinities. The integrated approach used in this work has revealed that inanga have many characteristics that facilitate acclimation. These characteristics range from those that present at a whole body level all the way down to a molecular level.

Freshwater inanga are able to absorb Na^+ from the hypo-osmotic environment. At a whole body level inanga regulate Na^+ using a saturable, high affinity, low capacity uptake system which makes them extremely adept at extracting Na^+ from very dilute freshwater environments (Chapter 4). This effect is most likely mediated by the gill, but it is possible that the scalelesss nature of the inanga integument may also have a role, as has been seen in some other fish species (Marshall, 1995). At a tissue level the complex structural arrangement created by the filaments and lamellae of the gill (Chapter 3) provides a large surface for ion exchange. While the inanga gill was morphologically similar to other euryhaline teleosts it displayed high apical crypt and MRC density that allows for greater ion absorption in freshwater environments. In seawater, inanga remodel their gills to facilitate ion secretion in the hyper-osmotic environment (Chapter

3). The gill epithelium becomes thickened due to an increase in MRCs, which are essential for ion secretion (Evans et al., 1999).

The NKA is central to ion regulation as it not only transports important ions such as Na^+ and K^+, but it also provides the driving force for other transporters (Hwang and Lee, 2007). In high salinties inanga increased NKA activity in an effort to secrete the excess Na^+, diffusively gained from the hyper-osmotic environment (Chapter 4). This increase in NKA activity was most likely a reflection of the increased proliferation of NKA-containing MRCs (Chapter 3). The NKA activities seen in freshwater- and 50% seawater-acclimate inanga were similar. This suggests that the inanga gill is capable of supporting ion regulation in brackish waters without a significant increase in NKA activities, and the energetically-expensive changes in gill structure and function that accompany such a change.

Molecular investigation of NKA showed inanga displayed salinity-induced changes in the expression of all three α NKA isoform variants (Chapter 5). While isoform α1a showed a role in freshwater, as is seen in other fish species (e.g. Richards et al., 2003), α1b expression suggested it also played more of a role in freshwater than in seawater as other studies suggest. None of the salinity-induced changes could quantitatively explain the increased NKA activity in seawater suggesting that different isoforms may convey different activities, there is also regulation of NKA at a post-transcriptional level, and/or other isoforms or subunits may have a significant role.

The impact of the osmoregulatory hormones, cortisol and prolactin on NKA activity and isoform expression was varied and may have been potentially compromised by the underlying effect of stress induced by handling and hormonal injection treatments. One clear pattern that did emerge was the combined effect of cortisol and prolactin in 100% seawater. Treatment with cortisol and prolactin resulted in a significant decrease in NKA activity (Chapter 4) and in the expression levels of all three isoforms (Chapter 5).

A major achievement of the research described in this thesis was the development of a new confocal-based technique that was able to describe for the first time intracellular Na^+ levels as a function of salinity in a euryhaline fish gill cell (Chapter 6). Gill cells from freshwater-acclimated inanga displayed lower $[Na^+]_I$ than cells from 50% and

100% seawater-acclimated inanga. Low $[Na^+]_i$ is advantageous in hypo-osmotic environments as it provides a gradient between the cell and the blood which is essential for generating electrochemical gradients (Evans et al., 2005), cell volume regulation (Lang, 2007) and other cellular homeostatic mechanisms. As salinity increased so did $[Na^+]_i$. A slightly higher $[Na^+]_i$ would help minimise the diffusive gradient for passive influx from the environment which would be of benefit in hyper-osmotic environments. Freshwater cells can maintain a Na^+ balance in response to 50% seawater, but in 100% seawater a higher $[Na^+]_i$ level resulted. Similarly, 100% seawater cells reduced $[Na^+]_i$ to a 'freshwater' level when placed in a dilute water, but maintained $[Na^+]_i$ at the 'seawater' level when placed in 50% seawater. This suggests inanga acclimated to freshwater or 100% seawater possess a distinct freshwater or seawater cell phenotype that enables them to maintain $[Na^+]_i$ at an optimal level. In contrast 50% seawater cells were equally adept at maintaining a constant $[Na^+]_i$ at any salinity, suggesting these cells are have the necessary constituents to regulate Na^+ in both lower and higher salinities, to achieve the $[Na^+]_i$ that is optimal for the physiology of the 50% seawater MRC. This novel LSCM approach is advantageous relative to existing transport models as it will allow the observation of cellular ion transport in real time, within a native filament structure displaying functional interaction of different cell types.

The overall the effects of amiloride in this study were unable to present a cohesive picture of a role for NHE in Na^+ ion transport in inanga (Chapter 6). This inconsistency in $[Na^+]_i$ response in inanga gill cells treated with amiloride, particularly in the freshwater inanga gill, coupled with the possibility of non-target effects of this drug, suggests that NHE is unlikely to be an important component of apical gill Na^+ transport in inanga. However, the possible presence of NHE isoforms that are resistant to amiloride cannot be ruled out and warrants further investigation.

7.2 Are inanga a model species?

This study showed that inanga are a valuable model species. Several characteristics such as their extreme ion uptake characteristics (bestowing a 'Krogh' model status) and their amenability to confocal-based studies make them an attractive model species.

One specific use for inanga is as a potentially valuable model for investigating metal toxicity. Metals such as copper and silver are known to be Na^+ transport pathway antagonists (Grosell et al., 2002). In fact there is a strong correlation between the rate of Na^+ transport and the sensitivity of an aquatic organism to the concentration of these metal ions in the water. Aquatic animals with rapid turnover of Na^+ also employ high affinity mechanisms for Na^+ absorption (Grosell et al., 2002). Given that inanga show an extremely high affinity for Na^+ uptake (Chapter 4), they are therefore predicted to exhibit high sensitivity to metals such as copper and silver. As yet there is little known regarding the sensitivity of inanga to metal toxicants. Future investigations that combine inanga with the confocal-based method developed in this study, may prove to be a powerful tool in studying the causes and implications of metal toxicity, both by examining the antagonised ion (e.g. via CoroNa green; Chapter 6) and also the toxicant metal (e.g. using Phen Green for copper; Kim and Ahner, 2006).

There are, however, some potential drawbacks to the utility of inanga as a model organism. These include the lack of basic physiological characterisation (relative to well-studied groups such as salmonids); a lack of understanding the targets of pharmacological agents (see Chapter 6), and the limited genomic knowledge (relative to species such as zebrafish; Ekker et al., 2007). There are also other, practical, considerations such as the high susceptibility to stress (see Chapter 5) and to fungal growth in a laboratory environment (personal observations). Some of these challenges could potentially be overcome by increased use and characterisation of inanga especially with the confocal-based method developed within this study.

One particularly issue that may be problematic in using inanga as a model species in ionoregulation work is the high levels of inter-individual variability that was noted in the current work. This may be partially attributed to the fact that inanga were sourced

from wild populations. Wild fish populations are more genetically diverse than farmed fish populations (McGinnity et al., 1997), leading to more experimental variation. The propagation of a laboratory-based homogeneous population of inanga may help differentiate the possible sources of experimental variation. There are laboratory protocols available for laboratory culture of inanga (Mitchell, 1989), but these are time-consuming and not always successful (C. N. Glover, personal communication). Much of the variation in physiological responses could also be related to inherent physiological rhythms. As a species with a defined life history (i.e. seasonal migration, spawning and senescence, diurnal tidal influences) there is a strong likelihood that intrinsic variations in physiology may result. Over the course of the current thesis the disruptions caused by the Christchurch earthquakes of 2010/2011 meant that different populations of inanga were used during this study. These populations were sourced from the wild at different times of the year and this may have contributed to the variation observed. Until these inherent patterns are well understood, they may also limit the utility of inanga as a model species.

7.3 Environmental context

Inanga are one of the very few fish species that are known to exhibit amphidromy. This specialised form of diadromy involves the migration of newly hatched fish to the ocean for feeding and growth, before returning to freshwater (McDowall, 2007). Amphidromy necessitates the ability for rapid salinity acclimation in order to balance the diverse challenges of diffusive ion gain (in seawater), and diffusive ion loss (in freshwater). This thesis illustrates the structural, molecular, biochemical and physiological processes underlying this process.

New Zealand has a relatively depauperate native fish population. There are two main groups, the bullies and the galaxiids (McDowall, 2001). The later group comprises inanga and approximately 37 other species. The galaxiid fish have radiated successfully in New Zealand freshwaters, and a component of their success must be attributed to their physiological capacity to adapt to new environments. However galaxiid fish are under increasing pressure from a number of different sources (McDowall 2006b). This is of particular important with respect to inanga, as this is the major species in the whitebait fishery. This fishery has been in decline over recent years (McDowall, 2006b). The whitebait fishery is now managed by the Department of Conservation, New Zealand which dictates in which rivers and estuaries whitebait fishing is permitted and sets seasonal fishing periods and fishing equipment restrictions (McDowall, 2006b). Inanga also face the threat of habitat destruction from intensification of agricultural practices such as the damming of rivers for irrigation purposes, pollution from run-off and general erosion. Metal pollution in particular (see section 7.2 above) may be an issue. There are also significant threats to galaxiids from introduced species such as the salmonids that are primarily thought to impact galaxiid populations by direct predation (McIntosh et al., 2010). One strategy for conservation is identifying waters where galaxiids may have a selective advantage over salmonids, and may therefore escape their predation effects (McIntosh etal., 2010). A large component of understanding fish habitat distribution is understanding their physiological capacities to withstand certain environmental conditions (e.g. salinity). Consequently, increased knowledge of inanga

physiology will provide critical information for the conservation of this species and its capacity to respond to environmental change both natural and man-made.

7.4 Future directions

The inanga used in this research were all sourced from wild populations that are generally heterogeneous in nature. Establishment of a homogenous population of inanga, followed by basic physiological characterisation would help address the possible sources of variation seen within this study. It was the intention of this study to replicate all experiments with the widely studied King salmon to compare and contrast with inanga. However due to the Christchurch earthquakes of 2010/2011 this was not possible. Basic physiological characterisation of salmon using the same experimental procedures would allow a nose-to-nose comparison which may help identify if variation seen is species- or experimentally-induced.

Some of the variation observed in the confocal studies using inhibitor amiloride may be a reflection of its promiscuous nature (Masareel et al., 2003). The use of more specific inhibitors such as phenamil for ENaC (Kleyman and Cragoe, Jr., 1988; Alvarez de Canessa et al., 2000) and HOE 694 for NHE (Woll et al., 1993; Reid et al., 2003) may offer further insight. However more extensive investigation of the exact inhibitory targets in inanga should be performed before firm conclusions can be reached.

Other species such as salmon display distinct life stage differences in osmoregulatory characteristics (McCormick, 2001; Björnsson et al., 2011). It would be of interest to compare physiological characteristics of different life stages such as larva, juvenile and adult inanga to see if there are differences in physiology as a consequence of developmental stage.

The confocal method developed in this study has vast potential for future research in fish in general. Future work may include the use of other ion specific fluorescent dyes (e.g. for K^+) or the use of fluorescent transport inhibitors such as EIPA that inhibits NHE (Beltran et al., 2008), and would therefore also be a tool to localise NHE (Johnson and Spence, 2010). This study has focussed on MRCs as they are thought to be the predominant cells type involved in ion regulation (Evans et al., 1999). It would be of interest to compare the responses of other cells types such as PVCs and ACs to this method may offer further insight into ionic regulation.

The presence of isoform switching has been demonstrated in inanga but there is much scope for future research in this area. Further characterisation of NKA isoforms to identify seawater-dependent isoforms would greatly add to the understanding of isoform switching and may help explain the discrepancies seen between isoform expression and NKA activity.

ACKNOWLEGEMENTS

I would like to sincerely thank my supervisor, Dr. Chris Glover, for his encouragement and support during what has been an eventful and often frustrating project. His expertise, guidance and enthusiasm for this project have been invaluable.

Thanks to my associated supervisor Dr. David Collings for his ideas and suggestions throughout the project. I would also like to thank the technical staff from the School of Biological Sciences, in particular Neil Andrews, Manfred Ingerfeld, Gavin Robinson and Rennie Bishop for their technical support.

Many thanks to Dr. Carol Bucking (University of Ottawa, Canada), and Dr. Pål Olsvik (National Institute of Nutrition and Seafood Research, Norway) for their excellent advice regarding qPCR experiments.

Thank you to Dr. Arvind Varsani and members of the Virology Research Group (University of Canterbury) for providing a work space and assistance for the molecular work.

A big thank you to Prof. Bill Davison and Selwyn Cox for looking after the fish during the numerous earthquake-imposed closures.

Thank you to New Zealand King Salmon and Fish and Game Canterbury and in particular Dirk Barr for providing the salmon used in this project.

Thank you to Mauricio Urbina (University of Canterbury, New Zealand) and Prof. Patricia Schulte (University of British Columbia, Canada) for allowing access to their unpublished data.

I would like to acknowledge funding from the Royal Society of New Zealand Marsden Grant (UOC0711) and University of Canterbury, College of Science Grant.

Finally, I would like to thank my family and friends for their unwavering support during this project.

CHAPTER 8 REFERENCES

Ahlemeyer, B., Weintraut, H. and Schoner, W. (1992). Cultured chick-embryo heart cells respond differently to ouabain as measured by the increase in their intracellular Na^+ concentration. *Biochimica et Biophysica Acta - Molecular Cell Research* **1137**, 135-142.

Alberts, B., Johnson, A., Lewis, J., Raff, M., Roberts, K. and Walter, P. (2002). Molecular Biology of the Cell. New York: Garland Science.

Albrecht, R. M. and Oliver, J. A. (2011). Labeling considerations for confocal microscopy. In *Basic Confocal Microscopy* (eds. R. L. Price and W. G. Jerome). New York: Springer.

Allendorf, F. W. and Thorgaard, G. H. (1984). Tetraploidy and the evolution of Salmonid fishes. In *Evolutionary Genetics of Fishes*, (ed. B. J. Turner), pp. 1-53. New York: Plenum Press.

Aluru, N. and Vijayan, M. M. (2009). Stress transcriptomics in fish: A role for genomic cortisol signaling. *General and Comparative Endocrinology* **164**, 142-150.

Alvarez de Canessa, C. M., Fyfe, G. K. and Zhang, P. (2000). Structure and regulation of amiloride-sensitive sodium channels. *Annual Review of Physiology* **62**, 573-594.

Amorino, G. P. and Fox, M. H. (1995). Intracellular Na^+ measurements using sodium green tetraacetate with flow cytometry. *Cytometry* **21**, 248-256.

Andrews, P. M., Petroll, W. M., Cavanagh, H. D. and Jester, J. V. (1991). Tandem scanning confocal microscopy (TSCM) of normal and ischemic living kidneys. *American Journal of Anatomy* **191**, 95-102.

Ara, N., Iijima, K., Asanuma, K., Yoshitake, J., Ohara, S., Shimosegawa, T. and Yoshimura, T. (2008). Disruption of gastric barrier function by luminal nitrosative stress: a potential chemical insult to the human gastro-oesophageal junction. *Gut* **57**, 306-313.

Avella, M., Berhaut, J. and Payan, P. (1994). Primary culture of gill epithelial cells from the sea bass *Dicentrarchus labrax*. *In Vitro Cellular and Developmental Biology - Animal* **30 A**, 41-49.

Baker, C. F. and Hicks, B. J. (2003). Attraction of migratory inanga (*Galaxias maculatus*) and koaro (*Galaxias brevipinnis*) juveniles to adult galaxiid odours. *New Zealand Journal of Marine and Freshwater Research* **37**, 291-299.

Barnett, R. E. (1970). Effect of monovalent cations on the ouabain inhibition of the sodium and potassium ion activated adenosine triphosphatase. *Biochemistry* **9**, 4644-4648.

Bellamy, D. (1961). Movements of potassium, sodium and chloride in incubated gills from the silver eel. *Comparative Biochemistry and Physiology* **3**, 125-135.

Beltrán, A. R., Ramírez, M. A., Carraro-Lacroix, L. R., Hiraki, Y., Rebouças, N. A. and Malnic, G. (2008). NHE1, NHE2, and NHE4 contribute to regulation of cell pH in T84 colon cancer cells. *Pflügers Archive European Journal of Physiology* **455**, 799-810.

Björnsson, B. T., Stefansson, S. O. and McCormick, S. D. (2011). Environmental endocrinology of salmon smoltification. *General and Comparative Endocrinology* **170**, 290-298.

Blanco, G. and Mercer, R. W. (1998). Isozymes of the Na-K-ATPase: Heterogeneity in structure, diversity in function. *American Journal of Physiology* **275**, F633-F650.

Blum, H., Nioka, S. and Johnson, R. G. (1990). Activation of the Na^+,K^+-ATPase in *Narcine brasiliensis*. *Proceedings of the National Academy of Sciences of the United States of America* **87**, 1247-1251.

Boisen, A. M. Z., Amstrup, J., Novak, I. and Grosell, M. (2003). Sodium and chloride transport in soft water and hard water acclimated zebrafish (*Danio rerio*). *Biochimica et Biophysica Acta - Biomembranes* **1618**, 207-218.

Bole-Feysot, C., Goffin, V., Edery, M., Binart, N. and Kelly, P. A. (1998). Prolactin (PRL) and its receptor: Actions, signal transduction pathways and phenotypes observed in PRL receptor knockout mice. *Endocrine Reviews* **19**, 225-268.

Bolis, C. L., Piccolella, M., Dalla Valle, A. Z. and Rankin, J. C. (2001). Fish as model in pharmacological and biological research. *Pharmacological Research* **44**, 265-280.

Bozzola, J. J. and Russell, L. D. (1999). Electron Microscopy: Principles and Techniques for Biologists. Sudbury, MA: Jones and Barlett Learning.

Breves, J. P., Seale, A. P., Helms, R. E., Tipsmark, C. K., Hirano, T. and Grau, E. G. (2011). Dynamic gene expression of GH/PRL-family hormone receptors in gill and kidney during freshwater-acclimation of Mozambique tilapia. *Comparative Biochemistry and Physiology A - Molecular and Integrative Physiology* **158**, 194-200.

Brisson, M., Hall, S., Hamby, R. K., Park, R. and Srere, H. K. (2004). Optimization of single and multiplex real-time PCR. In *A-Z of quantitative PCR* (ed. S. A. Bustin). La Jolla, CA: International University Line.

Burridge, C. P., McDowall, R. M., Craw, D., Wilson, M. V. H. and Waters, J. M. (2012). Marine dispersal as a pre-requisite for Gondwanan vicariance among elements of the galaxiid fish fauna. *Journal of Biogeography* **39**, 306-321.

Bustin, S. A. (2000). Absolute quantification of mRNA using real-time reverse transcription polymerase chain reaction assays. *Journal of Molecular Endocrinology* **25**, 169-193.

Bustin, S. A. (2004). A-Z of quantitative PCR. La Jolla, CA: International University Line.

Bystriansky, J. S., Richards, J. G., Schulte, P. M. and Ballantyne, J. S. (2006). Reciprocal expression of gill Na^+/K^+-ATPase α-subunit isoforms α1a and α1b during sea water acclimation of three salmonid fishes that vary in their salinity tolerance. *Journal of Experimental Biology* **209**, 1848-1858.

Bystriansky, J. S., Frick, N. T., Richards, J. G., Schulte, P. M. and Ballantyne, J. S. (2007). Failure to up-regulate gill Na^+,K^+-ATPase α-subunit isoform α1b may limit seawater tolerance of land-locked Arctic char (*Salvelinus alpinus*). *Comparative Biochemistry and Physiology A - Molecular and Integrative Physiology* **148**, 332-338.

Campbell, N. A. and Reece, J. B. (2005). Biology. San Francisco, CA: Benjamin Cummings.

Carrier, J. C. and Evans, D. H. (1976). The role of environmental calcium in freshwater survival of the marine teleost, *Lagodon rhomboides*. *Journal of Experimental Biology* **65**, 529-538.

Chakrabotri, R. K., Weisbart, M. and Chakrabotri, A. (1987). The presence of corticosteroid receptor activity in the gills of the brook trout, *Salvelinus fontinalis*. *General and Comparative Endocrinology* **66**, 323-332.

Chandler, D. E. and Roberson, R. W. (2009). Bioimaging: Current Concepts in Light and Electron Microscopy. Sudbury, MA: Jones & Bartlett Publishers.

Chernyavskiy, O., Vannucci, L., Bianchini, P., Difato, F., Saieh, M. and Kubinova, L. (2009). Imaging of mouse experimental melanoma *in vivo* and *ex vivo* by combination of confocal and nonlinear microscopy. *Microscopy Research and Techniques* **72**, 411-423.

Chessman, B. C. and Williams, W. D. (1975). Salinity tolerance and osmoregulatory ability of *Galaxias maculatus* (Jenyns) (Pisces, Salmoniformes, Galaxiidae). *Freshwater Biology* **5**, 135-140.

Choe, K. P., Kato, A., Hirose, S., Plata, C., Sindić, A., Romero, M. F., Claiborne, J. B. and Evans, D. H. (2005). NHE3 in an ancestral vertebrate: Primary sequence, distribution, localization, and function in gills. *American Journal of Physiology - Regulatory, Integrative and Comparative Physiology* **289**, R1520-R1534.

Claiborne, J. B., Walton, J. S. and Compton-McCullough, D. (1994). Acid-base regulation, branchial transfers and renal output in a marine teleost fish (the long-horned sculpin *Myoxocephalus octodecimspinosus*) during exposure to low salinities. *Journal of Experimental Biology* **193**, 79-95.

Claiborne, J. B., Blackston, C. R., Choe, K. P., Dawson, D. C., Harris, S. P., Mackenzie, L. A. and Morrison-Shetlar, A. I. (1999). A mechanism for branchial acid excretion in marine fish: Identification of multiple Na^+/H^+ antiporter (NHE) isoforms in gills of two seawater teleosts. *Journal of Experimental Biology* **202**, 315-324.

Clarke, A. P. and Potts, W. T. W. (1998). Isolated filament potentials and branchial ion fluxes in the European flounder (*Platichthys flesus* L.). Evidence for proton pump-mediated sodium uptake. *Journal of Zoology* **246**, 433-442.

Cornell-Bell, A. H., Finkbeiner, S. M., Cooper, M. S. and Smith, S. J. (1990). Glutamate induces calcium waves in cultured astrocytes: Long-range glial signaling. *Science* **247**, 470-173.

Cornish-Bowden, A. C. (1979). Fundamentals of Enzyme Kinetics. London: Butterworth and Co.

Cossins, A. R. and Crawford, D. L. (2005). Fish as models for environmental genomics. *Nature* **6**, 324-332.

Cutler, C. P., Sanders, I. L., Hazon, N. and Cramb, G. (1995). Primary sequence, tissue-specificity and expression of the Na^+,K^+-ATPase α-1 subunit in the European eel (*Anguilla anguilla*). *Comparative Biochemistry and Physiology B - Biochemistry and Molecular Biology* **111**, 567-573.

Daborn, K., Cozzi, R. R. F. and Marshall, W. S. (2001). Dynamics of pavement cell-chloride cell interactions during abrupt salinity change in *Fundulus heteroclitus*. *Journal of Experimental Biology* **204**, 1889-1899.

Dailey, M., Manders, E. M. M., Soll, D. and Terasaki, M. (2006). Confocal microscopy of live cells. In *Handbook of Biological Confocal Microscopy, 3rd edition* (ed. J. B. Pawley), pp. 381-403. New York: Springer.

De Proost, I., Pintelon, I., Brouns, I., Kroese, A. B. A., Riccardi, D., Kemp, P. J., Timmermans, J. P. and Adriaensen, D. (2008). Functional live cell imaging of the pulmonary neuroepithelial body microenvironment. *American Journal of Respiratory Cell and Molecular Biology* **39**, 180-189.

Demaurex, N., Orlowski, J., Brisseau, G., Woodside, M. and Grinstein, S. (1995). The mammalian Na^+/H^+ antiporters NHE-1, NHE-2, and NHE-3 are electroneutral and voltage independent, but can couple to an H^+ conductance. *Journal of General Physiology* **106**, 85-111.

Despa, S. and Bers, D. M. (2003). Na/K pump current and $[Na]_i$ in rabbit ventricular myocytes: Local $[Na]_i$ depletion and Na buffering. *Biophysical Journal* **84**, 4157-4166.

Despa, S., Islam, M. A., Weber, C. R., Pogwizd, S. M. and Bers, D. M. (2002). Intracellular Na^+ concentration is elevated in heart failure but Na/K pump function is unchanged. *Circulation* **105**, 2543-2548.

Eddy, F. B. and Chang, Y. J. (1993). Effects of salinity in relation to migration and development in fish. In *The Vertebrate Gas Transport Cascade: Adaptation to Environment and Mode of Life* (eds. J. Eduardo and P. W. Bicudo), pp. 35-42. Boca Raton, FL: CRC Press.

Edwards, S. L., Tse, C. M. and Toop, T. (1999). Immunolocalisation of NHE3-like immunoreactivity in the gills of the rainbow trout (*Oncorhynchus mykiss*) and the blue-throated wrasse (*Pseudolabrus tetrious*). *Journal of Anatomy* **195**, 465-469.

Ekker, S. C., Stemple, D. L., Clark, M., Chien, C. B., Rasooly, R. S. and Javois, L. C. (2007). Zebrafish genome project: Bringing new biology to the vertebrate genome field. *Zebrafish* **4**, 239-251.

Esaki, M., Hoshijima, K., Kobayashi, S., Fukuda, H., Kawakami, K. and Hirose, S. (2007). Visualization in zebrafish larvae of Na^+ uptake in mitochondria-rich cells whose differentiation is dependent on foxi3a. *American Journal of Physiology - Regulatory, Integrative and Comparative Physiology* **292**, R470-R480.

Evans, D. H. (1973). Sodium uptake by the sailfin molly, *Poecilia latipinna*: Kinetic analysis of a carrier system present in both fresh-water acclimated and sea-water acclimated individuals. *Comparative Biochemistry and Physiology* **45A**, 843-850.

Evans, D. H. (1984). The roles of gill permeability and transport mechanisms in euryhalinity. In *Fish Physiology, Vol. X, Part B: Gills- Ion and Water Transfer* (eds W. S. Hoar and D. J. Randall), pp. 239-283. New York: Academic Press.

Evans, D. H. (1998). The Physiology of Fishes. New York: CRC Press.

Evans, D. H. (2008). Teleost fish osmoregulation: What have we learned since August Krogh, Homer Smith, and Ancel Keys. *American Journal of Physiology - Regulatory, Integrative and Comparative Physiology* **295**, 704-713

Evans, D. H., Piermarini, P. M. and Potts, W. T. W. (1999). Ionic transport in the fish gill epithelium. *Journal of Experimental Zoology* **283**, 641-652.

Evans, D. H., Piermarini, P. M. and Choe, K. P. (2005). The multifunctional fish gill: Dominant site of gas exchange, osmoregulation, acid-base regulation, and excretion of nitrogenous waste. *Physiological Reviews* **85**, 97-177.

Eyckmans, M., Tudorache, C., Darras, V. M., Blust, R. and De Boeck, G. (2010). Hormonal and ion regulatory response in three freshwater fish species following waterborne copper exposure. *Comparative Biochemistry and Physiology C - Toxicology & Pharmacology* **152**, 270-278.

Farrell, A. P. (2011). Encyclopedia of Fish Physiology: From Genome to Environment. Burlington: Academic Press.

Febry, R. and Lutz, P. (1987). Energy partitioning in fish: The activity-related cost of osmoregulation in a euryhaline cichlid. *Journal of Experimental Biology* **128**, 63-85.

Fenwick, J. C., Wendelaar Bonga, S. E. and Flik, G. (1999). *In vivo* bafilomycin-sensitive Na^+ uptake in young freshwater fish. *Journal of Experimental Biology* **202**, 3659-3666.

Fiol, D. F. and Kültz, D. (2007). Osmotic stress sensing and signaling in fishes. *FEBS Journal* **274**, 5790-5798.

Franklin, N.M., Adams, M.S., Stauber, J.L., and Lim, R.P. (2001). Development of an improved rapid enzyme inhibition bioassay with marine and freshwater microalgae using flow cytometry. *Archieves of Environmental Contamination and Toxicology* **40**, 469-480.

Garty, H., Lindzen, M., Scanfano, R., Aizman, R., Fuzesi, M., Goldshleger, R., Farman, N., Blostein, R. and Karlish, S. J. D. (2002). A functional interaction between CHIF and Na,K-ATPase: Implication for regulation by FXYD proteins. *American Journal of Physiology - Renal Physiology* **283**, F607-F615.

Gilmour, K. M., Perry, S. F., Esbaugh, A. J., Genz, J., Taylor, J. R. and Grosell, M. (2012). Compensatory regulation of acid-base balance during salinity transfer in rainbow trout (*Oncorhynchus mykiss*). *Journal of Comparative Physiology B: Biochemical, Systemic, and Environmental Physiology* **182**, 259-274.

Glover, C. N. (2007). Cellular and molecular approaches to the investigation of piscine osmoregulation: Current and future perspectives. In *Fish Osmoregulation* (eds. B. Baldisserotto, J. M. Mancera and B. G. Kapoor), pp. 177-234. Enfield, NH: Science Publishers.

Glover, C. N., Pane, E. F. and Wood, C. M. (2005). Humic substances influence sodium metabolism in the freshwater crustacean *Daphnia magna*. *Physiological and Biochemical Zoology* **78**, 405-416.

Goldstein, J., Newbury, D. E., Joy, D. C., Lyman, C. E., Echlin, P., Lifshin, E., Sawyer, L. and Michael, J. R. (2003). Scanning Electron Microscopy and X-ray Microanalysis. New York: Springer.

Goss, G. G., Laurent, P. and Perry, S. F. (1994). Gill morphology during hypercapnia in brown bullhead (*Ictalurus nebulosus*): Role of chloride cells and pavement cells in acid-base regulation. *Journal of Fish Biology* **45**, 705-718.

Grosell, M., Nielsen, C. and Bianchini, A. (2002). Sodium turnover rate determines sensitivity to acute copper and silver exposure in freshwater animals. *Comparative Biochemistry and Physiology - C Toxicology and Pharmacology* **133**, 287-303.

Grupcheva, C. N., Laux Fenton, W. T., Green, C. R. and McGhee, C. N. J. (2003). *In vivo* and *ex vivo* confocal analysis of a rat model demonstrating transient 'epithelialization of the endothelium'. *Clinical and Experimental Ophthalmology* **30**, 191-195.

Gry, M., Rimini, R., Strömberg, S., Asplund, A., Pontén, F., Uhlén, M. and Nilsson, P. (2009). Correlations between RNA and protein expression profiles in 23 human cell lines. *BMC Genomics* **10**, 365.

Grynkiewicz, G., Poenie, M. and Tsien, R. Y. (1985). A new generation of Ca^{2+} indicators with greatly improved fluorescence properties. *Journal of Biological Chemistry* **260**, 3440-3450.

Harootunian, A. T., Kao, J. P. Y., Eckert, B. K. and Tsien, R. Y. (1989). Fluorescence ratio imaging of cytosolic free Na^+ in individual fibroblasts and lymphocytes. *Journal of Biological Chemistry* **264**, 19458-19467.

Hawkings, G. S., Galvez, F. and Goss, G. G. (2004). Seawater acclimation causes independent alterations in Na^+/K^+- and H^+-ATPase activity in isolated mitochondria-rich cell subtypes of the rainbow trout gill. *Journal of Experimental Biology* **207**, 905-912.

Hazon, N. and Balment, R. J. (1998). Endocrinology. In *The Physiology of Fishes*, (ed. D. H. Evans), pp. 441-463. Boca Raton, FL: CRC Press.

Herndon, T. M., McCormick, S. D. and Bern, H. A. (1991). Effects of prolactin on chloride cells in opercular membrane of seawater-adapted tilapia. *General and Comparative Endocrinology* **83**, 283-289.

Hirano, T. (1986). The spectrum of prolactin action in teleosts. In *Comparative Endocrinology, Developments and Directions* (ed. C. L. Ralph), pp. 53-74. New York: Alan R. Liss.

Hirata, T., Kaneko, T., Ono, T., Nakazato, T., Furukawa, N., Hasegawa, S., Wakabayashi, S., Shigekawa, M., Chang, M. H., Romero, M. F. and Hirose, S. (2003). Mechanism of acid adaptation of a fish living in a pH 3.5 lake. *American Journal of Physiology - Regulatory, Integrative and Comparative Physiology* **284**, R1199-R1212.

Hirose, S., Kaneko, T., Naito, N. and Takei, Y. (2003). Molecular biology of major components of chloride cells. *Comparative Biochemistry and Physiology B - Biochemistry and Molecular Biology* **136**, 593-620.

Hoar, W. S. (1988). The physiology of smolting salmonids. In *Fish Physiology, Vol. XI, Part B: The Physiology of Developing Fish - Viviparity and Posthatching Juveniles* (eds W. S. Hoar and D. J. Randall), pp. 275-343. New York: Academic Press.

Hochachka, P. W. and Somero, G. N. (2002). Biochemical Adaptation. Oxford, U.K.: Oxford University Press.

Hwang, P. P. and Lee, T. H. (2007). New insights into fish ion regulation and mitochondrion-rich cells. *Comparative Biochemistry and Physiology A - Molecular and Integrative Physiology* **148**, 479-497.

Hwang, P. P., Lee, T. H. and Lin, L. Y. (2011). Ion regulation in fish gills: Recent progress in the cellular and molecular mechanisms. *American Journal of Physiology - Regulatory, Integrative and Comparative Physiology* **301**, R28-R47.

Innis, M. A., Gelfand, D. H., Sninsky, J. J. and White, T. J. (1990). PCR Protocols: A Guide to Methods and Applications. San Diego, CA: Academic Press.

Jankowski, J. A. Z. and Polak, J. M. (1996). Clinical Gene Analysis and Manipulation: Tools, Techniques and Troubleshooting. Cambridge: Cambridge University Press.

Johnson, G. D. and Patterson, C. (1996). Relationships of lower euteleostean fishes. In *Interrelationship of Fishes*, (eds. M. J. L. Stiassny L. R. Parenti and G. D. Johnson), pp. 251-332. New York: Academic Press.

Johnson, I. and Spence, M. T. Z. (2010). The Molecular Probes Handbook: A Guide to Fluorescent Probes and Labeling Technologies. Eugene, OR: Life Technologies Corporation.

Kajimura, S., Hirano, T., Visitacion, N., Moriyama, S. and Aida, K. (2003). Dual mode of cortisol action on GH/IGF-1/IGF binding proteins in the tilapia, *Oreochromis mossambicus*. *Journal of Endocrinology* **178**, 91-99.

Karnaky, Jr., K. J. (1998). Osmotic and ionic regulation. In *The Physiology of Fishes* (ed. D. H. Evans), pp. 157-176. Boca Raton, FL: CRC Press.

Karnaky, Jr., K. J., Kinter, L. B., Kinter, W. B. and Stirling, C. E. (1976). Teleost chloride cell. II Autoradiographic localization of gill Na^+, K^+-ATPase in killifish (*Fundulus heteroclitus*) adapted to low and high salinity environments. *Journal of Cell Biology* **70**, 157-177.

Katoh, F. and Kaneko, T. (2003). Short-term transformation and long-term replacement of branchial chloride cells in killifish transferred from seawater to freshwater, revealed by morphofunctional observations and a newly established 'time-differential double fluorescent staining' technique. *Journal of Experimental Biology* **206**, 4113-4123.

Katoh, F., Hasegawa, S., Kita, J., Takagi, Y. and Kaneko, T. (2001). Distinct seawater and freshwater types of chloride cells in killifish, *Fundulus heteroclitus*. *Canadian Journal of Zoology* **79**, 822-829.

Kelly, S. P. and Wood, C. M. (2002a). Cultured gill epithelia from freshwater tilapia (*Oreochromis niloticus*): Effect of cortisol and homologous serum supplements from stressed and unstressed fish. *Journal of Membrane Biology* **190**, 29-42.

Kelly, S. P. and Wood, C. M. (2002b). Prolactin effects on cultured pavement cell epithelia and pavement cell plus mitochondria-rich cell epithelia from freshwater rainbow trout gills. *General and Comparative Endocrinology* **128**, 44-56.

Kelly, S. P., Chow, I. N. K. and Woo, Y. S. (1999). Effects of prolactin and growth hormone on strategies of hypoosmotic adaptation in a marine teleost, *Sparus sarba*. *General and Comparative Endocrinology* **113**, 9-22.

Kelly, S. P., Fletcher, M., Pärt, P. and Wood, C. M. (2000). Procedures for the preparation and culture of 'reconstructed' rainbow trout branchial epithelia. *Methods in Cell Science* **22**, 153-163.

Kerstetter, T. H., Kirschner, L. B. and Rafuse, D. D. (1970). On the mechanism of sodium ion transport by the irrigated gills of rainbow trout (*Salmo gairdneri*). *Journal of Experimental Biology* **56**, 342-359.

Kiilerich, P., Kristiansen, K. and Madsen, S. S. (2007a). Cortisol regulation of ion transporter mRNA in Atlantic salmon gill and the effect of salinity on the signalling pathway. *Journal of Endocrinology* **194**, 417-427.

Kiilerich, P., Kristiansen, K. and Madsen, S. S. (2007b). Hormone receptors in gills of smolting Atlantic salmon, *Salmo salar*: Expression of growth hormone, prolactin, mineralocorticoid and glucocorticoid receptors and 11β-hydroxysteroid dehydrogenase type 2. *General and Comparative Endocrinology* **152**, 295-303.

Kiilerich, P., Tipsmark, C. K., Borski, R. J. and Madsen, S. S. (2011). Differential effects of cortisol and 11-deoxycorticosterone on ion transport protein mRNA levels in gills of two euryhaline teleosts, Mozambique tilapia (*Oreochromis mossambicus*) and striped bass (*Morone saxatilis*). *Journal of Endocrinology* **209**, 115-126.

Kim, H. S. and Ahner, B. A. (2006). Calibration of Phen Green for use as a Cu (I) - selective fluorescent indicator. *Analytica Chemica Acta* **575**, 223-229.

King, J. A. C. and Hossler, F. E. (1991). The gill arch of the striped bass (*Morone saxatilis*). 4. Alterations in the ultrastructure of chloride cell apical crypts and chloride efflux following exposure to seawater. *Journal of Morphology* **209**, 165-176.

Kleyman, T. R. and Cragoe, Jr., E. J. (1988). Amiloride and its analogs as tools in the study of ion transport. *Journal of Membrane Biology* **105**, 1-21.

Kowalczyk, A., Boens, N., Meuwis, K. and Ameloot, M. (1997). Potential misevaluation of the ground-state dissociation constant from fluorimetric titrations: Application to the ion indicators SBFI, PBFI, and Fura-2. *Analytical Biochemistry* **245**, 28-37.

Krebs, H. A. (1975). The August Krogh principle: “For many problems there is an animal on which it can be most conveniently studied”. *Journal of Experimental Biology* **194**, 309-344.

Krogh, A. (1939). Osmotic Regulation in Aquatic Animals. Cambridge, MA: Cambridge University Press.

Kültz, D. (2001). Evolution of osmosensory MAP kinase signaling pathways. *American Zoologist* **41**, 743-757.

Kültz, D., Jürss, K. and Jonas, L. (1995). Cellular and epithelial adjustments to altered salinity in the gill and opercular epithelium of a cichlid fish (*Oreochromis mossambicus*). *Cell and Tissue Research* **279**, 65-73.

Kumai, Y. and Perry, S. F. (2011). Ammonia excretion via Rhcg1 facilitates Na^+ uptake in larval zebrafish, *Danio rerio*, in acidic water. *American Journal of Physiology - Regulatory, Integrative and Comparative Physiology* **301**, R1517-R1528.

Kwon, H. M. and Handler, J. S. (1995). Cell volume regulated transporters of compatible osmolytes. *Current Opinion in Cell Biology* **7**, 465-471.

Lang, F. (2007). Mechanism and significance of cell volume regulation. *Journal of the American College of Nutrition* **26**, 613S-623S.

Laurent, P. and Dunel, S. (1980). Morphology of gill epithelia in fish. *American Journal of Physiology* **238**, R147-R159.

Laurent, P. and Perry, S. F. (1990). Effects of cortisol on gill chloride cell morphology and ionic uptake in the freshwater trout, *Salmo gairdneri*. *Cell and Tissue Research* **259**, 429-442.

Laurent, P., Hõbe, H. and Dunel-Erb, S. (1985). The role of environmental sodium chloride relative to calcium in gill morphology of freshwater salmonid fish. *Cell and Tissue Research* **240**, 675-692.

Laurent, P., Chevalier, C. and Wood, C. M. (2006). Appearance of cuboidal cells in relation to salinity in gills of *Fundulus heteroclitus*, a species exhibiting branchial Na^+ but not Cl^- uptake in freshwater. *Cell and Tissue Research* **325**, 481-492.

Laurent, P., Wood, C. M., Wang, Y., Perry, S. F., Gilmour, K. M., Pärt, P., Chevalier, C., West, M. and Walsh, P. J. (2001). Intracellular vesicular trafficking in the gill epithelium of urea-excreting fish. *Cell and Tissue Research* **303**, 197-210.

Li, J., Eygensteyn, J., Lock, R. A. C., Wendelaar Bonga, S. E. and Flik, G. (1997). Na^+ and Ca^{2+} homeostatic mechanisms in isolated chloride cells of the teleost *Oreochromis mossambicus* analysed by confocal laser scanning microscopy. *Journal of Experimental Biology* **200**, 1499-1508.

Lin, H., Pfeiffer, D. C., Vogl, A. W., Pan, J. and Randall, D. J. (1994). Immunolocalization of H^+-ATPase in the gill epithelia of rainbow trout. *Journal of Experimental Biology* **195,** 169-183.

Lin, L. Y., Horng, J. L., Kunkel, J. G. and Hwang, P. P. (2006). Proton pump-rich cell secretes acid in skin of zebrafish larvae. *American Journal of Physiology - Cell Physiology* **290**, C371-C378.

Lingrel, J. B. (1992). Na,K-ATPase: isoform structure, function, and expression. *Journal of Bioenergetics and Biomembranes* **24**, 263-270.

Livak, K. J. and Schmittgen, T. D. (2001). Analysis of relative gene expression data using real-time quantitative PCR and the $2^{-\Delta\Delta Ct}$ method. *Methods* **25**, 402-408.

Lodish, H., Berk, A., Kaiser, C. A., Krieger, M., Scott, M. P., Bretscher, A., Ploegh, H. and Matsudaira, P. (2008). Molecular Cell Biology. New York: W.H. Freeman and Company.

Madsen, S. S. and Bern, H. A. (1992). Antagonism of prolactin and growth hormone: Impact on seawater adaptation in two salmonids, *Salmon trutta* and *Oncorhynchus kisutch*. *Zoological Science* **9**, 775-784.

Madsen, S. S., Kiilerich, P. and Tipsmark, C. K. (2009). Multiplicity of expression of Na^+,K^+-ATPase α-subunit isoforms in the gill of Atlantic salmon (*Salmo salar*): Cellular localisation and absolute quantification in response to salinity change. *Journal of Experimental Biology* **212**, 78-88.

Madsen, S. S., Jensen, M. K., Nohr, J. and Kristiansen, K. (1995). Expression of Na^+-K^+-ATPase in the brown trout, *Salmo trutta*: *In vivo* modulation by hormones and seawater. *American Journal of Physiology - Regulatory, Integrative and Comparative Physiology* **269**, R1339-R1345.

Maetz, J. (1971). Fish gills: Mechanisms of salt transfer in freshwater and seawater. *Philosophical Transactions of the Royal Society B: Biological Sciences* **262**, 209-251.

Maetz, J. (1973). Na^+/NH_4^+, Na^+/H^+ exchanges and NH_3 movement across the gill of *Carassius auratus*. *Journal of Experimental Biology* **58**, 255-275.

Mancera, J. M., Carrión, R. L. and Martín del Río, M. D. (2002). Osmoregulatory action of PRL, GH, and cortisol in the gilthead seabream (*Sparus aurata* L.). *General and Comparative Endocrinology* **129**, 95-103.

Mancera, J. M. and McCormick, S. D. (2000). Rapid activation of gill Na^+,K^+-ATPase in the euryhaline teleost *Fundulus heteroclitus*. *Journal of Experimental Zoology* **287**, 263-274.

Mancera, J. M. and McCormick, S. D. (2007). Role of prolactin, growth hormone, insulin-like growth factor I and cortisol in teleost osmoregulation. In *Fish Osmoregulation*, (eds. B. Baldisserotto J. M. Mancera and B. G. Kapoor). New Hampshire: Science Publishers.

Manzon, L. (2002). The role of prolactin in fish osmoregulation: A review. *General and Comparative Endocrinology* **125**, 291-310.

Marshall, W. S. (1995). Transport processes in isolated teleost epithelia: Opercular epithelium and urinary bladder. In *Fish Physiology, vol. XIV: Cellular and Molecular Approaches to Fish Ionic Regulation* (eds. C. M. Wood and T. J. Shuttleworth), pp. 1-23. London: Academic Press.

Marshall, W. S. (2002). Na^+, Cl^-, Ca^{2+}, Zn^{2+} transport by fish gills: Retrospective review and prospective synthesis. *Journal of Experimental Zoology* **293**, 264-283.

Marshall, W. S. and Bellamy, D. (2010). The 50 year evolution of *in vitro* systems to reveal salt transport functions of teleost fish gills. *Comparative Biochemistry and Physiology A - Molecular and Integrative Physiology* **155**, 275-280.

Marshall, W. S., Bryson, S. E., Midelfart, A. and Hamilton, W. F. (1995). Low conductance anion channel activated by cAMP in teleost Cl^- secreting cells. *American Journal of Physiology - Regulatory, Integrative and Comparative Physiology* **268**, R963-R969.

Martill, D. M. and Harper, L. (1990). An application of critical point drying to the comparison of modern and fossilized soft tissues of fishes. *Palaeontology* **33**, 423-428.

Masareel, B. A., Pochet, L. and Laeckmann, D. (2003). An overview of inhibitors of Na^+/H^+ exchange. *European Journal of Medicinal Chemistry* **38**, 547-554.

Matsuo, A. Y. O., Playle, R. C., Val, A. L. and Wood, C. M. (2004). Physiological action of dissolved organic matter in rainbow trout in the presence and absence of copper: Sodium uptake kinetics and unidirectional flux rates in hard and softwater. *Aquatic Toxicology* **70**, 63-81.

Mazon, A. de F., Nolan, D. T., Lock, R. A. C., Wendelaar Bonga, S. E. and Fernandes, M. N. (2007). Opercular epithelial cells: A simple approach for *in vitro* studies of cellular responses in fish. *Toxicology* **230**, 53-63.

McCormick, S. D. (1990). Fluorescent labelling of Na^+, K^+-ATPase in intact cells by use of a fluorescent derivative of ouabain: Salinity and teleost chloride cells. *Cell and Tissue Research* **260**, 529-533.

McCormick, S. D. (1993). Methods for non-lethal gill biopsy and measurement of Na^+/K^+-ATPase activity. *Canadian Journal of Fisheries and Aquatic Sciences* **50**, 656-658.

McCormick, S. D. (1995). Hormonal control of gill Na^+, K^+-ATPase and chloride cell function. In *Fish Physiology, vol. XIV: Cellular and Molecular Approaches to Fish Ionic Regulation* (eds. C. M. Wood and T. J. Shuttleworth), pp. 285–315. London: Academic Press.

McCormick, S. D. (1996). Effects of growth hormone and insulin-like growth factor I on salinity tolerance and gill Na^+, K^+-ATPase in Atlantic salmon (*Salmo salar*): Interaction with cortisol. *General and Comparative Endocrinology* **101**, 3-11.

McCormick, S. D. (2001). Endocrine control of osmoregulation in teleost fish. *American Zoologist* **41**, 781-794.

McCormick, S. D., Regish, A. M. and Christensen, A. K. (2009). Distinct freshwater and seawater isoforms of Na^+/K^+-ATPase in gill chloride cells of Atlantic salmon. *Journal of Experimental Biology* **212**, 3994-4001.

McCormick, S. D., Regish, A., O'Dea, M. F. and Shrimpton, J. M. (2008). Are we missing a mineralocorticoid in teleost fish? Effects of cortisol, deoxycorticosterone and aldosterone on osmoregulation, gill Na^+,K^+-ATPase activity and isoform mRNA levels in Atlantic salmon. *General and Comparative Endocrinology* **157**, 35-40.

McCormick, S. D., Sundell, K., Björnsson, B. T., Brown, C. L. and Hiroi, J. (2003). Influence of salinity on the localization of Na^+/K^+-ATPase, $Na^+/K^+/2Cl^-$ cotransporter (NKCC) and CFTR anion channel in chloride cells of the Hawaiian goby (*Stenogobius hawaiiensis*). *Journal of Experimental Biology* **206**, 4575-4583.

McCormick, S. D., Shrimpton, J. M., Carey, J. B., O'Dea, M. F., Sloan, K. E., Moriyama, S. and Björnsson, B. T. (1998). Repeated acute stress reduces growth rate of Atlantic salmon parr and alters plasma levels of growth hormone, insulin-like growth factor I and cortisol. *Aquaculture* **168**, 221-235.

McDowall, R. M. (1988). Diadromy in fishes: Migrations between freshwater and marine environments. London: Croom Helm.

McDowall, R. M. (1990). When galaxiid and salmonid fishes meet - a family reunion in New Zealand. *Journal of Fish Biology* **37**, 35-43.

McDowall, R. M. (1997). The evolution of diadromy in fishes (revisited) and its place in phylogenetic analysis. *Reviews in Fish Biology and Fisheries* **7**, 443-462.

McDowall, R. M. (2001). Freshwater Fishes of New Zealand. Auckland: Reed.

McDowall, R. M. (2002). The origin of the salmonid fishes: Marine, freshwater...or neither? *Reviews in Fish Biology and Fisheries* **11**, 171-179.

McDowall, R. M. (2006a). Crying wolf, crying foul, or crying shame: Alien salmonids and a biodiversity crisis in the southern cool-temperate galaxioid fishes? *Reviews in Fish Biology and Fisheries* **16**, 233-422.

McDowall, R. M. (2006b). Fish, fish habitats and fisheries in New Zealand. *Aquatic Ecosystem Health and Management* **9**, 391-405.

McDowall, R. M. (2007). On amphidromy, a distinct form of diadromy in aquatic organisms. *Fish and Fisheries* **8**, 1-13.

McDowall, R. M. and Pole, M. (1997). A large galaxiid fossil (Teleostei) from the Miocene of Central Otago, New Zealand. *Journal of the Royal Society of New Zealand* **27**, 193-198.

McDowall, R. M., Mitchell, C. P. and Brothers, E. B. (1994). Age at migration from the sea of juvenile *Galaxias* in New Zealand (Pisces, Galaxiidae). *Bulletin of Marine Science* **54**, 385-402.

McGinnity, P., Stone, C., Taggart, J. B., Cooke, D., Cotter, D., Hynes, R., McCamley, C., Cross, T. and Ferguson, A. (1997). Genetic impact of escaped farmed Atlantic salmon (*Salmo salar* L.) on native populations: Use of DNA profiling to assess freshwater performance of wild, farmed and hybrid progeny in a natural river environment. *ICES Journal of Marine Science* **54**, 998-1008.

McIntosh, A. R., McHugh, P. A., Dunn, N. R., Goodman, J. M., Howard, S. W., Jellyman, P. G., O'Brien, L. K., Nyström, P. and Woodford, D. J. (2010). The impact of trout on galaxiid fishes in New Zealand. *New Zealand Journal of Ecology* **34**, 195-206.

Meier, S. D., Kovalchuk, Y. and Rose, C. R. (2006). Properties of the new fluorescent Na^+ indicator CoroNa Green: Comparison with SBFI and confocal Na^+ imaging. *Journal of Neuroscience Methods* **155**, 251-259.

Meredith, A. S., Davie, P. S. and Forster, M. E. (1982). Oxygen uptake by the skin of the Canterbury mudfish, *Neochanna burrowsius*. *New Zealand Journal of Zoology* **9**, 387-390.

Mitchell, C. P. (1989). Laboratory culture of *Galaxias maculatus* and potential applications. *New Zealand Journal of Marine & Freshwater Research* **23**, 325-336.

Mommsen, T. P., Vijayan, M. M. and Moon, T. W. (1999). Cortisol in teleosts: Dynamics, mechanisms of action, and metabolic regulation. *Reviews in Fish Biology and Fisheries* **9**, 211-268.

Morgan, I. J., Potts, W. T. W. and Oates, K. (1994). Intracellular ion concentrations in branchial epithelial cells of brown trout (*Salmo trutta* L.) determined by X-ray microanalysis. *Journal of Experimental Biology* **194**, 139-151.

Myers, G. S. (1949). Usage of anadromous, catadromous and allied terms for migratory fishes. *Copeia*, 89-97.

Negulescu, P. A., Harootunian, A., Tsien, R. Y. and Machen, T. E. (1990). Fluorescence measurements of cytosolic free Na concentration, influx and efflux in gastric cells. *Molecular Biology of the Cell* **1**, 259-268.

Nilsen, T. O., Ebbesson, L. O. E., Madsen, S. S., McCormick, S. D., Andersson, E., Björnsson, B. T., Prunet, P. and Stefansson, S. O. (2007). Differential expression of gill Na^+,K^+-ATPase α- and β-subunits, Na^+,K^+,$2Cl^-$ cotransporter and CFTR anion channel in juvenile anadromous and landlocked Atlantic salmon *Salmo salar*. *Journal of Experimental Biology* **210**, 2885-2896.

Nolan, T., Hands, R. E. and Bustin, S. A. (2006). Quantification of mRNA using real-time RT-PCR. *Nature Protocols* **1**, 1559-1582.

Nordlie, F. G. (2009). Environmental influences on regulation of blood plasma/serum components in teleost fishes: A review. *Reviews in Fish Biology and Fisheries* **19**, 481-564.

O'Rourke, N. A. and Fraser, S. E. (1990). Dynamic changes in optic fiber terminal arbors lead to retinotopic map formation: An *in vivo* confocal microscopic study. *Neuron* **5**, 159-171.

Olsvik, P. A., Lie, K. K., Jordal, A. E. O., Nilsen, T. and Hordvik, I. (2005). Evaluation of potential reference genes in real-time RT-PCR studies of Atlantic salmon. *BMC Molecular Biology* **6**, 21.

Onken, H., Tresguerres, M. and Luquet, C. M. (2003). Active NaCl absorption across posterior gills of hyperosmoregulating *Chasmagnathus granulatus*. *Journal of Experimental Biology* **206**, 1017-1023.

Orlando, C., Pinzani, P. and Pazzagli, M. (1998). Developments in quantitative PCR. *Clinical Chemistry and Laboratory Medicine* **36**, 255-269.

Paddock, S. W., Fellers, T. J. and Davidson, M. W. (2012). Confocal microscopy: Basic concepts. Nikon.
http://www.microscopyu.com/articles/confocal/confocalintrobasics.html

Paredes, R. M., Etzler, J. C., Watts, L. T., Zheng, W. and Lechleiter, J. D. (2008). Chemical calcium indicators. *Methods* **46**, 143-151.

Park, M., Lee, H., Lee, J. S., Byun, M. O. and Kim, B. G. (2009). *In planta* measurements of Na^+ using fluorescent dye CoroNa Green. *Journal of Plant Biology* **52**, 298-302.

Parks, S. K., Tresguerres, M. and Goss, G. G. (2008). Theoretical considerations underlying Na^+ uptake mechanisms in freshwater fishes. *Comparative Biochemistry and Physiology C - Toxicology & Pharmacology* **148**, 411-418.

Pärt, P. and Wood, C. M. (1996). Na/H exchange in cultured epithelial cells from fish gills. *Journal of Comparative Physiology B: Biochemical, Systemic, and Environmental Physiology* **166**, 37-45.

Pawert, M., Müller, E. and Triebskorn, R. (1998). Ultrastructural changes in fish gills as biomarker to assess small stream pollution. *Tissue and Cell* **30**, 617-626.

Pawley, J. B. (2006). Handbook of confocal microscopy. New York: Springer Science.

Perry, S. F. (1997). The chloride cell: Structure and function in the gills of freshwater fishes. *Annual Review of Physiology* **59**, 325-347.

Perry, S. F. and Walsh, P. J. (1989). Metabolism of isolated fish gill cells: Contribution of epithelial chloride cells. *Journal of Experimental Biology* **144**, 507-520.

Perry, S. F. and Gilmour, K. M. (2006). Acid-base balance and CO_2 excretion in fish: Unanswered questions and emerging models. *Respiratory Physiology and Neurobiology* **154**, 199-215.

Perry, S. F., Goss, G. G. and Laurent, P. (1992). The interrelationships between gill chloride cell morphology and ionic uptake in four freshwater teleosts. *Canadian Journal of Zoology* **70**, 1737-1742.

Perry, S. F., Beyers, M. L. and Johnson, D. A. (2000). Cloning and molecular characterisation of the trout (*Oncorhynchus mykiss*) vacuolar H^+-ATPase B subunit. *Journal of Experimental Biology* **203**, 459-470.

Petr, M. J. and Wurster, R. D. (1997). Determination of *in situ* dissociation constant for Fura-2 and quantitation of background fluorescence in astrocyte cell line U373-MG. *Cell Calcium* **21**, 233-240.

Petroll, W. M., Cavanagh, H. D. and Jester, J. V. (1993). Three-dimensional imaging of corneal cells using *in vivo* confocal microscopy. *Journal of Microscopy* **170**, 213-219.

Pfaffl, M. W. (2004). Quantification strategies in real-time PCR. In *A-Z of quantitative PCR* (ed. S. A. Bustin), pp. 87-112. La Jolla, CA: International University Line.

Pisam, M., Prunet, P., Boeuf, G. and Rambourg, A. (1988). Ultrastructural features of chloride cells in the gill epithelium of the Atlantic salmon, *Salmo salar*, and their modifications during smoltification. *American Journal of Anatomy* **183**, 235-244.

Pisam, M., Auperin, B., Prunet, P., Rentier-Delrue, F., Martial, J. and Rambourg, A. (1993). Effects of prolactin on α and β chloride cells in the gill epithelium of the saltwater adapted tilapia *Oreochromis niloticus*. *Anatomical Record* **235**, 275-284.

Playle, R. C. and Wood, C. M. (1989). Water chemistry changes in the gill micro-environment of rainbow trout: experimental observations and theory. *Journal of Comparative Physiology - B Biochemical, Systemic, and Environmental Physiology* **159**, 527-537.

Potts, W. T. W. and Evans, D. H. (1966). The effects of hypophysectomy and bovine prolactin on salt fluxes in fresh-water adapted *Fundulus heteroclitus*. *Biological Bulletin* **131**, 362-368.

Prunet, P. and Auperin, B. (1995). Prolactin receptors. In *Fish Physiology, vol. XIII: Molecular Endocrinology of Fish* (eds. N. M. Sherwood, C. L. Hew, A. P. Farrell and D.J. Randall), pp. 367–392. London: Academic Press.

Prunet, P., Sturm, A. and Milla, S. (2006). Multiple corticosteroid receptors in fish: From old ideas to new concepts. *General and Comparative Endocrinology* **147**, 17-23.

Qiagen. (2010). Critical Factors for Successful Real-time PCR Germantown, MD: Qiagen. www.qiagen.com/literature/render.aspx?id=23490

Raven, P. H. and Axelrod, D. I. (1972). Plate tectonics and Australasian paleobiogeography. *Science* **176**, 1379-1386.

Reid, S. D., Hawkings, G. S. and Goss, G. G. (2003). Localization and characterization of a phenamil-sensitive Na^+ flux in isolated rainbow trout gill epithelial cells. *Journal of Experimental Biology* **206**, 551-559.

Reynolds, I. J. (2001). Measurement of cation movement in primary cultures using fluorescent dyes. *Current Protocols in Neuroscience* **7**, 11.1-11.17.

Richards, J. G., Semple, J. W., Bystriansky, J. S. and Schulte, P. M. (2003). Na^+/K^+-ATPase α-isoform switching in gills of rainbow trout (*Oncorhynchus mykiss*) during salinity transfer. *Journal of Experimental Biology* **206**, 4475-4486.

Rochat, T., Lacroix, J. S. and Jornot, L. (2004). N-acetylcysteine inhibits Na^+ absorption across human nasal epithelial cells. *Journal of Cellular Physiology* **201**, 106-116.

Sakamoto, T. and McCormick, S. D. (2006). Prolactin and growth hormone in fish osmoregulation. *General and Comparative Endocrinology* **147**, 24-30.

Sangiao-Alvarellos, S., Arjona, F. J., Miguez, J. M., Martín del Río, M. P., Soengas, J. L. and Mancera, J. M. (2006). Growth hormone and prolactin actions on osmoregulation and energy metabolsim of gilthead seabream (*Sparus auratus*). *Comparative Biochemistry and Physiology A - Molecular and Integrative Physiology* **144**, 491-500.

Scheiner-Bobis, G. and Schoner, W. (2001). A fresh facet for ouabain action. *Nature Medicine* **7**, 1288-1289.

Schreck, C. B. (1981). Stress and compensation in teleostean fishes: Response to social and physical factors. In *Sress and Fish* (ed. A. D. Pickering), pp. 295-321. New York: Academic Press.

Scott, G. R., Richards, J. G., Forbush, B., Isenring, P. and Schulte, P. M. (2004). Changes in gene expression in gills of the euryhaline killifish *Fundulus heteroclitus* after abrupt salinity transfer. *American Journal of Physiology - Cell Physiology* **287**, C300-C309.

Scott, G. R., Claiborne, J. B., Edwards, S. L., Schulte, P. M. and Wood, C. M. (2005). Gene expression after freshwater transfer in gills and opercular epithelia of killifish: Insight into divergent mechanisms of ion transport. *Journal of Experimental Biology* **208**, 2719-2729.

Seidelin, M. and Madsen, S. S. (1999). Endocrine control of Na^+,K^+-ATPase and chloride cell development in brown trout (*Salmo trutta*): Interaction of insulin-like growth factor I with prolactin and growth hormone. *Journal of Endocrinology* **162**, 127-135.

Semple, J. W., Green, H. J. and Schulte, P. M. (2002). Molecular cloning and characterization of two Na/K-ATPase isoforms in *Fundulus heteroclitus*. *Marine Biotechnology* **4**, 512-519.

Shephard, K. L. (1992). Studies on the fish-microclimate: Interactions between gill, tissue, mucus and water quality. *Environmental Biology of Fishes* **34**, 409-420.

Shiraishi, K., Matsuda, M., Mori, T. and Hirano, T. (1999). Changes in the expression of prolactin- and cortisol-receptor genes during early-life stages of euryhaline tilapia (*Oreochromis mossambicus*) in fresh water and seawater. *Zoological Science* **16**, 139-146.

Shrimpton, J. M. and McCormick, S. D. (1998). Regulation of gill cytosolic corticosteroid receptors in juvenile Atlantic salmon: Interaction effects of growth hormone with prolactin and triiodothyronine. *General and Comparative Endocrinology* **112**, 262-274.

Shrimpton, J. M., Bernier, N. J. and Randall, D. J. (1994). Changes in cortisol dynamics in wild and hatchery-reared juvenile coho salmon (*Oncorhynchus kisutch*) during smoltification. *Canadian Journal of Fisheries and Aquatic Sciences* **51**, 2179-2187.

Smith, C. L. (2011). Basic confocal microscopy. *Current Protocols in Neuroscience* **56**, 2.2.1-2.2.18.

Steward, N., Martin, R., Engasser, J. M. and Goergen, J. L. (1999). A new methodology for plant cell viability assessment using intracellular esterase activity. *Plant Cell Reports* **19**, 171-176.

Svoboda, K., Denk, W., Kleinfeld, D. and Tank, D. (1997). *In vivo* dendritic calcium dynamics in neocortical pyramidal neurons. *Nature* **385**, 161-165.

Szmacinski, H. and Lakowicz, J. R. (1997). Sodium green as a potential probe for intracellular sodium imaging based on fluorescence lifetime. *Analytical Biochemistry* **250**, 131-138.

Takahashi, A., Camacho, P., Lechleiter, J. D. and Herman, B. (1999). Measurement of intracellular calcium. *Physiological Reviews* **79**, 1089-1125.

Tamura, K., Peterson, D., Peterson, N., Stecher, G., Nei, M. and Kumar, S. (2011). MEGA5: Molecular evolutionary genetics analysis using maximum likelihood, evolutionary distance, and maximum parsimony methods. *Molecular Biology and Evolution* **28**, 2731-2739.

Taylor, A. and Windhager, E. E. (1979). Possible role of cytosolic calcium and Na-Ca exchange in regulation of transepithelial sodium transport. *American Journal of Physiology - Renal Physiology* **236**, F505-F512.

Thorgaard, G. H., Bailey, G. S., Williams, D., Buhler, D. R., Kaattari, S. L., Ristow, S. S., Hansen, J. D., Winton, J. R., Bartholomew, J. L., Nagler, J. J., Walsh, P. J., Vijayan, M. M., Devlin, R. H., Hardy, R. W., Overturf, K. E., Young, W. P., Robison, B. D., Rexroad, III., C. and Palti, Y. (2002). Status and opportunities for genomics research with rainbow trout. *Comparative Biochemistry and Physiology B - Biochemistry and Molecular Biology* **133**, 609-646.

Tipsmark, C. K. and Madsen, S. S. (2009). Distinct hormonal regulation of Na^+,K^+-ATPase genes in the gill of Atlantic salmon (*Salmo salar* L.). *Journal of Endocrinology* **203**, 301-310.

Tipsmark, C. K., Mahmmoud, Y. A., Borski, R. J. and Madsen, S. S. (2010). FXYD-11 associates with Na^+-K^+-ATPase in the gill of Atlantic salmon: regulation and localization in relation to changed ion-regulatory status. *American Journal of Physiology - Regulatory, Integrative and Comparative Physiology* **299**, R1212-R1223.

Tipsmark, C. K., Madsen, S. S., Seidelin, M., Christensen, A. S., Culter, C. P. and Cramb, G. (2002). Dynamics of Na^+,K^+,$2Cl^-$ cotransporter and Na^+,K^+-ATPase expression in the branchial epithelium of brown trout (*Salmo trutta*) and Atlantic salmon (*Salmo salar*). *Journal of Experimental Zoology* **293**, 106-118.

Törnquist, K. and Ekokoski, E. (1993). Intracellular free sodium concentrations in GH4C1 cells. *Journal of Cellular Physiology* **154**, 608-614.

Trachtenberg, J. T., Chen, B. E., Knott, G. W., Feng, G., Sanes, J. R., Welker, E. and Svoboda, K. (2002). Long-term *in vivo* imaging of experience-dependent synaptic plasticity in adult cortex. *Nature* **420**, 788-794.

Uchida, K., Kaneko, T., Yamauchi, K. and Hirano, T. (1996). Morphometrical analysis of chloride cell activity in the gill filaments and lamellae and changes in Na^+,K^+-ATPase activity during seawater adaptation in chum salmon fry. *Journal of Experimental Biology* **276**, 193-200.

Urbina, M. A., Forster, M. E. and Glover, C. N. (2011). Leap of faith: Voluntary emersion behaviour and physiological adaptations to aerial exposure in a non-aestivating freshwater fish in response to aquatic hypoxia. *Physiology & Behavior* **103**, 240-247.

Urbina, M. A., Glover, C. N. and Forster, M. E. (2012). A novel oxyconforming response in the freshwater fish *Galaxias maculatus*. *Comparative Biochemistry and Physiology A - Molecular and Integrative Physiology* **161**, 301-306.

Utida, S. T., Hirano, H., Oide, M., Ando, D., Johnson, W. and Bern, H. A. (1972). Hormonal control of the intestine and urinary bladder in teleost osmoregulation. *General and Comparative Endocrinology* **3**, 317-327.

Valasek, M. A. and Repa, J. J. (2005). The power of real-time PCR. *Advances in Physiology Education* **29**, 151-159.

VandeVen, M., Balut, B., Baron, S., Smets, I., Steels, P. and Ameloot, M. (2010). Analysis of mitochondrial pH and ion concentrations. In *Methods in Molecular Biology, vol. 591, Part 2: Live Cell Imaging- Methods and Protocols*, (ed. D. B. Papkovsky), pp. 275-209. New York: Humana Press.

Van Der Heijden, A. J. H., Verbost, P. M., Eygensteyn, J., Li, J., Wendelaar Bonga, S. E. and Flik, G. (1997). Mitochondria-rich cells in gills of tilapia (*Oreochromis mossambicus*) adapted to fresh water or sea water: Quantification by confocal laser scanning microscopy. *Journal of Experimental Biology* **200**, 55-64.

Van Grieken, R. and Markowicz, A. (2001). Handbook of X-ray Spectrometry. New York: Marcel Dekker.

Van Guilder, H. D., Vrana, K. E. and Freeman, W. M. (2008). Twenty-five years of quantitative PCR for gene expression analysis. *BioTechniques* **44**, 619-626.

van Pelt-Verkuli, E., van Belkum, A. and Hays, J. P. (2008). Principles and Technical Aspects of PCR Amplification. New York: Springer.

Vandesompele, J., De Preter, K., Pattyn, F., Poppe, B., Van Roy, N., De Paepe, A. and Speleman, F. (2002). Accurate normalization of real-time quantitative RT-PCR data by geometric averaging of multiple internal control genes. *Genome Biology* **3**, 34

Venkatesh, B. (2003). Evolution and diversity of fish genomes. *Current Opinion in Genetics and Development* **13**, 588-592.

Voipio, J., Pasternack, M. and MacLeod, K. (1994). Ion-sensitive microelectrodes. In *Microelectrode Techniques: The Plymouth Workshop Handbook* (ed. D. Ogden), pp. 275-316. Cambridge: The Company of Biologists.

Walrond, C. (2009). Trout and salmon. In *Te Ara - the Encyclopedia of New Zealand*. http://www.TeAra.govt.nz/en/trout-and-salmon/2/5

Walrond, C. (2011). Whitebait and whitebaiting. In *Te Ara - the Encyclopedia of New Zealand* http://www.TeAra.govt.nz/en/whitebait-and-whitebaiting/1/1

Waters, J. M., López, J. A. and Wallis, G. P. (2000). Molecular phylogenetics and biogeography of galaxiid fishes (Osteichthyes: Galaxiidae): Dispersal, vicariance, and the position of *Lepidogalaxias salamandroides*. *Systematic Biology* **49**, 777-795.

Wilfinger, W. W., Mackey, K. and Chomczynski, P. (1997). Effect of pH and ionic strength on the spectrophotometric assessment of nucleic acid purity. *BioTechniques* **22**, 474-481.

Wilkie, M. P. (1997). Mechanisms of ammonia excretion across fish gills. *Comparative Biochemistry and Physiology* **118**, 39-50.

Wilmer, P., Stone, G. and Johnston, I. (2004). Environmental Physiology of Animals, 2nd edition. London: Wiley-Blackwell.

Wilson, J. M. and Laurent, P. (2002). Fish gill morphology: Inside out. *Journal of Experimental Zoology* **293**, 192-213.

Wilson, J. M., Randall, D. J., Donowitz, M., Vogl, A. W. and Ip, A. K. Y. (2000b). Immunolocalization of ion-transport proteins to branchial epithelium mitochondria-rich cells in the mudskipper (*Periophthalmodon schlosseri*). *Journal of Experimental Biology* **203**, 2297-2310.

Wilson, J. M., Laurent, P., Tufts, B. L., Benos, D. J., Donowitz, M., Vogl, A. W. and Randall, D. J. (2000a). NaCl uptake by the branchial epithelium in freshwater teleost fish: An immunological approach to ion-transport protein localization. *Journal of Experimental Biology* **203**, 2279-2296.

Wittwer, C. T., Herrmann, M. G., Moss, A. A. and Rasmussen, R. P. (1997). Continuous fluorescence monitoring of rapid cycle DNA amplification. *BioTechniques* **22**, 130-138.

Woll, E., Ritter, M., Offner, F., Lang, H. J., Scholkens, B., Haussinger, D. and Lang, F. (1993). Effects of HOE 694 - A novel inhibitor of Na^+/H^+ exchange - On NIH 3T3 fibroblasts expressing the RAS oncogene. *European Journal of Pharmacology - Molecular Pharmacology Section* **246**, 269-273.

Wood, C. M. and Le Moigne, J. (1991). Intracellular acid-base responses to environmental hyperoxia and normoxic recovery in rainbow trout. *Respiratory Physiology* **86**, 91-113.

Wood, C. M. and Pärt, P. (1997). Cultured branchial epithelia from freshwater fish gills. *Journal of Experimental Biology* **200**, 1047-1059.

Wood, C. M., Kelly, S. P., Zhou, B., Fletcher, M., O'Donnell, M., Eletti, B. and Pärt, P. (2002). Cultured gill epithelia as models for the freshwater fish gill. *Biochimica et Biophysica Acta - Biomembranes* **1566**, 72-83.

Wright, S. H. (1991). The interface of animal and environment: Strategies and constraints on the maintenance of solute balance. In *Biochemistry and Molecular Biology of Fishes*, vol. 1, (eds. P. W. Hochachka and T. P. Mommsen), pp. 165-180. Amsterdam: Elsevier.

Wu, S. M., Ding, H. R., Lin, L. Y. and Lin, Y. S. (2008). Juvenile tilapia (*Oreochromis mossambicus*) strive to maintain physiological functions after waterborne copper exposure. *Archives of Environmental Contamination and Toxicology* **54**, 482-492.

Yabu, T., Imamura, S., Mohammed, M. S., Touhata, K., Minami, T., Terayama, M. and Yamashita, M. (2011). Differential gene expression of HSC70/HSP70 in yellowtail cells in response to chaperone-mediated autophagy. *FEBS Journal* **278**, 673-685.

APPENDIX A: PRIMER DESIGN AND OPTIMISATION

Methods A

A.1 Primer design

A.1.1 Primer length

Primers are usually designed to be between 18-25 base pairs long with an ideal length of 20 base pairs. This provides a sufficiently long sequence to maximise specificity but is also short enough to facilitate ease of binding (Bustin, 2000, 2004; Nolan et al., 2006).

A.1.2 Primer Melting Temperature

The primer melting temperature (T_m) is the temperature at which one half of the DNA duplex will dissociate to become single stranded. The stability of a primer-template DNA duplex can be measured by its T_m (van Pelt-Verkuli et al., 2008). The ideal temperature range is between 58-64°C with 60°C being preferred. The T_m of each primer should not differ by more than 4°C from its pair in order for both primers to bind simultaneously and efficiently amplify the product.

A.1.3 GC Content

Binding between the bases guanine (G) and cysteine (C) is stronger than that between adenosine (A) and thymine (T) due to the three hydrogen bonds they share (Alberts et al., 2002). Ideally the GC content of the primer should be around 50% as this helps stabilise mismatches (Nolan et al., 2006). GC-rich regions can be difficult to amplify, and therefore primers with more than 60% GC content are also avoided.

A.1.4 Secondary Structure

Intermolecular and intramolecular interactions in primers can produce a variety of secondary structures that can lead to a decreased yield or absence of product in the PCR reaction (Nolan et al., 2006). Secondary structures may sequester reagents and primers, reducing the availability of these components for the preferred template reaction.

There are three types of secondary structures: hairpins, primer self-dimers, and cross dimers (Bustin, 2004). Hairpins occur when intramolecular interactions within an individual primer are high and it bonds to itself. Primer self-dimers occur when intermolecular interactions between two of the same primers (i.e. between two forward primers or two reverse primers) are high and they bind to each other. Cross dimers are similar but occur between a forward and a reverse primer. All candidate primers were analysed *in silico* for the existence of secondary structures using OligoAnalyzer 3.1.

A.1.5 Consecutive base pairs

Runs of single base pairs in the primers (i.e. more than three or four bases (particularly G or C) in a row) are avoided as they can cause slippage of the DNA polymerase (Nolan et al., 2006). If slipping occurs this can produce an inaccurate template.

A.1.6 Amplicon size

Primers designed to select for a small amplicon of around 100 base pairs (bp) are preferred as they lead to a more efficient reaction (Brisson et al., 2004; Nolan et al., 2006). Small amplicons require shorter polymerisation times for replication, meaning that amplification of larger contaminants such as genomic DNA is less likely (Nolan et al., 2006). Large amplicons are also more prone to replication errors than small amplicons and so should be avoided.

A.1.7 Specificity

To determine the specificity of each primer pair for its target sequences, all primers were aligned with the other non-target isoforms to ensure they did not prime to non-target templates. This was performed using the alignment software MEGA Version 5.0 (Tamura et al., 2011). Because of the similarity of the three NKA isoforms sequences, the primers all showed some degree of priming. To help reduce this, the primers with the least similarity to the non-targets were selected and mismatches were designed to occur in the 3’ end of the primer.

A.2 Primer optimisation

A.2.1 Temperature gradient

Annealing temperature is critical for PCR specificity as a low annealing temperature will cause non-specific binding (Innis et al., 1990). The annealing temperature should theoretically be 5°C below the T_m of the primer pair. A temperature gradient can be performed by exposing the primer sets to a variety of temperatures above and below the T_m. All primer sets were design to have a T_m of 60°C so temperature gradient was performed from 49.8°C to 65.1°C, using a PCR-based assessment. PCR-based assessment of primers is a simple and cost-effective way to initially assess their suitability. Simple PCR involves the priming and amplification of the target sequence under similar conditions as the qPCR. The PCR products are then examined via electrophoretic separation with the most appropriate annealing temperature indicated by the brightest band.

PCR reactions were performed using KAPA Taq Ready Mix DNA Polymerase (Kapa Biosystems), and an Eppendorf Mastercycler e*p* gradient *S* PCR machine. Reactions were performed using representative cDNA (pooled cDNA samples from freshwater-, 50% seawater- and 100% seawater-acclimated inanga) to give a final reaction concentration of 5 ng/µL. Final reaction concentrations were 200 nM of forward and reverse primer and Taq DNA polymerase 0.025 U/µL, 1X buffer, and 0.2 mM dNTPs (Table A.1). The Eppendorf Master cycler allows the annealing temperature for each individual reaction well to be specified so all possible annealing temperatures can be tested in the same reaction. The thermal profile used is shown in Table A.2. After PCR cycling, 5 µL of each product was run on a 2% gel at 100 volts for 45 minutes. A Hyperladder IV molecular weight ladder was also included to allow the size of the bands to be determined. The gel was imaged using a Syngene G:Box Gel Documentation system (Synoptics Group) and the brightest band was determined using the Syngene G:Box Gel Doc software.

Table A.1 Reaction compositions for primer annealing temperature gradient experiment

Reagents	Volume (µL) per reaction
Forward primer (10 nM)	0.4
Reverse primer (10 nM)	0.4
KAPA Taq DNA polymerase	10
cDNA (100ng/µL)	1
Water	8.2
Total volume	20

Table A.2 Thermal cycling conditions for primer annealing temperature gradient experiment

Step	Temperature °C	Duration	Cycles
Denature	95	2 minutes	
Annealing	Gradient between 49.8 – 65.1	30 seconds	30
Extension	72	15 seconds	
Final extension	72	1 minute	

A.2.2 Primer concentration

Suboptimal concentrations of primers can lead to primer-dimer formation which leads to poor or absent yield of product in the PCR reaction (Nolan et al., 2006). To test the most appropriate primer concentration, a matrix of primer concentrations was analysed using RT-PCR. Working 1 µM primers stocks were prepared and the appropriate volume to give a graded series of primer concentrations was added to a single strip tube along with KAPA SYBR® Fast qPCR master mix (2X) (Kapa Biosystems), cDNA and molecular pure water to give a 20 µL reaction volume (Table A.3). Standard curves were prepared to assess reaction efficiency by serially diluting a pooled cDNA sample, to cover the entire dynamic range of the specimens.

The reactions were prepared in duplicates and run on a Rotor-Gene Q Realtime PCR instrument (Qiagen) set with the thermal cycle indicated in Table A.4. The master mix used contained a hot-start DNA polymerase enzyme that shows no enzymatic activity at room temperature and therefore requires activation by exposure to a high temperature (first step - enzyme activation; Table A.4). This prevented primer-dimer formation and mispriming during reaction set-up and initial cycling steps (Qiagen, 2010). Melt curve analysis was performed at the end of 40 cycles to determine if a single product was formed or if primer-dimers were present. Selection of the appropriate primer concentration was based on the minimum concentration of each primer that produced the lowest C_t value with the least amount of nonspecific amplification (Nolan et al., 2006).

Table A.3 Reaction components for primer concentration experiment

	Volume added to each reaction (µL)				
Final reaction concentration of forward/reverse primers (nM)	**Forward primer (1 µM)**	**Reverse primer (1 µM)**	**KAPA SYBR® Fast**	**cDNA (10 ng/µL)**	**Molecular pure water**
50/50	0.5	0.5	10	2	7
50/100	0.5	1	10	2	6.5
50/150	0.5	1.5	10	2	6
50/200	0.5	2	10	2	5.5
50/300	0.5	3	10	2	4.5
100/50	1	0.5	10	2	6.5
100/100	1	1	10	2	6
100/150	1	1.5	10	2	5.5
100/200	1	2	10	2	5
100/300	1	3	10	2	4
150/50	1.5	0.5	10	2	6
150/100	1.5	1	10	2	5.5
150/150	1.5	1.5	10	2	5
150/200	1.5	2	10	2	4.5
150/300	1.5	3	10	2	3.5
200/50	2	0.5	10	2	5.5
200/100	2	1	10	2	5
200/150	2	1.5	10	2	4.5
200/200	2	2	10	2	4
200/300	2	3	10	2	3
300/50	3	0.5	10	2	4.5
300/100	3	1	10	2	4
300/150	3	1.5	10	2	3.5
300/200	3	2	10	2	3
300/300	3	3	10	2	2

Table A.4 qPCR thermal cycling conditions for primer concentration experiment

Step	**Temperature °C**	**Duration**	**Cycles**
Enzyme activation	95	10 minutes	Hold
Denature	95	30 seconds	40
Annealing	60	30 seconds	
Extension	72	30 seconds	
Melt curve analysis	60 - 95	1 second per step	

Results A

A.3.1 Primer optimisation

Temperature-gradient PCR revealed the optimum annealing temperature for all primer sets was 60°C as indicated by the brightest band as identified by Syngene G:Box Gel Doc software. High annealing temperatures tend to result in more specific binding relative to lower temperatures, so when multiple bands showed equal intensity the higher annealing temperature was selected (Figure A.1).

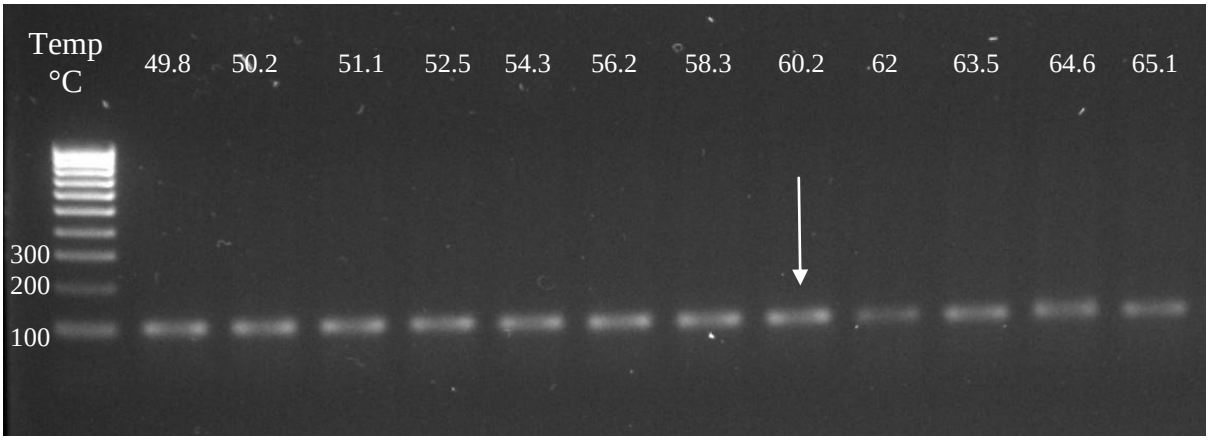

Figure A.1 Electrophoresis gel of temperature gradient PCR for α1a primers. The brightest bands were seen at 56.2, 58.3 and 60.2 °C so 60°C was selected as the annealing temperature (arrow). The Hyperladder IV indicates the band size in basepairs.

The results from the primer concentration matrix experiments indicated that for α1b, α1c and 18S, 200 nM of each forward and reverse primer was optimal. This concentration produced the lowest Ct value, with the least amount of nonspecific amplification, and no primer dimerisation was recorded (data not shown). For α1a 150 nM of each forward and reverse primer was selected, based on similar criteria.

During primer optimisation it became evident that the EF1a and βA primers were non-specific and produced more than one product (Figure A.2)

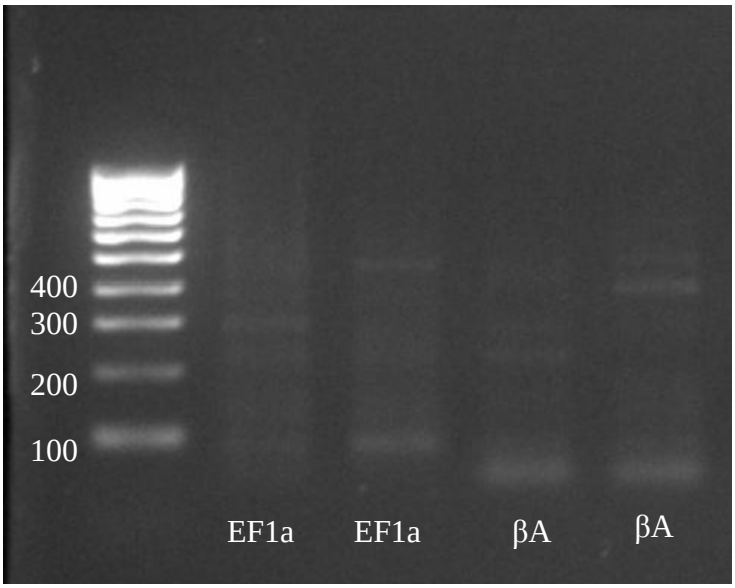

Figure A.2 Electrophoresis gel of temperature gradient PCR for EF1a and βA primers. Multiple bands are seen indicating multiple products are produced. The Hyperladder IV indicates the band size in basepairs.